2

OPTIMAL PROCESSING OF KUMARA

A thesis presented in patial fulfilment of the requirements for the degree of
Doctor of Philosophy in Bioprocess Engineering
Massey University
Palmerston North
New Zealand

Juan Antonio Canumir-Veas

Agronomist Engineer, M.S. in Agriculture Engineering

2004

...para mi padre...

...ese error consiste en creer que describir mas explicar, es igual a comprender...
...comprender es algo mas profundo, y no tiene que ver con la ciencia...
...sino mas bien con la percepción, osea con la capacidad de iluminación...
...este mundo necesita ser comprendido, mas que conocido, pero insistimos an acumular mas conocimiento de él...
M. MaxNeef

ABSTRACT

The colour and texture change of kumara (*Ipomoea batatas L.*) during the cooking process has been studied. A model was developed as a tool to understand how of these characteristics could be optimised in terms of cooking temperature and time.

After cooking, kumara undergoes an intensive darkening discolouration due to a reaction between iron and phenolic compounds. The discoloration mechanism was separated into three consecutive steps. Cell modification occurs during cooking allowing iron and/or phenolic compounds (principally chlorogenic acid) to leave the cell. Once free, both elements combine to form a colourless iron-phenolic complex. In the presence of oxygen this complex oxidises to form a blue-black Fe^{3+} complex that is responsible for the dark colour. This mechanism was confirmed experimentally on roots of Owairaka Red and Toka Toka Gold kumara by measuring the colour parameters (a, b, L) over a range of cooking and storage conditions using a Minolta colorimeter.

Kinetics parameters for cellular modification during cooking and colour formation upon exposure to oxygen were determined. The results showed that the cell modification reaction followed first order kinetics with an activation energy and Arrhenius constant of $101 kJmol^{-1}$ and $4.56 mim^{-1}$ respectively. Upon exposure of cooked kumara to oxygen, colour formation occurs at a rate dependent on diffusion of oxygen into the kumara flesh. By chelation of iron through the use additives such as sodium pyrophosphate (SAPP) it is possible to prevent post cooking darkening in kumara.

Textural change was also studied and the mechanism was found to be a result of two main reactions, starch gelatinisation and cell wall disruption. Experiments were carried out to confirm this textural mechanism.

Experiments were carried out to measure the kinetics of textural change (fracture force) using Owairaka Red and Toka Toka Gold kumara. The results showed that texture kinetics

were temperature dependent and followed first order kinetics and the Arrhenius Law with activation energies of 162 and 125kJ/mol, and Arrhenius constants of 5.59E22 and 2.54E17min^{-1} for red and gold kumara respectively.

Attempts to measure cell wall disruption kinetics from changes in alcohol insoluble solids and total reducing sugars were not successful but literature data for pectin losses in potatoes showed close agreement with overall texture loss in kumara, suggesting that breakdown of the middle lamella is the primary cause of softening during cooking.

Using the kinetics data a model was formulated to predict temperature, texture and colour profiles through the product during cooking. Good comparisons were found between experimental data predictions from the model, for large kumara samples providing a partial validation of the model. The model was used to demonstrate the sensitivity of kumara quality and consistency to processing conditions. The use of the model was demonstrated with two industrially focussed case studies.

Acknowledgements

My deepest gratitude to Dr John Bronlund for his supervision, orientation and scientific support. His great scientific ability was extremely helpful in the development of my Ph.D. project.

I also wish to recognise the support of Dr. John Mawson and Michael Parker for their important contribution to improve this research. To Delta Produce, and Andre de Bruin for providing funds and raw material necessary during this research.

Many thanks to the Chilean Government, for awarding me the scholarship "Beca Presidente de la Republica" through Mideplan. Gracias Adriana del Pozo, por el apoyo en estos años *"un gran abrazo Adriana"*.

I wish to express my appreciation to all the staff at Institute of Technology and Engineering in particular my friends Lisa Valenzuela and Joan Brookes, and also Mike Sahayam and his family for their wonderful friendship

Thanks to Anne Marie Jackson, John Sykes, and Garry Radford.

I am grateful to Gary Field-Mitchell, John and Pauline Julian for reviewing my "English" in the final document and for their warm friendship, I really appreciate your support.

Thanks to all our Latin friends, we shared our typical traditions, and very good moments *"gracias amigos"*.

Precious thanks to all our kiwi friends, Michael and Ann Wilson, Mary and Terry Silcock, Catherine Widdup and Wallace Robinson.

Most of all thank you to my wonderful family, my most heartfelt thanks to Patty *"my boss"* for her love, undestanding, and to Carmen, Javi and JJ, "thank you God for my beautiful family".

There are so many people I am indebted to I cannot mention you all by name, you know who you are. Those who helped me in my work, and those who made my family and I so welcome in New Zealand, please take this as a personal "thank you"

TABLE OF CONTENTS

LISTS OF FIGURES

LISTS OF TABLES

CHAPTER 1: PROJECT OVERVIEW

1.1. BACKGROUND

In New Zealand sweet potato is also known as Kumara. Both are classified in the same taxonomic species (*Ipomoea batatas* L.). Maori travellers originally introduced them into New Zealand as they migrated southwards many centuries ago.

The New Zealand kumara production has good potential for export because it has significant advantages over other countries. New Zealand is free of major sweet potato pests and diseases, and produces product of high quality and high yields (Balasingham, 1984).

Currently kumara are sold as fresh product to the local market, but processed sweet potato is highly demanded by the Australian and Japanese food industries, because it can be used as a base ingredient in many processed foods, especially baby foods. Processed kumara offers a good opportunity for New Zealand to expand into these international markets.

The most critical problems for kumara processing are the discoloration or darkening of the product after cooking and texture change. Colour and texture (consistency) are important quality characteristics, and must be controlled to exact customer or market requirements.

An understanding of the cause and mechanisms of colour and texture changes are necessary to identify how the processing conditions can be manipulated in order to produce high quality processed kumara.

1.2. AIM

The aim of this project was to identify the mechanism of the after cooking discoloration reaction, and the mechanism of texture changes in kumara during cooking. Using this information, the kinetics of the key reactions influencing colour and texture were to be measured.

To integrate this knowledge, the cooking process was to be modelled to provide tools that can be applied to help control or design of industrial cooking processes that can produce high quality kumara products.

CHAPTER 2: LITERATURE REVIEW

2.1. GENERAL ASPECTS OF KUMARA

2.1.1. Botanical characteristics

The kumara is also known as the sweetpotato, sweet potato (English), kamote, camote o batata (Spanish). Taxonomically it is included in the Convolvulacea family, under the genus *Ipomoea* and the species is *Ipomoea batatas L.* (Decoteau, 2000).

2.1.1.1. Type of structure:

The sweet potato is a storage root; an enlarged lateral root and its function is the storage of energy. Consequently if a true botanical description is applied, it is not a tuber (like a white potato), but a root (like a carrot and beet) (Purcell and Sistrunk, 1982).

2.1.1.2. Phenotypic characterisation

The sweet potato storage root is highly variable in size and shape (Table 2-1). Sweet potato grown for the same time can have average size for the one cultivar of less than 40mm while the average size of another may be 100mm. It is possible to find roots from 0.1kg to over 1kg in weight, and in length from a few centimetres to over 30cm (Purcell and Sistrunk, 1982; Onwueme and Charles, 1994).

The surface can have defects, such as veins, horizontal constrictions, longitudinal grooves, and others like an alligator's skin (Huaman, 1991).

The colour is also highly variable, and is different for the skin and flesh. In each part, two colours can be distinguished, a predominant and a secondary colour. The distribution of the secondary flesh colour is also important to consider when a description of raw material is made. In a puree process however, the distribution of the flesh colour does not have relevance (Table 2-1) (Yen, 1974; Purcell and Sistrunk, 1982; Huaman, 1991).

Table 2-1 Typical shape of kumara

Shape	Description	Picture
Round	Almost circular, length to breadth ratio (L/B) about 1:1	
Round elliptic	L/B ratio 2:1	
Elliptic	L/B ratio no more than 3:1	
Ovate	Proximal end narrow, distal broad	
Obovate	Proximal end broad, distal narrow	
Oblong	Rectangular in outline. L/B ratio about 2:1	
Long oblong	L/B ratio of more than 3:1	
Long elliptic	L/B ratio of more than 3 to 1	
Long irregular or curved	Long irregular or curved	

Adapted from Huaman, (1991).

Table 2-2 Typical colour of kumara

Part of Storage root	*Predominant Colour*	*Secondary Colour*	*Other Colour Characteristics*
Skin	White Cream Yellow Orange Brownish orange Pink Red Purple-red Dark-purple	Absent White Cream Yellow Orange Brownish orange Pink Red Purple-red Dark-purple	*Intensity of Predominant colour* Pale Intermediate Dark
Flesh	White Cream Dark cream Pale yellow Dark yellow Pale orange Intermediate orange Dark orange Strongly pigmented	Absent White Cream Yellow Orange Pink Red Purple-red Purple Dark-purple	*Distribution of secondary colour* Absent Narrow ring in cortex Broad ring in cortex Scattered spots in flesh Narrow ring in flesh Broad ring in flesh Ring and other areas in flesh In longitudinal sections Covering most of the flesh Covering all flesh

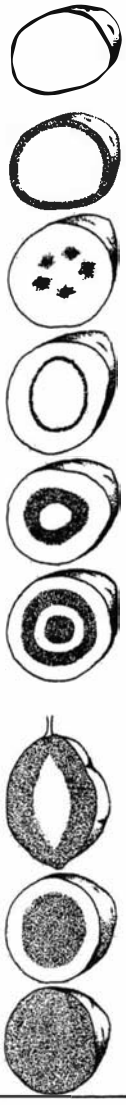

Adapted from Huaman (1991).

The colour of the flesh is difficult to determine, because exposure to the air on the cut sections can darken in some varieties more than others of similar colour. Differences in the amount of latex like exudate from the cut surface tend to obscure colour measurement (Yen, 1974).

2.1.2. Agricultural characteristics

The majority of New Zealand kumara, approximately 90% of product for fresh and processing industry, is grown in Northland and Taranaki. In the South Island a few districts grow kumara with only small production. Kumara is the 10th most popular vegetable in New Zealand (Sloss, 1994; Vegfed, 2001).

2.1.2.1. Varieties

External quality (shape, size and colour) is greatly influenced by cultivar (Purcell and Sistrunk, 1982).

In New Zealand, there are several different varieties of kumara, however the most common are those with a red–skinned and a creamy-white flesh (Owairaka Red) and those with a golden skin and flesh (Toka Toka Gold kumara) (Vegfed, 2001).

In general, sweet potato cultivars are grouped into two types; those with a deep yellow-orange colour that are soft, moist, and sweet when cooked; and those with a firm, dry, light-coloured mealy flesh. Soft-fleshed cultivars are becoming more popular and include Centennial, Nemagold, and Goldrush. Yellow Jersey is a prominent firm-fleshed cultivar (Decoteau, 2000).

The Grower organisation NZ Vegetable & Potato Growers Federation (Inc), reported that in June 1999, in New Zealand the planted area with kumara was 1000 ha, with 16,000 tonnes of production, concentrated in 90 growers (Vegfed, 2001).

2.1.2.2. Phase of growth

Sweet potato is a perennial plant, but is normally grown as an annual. Under cultivation it is vegetatively propagated from sprouts or vine cuttings. The growth occurs in three distinct phases; an initial phase when the fibrous roots grow extensively and there is only moderate growth of the sprouts; a middle phase when the vines undergo extensive growth, and the tubers are initiated, a tremendous increase in leaf area occurs during this phase; and a final phase when the storage root bulking occurs and very little further growth of vines and fibrous roots take place; total leaf area stays constant early in this phase, and then begins to decline (Onwueme and Charles, 1994; Decoteau, 2000)

2.1.2.3. *Production systems*

Production systems and postharvest treatment affect internal sensory quality and external appearance.

2.1.2.3.1. *Environmental:*

Sweet potato is a crop native to the tropics, and is grown best in regions with 750-1250mm per year of rainfall, with warms days and nights. The optimum temperatures for growth are 20-28°C and with 4 or 5 frost-free months (Purcell and Sistrunk, 1982; Mayhew and Penny, 1988; Decoteau, 2000).

The level of light also influences storage root formation. Growth is promoted by short day-lengths and retarded by long day-lengths, also, the normal growth and development of storage roots can only occur in the absence of light. When the kumara roots have already developed and are growing, exposure to light results in a cessation of storage root enlargement, a decrease in the starch content, and an increase in the fibre content (Onwueme and Charles, 1994).

2.1.2.3.2. *Planting:*

A common spacing is 25-30cm between plants and 60-105cm between rows. Plants' spacing depends on soil fertility and availability of irrigation water. Wide spacing on fertile soils results in excessive jumbo roots and rougher roots. Close spacing on very sandy soil results in undersized roots (Onwueme and Charles, 1994; Decoteau, 2000).

2.1.2.3.3. *Soil:*

The soil textures affect the quality of the root. Heavy soils should be avoided, as the storage roots tend to be badly shaped and difficult to lift. In general, rich and heavy soils produce high yields of low-quality roots, on the other hand extremely poor, sandy soils produce low yields of high quality roots. Sweet potato yields more and better quality roots on well-drained, sandy loam or silt loam soil. These soil conditions are best met in New Zealand around Dargaville, Northland.

Poor surface drainage of the field may cause wet spots, and reduce yields which cause sweet potatoes to be large, misshapen, cracked, and rough skinned.

Finally soil temperatures below 12-15°C will damage the roots and cause rotting and off-flavour (Purcell and Sistrunk, 1982; Mayhew and Penny, 1988; Decoteau, 2000).

2.1.2.3.4. *Irrigation:*

Sweet potatoes need about 25-35mm of water each week. Severely wet soil conditions may lead to off-flavour, decreased yield, and roots that darken when processed. These and other colour-problems will be discussed later (section 2.5.3)(Purcell and Sistrunk, 1982; Mayhew and Penny, 1988; Decoteau, 2000).

2.1.2.3.5. Fertilisation:

Sweet potatoes respond well to fertiliser, however, excessive nitrogen fertiliser in the soil delays the storage root formation (Onwueme and Charles, 1994; Decoteau, 2000).

2.1.2.3.6. Harvesting:

Kumara is ready for harvesting 3-8 months after planting, and occurs between December and February, but often the storage roots on a given plant do not reach maturity at the same time. This gives rise to differences in size and shape of the roots, which may have implications during processing.

There are manual and mechanised ways to carry out kumara-harvesting. In either case, it is important that the roots be free of surface wounds and bruises which may impair their storage life (Onwueme and Charles, 1994; Vegfed, 2001).

2.1.2.3.7. Post harvest Handling:

After harvest, kumara is usually cured. Artificial curing is done in a storage house at 27-29.5°C and 85-90% relative humidity for 4-7 days with ventilation. Curing time is dependent on the prevailing temperature at the time that the roots are harvested. The lower the temperature, the longer the period of curing is required.

There is less loss of moisture and respiration in cured roots than in uncured roots; thus, there is less shrinkage during storage. Curing also improves the sensory quality of baked sweet potatoes (Purcell and Sistrunk, 1982; Onwueme and Charles, 1994).

Storage at 13-16°C requires the use of refrigerated rooms. Below 10°C, chilling-injury sets in, resulting in internal breakdown of the tissues, susceptibility to decay, loss of flavour, and the raw material quality for the puree process is decreased. On the other hand, storage temperatures above 16°C increase the respiration rate, causing heat production, loss in dry matter (raw material weight loss) and also sprouting (Onwueme and Charles, 1994).

Ventilation is important too. Loss of flavour results when the oxygen is less than 7% and CO_2 more than 10%.

In short, the agricultural activities have an important impact on the quantity and quality of kumara raw material used in puree processing. The colours and flavours (chemical composition) of roots are two characteristics highly affected by differences in cultivars, pathogens, storage conditions and time, and also the curing process (Kays, 1992).

2.2. COMPOSITION OF SWEET POTATOES

2.2.1. Proximate composition

The proximate composition of fresh sweet potato is shown in Table 2-3 below.

The most important component in the storage roots of kumara is the carbohydrate-group; of these, the starch (a polysaccharide) is present at the greater levels (~70% of total dwt) (Kays, 1992).

The non-starch carbohydrates (other polysaccharides) include pectin substances (~2.5%), cellulose (~2% of total dwt), and hemicellulose (3-4%) As a group they are classed as dietary fibre. Commonly, kumara are selected for low fibre content (Kays, 1992; Woolfe, 1992b).

Table 2-3 Proximate composition of kumara storage roots.

Component	Composition (%) (1)	(2)	(3)	(4)
Moisture	69±2	61.2-89	50-81	70
Carbohydrates	21.6	6.17-38.75	9-39	27.3
Reducing sugars	*1.1*	*0.38-5.64*	*0.5-2.5*	*ni*
Non-starch carbohydrates	*4.5*	*0.49-4.71*	*0.5-7.5*	*ni*
Starch	16±2	*5.3-28.4*	*8-29*	*ni*
Protein	2.0	0.46-2.93	0.95-2.4	1.3
Ether extract	0.2	0.06-0.48	1.8-6.4	0.4
Mineral Matter	0.96	0.31-1.06	0.88-1.38	1.0

Adapted from (1) Visser et al., (1990) "New Zealand Kumara"; (2) Woolfe, (1992b) "South Pacific Kumara"; (3) Onwueme and Charles, (1994); and (4) Enachescu, (1995). ni: no information

The protein concentration is highly variable. It varies between cultivars, within cultivars (root to root), and depends as well on the environmental conditions, nitrogen fertiliser, length of growing season and storage. It is also not uniform throughout the storage roots, and is generally higher at the proximal (stem) end. The cross-sectional distribution shows a significantly higher concentration in the outer cortex close to the surface (Kays, 1992).

Cooking has a significant effect on the nutritional quality of the protein, with baking resulting in less loss than canning in syrup or dehydration of flakes. Once processed to a puree the protein was found to remain constant over a 6 month period with proper storage (Kays, 1992).

The lipid content of kumara is low and nutritionally insignificant (Woolfe, 1992b).

In the ash or mineral matter, potassium (K) is the element in the greatest concentration followed by phosphorus and calcium or magnesium, and then other elements as shown in Table 2-4 (Kays, 1992; Woolfe, 1992b).

Table 2-4 Ten most important mineral contents of sweet potato storage roots

Minerals	Composition (mg/100 g fwb) (1)	(2)	(3)	(4)
K	250-450	260	342-488	430
P	29-57	51	28-54	38
Ca	17-45	29	17-34	21
Mg	18-36	26	14-23	23
Na	8-45	52	13-30	ni
S	13-19	13	Ni	22
Si	0.9	ni	0.99	ni
F	0.86	ni	0.86	ni
Fe	0.5-0.9	0.49	0.59-0.86	0.57
Zn	0.22-0.63	0.59		0.25

Adapted from (1) Kays, (1992); (2) Woolfe, (1992b) "South Pacific Kumara"; (3) Woolfe, (1992b) "Raw kumara roots" and (4) Sloss, (1994) "New Zealand Kumara". fwb: fresh weight basis. ni: no information

2.2.2. Starch

Starch is the most important carbohydrate present in the root of sweet potato. Its function is as a store of energy reserves. Starch is a long, weighty and complex polysaccharide, which is stored in amyloplasts (storage tissue) within the roots. There are linear relationships between root dry weight and the starch content (Kays, 1992; Woolfe, 1992b).

In kumara there are two categories of starch. One is a transitory starch that is formed in the leaves during the day and then degraded, converted to sucrose, and translocated out during the night. The second is a reserve starch that is synthesised and stored in the edible storage roots of the plants. This secondary type is more important to consider when the roots are used in food-processing (Kays, 1992).

2.2.3. Starch structure

The starch occurs as water-insoluble, roughly spherical granules (range diameter between 2 to 43μm, mean 25μm), which are semi-crystalline in nature (Morris, 1990; Tian *et al.*, 1991; Woolfe, 1992b).

Two structurally distinct polysaccharides can be extracted from starch, amylose and amylopectin (Figure 2-1). The amylose:amylopectin ratio is generally about 3:1 or 4:1 (Morris, 1990; Woolfe, 1992b). Amylopectin is a large, highly branched polymer of α-1,4-linked glucose chains branching through α-1,6 glucosidic links, composed of ~100,000 glucose units. Amylose is a linear polymer, which is smaller containing ~4000 glucose units. The amylose content of kumara is approximately 20% w/w (range is between 17.5-38%) (Morris, 1990; Woolfe, 1992b).

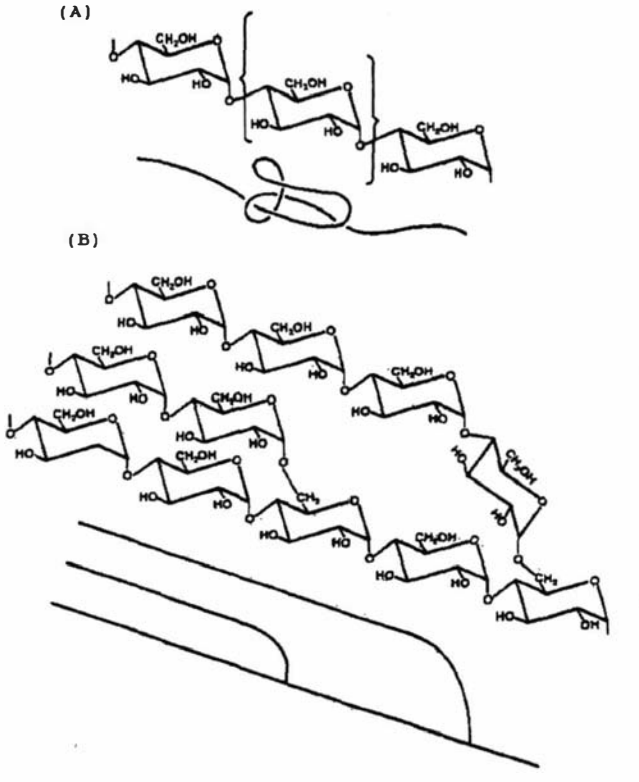

Figure 2-1 Starch molecule, (A) amylose and (B) amylopectin (Morris, 1990)

2.2.4. Other components

2.2.4.1. Enzymes

Sweet potatoes have more than forty enzymes that have been identified by different authors, each one catalysing a specific reaction (Kays, 1992).

Amylase (*α and β-amylase*) is one of the most important enzymes to consider in a processed root. These break down the starch and other complex polysaccharides, to shorter chain molecules (starch hydrolysis) (Woolfe, 1992b).

2.2.4.2. Organic acids

These constituents have an influence on the flavour, or in the taste sensation of the product. Different analyses (i.e. HPLC) show that differences in the amount of organic acids, depend on the cultivars or place of growth. Some of these acids are citric, malic, succinic, and quinic (Kays, 1992; Woolfe, 1992b). Sometimes, the concentrations of the

organic acids increase during processing but this could be partially attributable to water loss (Woolfe, 1992b).

2.2.4.3. Pigments and Vitamins

Sweet potato has three of the four primary classes of pigments, carotenoids, flavonoids and chlorophyll. However, only carotenoids and flavonoids are contained in the storage roots (Kays, 1992).

β-carotene and its close derivatives predominate in sweet potato, constituting 86 to 90% of carotenes present. Carotene is a precursor of vitamin A, and the orange and yellow colours of the roots are due to carotene present within the roots of the cultivar (Kays, 1992).

The flavonoid group contains anthocyanidins, flavones, catechins, flavonols, flavanones, and others, with colours ranging from yellows, oranges, reds, and blues to purple. These groups are water-soluble, unlike chlorophyll and carotenoids (Kays, 1992).

Kumara are also sources of ascorbic acid (vitamin C) and contain moderate amounts of thiamin (B_1), riboflavin (B_2) and others as given in Table 2-4.

Table 2-5 Vitamins present in kumara roots

Vitamin	Ranges (mg/100g)				
	(1)	(2)	(3)	(4)	(5)
Ascorbic acid	21-30	35±7	20-35	24	29-40
Niacin	0.6-0.7	0.175	0.2-0.8	0.60	
Thiamin	0.12-0.14	0.15	0.04-0.12	0.086	0.1
Riboflavin	0.05	0.0035	0.3-0.5	0.036	0.06
Carotene (Vit A)	0.035-1.68	0.076± 18	0.07->11	0.11	1-12

Adapted from (1) FAO, (1990); (2) Visser *et al.*, (1990) "New Zealand Kumara"; (3) Kays, (1992); (4) Woolfe, (1992) and (5) Onwueme *et al.*, (1994).

2.2.5. Flavour

Flavour is other important characteristic. It is a combination of odour and taste. The principal taste sensation of cooked kumara is its sweetness, due principally to the high concentration of simple carbohydrates (see Table 2-3). More than 30 volatile constituents have been identified in sweet potato, all of which contributed to the typical kumara aroma (Woolfe, 1992b). The flavours of sweet potato can be modified by post harvest practice, such as curing, increasing its quality (Purcell and Sistrunk, 1982).

Phenolic compounds have been related to a bitter flavour in cereals and vegetables, but in there is little information about the relationship between flavours and phenolics (Woolfe, 1992b).

2.3. PHYSIOLOGY

Sweet potato roots do not pass through stages of maturity, like in fruit, because it is a vegetative structure. For this reason they continue to grow larger as long as growing conditions are adequate (Purcell and Sistrunk, 1982).

2.3.1. Changes during storage

In the kumara root, there is a natural respiratory loss of dry matter during storage as well as transpiratory loss of water. Sweet potatoes stored under controlled conditions have been shown to lose water and CO_2 in such a way that the dry matter:water ratio changes little (Woolfe, 1992b).

The most important changes in sweet potato storage roots occur during the curing process. The environment, at which this process is carried out, stimulates the rapid synthesis of a periderm layer on the surface. Wounds are healed and the roots are protected from invasion by pathogens (Clark and Moyer, 1988).

2.3.2. Physiological disorders

Non-biological agents, commonly environmental factors in the field or in storage may produce many disorders with the loss of the raw materials quality.

2.3.2.1. Souring

Souring of harvested roots is caused by water-saturated soils for a prolonged period prior to harvest. Under low oxygen levels, the roots become asphyxiated, and ethanol and CO_2 is accumulated in the roots, causing high rates of decay during curing and

surviving roots undergo a significant shrinkage. Water-saturated soils also reduce carotenoid pigments, dry matter content and baking quality (Clark and Moyer, 1988).

2.3.2.2. Storage root cracking

Storage roots can crack or split in the field during the harvest or post harvest processing. The incidence of growth cracking is highly variable. It appears to result when the subcortical tissue expands more rapidly than the periderm, and may be a result of fluctuations in soil moisture, boron deficiency or excessive nitrogen. Sometimes cracking appears during digging. This occurs when the roots are dug from the warm, moist soil and exposed to too much cooled air.

Other cracking may appear during storage. Low temperatures increase these disorders but the cause of other splits, such as those close to the end of the root is unknown (Clark and Moyer, 1988).

2.3.2.3. Skinning

Skinning or surface abrasion can appear like a blemish on the periderm (Clark and Moyer, 1988). If the damage is not deep it is not important for processing (raw material-quality), because in most cases the roots have to be peeled when the process begins.

2.3.2.4. Sunscald

When the kumara roots are left exposed to the bright sunlight after they are dug, they are commonly damaged by sunscald. The colours of the skin change, turning to a purplish brown (Clark and Moyer, 1988).

2.3.2.5. Chilling and freezing injury

Kumara roots are sensitive to temperatures below 13°C during storage. Symptoms of chilling injury include an increase in the frequency of roots with decay, flavour changes, internal loss of colours and tissues that remain hard after cooking (or hardcore). Hardcore is an easily recognised disorder attributable to the cold exposure. Low temperature modifies pectic substances in the middle lamella (cell wall), so that the tissue remains rigid during cooking (Woolfe, 1992b;Clark and Moyer, 1988).

2.3.2.6. Internal Breakdown (Pithiness)

Sound storage roots that have been stored for long times, feel spongy when squeezed and may become significantly lighter in weight. When one of these is cut open, the flesh

has areas of white, spongy and dry tissue, interspersed within the normal tissues. The internal breakdown or pithiness is associated with the storage of roots in a warm, low-humidity environment for long periods (Clark and Moyer, 1988; Woolfe, 1992b).

2.4. PHYSICAL AND CHEMICAL PROPERTIES OF COOKED SWEET POTATO

Firmness is one of the important attributes determining the quality and marketability of canned sweet potato roots, and is dependent on the cultivar, geographical location of growth, cultivation practices, curing, storage and processing techniques. The softness increased with the chronological age of roots (even after a day delay between harvest and processing), and storage temperatures increases of 15 to 30°C (Woolfe, 1992b).

Truong *et al.* (1997) grouped sensory texture of cooked sweet potato into three main factors, namely moistness-firmness, particles and fibre. These attributes, including the mouthfeel (moistness, ease of swallow, chalkiness) and mechanical-type descriptors (cohesiveness, hardness, denseness, chewiness, adhesiveness), were highly correlated with shear stress of uniaxial compression, fracturability, hardness and gumminess of Texture Profile Analysis (TPA).

The colour is the other important quality attribute; to prevent the discoloration is an important objective in any process after harvest. Citric acid has been used to improve the colour of the canned product, and also combination of citric acid and calcium chloride before canning improves colour (Woolfe, 1992b).

2.4.1. Colour Changes and Browning reaction

There are many reasons for changes in colour in a fresh or in processed horticultural product. Browning reactions have been categorised as non-enzymatic or enzymatic browning.

2.4.1.1. Non enzymatic browning

In this group there are reactions such as Maillard and Strecker browning. Both impair proteinaceous nutritional value. In Maillard browning, a chemical reaction occurs between reducing sugars (mainly D-glucose) and a free amino acid or amino groups of a protein chain (lysine). The Strecker reaction is a degradation of the aminoacids to aldehydes, ammonia and carbon dioxide (BeMiller and Whistler, 1996; Damodaran, 1996).

Caramelisation is another non-enzymatic reaction. This occurs when carbohydrates (especially sucrose and reducing sugars) are heated without nitrogen-containing

compounds present. In general, thermolisis causes dehydration of the sugar molecule with introduction of double bonds and formation of anhydro rings. These double bonds absorb light and produce the colour. Caramelisation is facilitated by small amounts of acids and by some salts (BeMiller and Whistler, 1996).

2.4.1.2. Enzymatic browning

Enzymes are a group of proteins that catalyse many reactions using different substrates. There are three important enzymes responsible for the chemicals alterations of pigments in horticultural products; lipoxygenase, chlophyllase and polyphenol oxidase (Whitaker, 1996).

Lipoxidase has six important effects; bleaching of wheat and soybean flour, formation of disulphite bonds in gluten during dough formation, destruction of chlorophyll and carotenes, development of oxidative off flavours and aromas, oxidative damage to compounds like proteins and vitamins and oxidation of essential fatty acids (linoleic, linolenic and arachidonic) (Whitaker, 1996).

Chlorophyllase enzymes hydrolyse chlorophyll during storage of raw plant foods (Whitaker, 1996).

Polyphenol oxidase catalyses different reactions with a large number of phenols. One of these is the catechol forming *o*-Benzoquinone. This compound is unstable and undergoes further non-enzyme-catalysed oxidation by O_2 and polymerisation to give melanin. This is responsible for the undesirable brown discoloration in many fruits, and vegetables and deterioration of colour in juice (Whitaker, 1996).

The propensity of any given tissue to browning varies from one cultivar of a crop to another, due to variations in enzyme content, and the kinds and amounts of phenolic substrate present. Different methods are used to minimise this reaction such as, exclusion of oxygen, application of acidulants, heat inactivation of the enzyme and the use of inhibitors (sulphites) (Haard and Chism, 1996).

2.4.1.3. Post cooking darkening reaction

2.4.1.3.1. Definition

Post cooking or after cooking darkening reaction is a change in colour that in potato is expressed as a steel blue-grey colour after cooking. It is caused by the formation of an iron-chlorogenic acid complex (Mann and De Lambert, 1989).

2.4.1.3.2. Factors involved

Chlorogenic acid and isochlorogenic acid are members of a group of phenolic acids that are involved in colour formation. The majority of the phenolic compounds are formed

from quinic acid and caffeic acid (Figure 2-2). In sweet potato isochlorogenic acid is the predominant acid (Walter Jr. and Purcell, 1980; Mann and De Lambert, 1989; Ma *et al.*, 1992; Woolfe, 1992b).

Smith (1977) thoroughly reviewed after cooking darkening in potatoes. Some researchers (eg. Muneta 1959), found correlations between post cooking darkening and aqueous iron levels in potatoes. Other researchers did not find such relationships, suggesting that other factors such as citric and phosphoric acid levels complicate the extent of colour formation. Other researchers have investigated the differences in iron and darkening with position in potato tubers (eg. Wurster and Smith 1965). Generally after cooking darkening occurs the most in potato at the stem end where the iron levels are greatest. Similarly chlorogenic acid levels in potatoes are higher at the stem end, falling to lower levels towards apical end (Hughes 1958). Although there have been some correlations reported between blackening and chlorgenic acid, the best correlation was reported with the chlorogenic acid to citric acid ratio (Hughes and Swain 1962).

There are many other factors involved in the darkening process. One of these is the temperature. The discoloration occurs when the kumara roots are subject to elevated temperatures not high enough to denature enzymes but sufficient to disrupt cellular organisation and thus cause polyphenol oxidase to react with other compounds (Walter Jr. and Purcell, 1980; Mann and De Lambert, 1989).

Ma *et al.*, (1992), working with frozen sweet potato, found that the prevention of enzymatic darkening by blanching is the result of the reduction of the polyphenolic oxidase activity but not a reduction in phenol level.

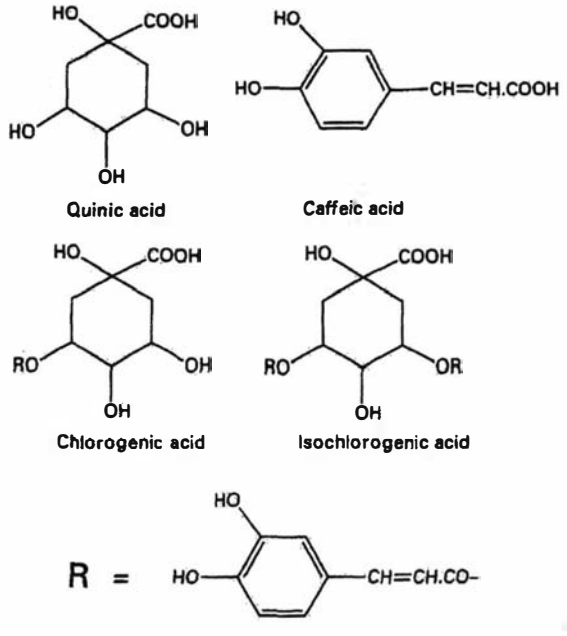

Figure 2-2 Phenolic compounds found in sweet potato (Woolfe, 1992b)

Methods to prevent darkening in potato include the use of chelating agents such as EDTA and sodium acid pyrophosphate (SAPP). It is thought that the mechanism for their effectiveness is the sequestering of iron in the tubers, thereby making it unavailable to reactor with the chlorogenic acid (Smith 1977).

Other approaches to avoid darkening are, producing cultivars with low discoloration potential, and some changes in the processing such as; additive use, pre-peeling heating, longer lye-peeling time (Walter Jr. and Purcell, 1980).

Muneta and Kaisaki (1985) also reported the formation of a complex of ascorbic acid plus ferrous iron (Fe^{2+}) which is a purple pigment similar to the after cooking darkening colour in potatoes, although the ascorbate-Fe^{2+} complex is much less stable than the chlorogenic acid-Fe^{3+} complex discussed above. In both cases the colour formation could be avoided by removal of iron from the system using sequestering agents such as SAPP, or elimination of oxygen.

2.4.2. Starch gelatinisation

2.4.2.1. Definition and kinetics

Gelatinisation occurs when the starch granules present in a hot solution are swelling. It is accompanied with a loss in order, loss of *birefringence*[1], the loss of crystallinity and the solubilisation of amylose (Morris, 1990; Woolfe, 1992b).

The kinetics of gelatinisation can be explained in Figure 2-3, where the viscosity is recorded as the sample is heated at a constant rate to the pasting temperature (95°C in this case) and then held at this temperature.

[1] Birefrigerence: different indexes of refraction for different polarisation (Sears, Zemansky and Young, 1987).

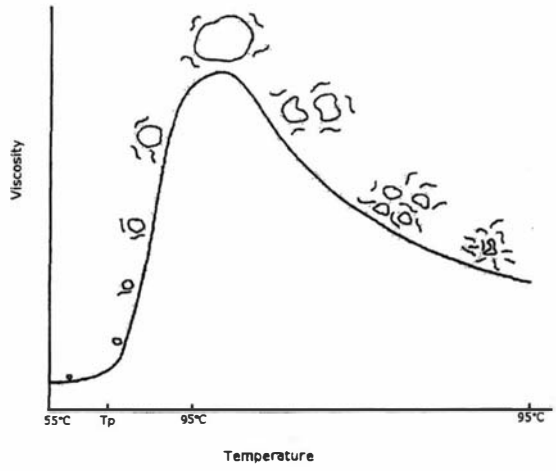

Figure 2-3 Starch molecule behaviour and viscosity changes, during gelatinisation process (Adapted from BeMiller and Whistler, 1996).

The process starts when the starch-water solution is heated to the pasting or gelatinisation temperature (Tp), after which the starch molecules swell and with this the viscosity increases, until some starch granules disintegrate as a granule suspension. At this points the viscosity decreases (BeMiller and Whistler, 1996).

2.4.2.2. Structured effects

Gelatinisation results in a fluid composed of porous, gelatinised and swollen granules with an amylopectin skeleton suspended in a hot amylose solution (Morris, 1990; Hoover, 1995). On cooling, the solution looks like a turbid viscoelastic paste or like an opaque elastic gel with high starch concentrations (>6% w/w) (Morris, 1990). Woolfe (1992b) reported that when cooled sweet potato, like cassava and cocoyam, gives a poor gel of low consistency.

2.4.2.3. Factors involved

Gelatinisation depends on the temperature, amount of water present, agitation during heating, type of starch and origin of tissue (species and cultivars) (Keetels *et al.*, 1996).

2.4.2.3.1. Temperature:

The gelatinisation of starch is an endothermic process. It is carried out when the starch suspension is heated over a characteristic temperature known as gelatinisation temperature (Tp). However an increase in temperature results in a decrease in viscosity. The temperature range over which the gelatinisation occurs depends on the starch:water ratio and granule type. The interaction between temperature and time is also important

and it has an effect on the mechanical behaviour and hence texture of the food (Orford *et al.*, 1987; Morris, 1990; Verlinden *et al.*, 1995; BeMiller and Whistler, 1996).

The temperature and/or the presence of shear, changes the rheological and structural character of the starch system (Keetels *et al.*, 1996).

2.4.2.3.2. Agitation:

Agitation or shear, during the gelatinisation process increases the extent of granule swelling and disintegration. With stirring, more starch molecules rupture and fragment causing a further decrease in viscosity (BeMiller and Whistler, 1996).

2.4.2.3.3. Concentration:

There are direct relationships between the concentration of starch and the texture of gels (Orford *et al.*, 1987). The quantity of the water is important, because heating the starch granules in excess water results in further granule swelling, additional leaching of amylose and other soluble components. The water-binding capacity of sweet potato starch gels ranges from 66.3 to 211.6% (Tian *et al.*, 1991).

Koch and Jane (2000) found no correlation between the amylose:amylopectin ratio of starch and gelatinisation time, but large starch granules required a longer time to complete the gelatinisation. Hoover (1995), said that the kinetics of aggregation, physical form and variation of the gel strength with concentration, show a dependence on amylose chain length.

2.4.2.3.4. Species or cultivars:

The starch gelatinisation depends also on the species or cultivars that the starch came from. The starch of sweet potatoes undergo more complete gelatinisation than corn starch and less than yam which are firm and increase in consistency with time. Potato and wheat starches have different behaviour. Potato starch swells more than wheat starch granules upon gelatinisation (Woolfe, 1992b; Keetels *et al.*, 1996).

2.4.2.4. Measurement of starch gelatinisation

Determination of starch gelatinisation can be measured by several methodologies. One method is measure the loss of birefringence using light microscopy (Zobel, 1984; Koch and Jane, 2000). During gelatinisation, structural changes occur in the starch granules. These changes can be followed with a scanning electron microscope (Zobel, 1984). Whistler (1984) used changes in light transmission as a basis for following gelatinisation

Starch swelling can be recorded using a Brabender Visco/amylo/graph, which records the viscosity continuously when the temperature is increased, held constant for a time, and then decreased (Zobel, 1984; BeMiller and Whistler, 1996; Navas *et al.*, 1999).

Other viscometers (*Scott Viscometer*, *Stein-Hall Cup* and *Brookfield Viscometer*. Rheometers), can also be used to follow gelatinisation of starch pastes.

Swelling power, in this case, is a measure of hydration capacity and is a measuring of granules swelling and their occluded water (Zobel, 1984). This can also be used to follow the progress of gelatinisation.

Selective digestion of the gelled starch granules by enzymes is an accurate method for measuring extents of gelatinisation. This method is especially used in the analysis of food where heterogeneity of mixture makes it difficult to detect changes in the starch (Zobel, 1984).

Gelatinisation can be described, as the melting of starch crystallites, which should be amenable to thermodynamic analysis. Investigations with DTA and DSC have shown the dependence between the temperature of melting and starch:water ratio (Zobel, 1984). Zobel (1984) also report the use of nuclear magnetic resonance (NMR) and laser light scattering for following gelatinisation in starch solutions.

2.4.3. Starch retrogradation

Retrogradation is the collective process of dissolved starch becoming less soluble, generally producing a viscoelastic, firm, rigid gel. The formation of the junction zones of a gel can be considered to be the first stage of an attempt by starch molecules to crystallise (BeMiller and Whistler, 1996).

Retrogradation depends on several variables including the molecular ratio of amylose and amylopectin. The structures of the amylose and amylopectin molecules, are determined by the botanical source of the starch, temperature, starch concentration and the presence and concentration of other substances like a surfactants and salts (Hoover, 1995; BeMiller and Whistler, 1996).

Retrogradation depends strongly on the concentration of starch. In starch water solutions the maximum crystallisation occurs in a 50-53% of starch solution (Hoover, 1995). The mechanism of starch crystallisation is instantaneous nucleation followed by growth of the crystalline regions over the temperature range -1 to 43°C. At higher storage temperatures, a more symmetrically perfect crystalline structure is formed (Hoover, 1995).

Morris (1990) described the effect of the quenching temperature *(T)* on the kinetics of the recrystallisation processes in amorphous polymers. The net rate of crystallisation, nucleation and growth will have maximum value at a temperature average between the glass transition temperature *(Tg)* and the crystal melting temperature *(Tm)* (see Figure 2-4).

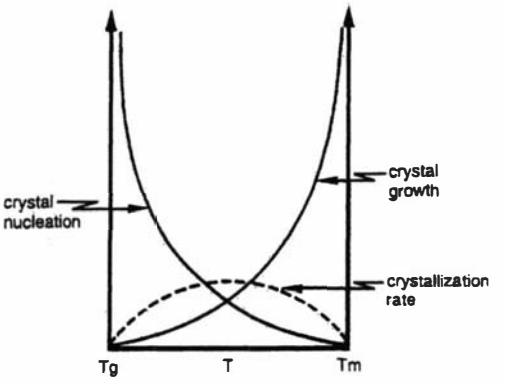

Figure 2-4 Crystallisation kinetics of partially crystalline polymers (Morris, 1990)

Lower storage temperatures, increase retrogradation rates in rice starch (Lima and Singh, 1993).

Sugars affect the melting temperature of retrograded starch. Many results suggest fructose and mannose enhance starch retrogradation while other sugars appear to retard retrogradation. Disaccharides and maltooligosaccharides are the most effective inhibitors of retrogradation (Hoover, 1995).

Lipids can also affect retrogradation. The retrogradation rate of normal and waxy starches decrease as the chain length of the lipid decreases. The rate also decreases in relation to the degree of unsaturation of the lipid and also decreases, as the proportion of monoglycerides increases. Monoglycerides are more effective than diglycerides, and those are more effective than triglycerides at inhibiting retrogradation. The reduction of the retrogradation in the presence of lipids could also correspond to a decrease in the mobility of those starch chains which are involved in double helix formation and lateral associations during recrystallisation (Hoover, 1995).

An increase in salt concentration leads to a reduction in the retrogradation rate (Hoover, 1995).

It is also possible to influence retrogradation during processing. In drum drying and pasting the amylose leaches from the starch granules to form a continuous phase when the product is cooled. In the case of extrusion, amylopectin forms the continuous phase and the product retrogrades more slowly (Oduro *et al.*, 2000)

Retrogradation behaviour can also be manipulated chemically. The introduction of acetyl, hydroxypropyl and phosphate groups into the starch molecule has been shown to interfere with the alignment of amylose chains and the outer linear chains of amylopectin during retrogradation. This enhances the freeze-thaw stability of the colloidal starch dispersion (Hoover, 1995).

2.4.4. Physical Properties of cooked sweet potato products

Szyperski *et al.*, (1986) describes the curves of the shear rate and the apparent viscosity in kumara puree, as a typical pseudoplastic behaviour.

2.4.4.1. Viscosity and gelatinisation temperature

After gelatinisation the sweet potato starch viscosity increases, because of granular swelling but also because of the effects of soluble substances which are released from the swollen granules through further heating or mechanical disruption (Tian *et al.*, 1991).

In Figure 2-5, the first peak viscosity A indicates the highest viscosity that may be encountered during the preparation of a usable paste, and B represents the viscosity at 95°C. C represents the viscosity after the starch paste has been held at 95°C for 1h, and shows the stability of the starch after cooking. D represents setback or retrogradation and shows the viscosity of the cooked paste. Finally E reflects the stability of the cooked starch after 1h at 35°C (Tian *et al.*, 1991).

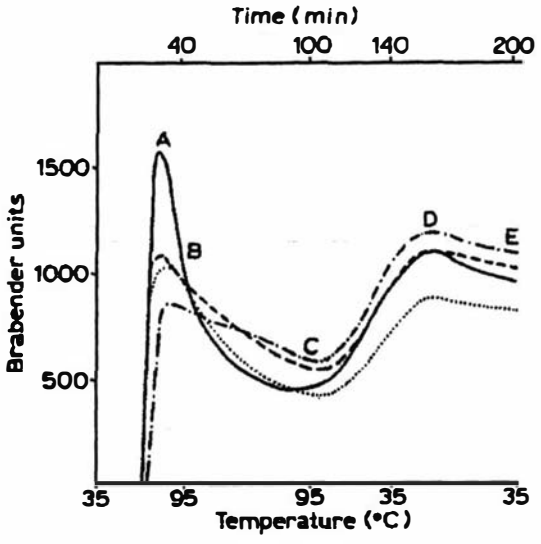

Figure 2-5 Brabender viscograms of three cultivars of sweet potato starch (Tian *et al.*, 1991)

Van Hal (2000) mentioned that most of the RVA (Rapid Visco Analyser) visco-amylograph pasting parameters of flour could not be used to indicate the pasting properties of the starch, because they were not significantly correlated. He showed that for 44 different genotypes in distilled water, there was a mean of peak viscosity (PV_{water}) of 156 RVU (Relative Viscosity Units) ranging from 40 to 309 RVU.

Collado and Corke (1996) using a DSC method, found the gelatinisation of sweet potato flour occurred between 69.9 to 92.9°C with peak temperature between 80.4 to 83.6°C. They also found significant differences in wheat and sweet potato (mixed) pasting characteristics. The highest peak and cold paste viscosity were those in which wheat had a high component in the paste, and the lowest was that of the composite containing ones of sweet potato genotypes (CL-946-25).

Navas *et al.* (1999), found that the gelatinisation temperature of sweet potato flour was between 68 to 81°C. They used a Brabender Duisgurg Amylograph to determine the viscosity. The highest viscosity (420BU [Brabender Unit]) occurred at 81°C.

Van Hal (2000), mentioned that Leonard and Schultz using a Viscograph found that sweet potato flour gelatinisation temperatures were between 74 to 78°C, and also mentioned that Iwe and Onuh found a pasting temperature of 79°C. However, Oduro *et al.* (2000), worked with seven new sweet potato varieties, using a Brabender Visco-Amylograph to determine the pasting characteristics. They showed that the lowest pasting temperature was between 72 and 73.3°C, and the peak of viscosity ranged 480BU to 600BU, being superior to that found by Navas *et al.* (1999) in sweet potato flour (Carolina cultivar).

High viscosity is desirable for industrial use, for which a high thickening power at high temperature is required. On cooling the paste to 50°C there is an increase in viscosity, indicating the tendency of starch particles to associate or retrograde (Oduro *et al.*, 2000).

Sweet potato starch properties are affected by environmental factors. Noda *et al.*(2001), analysed the impact of soil temperature on sweet potato starch, finding that the granule size (4μm), and amylose content (5%) increased as the soil temperature increased from 15 to 27°C and from 15 to 33°C respectively. Using DSC, large increases were found. Starch pasting properties measured by using a Rapid Viscoanalyzer, showed higher soil temperatures were generally associated with lower values of peak viscosity (range from 269-369RVU and 265 to 369RVU for Ayamurasaki and Sunnyred cultivars). The pasting temperatures were 65.3-82.4°C and 65.3-81.6°C for Ayamurasaki and Sunnyred cultivars respectively.

Noda *et al.* (2001), indicate that the quantitative molar distributions of amylopectin chain length analysed by HPAEC (High-performance anion-exchange chromatography) had a great impact on all the DSC parameters (T_0, T_p, ΔT). The amylose content was found to be independent.

2.4.4.2. Shear stress and textural properties

Walter *et al.* (2000) reported a high range shear stress value (8.61 to 39.28kPa) for cooked sweet potato puree. Moreover, there was a statistically significant correlation

coefficient between texture type and shear stress (r^2=0.77). In other words, there is a significant association between human perception of sensory texture by mastication force and the uniaxial compression force as measured by the TA.XT2 texture analyser.

Truong *et al.* (1997), defined the cooking time for given sweet potato cultivars was the time corresponding to the inflection point of its firmness (compressive stress at failure)-steaming time curve. They also correlated instrumental and sensory parameters of cooked sweet potato texture. Under uniaxial compression (Instron Testing Machine/500Ncell/plunger 5.7cm diameter compression plate), the results for compressive strain and stress at failure for raw material were ranged from 0.20 to 0.42 and from 822 to 1419.5kPa, and for cooked kumara samples, were 0.18-0.25 and 7.35-37.69kPa respectively. A strong inverse association between stress values and moistness or mealiness of the cooked samples was noted.

Texture profile analysis (TPA) showed fracturability of cooked sweet potatoes was 2.30-11.28N, hardness 2.92-11.92N, adhesiveness 0.13-0.59N, cohesiveness 0.04-0.08, springiness 0.08-0.20, and gumminess 0.11-0.94N (Truong *et al.*, 1997). Rao *et al.* (1975) showed that yield stress (using a rotational viscometer) is significantly correlated to the taste panel evaluation of mouthfeel for sweet potato puree.

Rao and Graham (1982) worked with Red Jewel and Centennial cultivars and using a rotational viscometer (Brookfield Rheology HBT), they found that although the parameters yield stress (8.95-16.82N/m^2) and flow behaviour index (n) (0.3782-0.5339) exhibited significant differences between cultivars, the coefficient of shear rate (k) did not (1.76-11.18). They found also, that the rheological parameters change with the storage time of puree. Increases in k value and n occurred with increased storage time. The yield stress variations depended on each cultivar.

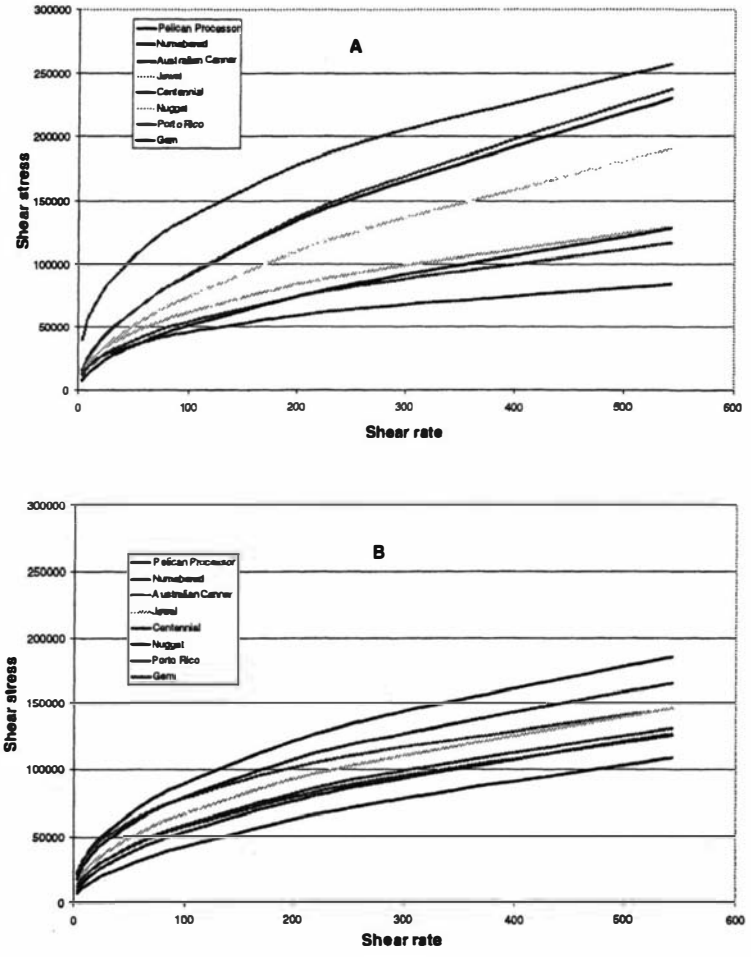

Figure 2-6 Flow curves of kumara cultivars tested after 5 (A) and 61 (B) days of storage (Rao and Graham, 1982)

Figure 2-6 shows the differences of the shear stress versus shear rate curves, for different cultivars, decreased with storage time for sweet potato puree (Rao and Graham, 1982).

2.5. PROCESSING OF THE SWEET POTATO

2.5.1. Overview of processing of sweet potato

The sweet potato has been a traditional staple food in developed countries, but in the last few years much effort has been done in order to change the status of these roots from a subsistence to a commercial commodity (van Den, 1992; Woolfe, 1992a).

Woolfe (1992a), described the main features of kumara as nutritional value and sensorial versatility.

Kumara has been processed or cooked[2] in different ways such as flours, flakes, dry, chips, starch productions, and as ingredient in noodles (see Table 2-6) (FAO, 1990; van Den, 1992; Woolfe, 1992b; Woolfe, 1992a; Sloss, 1994).

Table 2-6 Characteristics of sweet potato products

Product	Use
Fried chips/strips	Snack food
Dried chips/strips	Food preparations
Dried cubes	Food preparations
Dehydrated flakes	Breakfast food & food preparations
Flour	Baked products & food preparations
Starch	Food (noodles, backed products, food preparations, etc.)
	Industrial products (glucose syrup, alcohol, medicines, chemicals, textiles, etc.)
Canned/bottled products	Food preparations & baby food
Frozen products	Food preparations
Fermented products	Alcoholic drinks & fuel alcohol
Special products (candies, cracker, pies, paste, roasted, etc.)	Snack food, food preparations & ice cream

Adapted from Van Den, 1992.

2.5.2. Processing and nutritional value

Cooking produces an improvement in digestibility, increases the availability of nutrients, promotes the palatability and keeps quality and makes the product safer to eat (microbiologically clean) (Bradbury and Holloway, 1988; FAO, 1990).

The nutrients may be lost during cooking, in two ways: *Chemical change*, such as degradation, hydrolysis, oxidation, denaturation, i.e. vitamin, free amino acids, starch and protein, and *leaching* in to the cooking medium (i.e. vitamin, minerals, amino acids) (FAO, 1990).

Bradbury and Holloway (1988) worked with sweet potato and described the nutritional changes produced by three different thermal treatments, boiled (boiled water for 20 min), steamed (for 25 min) and baked products (oven at 200°C for 30 min). The results showed that dietary value increased because there was a high reduction in starch

[2] Cooking exposes the food to heat in a dry form or in a wet form (Bradbury and Holloway, 1988).

content, and maltose and sucrose levels increased after cooking. Dry baking reduced the moisture content (7-9%), but in the other two treatments these factors increased (1-4%). Finally in every case, the ash content was reduced significantly.

2.5.3. Unit operations for puree

Woolfe (1992b), described the unit operations involved in, "pre-processing" (Figure 2-7) and "pureeing processes" (Figure 2-8).

The pre-heating process (Figure 2-7) has as main advantage of the reduction of enzyme discoloration (phenolic oxidation) and the reduction of peeling time (Woolfe, 1992b).

Peeling is one important step in the process, its objective basically to remove the skin. However reduction in nutritional value and less browning can be other consequences. The effect in browning is because the phenolics (chlorogenic and isochlorogenic acids) are located in tissue directly below the periderm. 78% of phenolics were found to be concentrated in the outer 5-6mm of tissue which includes the periderm (Woolfe, 1992b). Peeling is an important factor in nutrient losses (carbohydrates, vitamins), in some instance in tubers the losses may run high as 25 to 30% (Harrington and Shaw, 1967).

The root or tuber can be peeled by chemical solution, heat or abrasion action.

Chemical solution; combines the effect of chemical attack and thermal shock. Different solutions (lye solution) can be used in this methodology. The most common approach is to use a hot sodium hydroxide solution (104°C), in different concentrations and times, depending on the type of the sweet potato root (5-6 min in 20% lye solution for cured kumara or 3-6 min in 10% for fresh sweet potato) (Woolfe, 1992b, Harrington and Shaw, 1967). The time is important because it has an effect on the amount of tissue removed, the gelatinisation of the starch present in the surface tissue and on cell wall detachment (Figure 2-9) (Walter Jr. and Schadel, 1982).

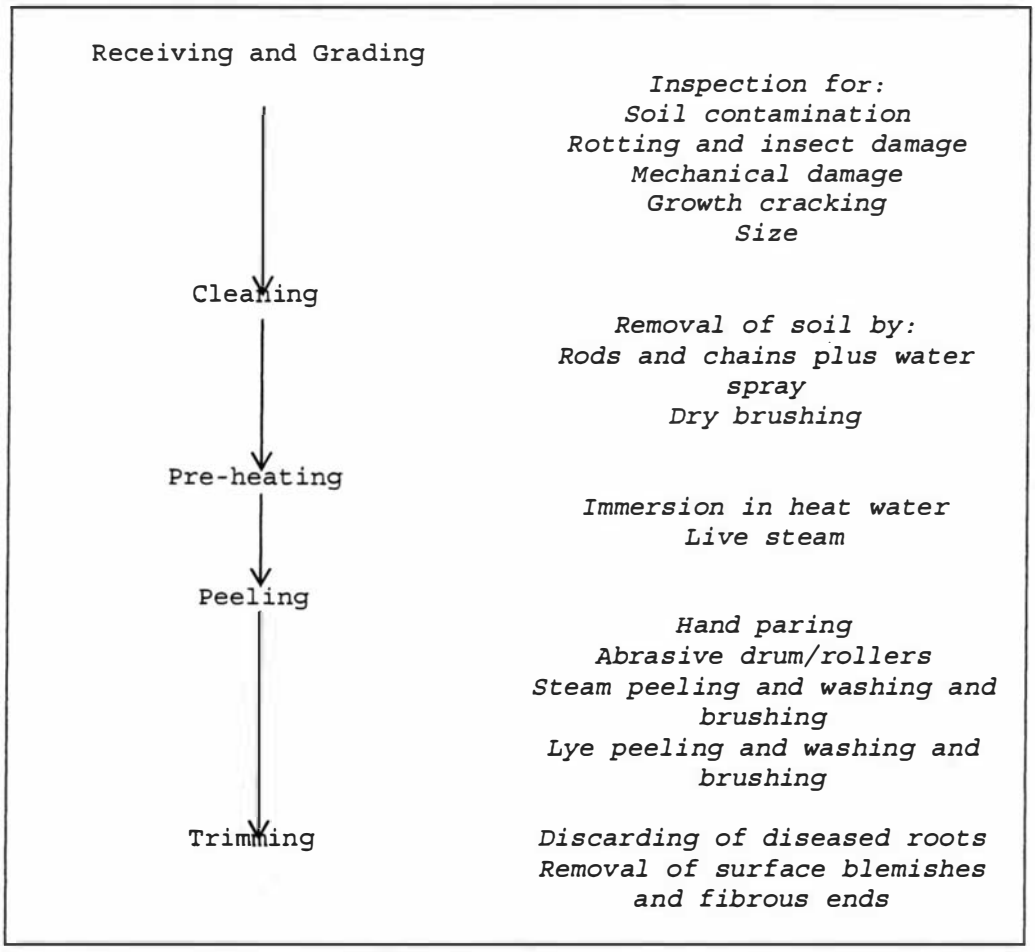

Figure 2-7 Pre-processing procedures (Woolfe, 1992b)

The discoloration after lye peeling in kumara occurs in the cambium area that is a PPO-DP (poliphenoloxidase - *o*-dihydroxyphenols) reaction induced by heat peeling. The heat induces breakdown of the lacticifers (Figure 2-10). These lacticifer compartments are disrupted the PPO and DP interact. The problems occur when the thermal treatment disrupts the lacticifers but it is not enough to inactivate the PPO present (Walter Jr. and Schadel, 1982)

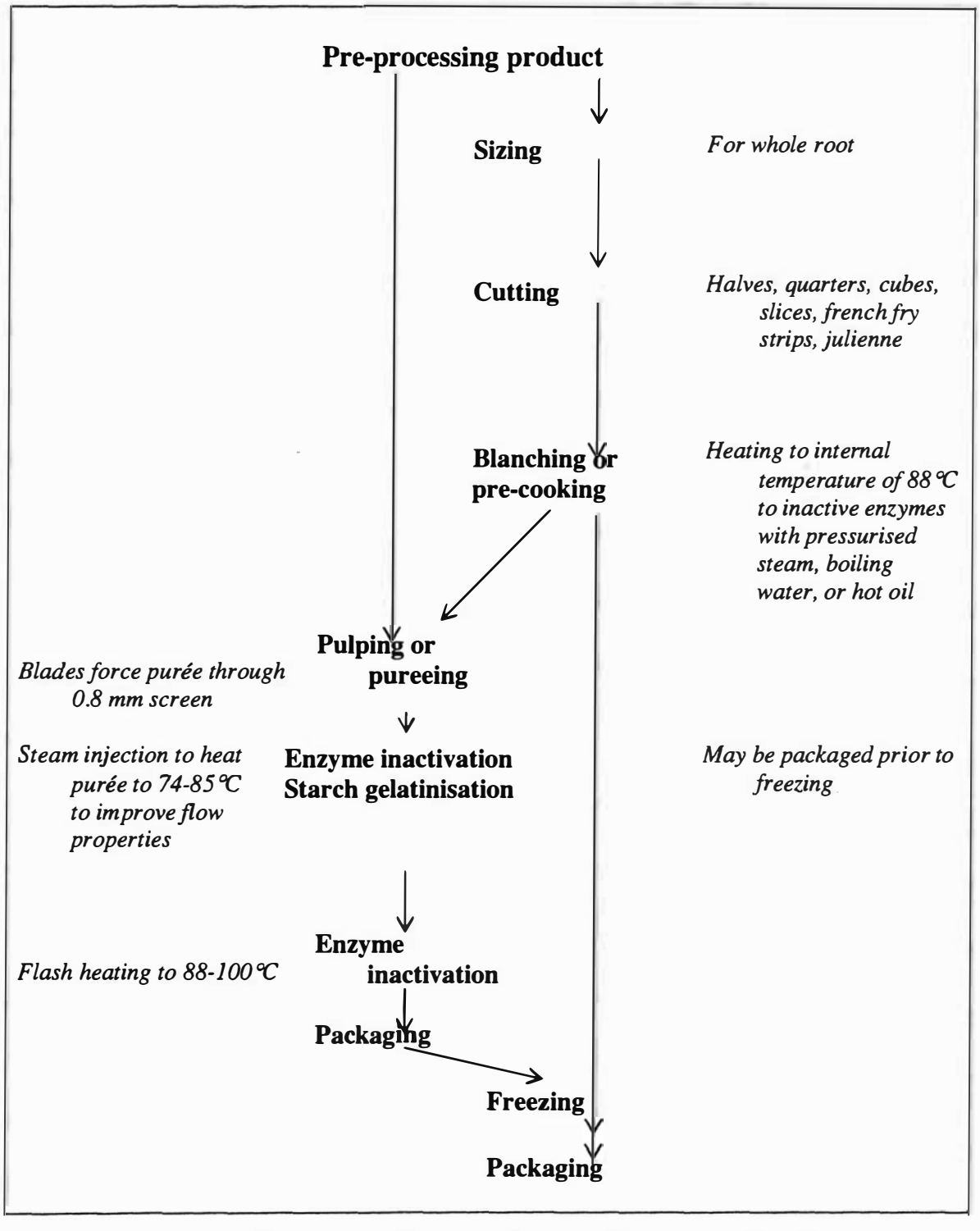

Figure 2-8 Pureeing and freezing processes (Woolfe, 1992b)

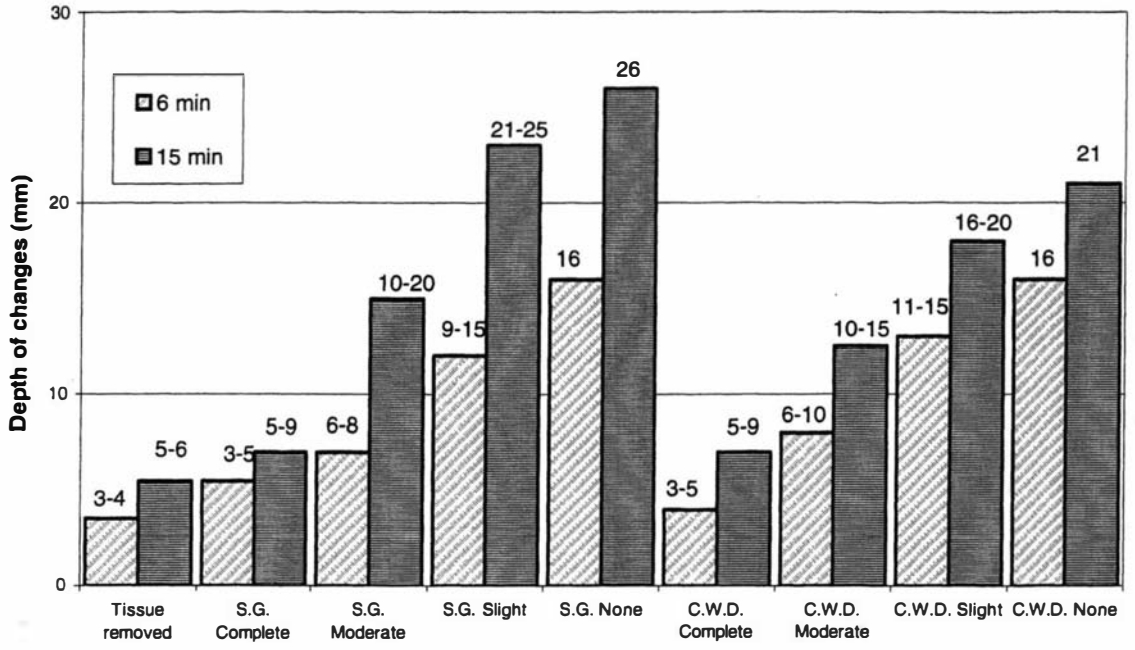

Figure 2-9 Effect of the lye peeling in kumara superficial tissue (Adapted from Walter and Schadel, 1982).

S.G.; starch gelatinisation: C.W.D.; cell wall detachment

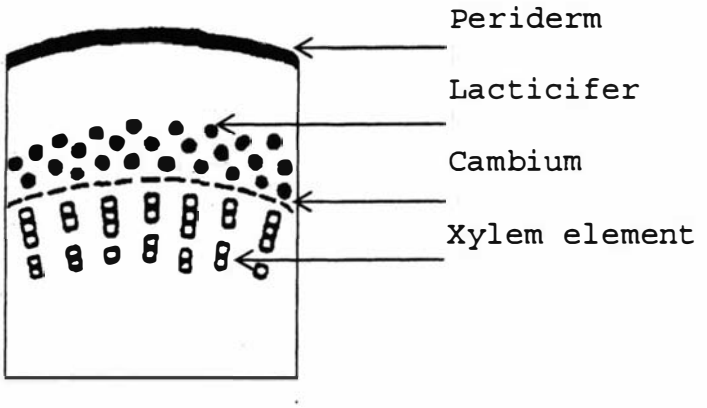

Figure 2-10 Kumara Transverse sections with relative locations of tissues and cell types (Walter Jr. and Schadel, 1982)

Super heated steam; in this methodology super-heated steam has been used followed by flash cooling by direct injection of cold water into the peeler chamber (Woolfe, 1992b).

Mechanical abrasion; the peelers, can be by batch or continuous system. Batch-type peelers usually consist of vertical cylindrical containers for holding the potatoes, with a rotating disk forming the bottom. Turning of the disk rotates the potatoes so that they contact the abrasive surfaces, which may be on the disk or the sides or on both. Continuous abrasion peelers vary in design, but they have the same elements found in the simple design of the batch-type peeler. Round product are much more suitable for abrasive peeling than the long types, non uniformity in size has been observed to cause uneven peeling with most abrasive peelers. Losses are greater for small than for large potatoes (Harrington and Shaw, 1967).

Washing is necessary after peeling to clean the surface of waste materials like chemicals (lye solution) or other compounds (Woolfe, 1992b).

Trimming to remove surface imperfections, due to mechanical damage, disease or insects and the fibrous end then follows (Woolfe, 1992b).

The kumara mash process can be done by a combination of mechanical operation, temperature treatment and use of enzymes. Size reduction (cutting) is done to reduce the thermal time but it is also important in gelatinisation uniformity of the root slice. Verlinden *et al.* (1995), used a model to estimate the starch gelatinisation in a potatoes slice (width=5mm and ratio=10mm) during cooking. They found differences of 10°C in temperature, and more than 60% of the fraction ungelatinised, starch occurred between the centre and the surface of the slice, after 45s of cooking in water at 82°C.

Few studies have been reported to study the temperature profile in whole sweet potato or sliced roots during cooking. Wadsworth and Spadaro (1970) developed a mathematical model (finite difference methods) to study the temperature distribution in whole kumara roots during immersion heating. The results showed that in roots with 2.54cm (1in.) diameter, the centre of root had the same temperature as the water, within 15 min. A greater than 7.62cm diameter, the centre of the root took more than 60 min for centre to be heated.

Hagenimana *et al.* (1994) state that the pH optimum ranged between 5.8-6.4 and 5.3-5.8, and optimum temperature was 71.5 and 53.0°C for α- and β- amylase respectively. They found that α-amylase was heat labile in the absence of Ca^{+2}. Calcium is required for the activity and thermal stability of α-amylase. β-amylase activity was affected by heat , and was not dependent on any metal for activation.

2.6. CONCLUSIONS

The composition of kumara roots is highly variable between cultivars. Many works have also demonstrated that the different agricultural practices such as fertilisation, growing location, and irrigation have an influence on the roots. The curing processes doing in post harvest treatment and storage conditions also have influence in the physic-chemical characteristics of kumara root.

Many authors have studied the chemical composition of sweet potato, describing starch as the main constituent with, protein, enzymes and other components. Different research has been done studying chemical reactions such as starch gelatinisation and retrogradation, and changes in colours in these materials.

Many works were reported for the physical and pasting properties of sweet potato flour, however few reports are available those explain how the raw kumara characteristics influence the physic-chemical characteristics of cooked or pureed products.

Kumara colour is likely to behave in a similar way to potatoes. Mechanical peeling will promote enzymatic browning due to the action of polyphenol oxidase. This reaction can be avoided by steam peeling which would denature the enzyme. Of more importance to kumara colour is post cooking darkening. This is believed to be due to an iron-phenol complex that forms on cooking. This will be the focus of the next chapter.

CHAPTER 3: THE MECHANISM OF POST COOKING DARKENING IN KUMARA

3.1. INTRODUCTION

Colour is one of the most important quality characteristics of the processed kumara. A good colour is clear, bright and even shiny, while product with a bad colour is dark (ranging from blue black to brown) and opaque. One of the most significant problems in the manufacturing of the processed kumara products is post-cooking discoloration or darkening. To identify solutions to this problem, it is necessary to understand the reaction mechanism and what compositional or processing factors promote or reduce discoloration. Once the reaction mechanism is understood, optimisation of kumara processing can be carried out.

There are two reaction mechanisms described in the literature for discoloration of fruit and vegetable. The first is enzymatic browning, which can occur after peeling. Polyphenolic compounds in sweet potato are located in specific cells between the periderm and xylem called the lacticifer. When these cells are disrupted (e.g. by mechanical or chemical peeling), the phenols are oxidised by the action of polyphenoloxidase (PPO) enzyme in the presence of oxygen. This reaction produces quinones that combine with the free amino acids to form a coloured molecule (Walter Jr. and Purcell, 1980; Walter Jr. and Schadel, 1982; Woolfe, 1992).

In plants, PPO is principally located in chloroplast thylakoid membranes, and from several fruit and vegetables plants the enzyme shows maximum activity in the temperature range of 20 and 35°C (Lamikanra, 2002). PPO can be inactivated by moderate thermal treatment (at temperature higher than 40°C), and therefore is not likely to be the cause of post-cooking darkening.

The second discoloration reaction mechanism is summarised in Figure 3-1, and involves formation of a coloured iron-phenolic complex (Mann and De Lambert, 1989). Three

steps are proposed for the discoloration of other vegetables and fruits (Woolfe, 1992b; Lattanzio *et al.*, 1994). In the first step, cell modification occurs promoted by mechanical, chemical or thermal factors. This modification releases iron and phenolic compounds (chlorogenic acid [CA] and isochlorogenic acid [ICA]) into the system, and these combine to form a colourless complex (second step). In the final step, iron is oxidised from Fe^{2+} to Fe^{3+} in the presence of oxygen, resulting in a blue/black coloured complex.

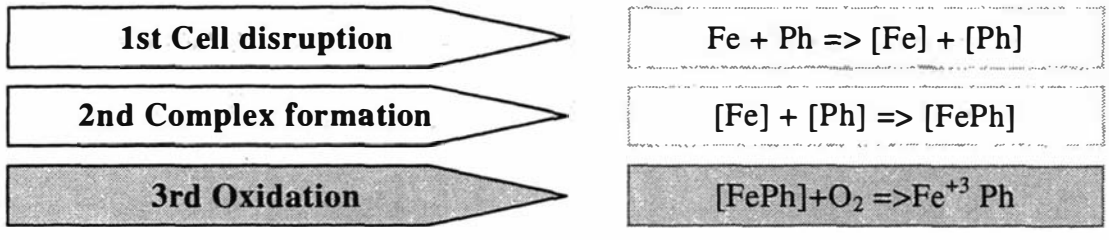

Figure 3-1 Proposed discoloration reaction mechanism for kumara

The objective of the present work is to confirm that the darkening reaction in cooked kumara is consistent with this mechanism.

3.2. EXPERIMENTAL METHODOLOGY

3.2.1. Total Iron

Gold kumara samples from eleven locations were analysed. Two slices from the centre of each root were taken, one for the total iron determination and the other for the total phenol and chlorogenic acid (CA) determination.

The methodology for determination of total iron in the kumara samples was carried out according to the AOAC official method 975.03 (Cunniff, 1996).

A 1g sample (dried) was taken and placed in into glazed, high-form porcelain crucibles. The samples were ashed for 2h at 500°C, and cooled. The ash samples were moistened with 10 drops of deionized water and 3-4mL of HNO_3 (50%) was added. The excess HNO_3 was evaporated on a hot plate set at 100-120°C. The samples were returned to the crucible ashed for an additional 1h at 500°C and cooled. The ashed samples were then dissolved in 10mL HCl (50%) and transferred quantitatively to a 50mL volumetric flask. The volume was made up to 50mL with deionised water.

The determinations were carried out using an Atomic Absorption Spectrophotometer, model GBC 933AA. An iron standard was used to make a calibration curve over the range 0, 2, 4, 6, 8 and, 10ppm.

3.2.2. Total phenol and CA

To measure total phenols and CA in kumara, 250mg of dry samples were taken and 15mL of ethanol (EtOH) was added. The samples were sonicated for 30 seconds, three times, and then water was added to make up 100mL (stock solution).

For total phenol analysis Folin-Ciocalteu reagent was used. A phenol stock solution was made, by taking 0.500g of dry gallic acid in a 15% ethanol/water solution, then made up to 100mL in a volumetric flask.

1mL from the stock solution was placed into each replicate 100mL volumetric flasks and 60mL water was added and mixed. Finally, 5mL of Folin-Ciocaleu reagent was added and mixed well. After 30 seconds and before 8 minutes, 15mL of 20% sodium carbonate solution was added. It was mixed and brought to required volume with water. The solutions were allowed to stand for 2h at room temperature (20°C) and the absorbance at 760nm was measured against the blank. The absorbance was taken using a Hitachi U-2000 spectrophotometer.

To determine a calibration curve for phenol, the same procedure was followed using 1, 2, 3, 5, and 10mL aliquots of gallic acid standard solution in place of the kumara samples. This gave total phenol levels of 0, 50, 150, 250, and 500mg/L.

CA levels were determined from the same stock solution used to determined total phenol by measurement of absorbance at 325nm using the method of Lugasi *et al.*,

(1999). This was then compared to a standard curve calculated by using pure CA (Merk, 98%) dissolved in a 15% ethanol water solution.

3.2.3. Raw material and preparation of samples

The raw material was provided by Delta Produce Ltd. Two kumara cultivars were used in this research, Toka Toka Gold and Owairaka Red. Samples were cleaned and peeled manually in order to avoid any effects of chemical or thermal modification of cellular material. Immediately after peeling, the roots were placed in water at room temperature to exclude oxygen from promoting oxidative reactions. Additives were added to this water in some cases, depending on the treatment. Samples were cut into slices of 1cm thickness before cooking treatment.

3.2.4. Cooked parameters and packaging characteristics

The samples were vacuum packed into either metallised or transparent bags, and then cooked either at 121°C for 20 minutes in a steam retort or in a controlled temperature water bath at 15 to 85°C for 30 minutes. After cooking, the samples were cooled quickly by immersion in cool water (15°C). The transparent bags (PD-961) were composed of three layers: 12μm polyester, 25μm nylon and 100μm cast polypropilene. The non transparent metallised bags composed four layers; 12μm polyester, 9μm aluminium foil, 25μm nylon and 100μm cast polypropylene.

3.3. COLOUR DETERMINATION IN KUMARA

A reliable colour measurement method was required. The most common method used in whole vegetables is colorimetry, which characterise the colour in three parameters or coordinates *L*, *a*, and *b*.

3.3.1. Colour measurement; instrument and colour parameter

A Minolta colorimeter (model L-200) was used to measure the colour. The instrument was calibrated against a white blank tile (*x=0.3140, y=0.3212, Y=93.80*). *L, a*, and *b* values were recorded, and the colour difference (ΔE) was calculated using Equation 3-1, where *x*, *y* and *Y* represent of coordinate of the CAE chromaticity scale and a, b, L correspond of Hunter values.

The standard colour was taken as the colour immediately after the samples were exposed to the air (time=0), and the sample colour measurements were taken 20 or more minutes after the bags cooking the samples were opened. In this way, a steady state of colour was achieved.

$$\Delta E = \sqrt{(a_{sample} - a_{standard})^2 + (b_{sample} - b_{standard})^2 + (L_{sample} - L_{standard})^2} \qquad \textit{Equation 3-1}$$

Where;

a: colour value to measure the red-blue range
b: colour value to measure the yellow-green range
L: colour parameter to measure the white-black range

3.3.2. Colour measurement position

To obtain reliable experimental measurements of colour change, the natural variability of the raw material must be considered. For this reason two preliminary experiments were carried out to assess the variability of kumara colour with position in a kumara slice. Five points on the slice surface were selected (see insert of Figure 3-2): Point 1 was located at the centre, and the others on the external part of the slice (slice edge). Three replicate measurements were taken at each location. One slice was selected to represent good colour, one poor colour and another of intermediate colour quality.

The results are shown in Figure 3-2 and clearly demonstrate that the colorimeter could adequately separate the samples into three groups. If was latter shown that the rate of colour development can take up to 50 minutes (see section 4.6). For this reason it is likely that the standard deviation measured in this experiment could have been reduced of samples were left longer before colour measurement. Despite this factor it is clear that the colorimeter was accurate enough to use in future experiments. As expected, the

good colour slices showed less ΔE than the bad and intermediate colour slices. However, it can be seen that there are significant differences in colour between measurements taken at different locations across the slice. For this reason it was important in future experiments that measurements were made at a consistent location.

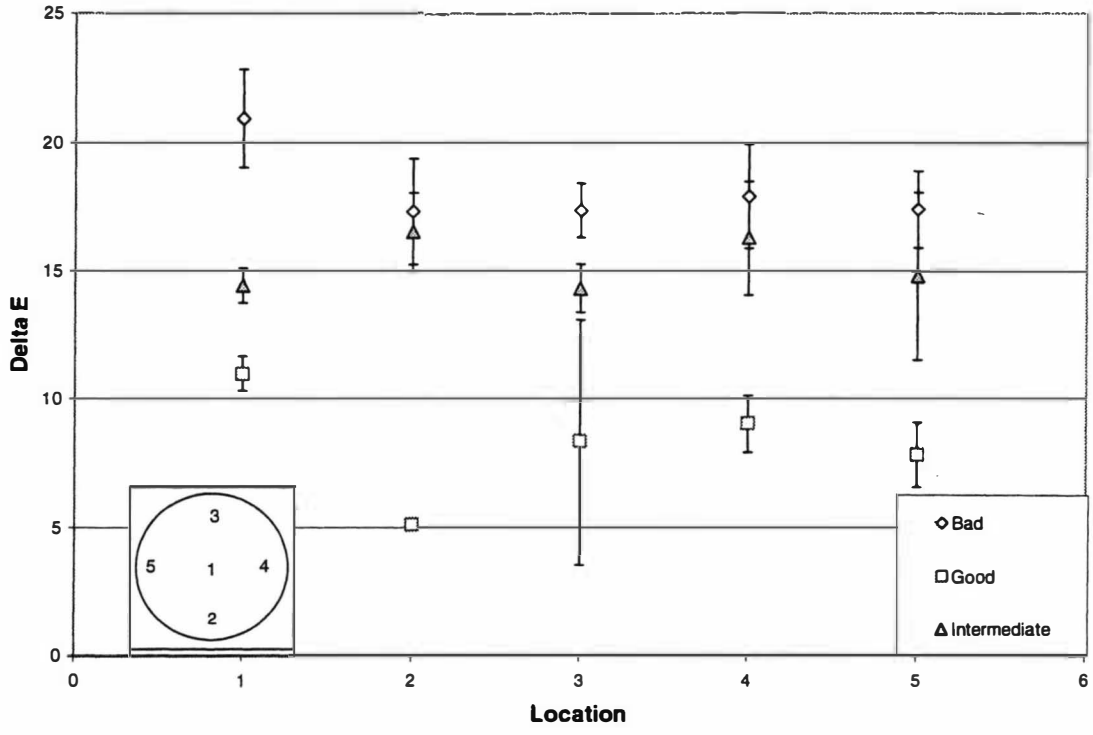

Figure 3-2 Colour variation (ΔE) on the kumara slice surface. The insert on the left side of the figure shows the position on the roots slice at which colour was measured (see raw data Appendix A3).

3.3.3. Colour variation between roots

Kumara roots exhibit a large variation in chemical composition and physical characteristics. These differences are due to a number of factors including variety, soil type, fertilisation, irrigation, post harvest management, curing process, etc. (Purcell and Sistrunk, 1982; Mayhew and Penny, 1988; Huaman, 1991; Kays, 1992; Onwueme and Charles, 1994; Decoteau, 2000). As a consequence it was likely that colour changes would vary markedly in samples obtained from different roots. To investigate this effect, twelve replicates of Toka Toka Gold kumara and eight of Owairaka Red kumara samples were prepared and analysed as described above. In both cultivars, large variations at ΔE were observed between roots (Figure 3-3).

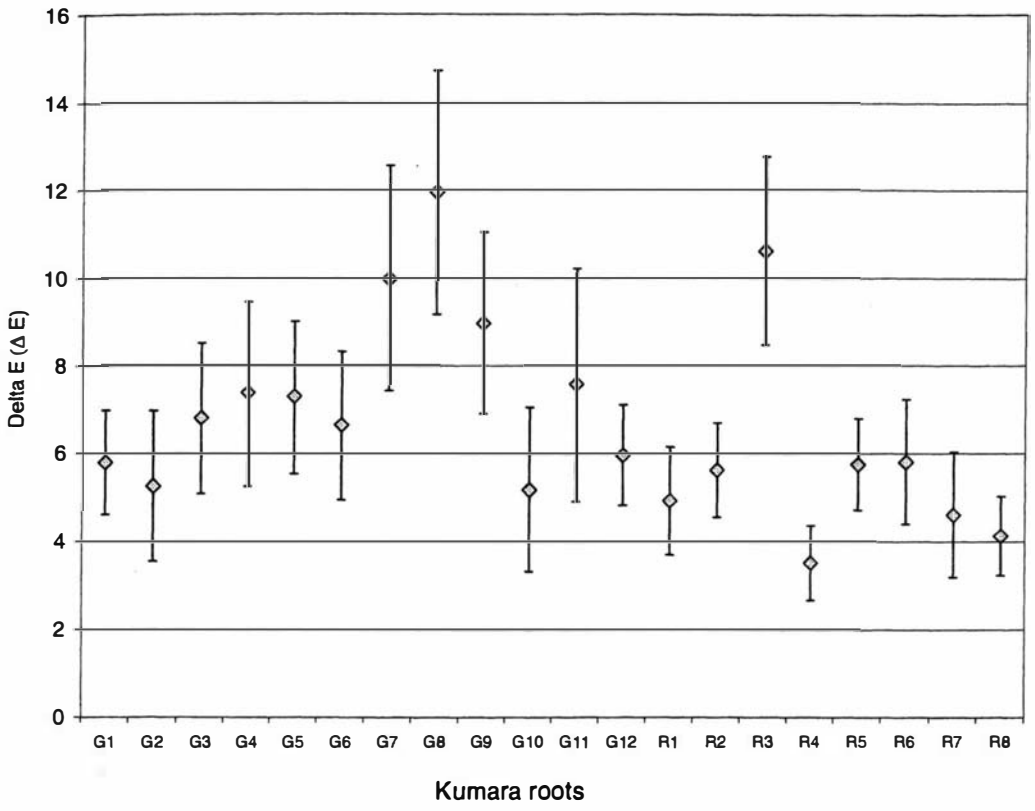

Figure 3-3 Colour variation (ΔE) between different cooked kumara root slices of Toka Toka Gold (G) and Owairaka Red (R) (see raw data Appendix A3).

In order to avoid the effect of between batch differences, subsequent experiments were performed using a blocked design. Replicate roots were selected and slices from each root were subjected to different cooking or storage treatments. In this way the root to root variation could be removed from the resulting data by statistically using the SAS (version 8.02) software package.

3.4. COMPARISON OF COMPOSITION WITH COLOUR CHANGE IN KUMARA

The aim of this experiment was to determine if any correlation exists between the levels of the components identified as contributing to the proposed colour change mechanism; iron, phenols and CA. 10 gold roots were selected, prepared, and cooked as described in 3.2 above. The colour change (ΔE) was determined as well as total phenol and CA levels in each sample.

3.4.1. Total iron and phenolic levels in gold kumara

Table 3-1 shows the total iron and phenol concentrations (mg/L), of cooked kumara slices from ten different growing locations, along with colour change after cooking and chlorogenic acid levels for the selected samples.

Table 3-1 Total phenol and total iron composition in cooked Toka Toka Gold kumara from ten different places.

	Analysis									
Identification	**Moisture** *%*		**Total phenol** *mg/100gfwb*		**Iron** *mg/100gfwb*		**ΔE**		**CA** *mg/100 g*	**CA/Ph**
(Place)	Mean	S.E	Mean	S.E	Mean	S.E.	Mean	S.E		*
Ga	70.48	1.56	16.75	8.46	1.36	0.27	8.81	0.30	1.04	0.036
Gb	73.88	1.45	11.81	3.86	1.66	0.27	8.92	0.70	1.34	0.132
Gc	71.24	0.90	34.04	3.64	2.12	0.86	11.08	1.08		
Gd	72.38	0.77	23.89	2.84	1.79	0.66	8.35	0.34		
Ge	71.37	1.03	15.23	2.71	2.26	0.35	9.05	0.20	1.81	0.140
Gf	67.55	0.92	22.80	7.57	1.93	0.28	11.97	0.37		
Gg	69.70	1.05	14.02	4.61	2.12	0.79	8.56	0.49		
Gh	71.61	1.37	16.38	5.00	1.49	0.20	6.80	0.95	1.40	0.036
Gi	72.23	0.75	19.69	5.96	1.68	0.26	8.48	0.80	1.49	0.078
Gj	73.45	1.50	21.29	1.60	1.84	0.43	7.86	0.54		
Average	*71.39*	*1.13*	*19.59*	*4.63*	*1.82*	*0.44*	*8.99*	0.58	*1.41*	

(*) Note that the ratios CA/Ph were obtained for some samples, the means of iron and total phenol were not considered.

The average of the total phenol composition was 19.59mg/100g f.w.b.. This is higher than those reported by Lugasi *et al.* (1999), who worked with potato tubers. They

reported values of 15.5mg/100g f.w.b. and 17.3mg/100g f.w.b. for Agria and Kennebec cultivars. Walter Jr. *et al.*, (1979), found similar phenolic content on sweet potatoes (cv. Jewel 18.51mg/100g f.w.b, and c.v. Julian 22.38mg/100g f.w.b).

Chlorogenic acid levels in the kumara samples ranged from 3.9 to 7.1mg/100gd.w.b.. This corresponded to 3.6 to 14.4% of the level of total phenols. Griffiths *et al.*, (1992) determined the CA and phenol content of 12 potato samples of freeze-dried powders. Their results CA/total phenol percentage were 14.1% to 20.21%, much higher than the data obtained in this experiment. In data reported by Walter Jr. *et al.* (1979), the relationship within sweet potato cultivars was higher than observed in kumara in this work (39.6 to 55.9%).

The similarity of results achieved in this study compared with the literature for similar products suggest the phenol and CA values are sensible.

The average total iron content was 1.82mg/100g f.w.b, which was lower that the content reported by Olaofe (1988), 14 mg/100fwb, but higher than the data given by van Den (1992), 0.8 mg/100fwb, and other authors (see Table 2-4).

It is clear from the data that there is a no clear correlation between the colour change observed after cooking and the levels of total iron or phenol in kumara. Hughes and Swain (1962) also observed no correlation between iron levels and post cooking darkening in potato despite the effectiveness of sodium acid pyrophosphate (SAPP), which acts to chelate the iron, by eliminating the colour change in potato. A possible explanation of this is that the colour change is dependent only on free iron, but this is not differentiated from bound iron in the system by measurement methods.

There was also no trend in the data demonstrating a dependency of ΔE on the chlorogenic acids levels in kumara.

Hughes and Swain (1962) observed a complicated relationship between CA/citric acid ratio and darkening, except that the relationship varied with position in potato.

To confirm these results an additional experiment was carried out in which CA and total phenolic levels in gold kumara roots were compared with colour change after cooking.

These results are shown in table 3-2 below, however no relationship between colour development was observed for these compositional measurements either.

Table 3-2 Comparison between total phenols (TPh), chlorogenic acid (CA) composition against colour change (ΔE) after cooking Toka Toka Gold kumara

Samples	ΔE	Moisture %	Total Phenol mg/100gfwb	CA
Ga	9.67	67.60	16.656	1.67
Gb	12.44	70.93	19.914	1.99
Gc	11.87	70.77	20.276	2.03
Gd	11.34	73.54	19.552	1.96
Ge	6.35	68.05	21.001	2.10
Gf	7.96	67.25	22.811	2.28
Gg	10.08	71.43	19.552	1.96
Gh	9.44	71.45	21.363	2.14
Gi	12.97	72.85	23.897	2.39
Gj	10.59	69.51	12.673	1.27
Average	*10.59*	*69.51*	*19.77*	*1.98*

The results of these experiments would seem to invalidate the proposed mechanism. Due to uncertainty though as to the levels of free iron and as to which phenolic compounds in addition to CA could be involved in the colour formation reaction, further experiments were carried out to test the mechanism.

3.5. THE EFFECT OF COOKING TEMPERATURE ON DISCOLORATION

In the first step of the discoloration mechanism, it is hypothesised that the cells are disrupted causing release of the iron and/or phenolic compounds that participate in dark colour formation and that modification can be promoted by mechanical, chemical or thermal factors. High temperature conditions are encountered in a number of unit operations used in vegetables or fruit processing (e.g. peeling, blanching, cooking, etc) and are focus of this work.

The objective of this experiment was to quantify the effect of temperature on the cell modification, and the formation of dark colour in the product.

Samples of Toka Toka Gold kumara were prepared as described above. No additives were used to ensure nothing other then cell modification altered the extent of the discoloration reaction. Seven water baths were used to cook the samples at a range of different temperatures between 15 to 85°C, for 30 minutes. The numbers of replicates at each temperature ranged from six to twelve. After cooking, the samples were cooled by immersion in cool water (15°C) and then exposed to the air for 30 minutes before taking measurements. This was done to ensure the oxidation step of the reaction mechanism did not limit the extent of reaction. *L* value, was used to quantify the discoloration reaction. Previous experiments have demonstrated that colour changes were due at *L* and *b* values changes, both values had the same importance.

Figure 3-4 shows the results of the *L* value measured in the kumara cooked at different temperatures. The extent of discoloration increased (as show by reduced *L*) when the temperature was increased over 53°C.

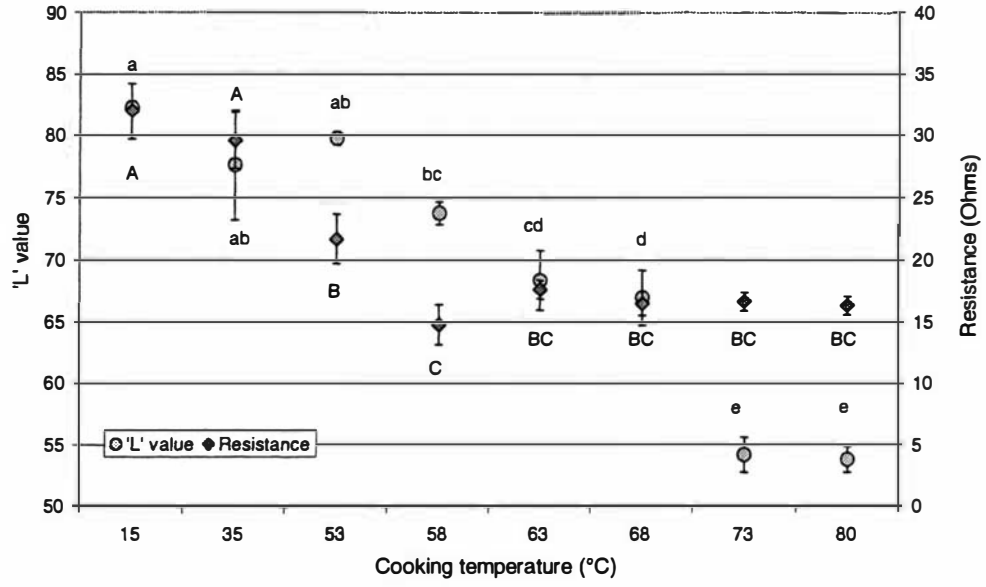

Figure 3-4 Cooking temperature effect on discoloration (L) and electrical resistance of cooked Toka Toka Gold kumara slices (see raw data Appendix A3).

(*) Different letters (capitol for resistance, and lower case for L value) show statistical differences, according to t-test (P≤0.05).

To confirm that the discoloration increase above 53°C was due to cell modification the electrical resistance of the slices was also measured. A multimeter Hung Chang (HC-5050E) was used to determine the electrical resistance (Ohms). The electrodes were separated by 2cm, and each sample was inserted into the fresh kumara to a depth of 0.5cm.

The results are shown in Figure 3-4 and demonstrate that cell modification is starts between 35 and 53°C. Cell modification releases solutes into the free water present in the kumara flesh, resulting in a decreased electrical resistance. These results are in accordance with other studies that have measured injury of vegetable cell membranes by changes in electrical resistance (Liu *et al.*, 1989).

Overall these results are consistent with the hypothesis of post cooking darkening reaction. Colour change is observed at temperatures above 53°C. Similarly the decrease in electrical resistance occurs at similar cooking temperatures. This suggests that avoiding or minimising cell modification during processing should allow reduction of the discoloration problem. This might be possible by the addition of calcium salts, which are known to strengthen cell walls, or by promoting the activity of pectin methylesterase enzyme which has a stabilising effect on cell walls if Ca^{2+} is present (Fennema, 1996).

3.6. THE EFFECT OF IRON ON DISCOLORATION

The second and third steps in the hypothesised reaction mechanism are dependent on the presence of free iron and oxygen. In the second step of the hypothesised mechanism, the free iron and phenols form a colourless complex. If this complex is not formed the discoloration does not occur. For the third step in the proposed mechanism it is necessary to have the presence of oxygen. To investigate the effect of limiting the availability of free iron and oxygen on colour formation, a factorial experiment was developed.

Kumara slices were prepared as described above and cooked at 120°C for 20 minutes. At this time and temperature, completed cell modification could be assured and

therefore the extent of discoloration would be limited by reaction 2 and 3 of the proposed mechanism.

To study the second step of the mechanism (the reaction between iron and phenols), the slices were soaked in a 3% sodium acid pyrophosphate (SAPP) solution before cooking. SAPP is a chemical compound that binds free iron (and another cations), effectively removing it from the reaction.

The third reaction in the mechanism is iron-oxidation (Fe^{2+} to Fe^{3+}) (Walter Jr. and Schadel, 1982; Lattanzio *et al.*, 1994). This was investigated by exposing the packed samples to the air (oxygen). The number of replicates was twelve for Toka Toka Gold kumara and eight for Red kumara.

Figure 3-5 shows the results of colour change (ΔE) on Owairaka Red and Toka Toka Gold roots, with and without SAPP treatment prior to packaging and cooking.

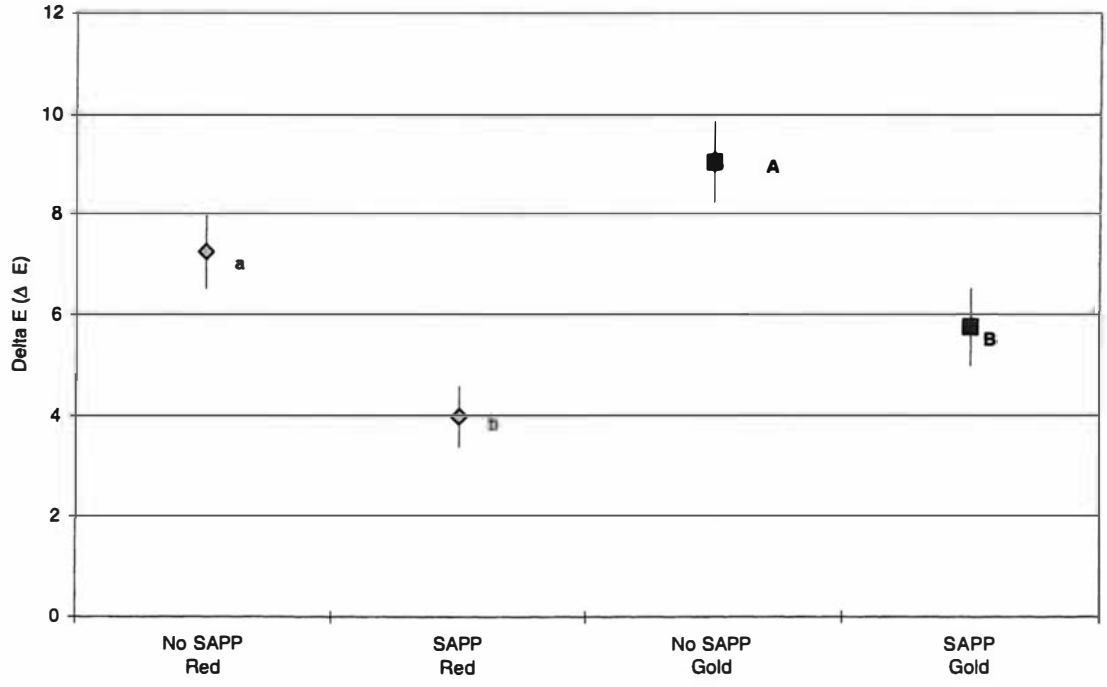

Figure 3-5 Sodium acid pyrophosphate (SAPP 3% w/v) effect on colour (ΔE) on Toka Toka Gold and Owairaka Red Kumara

**Different letters show statistical differences, according to t-test (P≤0.05)*

Figure 3-5 shows that the colour difference was low when SAPP was used to bind iron in both Owairaka Red and Toka Toka Gold kumara. These results support the proposed mechanism for discoloration, and that there is a direct relationship between free iron levels and the degree of darkening after cooking. On the other hand, as reported in 3.3.1, the colour differences measured in different kumara roots did not correlate with the total iron concentration measured in the same sample.

These results appear contradictory. A possible explanation for these results is that iron is present in excess in untreated kumara and normally the reaction is limited by the level of CA. By adding SAPP, the reaction extent becomes limited by the levels of iron in the sample. Another explanation is that the extent of discoloration is dependent on free iron levels in kumara not correlated with total iron in the sample.

3.7. THE EFFECT OF OXYGEN ON DISCOLORATION

Figure 3-6, shows the effect of oxygen on cooked kumara slice colour. The samples that were excluded from oxygen were done so by packaging the product in metallised bags prior cooking. These bags had very low permeability to oxygen.

In the presence of oxygen, the slices showed high discoloration especially for Toka Toka Gold kumara, where very little change was observed in samples without oxygen. These results support the proposition that the iron is initially in the reduced state (Fe^{2+}) in the complex (colourless), but when the iron is oxidised to form Fe^{3+}, the dark blue/black colour appears. It was interesting to note that in cooked samples vacuum packed in transparent bags, a slow colour change was observed over 35 days storage at room temperature. These transparent bags were slightly permeable to oxygen, demonstrating that the rate of colour formation is very dependent on oxygen.

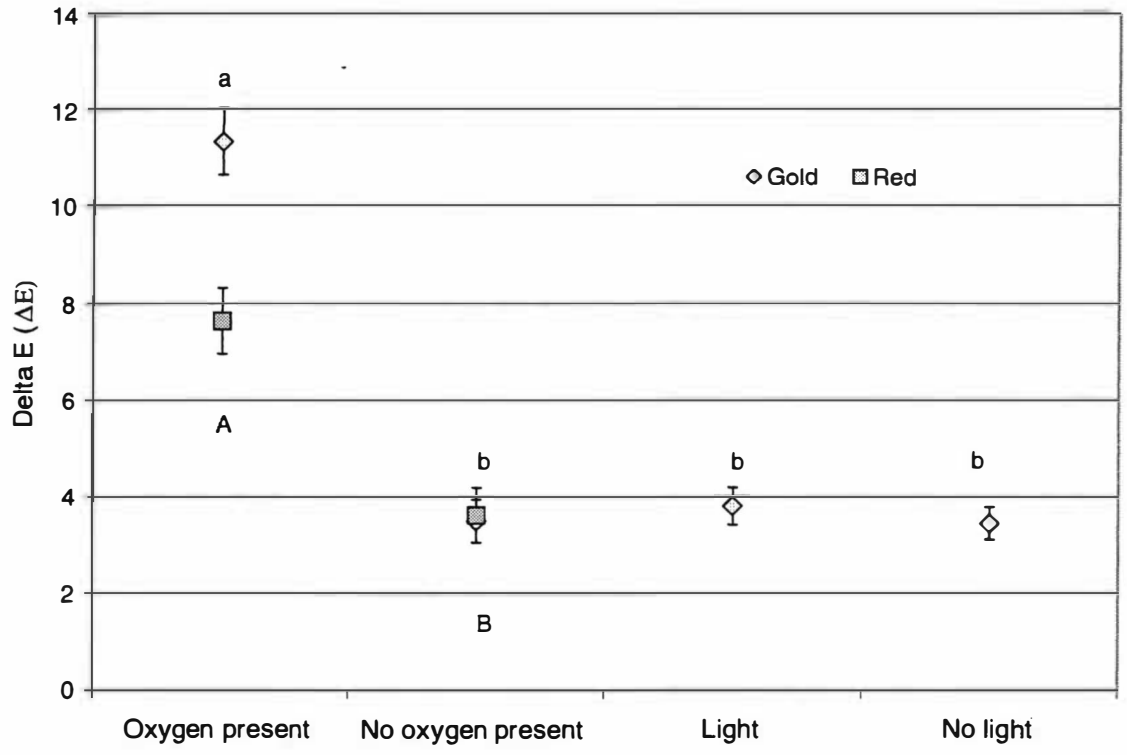

Figure 3-6 Oxygen effect and light effect on colour difference (ΔE) on Toka Toka Gold and Owairaka Red kumara slices.

**Different letters show statistical differences, according to t-test ($P \leq 0.05$)*

3.8. THE EFFECT OF LIGHT ON DISCOLORATION

Light can be an important factor promoting colour change in many products including oils, dairy products and others.

To investigate the effect of the light on the discoloration reaction, samples of Toka Toka Gold kumara were selected and prepared as described above. Twelve replicates were carried out. The samples were packed in transparent bags and stored for 48 hour at ambient conditions (22°C) after cooking. Half the samples were stored in dark conditions and the remainder stored under natural light. After storage, the colour in each sample was measured.

The results shown in Figure 3-6 demonstrate that the light had no effect on the cooked kumara discoloration reaction.

3.9. CONCLUSION

The results of the preliminary experiment support the mechanism proposed for the discoloration reaction in cooked kumara, except that there was no significant correlation between total phenol, chlorogenic acid, or total iron and colour changes in kumara samples. These results are not in agreement with Walter Jr. *et al.* , (1980), who found that browning was significantly correlated to the phenolic content in sweet potato cultivars. Similarly Hughes *et al.*, (1962) demonstrated a correlation between after cooking blackening in potatoes and chlorogenic acid levels.

The control of discoloration using SAPP showed that the free iron could be the limiting element for the discoloration reaction on kumara. The use of SAPP to sequester the iron was found long time ago (Rogers and Reynolds, 1949; Irani and Morgenthaler, 1963), and the use of SAPP to avoid colour changes after cooking is common in the potato processing industry.

CHAPTER 4: THE KINETICS OF POST COOKING DARKENING REACTIONS IN KUMARA

4.1. INTRODUCTION

Colour is an important quality attribute for cooked kumara and in industrial processing, it is necessary to optimise the kumara cooking process to achieve an acceptable colour for the cooked product. In chapter 3, the discoloration reaction was investigated and it was shown that it could be described in three steps. For each step, there are limiting factors that determine the extent of the reaction. In the first step, cell modification at high temperatures during cooking, releases iron and phenols into free solution. The second step is a reaction between free iron and phenolic compounds. This reaction depends on the quantity of free iron or phenolic available for the reaction, which ever is limiting. Oxidation of the iron-phenolic complex occurs in the third step. The oxidised iron present in the resulting complex gives the blue/black appearance to the sample. The availability of oxygen is critical in determining the extent of this reaction.

The objective of this chapter was to develop a temperature dependent kinetics model, to describe the three different reactions involved in the discoloration of cooked kumara, and to quantify the effect of the limiting factors on the discoloration reaction.

4.2. METHODOLOGIES AND EXPERIMENTAL APPROACH

4.2.1. General experimental aspects

The colour kinetics was determined according to the hypothesis that the discoloration reaction in kumara follows the three steps explained above. First of all, (1) the effect of cooking time and temperature, (2) free iron concentration, and the (3) oxygen

concentration on discoloration were studied. A series of experiments were designed in a ways that allowed the quantification of each of these three reactions independently by simple measurement of colour of the kumara slices using the Minolta chromameter described in chapter 3.

4.2.2. Preparation of sample

Gold roots harvested during the 2002 season were used. All the samples for each replicate were taken from one root, to avoid root to root variation. The peeling process was made manually in order to avoid any biochemical/chemical effects. Slices of 1cm thickness were cut from the roots and were vacuum packed into metallised bags (12 μm Polyester [PET], 9 μm Foil, 25 μm Nylon and 100 μm Cast Poly Prop [CPP]).

4.2.3. Colour measurement

The colour determination was carried out using the Minolta chromameter CR-200. The colour parameter ***L***, ***a*** and ***b*** were recorded.

The standard reading was done on the cooked slices, immediately after samples were exposed to the air ($a_{standard}$, $b_{stardard}$ and $L_{standard}$). ΔE is then given by the *Equation 4-1*.

$$\Delta E = \sqrt{(a_{sample} - a_{standart})^2 + (b_{sample} - b_{standard})^2 + (L_{sample} - L_{standard})^2} \qquad \textit{Equation 4-1}$$

where,

- L parameter is a measure of the white-black range
- a value is a measure of the red-blue range
- b value is measure of the yellow-green range

4.2.4. Kinetics studies

In order to determine the order of the reactions, ΔE versus time (minutes) data was expressed as to the extent of reaction (X) as calculated with *Equation 4-2*.

$$X = 1 - \left(\left(\Delta E_{\infty} - \Delta E_{a} \right) / \left(\Delta E_{\infty} - \Delta E_{i} \right) \right)$$ *Equation 4-2*

where,

- X is the extent of reaction (dimensionless)
- ΔE_{∞} is the colour difference at infinite time
- ΔEa is a colour difference at anytime
- ΔEi is the initial colour difference after cooking but before any colour development (t=0min)

If the reactions follow first order kinetics, the rate of reaction can be obtained by plotting *ln(k)* versus *t (time)*, and using the *Equation 4-3*. The slope is negative so the rate constant *(-k)* is negative.

$$\ln(1 - X) = -kt$$ *Equation 4-3*

where,

- k is a rate constant (min^{-1})
- t is time (min)

The Arrhenius law is often used to describe the dependence of the rate constant. This relation is shown as *Equation 4-4* below (Leve: piel, 1999).

$$k = k_o \exp(-E_A / RT)$$ *Equation 4-4*

where,

- k_o is Arrhenius equation constant (min^{-1})
- EA is the activation energy (J mol^{-1})
- T is absolute temperature (°K)
- R is the universal gas constant (8.134 [J $mol^{-1} \cdot K^{-1}$])(Cooper and Le Fevre, 1996)

4.3. COOKING TIME AND TEMPERATURE

The first step of the discoloration reaction is cell modification or alteration, which is promoted by high temperatures. This reaction can be described by the following Figure 4-1.

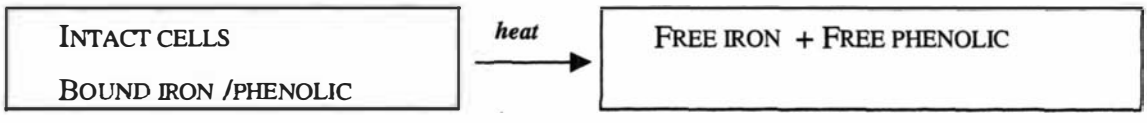

Figure 4-1 Outline of the first steps of the discoloration mechanism

The effect of temperature on the reaction rate was studied. The basic concept behind this experimental design was to cook kumara samples for different times at each temperature and then rapidly cool them in an ice water slurry to halt the cell alteration reaction at that point. The colour was then evaluated after 3h of exposure to oxygen in the ambient air. This time before measurement allowed for diffusion of iron, phenolic and oxygen through the kumara slice. Because there was no attempt to control the extent of either the second and third reaction in the mechanism, the kinetics data reflected the rate at only the cell modification process. The cooking temperatures investigated were 50, 55, 65, 70, and 80°C.

4.3.1. Cooking time

An analytical solution for heat conduction in an infinite slab was used, applying *Equation 4-5* to *Equation 4-7* to calculate the rate of heating in the kumara slices. Specific heat, density, and thermal conductivity values were used from potatoes with similar moisture content to the kumara samples (71.8 ± 2.86% w/w) used in these experiments (Rahman, 1995).

$$Fo = \frac{\lambda * t}{\rho * cp * R_x^{\,2}} \qquad \textit{Equation 4-5}$$

where,

F_o is the Fourier number (dimensionless)
λ is the thermal conductivity (W m^{-1} K^{-1})
t is the time (s)
ρ is the density (Kg m^{-3})
cp is the specific heat capacity (J kg^{-1} $°C^{-1}$)
R_x is the slice half of thickness (m)

$$Yav = (\theta av - \theta a)/(\theta i - \theta a) \qquad \textit{Equation 4-6}$$

where,

Yav is the fractional unaccomplished temperature change (dimensionless)
θav is the average temperature in solid slice (°C)
θa is the external medium temperature (°C)
θi is the slice initial temperature (°C)

$$Yav = 8/\pi^2 * \sum_{m=0}^{\infty}\left(\frac{1}{(2m+1)^2}\exp\left[-(2m+1)^2 * \pi^2/4 * Fo\right]\right) \qquad \textit{Equation 4-7}$$

It was found that after 5 minutes of cooking the average temperature had reached 95% of the cooking temperature (Figure 4-2). As a result it was safe to conclude that the changes in colour which occurred over a much longer time frame were not due to the dynamics of heating and that an assumption of isothermal reaction was appropriate for kinetic analysis of the data.

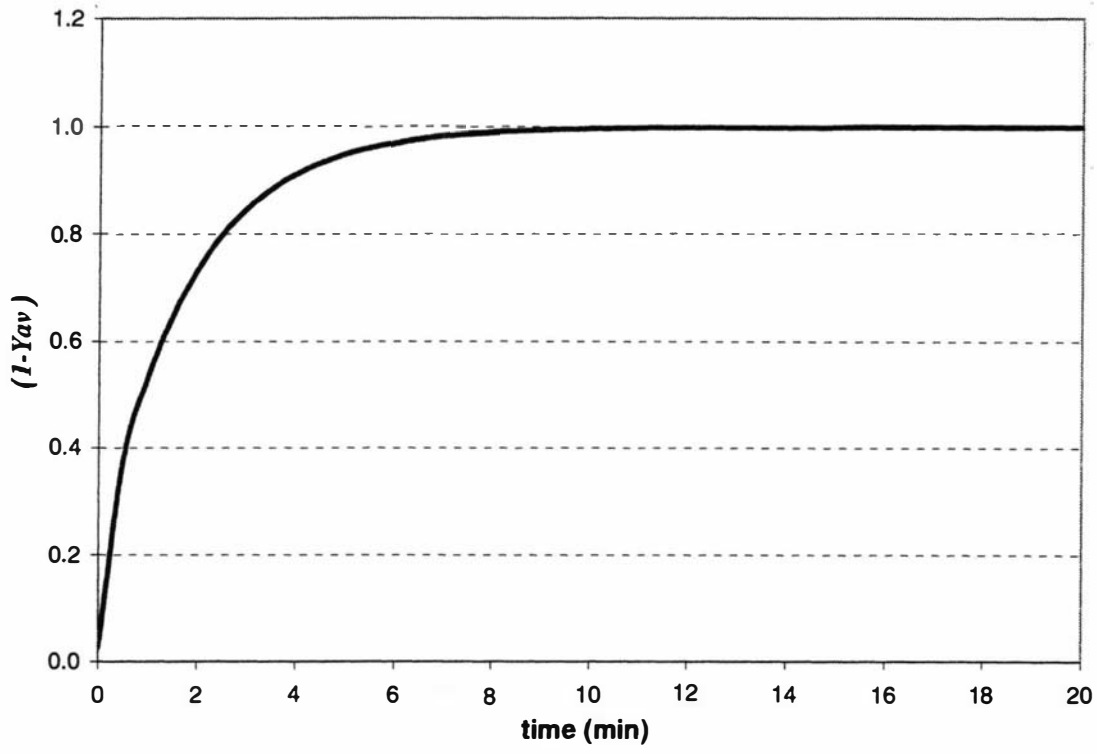

Figure 4-2 Cooking time needed to reach different extent of temperature, in 1cm slab

4.3.2. Results

Figure 4-3 shows the results of colour difference in cooked kumara as a function of time. The samples cooked at 50°C, showed little colour change, because the temperature was not adequate to promote significant cell disruption during the time the samples were cooked (60min).

On the other hand the sample cooked at 80°C showed high ΔE value after only 5 minutes of cooking because at this high temperature cells were destroyed quickly promoting the discoloration reaction. Between 55 to 70°C the samples showed clear changes in ΔE as the cooking time increased. With these it was possible to calculate the reaction rate.

At 80°C the discoloration reaction reached the maximum within 5-10 minutes. This time is similar to the time required for heating of the slice to reach the cooking

temperature, the limiting factor for colour change could be the rate of heat transfer through the sample. As a result, the data measured at 50 and 80°C were not included in the kinetic analysis.

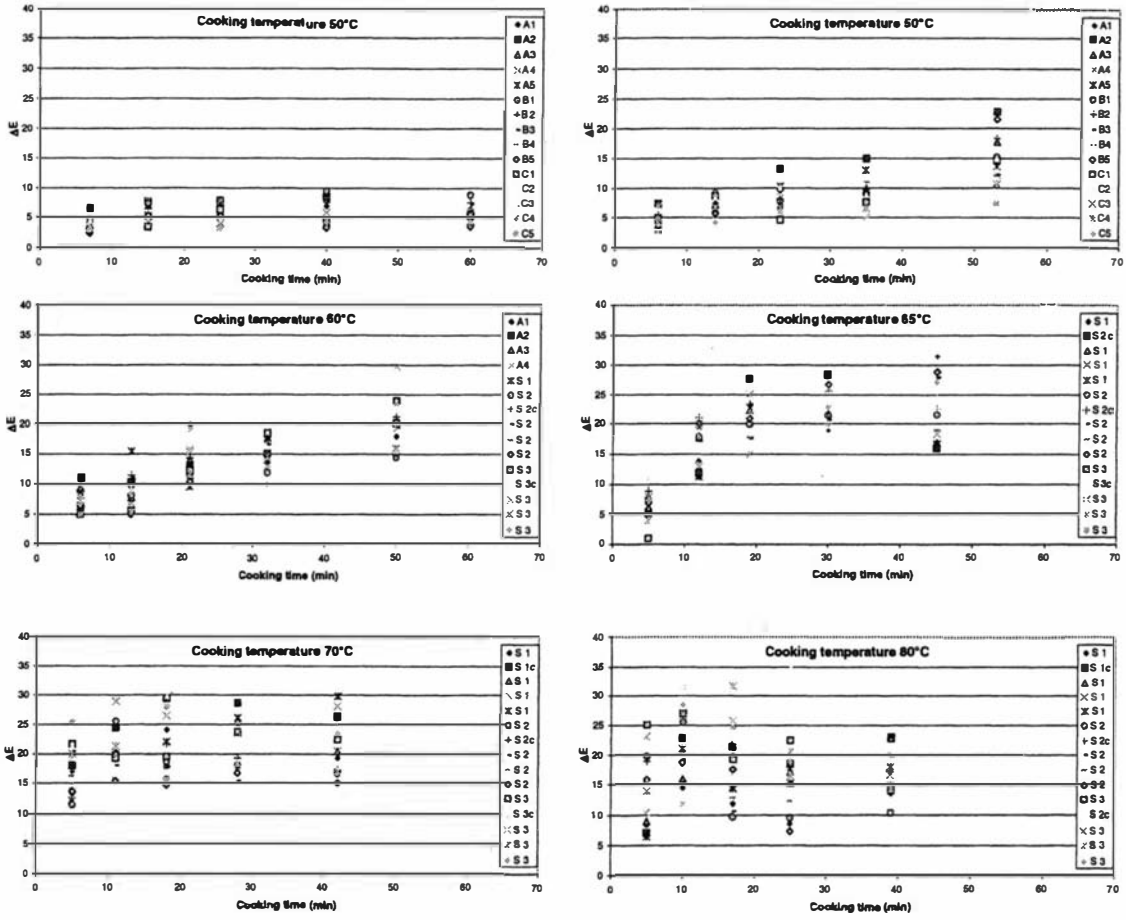

Figure 4-3 Colour difference (ΔE) in cooked gold kumara slices due to cell modification (see raw data Appendix A3).

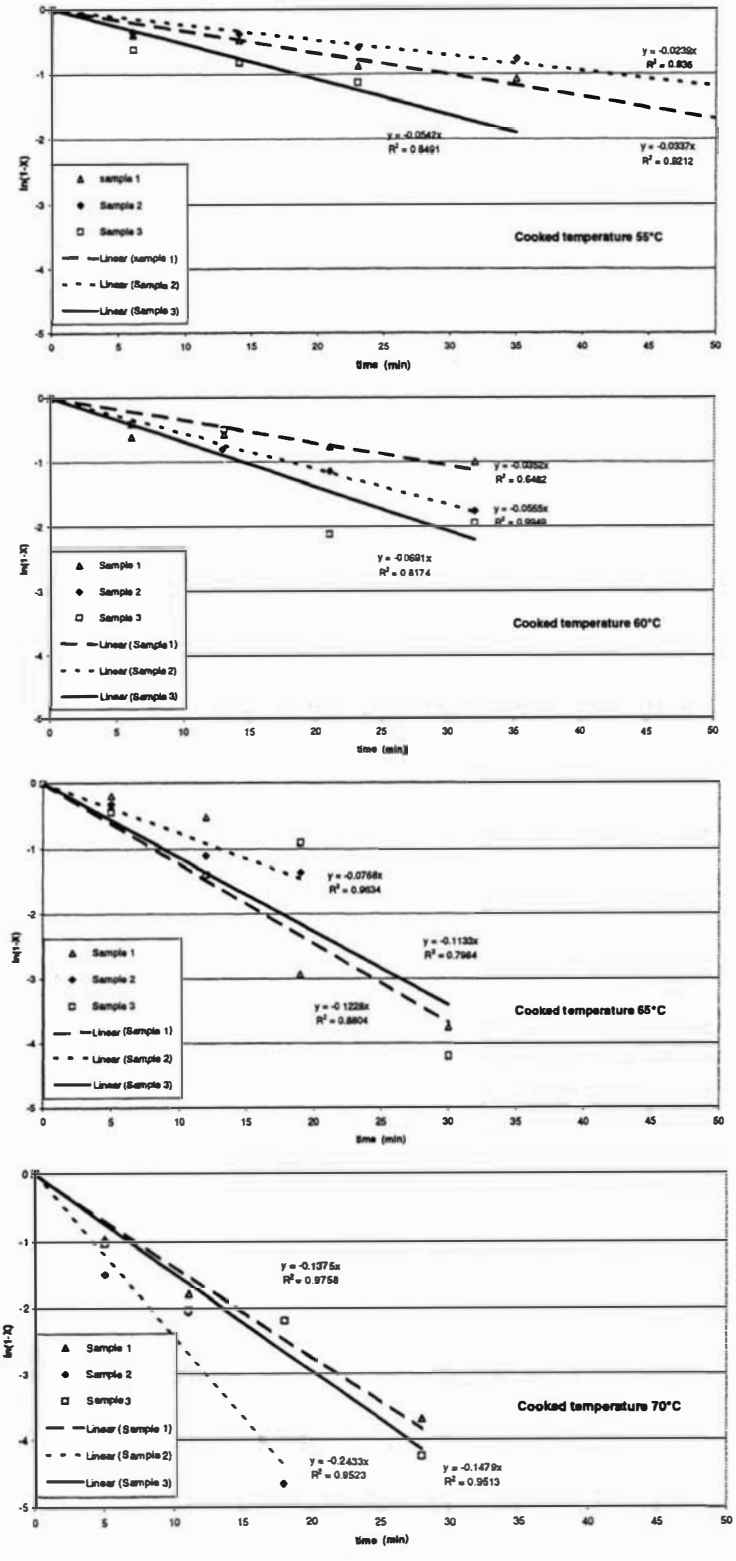

Figure 4-4 Rate of discoloration reaction on Gold kumara slice

The data for ΔE of the treatment 55, 60, 65, and 70°C was used to calculate the extent of reaction (X) using *Equation 4-2*. The extent of reaction was plotted against time and a straight line was fitted using least square regression (see Figure 4-4). The rate constant was calculated from the slope, and was found to increase when the cooking temperature was increased.

The Arrhenius parameters (***ko*** and ***E***) were obtained from an Arrhenius plot (natural log of k versus 1/T) (see Figure 4-5).

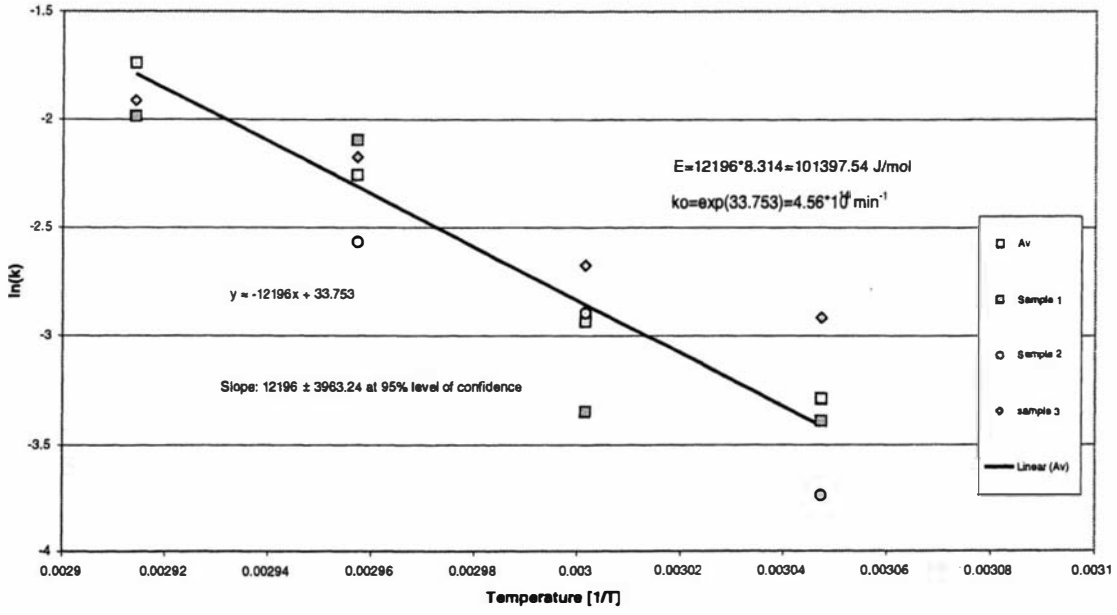

Figure 4-5 Arrhenius plot of kumara discoloration reaction rate versus cooked temperature (see raw data Appendix A3).

The activation energy *(Ea)* and Arrhenius constant *(ko)* were 101kJ mol^{-1} and $4.56 \cdot 10^{14}$ min^{-1}. The activation energy shows that the reaction is reasonably sensitive to temperature (e.g. a 10°C increase in temperature will increase the reaction rate by 2.5 times).

Using the Arrhenius parameters, predictions were made and compared to the trial data for the cooking times between 55 and 70°C (Figure 4-6) to ensure adequate predictions were possible using the kinetic model.

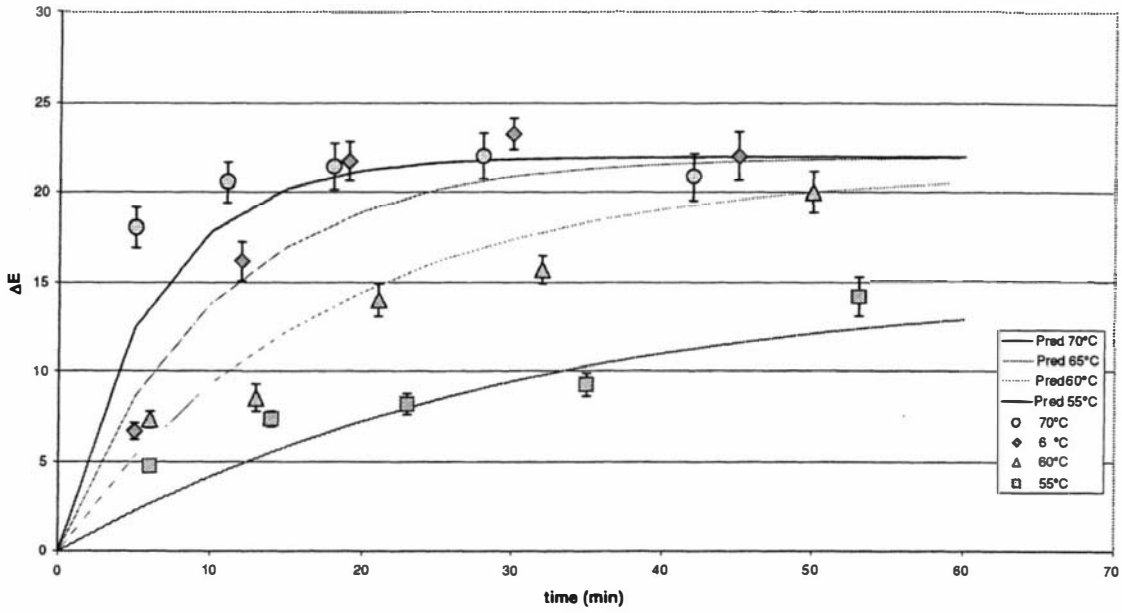

Figure 4-6 Prediction of trial data, for ΔE behaviour under different cooking temperature and time

4.4. THE EFFECT OF FREE IRON ON THE DARKENING REACTION

In the second step of the post cooking kumara discoloration reaction mechanism, free iron and phenolic compounds react and form a complex (Figure 4-7). This complex is colourless when the iron is in its reduced state (Fe^{+2}).

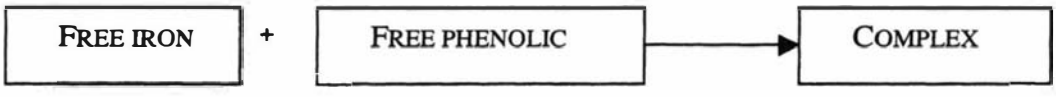

Figure 4-7 Summary of the complex formation step in darkening reaction mechanism

It follows that the amount of free iron and phenolic compounds are important factors, which can limit the extent of the reaction.

4.4.1. SAPP characteristics

The amount of free iron can be reduced by addition of chemical binders, such as sodium acid pyrophosphate (SAPP=$Na_2H_2P_2O_7$), and is used extensively in the potato processing industry for prevention of post cooking darkening (Rogers and Reynolds, 1949; Irani and Morgenthaler, 1963; Harwood *et al.*, 1995; Anonymous, 2002).

4.4.2. Process factors

Slices from one kumara were soaked in solutions with different concentrations of SAPP (0, 0.5, 1.0, 1.5, 2.0, 2.5, and 3.0%). The time necessary to reach a uniform concentration through the slice was 43.8min as calculated following the *Equation 4-8* (Saravacos and Maroulis, 2001). A diffusivity value of $9.51*10^{-9}$, $m^2\ s^{-1}$, was used for this calculation by interpolating measured data from Savaracos and Maroulis (2001) over a range of moisture contents. To ensure equilibrium had been reached, the samples were soaked in each solution for 2h prior to vacuum packing and cooking.

$$t = R_x^2 / D_m \qquad \textit{Equation 4-8}$$

where,

t	is time (s)
Rx	is the half of the slice thickness (m)
Dm	is mass diffusivity ($m^2\ s^{-1}$)

The volume of SAPP solution in the different treatment solutions was more than 10 times the volume of the samples to ensure the SAPP concentration was not significantly diluted from displacement of the free moisture of the kumara.

The colour difference (ΔE) was calculated according to *Equation 4-1*.

In this experiment the kinetics of reaction were not determined, only the extent of reaction at the point where no further colour change was observed. Previous experiments demonstrated that the rate of this reaction is fast compared with the cell modification reaction and for oxidation. The only factor likely to affect the rate of the

complex formation is due to diffusion of the substrates Fe^{2+} and CA from different locations in the kumara. There was no sign of any significant time dependence in any of the experiments carried out.

4.4.3. Results of kinetics

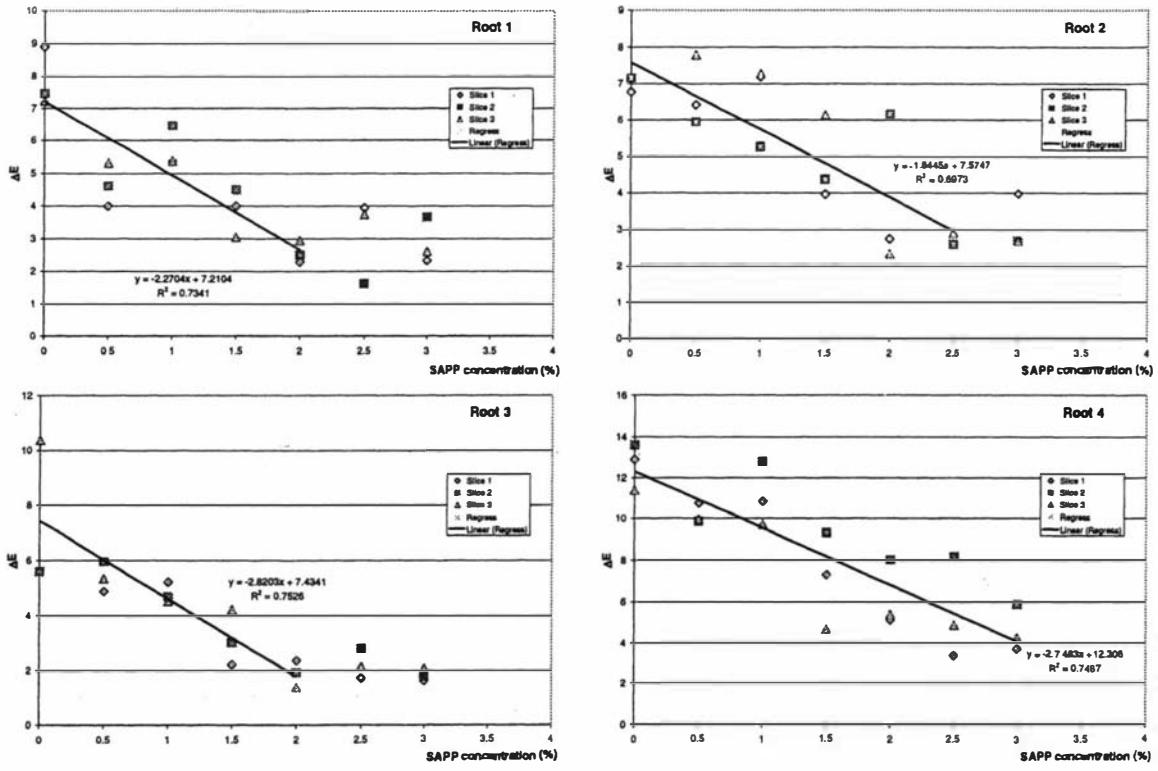

Figure 4-8 The dependence of the extent of discoloration *(ΔE)* on SAPP concentration

Figure 4-8 demonstrates how increasing concentrations of SAPP can reduce the extent of colour change in kumara after cooking. For each of the four different roots analysed there is a linear reduction in ΔE until a background level of about 2-3 is reached. Adding SAPP after this level has no further effect on colour change reduction. A colour value of ΔE=3 represent a good colour with no evidence of post cooking darkening.

The slopes of the linear regions of the plot on Figure 4-8 are similar with an average value of 2.42. This provides a useful starting point for determining the optimal level of SAPP to use to avoid after cooking darkening. Kumara samples should be cooked to

completion (e.g. 100°C 20min) and exposed to air before measurement of ΔE_o as described for these experiments described above. The optimal SAPP concentration ([SAPP]) can then be estimated using *Equation 4-9*.

$$[SAPP] = \frac{\Delta E_o - 3}{2.42} \qquad \textit{Equation 4-9}$$

where,

[SAPP] is estimated concentration of SAPP to avoid after cooking darkening

Theoretically the sequestering capacity of SAPP could be used to estimate the free concentration of iron in kumara samples. There have been various studies reporting the sequestration capacity of various metal ions by SAPP. From the data of Harwood *et al.* (1995), 1mg of SAPP can sequester 0.098mgFe^{2+} or 0.839mg Fe^{3+}. Similar magnitudes have been reported by Rogers and Reynolds (1949), Irani and Morgenthaler (1963) and Anonymous (2002). It is clear from simple calculations (137mgFe^{2+}/100fwb or 1,678mgFe^{3+}/100gfwb), that the iron sequestering capacity at a 2%SAPP solution, is much greater than the total iron levels measured in kumara (1.82mg/100gfwb- see section 3.4.1). This can be partly explained by the high concentrations of calcium and magnesium present in kumara (see table 2-4) which are also sequestered by SAPP. In any case, the SAPP levels required for prevention of colour change are similar to those suggested by Astris Ltd for potatoes (2 to 2.5 for whole and frozen mashed product) (Anonymous, 2002).

4.5. EFFECT OF OXYGEN LEVELS

The third reaction in the darkening of kumara after cooking is iron oxidation of the iron-phenolic complex. It can be described as follows in Figure 4-9.

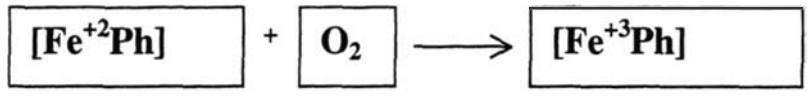

Figure 4-9 Summary of oxidation step of the post cooking darkening reaction

The complex in the reduced state is colourless but in the oxidised state has a dark, brown- blue coloration.

4.5.1. Methodology and process factors

During the measurement of the kinetics of this step of the reaction mechanism, the samples were cooked at 100°C for 25minutes to ensure completion of the cell modification reaction. In all cases, metallised packing was used to avoid the presence of oxygen until the start of the experiment. These conditions allowed the rates of the first two stages in the reaction to be maximised, so that the third stage is the limiting factor.

In order to study the effect of the oxygen levels on the kinetic of discoloration, slices from the same root were exposed (after cooking) to four different oxygen levels at ambient temperature. An anaerobic system chamber (Model 1028) was used to control the environmental oxygen.

4.5.1.1. *Operation procedure of Anaerobic system:*

For this procedure nitrogen gas was connected to the anaerobiotic gas connection at the back of the unit. Prior to start up, a vacuum was applied to the interchange with both interchanges doors closed, to check the vacuum pump and to ensure that the interchange was holding a vacuum.

a) The nitrogen supply was turned on at the source and adjusted to the low stage pressure of 10-15PSI. All connections were checked for leaks.

b) The outer door was secured and clamped shut.

c) The inner door was opened.

d) The incubator door was opened.

e) The catalyst fan switch was turned on.

f) The manual fill knob was turned fully counterclockwise.

g) The start button was pushed. This caused the vacuum system to pump out the atmospheric gas. It was automatically shut off and the work chamber was filled with nitrogen.

h) When the chamber was full, the start button was pushed again.

i) Step g was repeated.

j) The manual fill knob was turned off when the procedure was completed.

k) The nitrogen at the source was turned off.

4.5.1.2. *Gas analysis*

The oxygen levels were tested continuously with an oxygen meter (model YSI 57, probe 5700), and with a gas analyser (Hewlett Packard) periodically. For the gas analyser, 1mL samples were tested 7 or 8 times during each treatment. The samples were taken using gas tight syringes (1mL) inside the work chamber. After the samples were taken the syringe's needle was sealed with a rubber bung, to prevent concentration change in the air samples.

4.5.2. Results

The oxygen concentrations for the different treatments were 6.1, 9.9, 13.8, and 21%. The plots of the raw data are shown in Figure 4-10. These curves follow a first order trend, similar to the results observed for the cooking temperature.

From Figure 4-10 the rate of reaction was calculated by following the same methodology as for cooking temperature. Figure 4-11 shows the first order plots for different oxygen levels. It can be seen that the slopes (rate constant) increase when the oxygen concentrations increased.

It is clear from these results that the oxygen concentration has an influence on the discoloration rate reaction. Figure 4-12 shows that the rate of reaction is directly proportional to oxygen concentration. It is also evident that under anaerobic conditions the iron remained in the reduced state (Fe^{2+}) as no colour changes were observed.

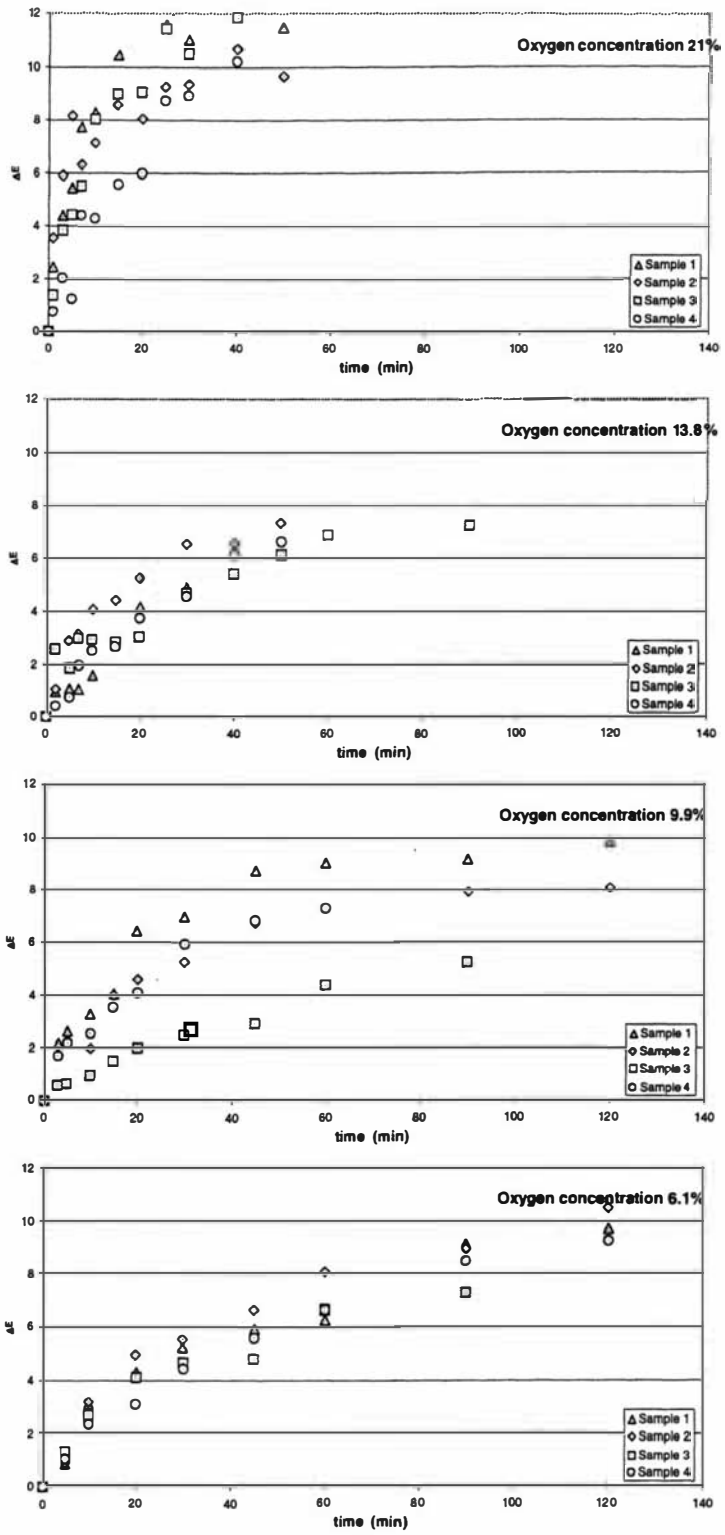

Figure 4-10 Colour difference (ΔE), under four oxygen concentrations (see raw data Appendix A3).

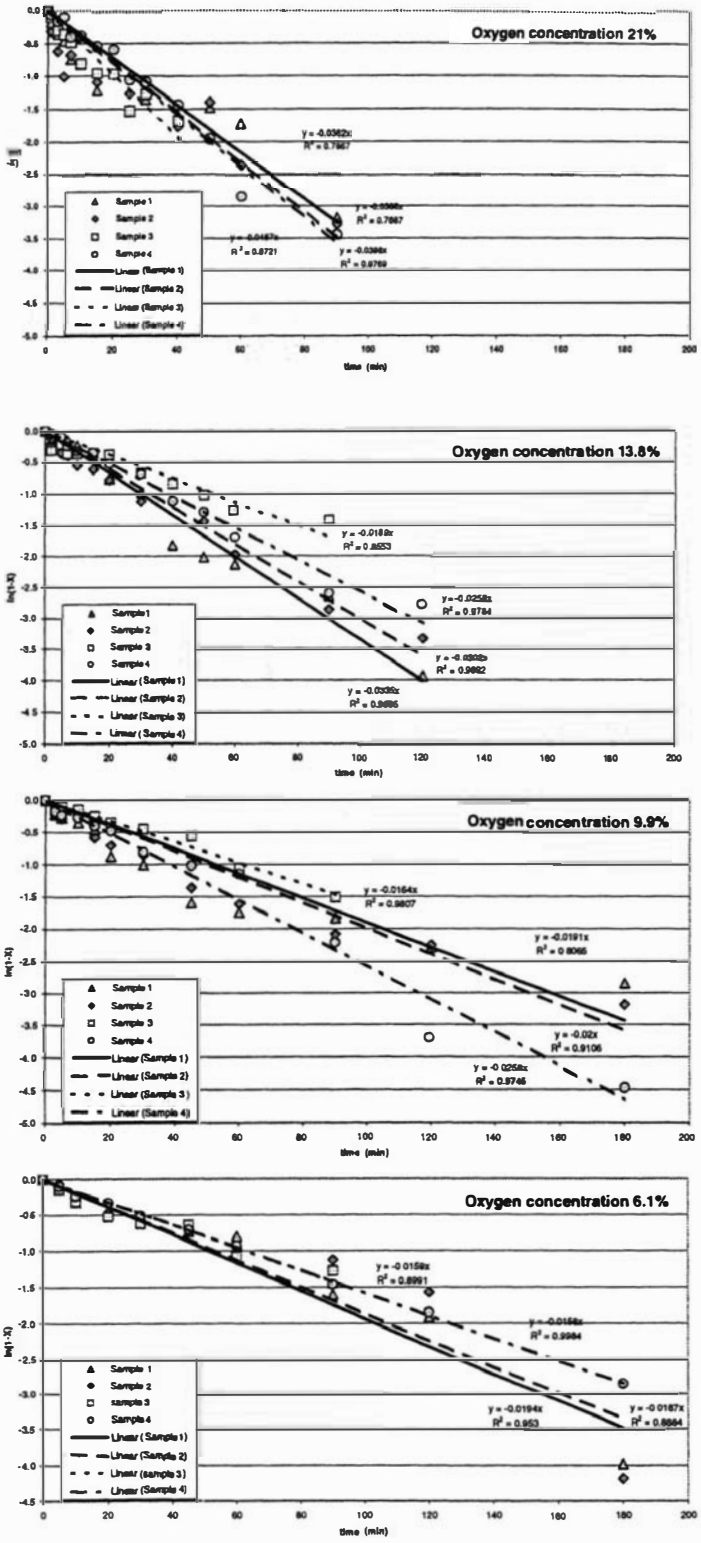

Figure 4-11 Discoloration rates in four oxygen concentrations

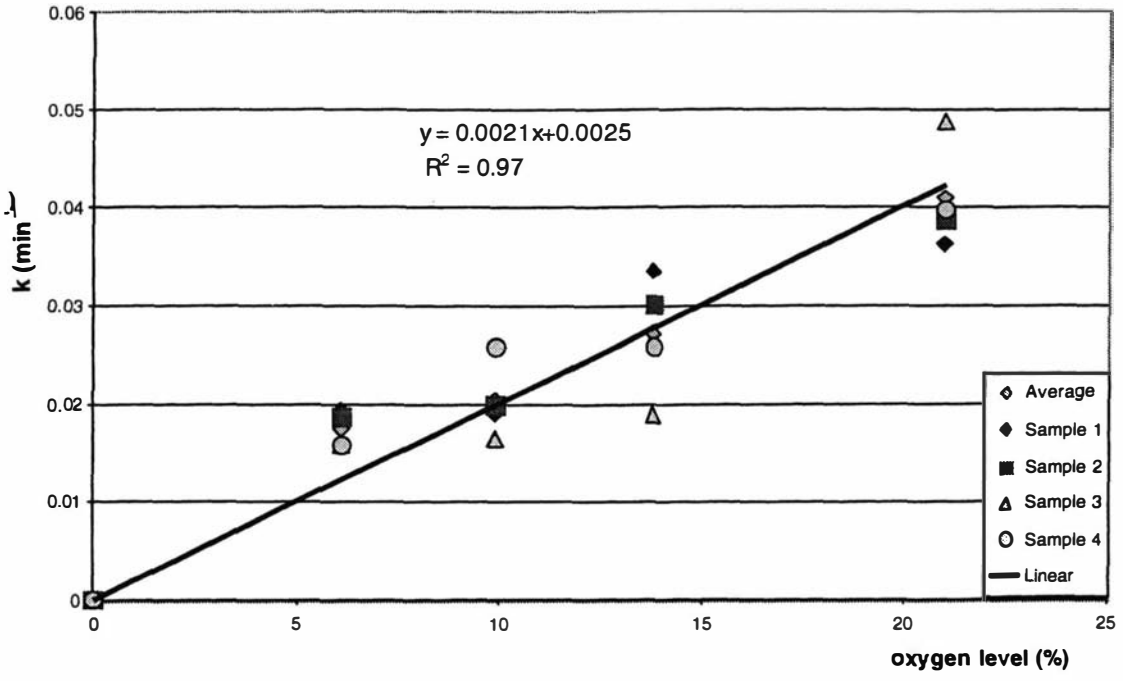

Figure 4-12 Change on the discoloration rates in four oxygen concentrations (see raw data Appendix A3).

An overall model for the reaction rate can then be given by *Equation 4-10* below, where k' is 0.0021min^{-1} $\%0_2^{-1}$. This shows that the reaction is first order with respect to oxygen concentration.

$$k = k'[O_2] + 0.0025 \qquad \textit{Equation 4-10}$$

The prediction of the colour changes (ΔE) observed in the experiment, using the model, is shown in Figure 4-13. The predicted data are in reasonable agreement with the trial data.

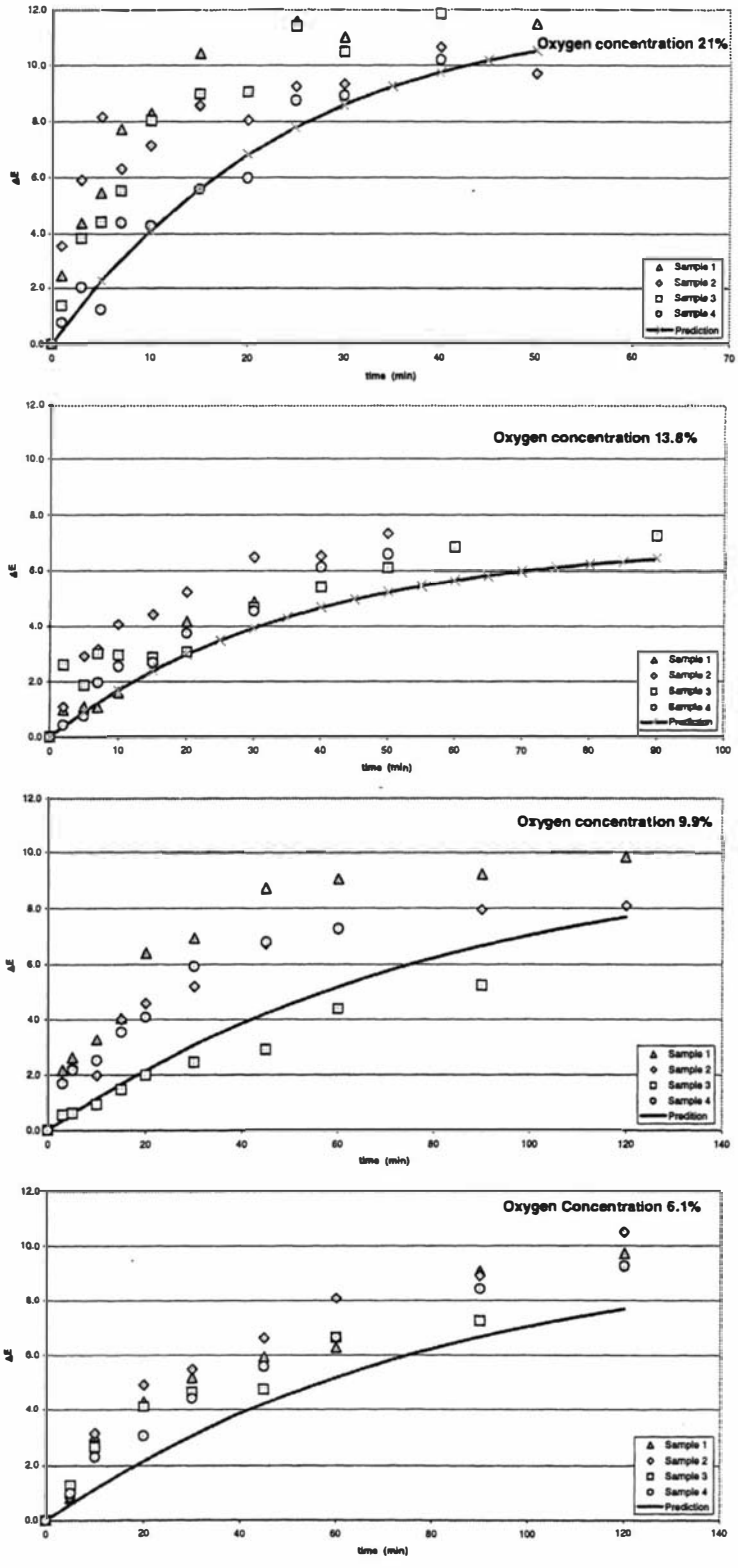

Figure 4-13 Comparison of prediction using model with real data

4.6. THE EFFECT OF STORAGE TEMPERATURE

In order to determine the effect of temperature on the oxidation step of darkening kinetics reaction, an experiment was carried out at ambient oxygen levels,.

Four storage temperatures were selected to measure the discoloration kinetics (4, 20, 30, and 40°C). The samples were cooked at 100°C for 25 minutes, to ensure all cells were disrupted. No SAPP was used during the process.

L, *a*, and *b* values were recorded, and the colour difference *(ΔE)* was calculated (*Equation 4-1*) at regular time intervals after the samples were exposed to air. The extent of the reaction (*X*) was calculated using *Equation 4-2* and a first order plot was constructed (Figure 4-15), the rate constants at each temperature were calculated using least square regression, according to *Equation 4-3*. The Arrhenius parameters (*Equation 4-4*) were determined by from an Arrhenius plots (Figure 4-16).

In all the samples the data followed first-order reaction kinetics (Figure 4-14). The change in colour difference was high during the first period of the samples in aerobic conditions. The rate of colour change decreased over time. This tendency of discoloration over time was the same in the four storage temperatures studied.

The same behaviour for colour changes are found for other vegetables which generally follow first order kinetics (Ahmed *et al.*, 2001).

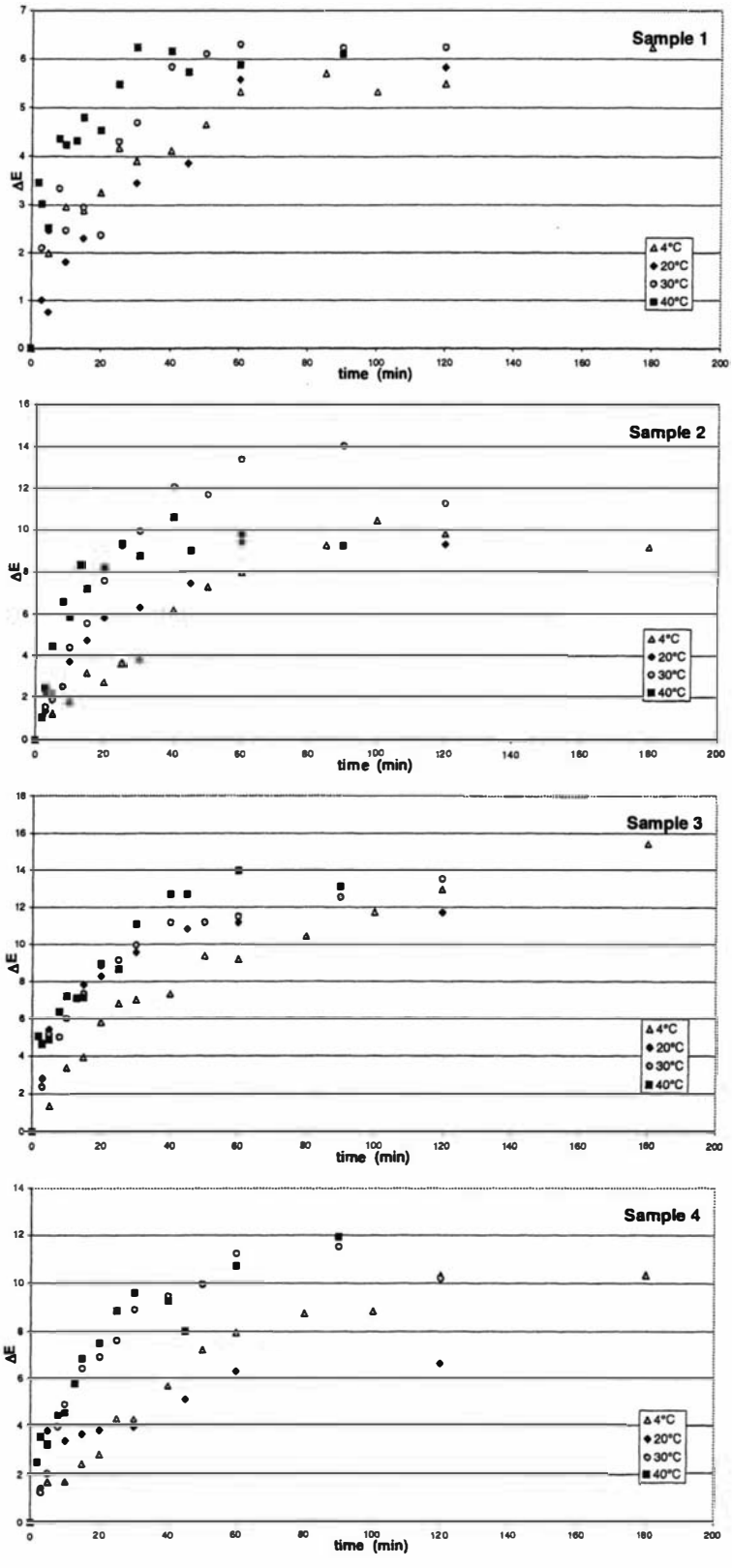

Figure 4-14 Colour differences (ΔE) in cooked gold kumara slice, stored under different temperatures (see raw data Appendix A3).

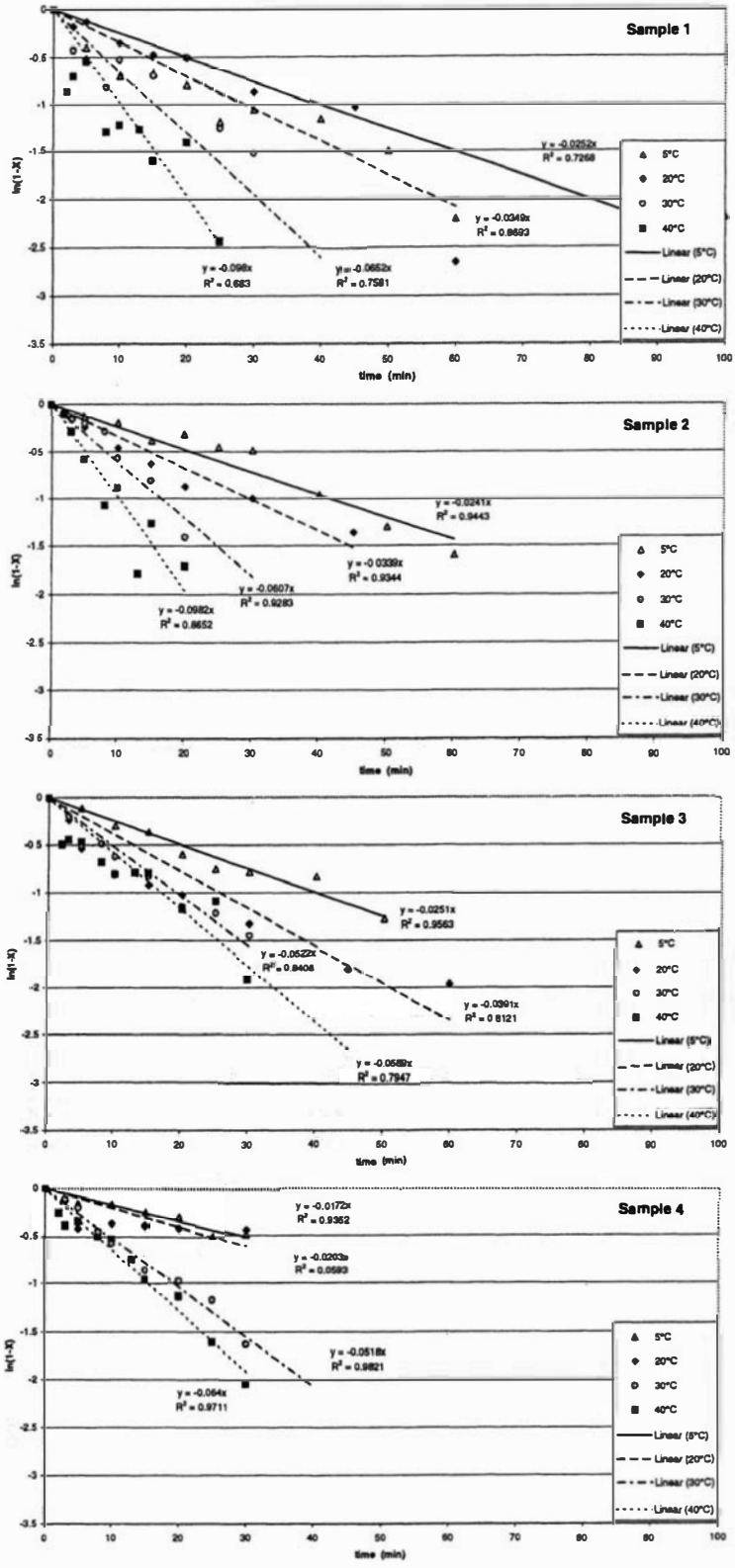

Figure 4-15 First order plots for darkening reaction at different environmental temperatures

The rate of reaction for the different samples of gold kumara increased when the temperature was increased (Figure 4-15).

In Figure 4-16 the Arrhenius constant (k_o) is the intercept and the activation energy (E_A/R) is the slope of the line.

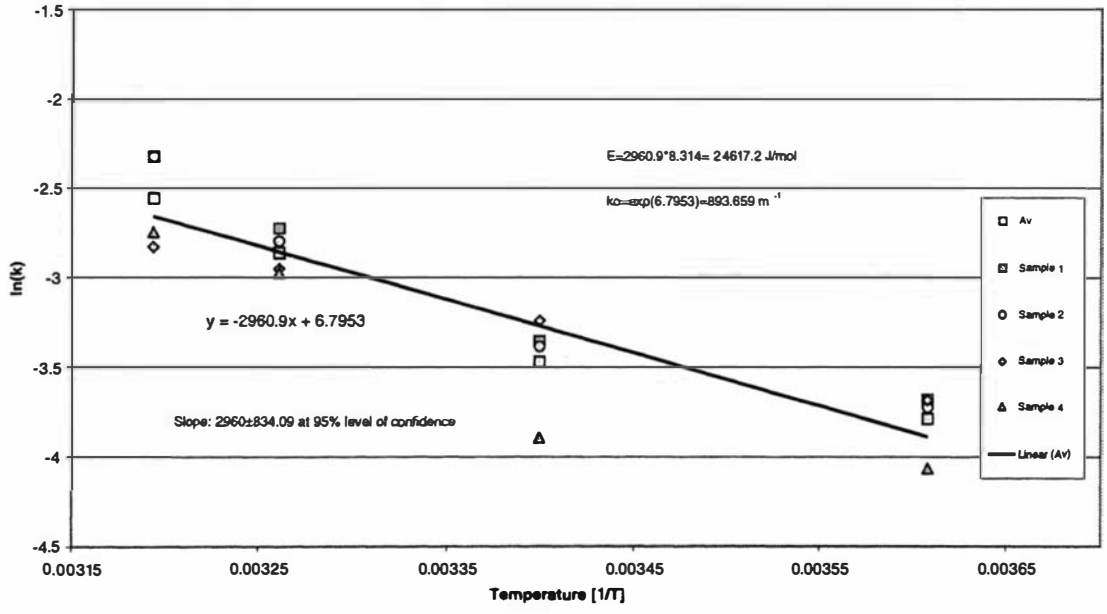

Figure 4-16 Arrhenius plot for cooked Gold kumara slices, at different storage temperatures

The average values for k_o were 894 min^{-1} and E_a25kJ mol^{-1}. If the oxygen dependency discussed in section 4.5.2 above is considered together with the temperature effects, an overall equation for the rate constant can be developed (see *Equation 4-11*).

$$k = k'[O_2]\exp\left(-E_a/RT\right) \qquad \textit{Equation 4-11}$$

where,

k_o'=42.6min^{-1}%O_2

The trial data was predicted with the model considering the calculated Arrhenius parameters. The curves shown in Figure 4-17 are very close, suggesting the kinetic model is suitable to describe colour changes in kumara after cooking.

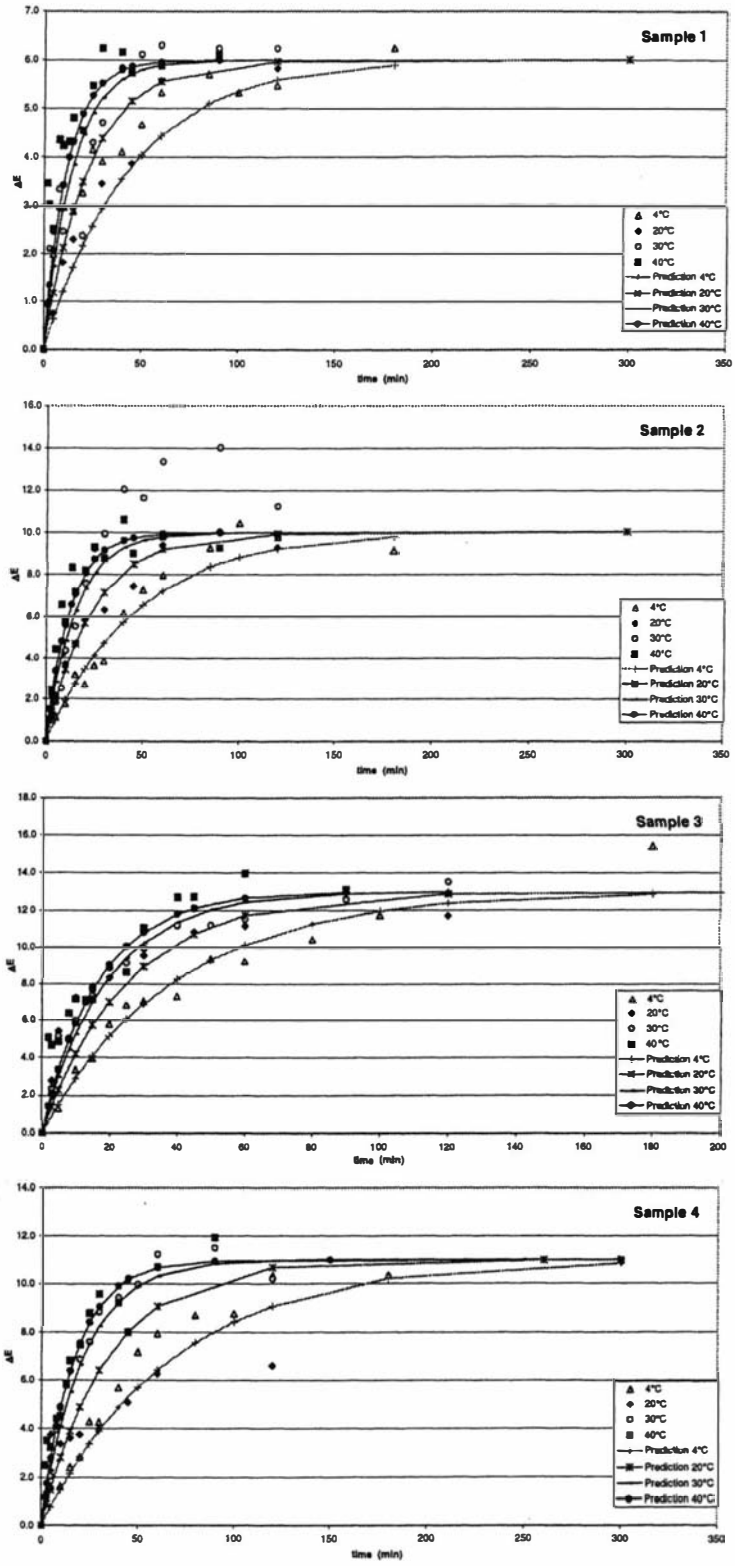

Figure 4-17 Raw data and predicted values by the model

The parameters *L, a,* and *b* were analysed in the same way as for ΔE above. The results showed that the *a* values had no great influence in the discoloration reaction, and that the *b* and *L* values, followed the same trends as ΔE. Both parameters followed a first-order reaction kinetics and, the Ea was 20 and 24kJ/mol and k_o was 159 and 574min^{-1} for *b* and *L* respectively.

The variation in the colour (ΔE) was promoted principally by differences in *b* and *L* in the kumara slices after cooking, but both had a similar importance. This is shown by the linear relationship between *b* and *L* extent of reaction observed in Figure 4-18.

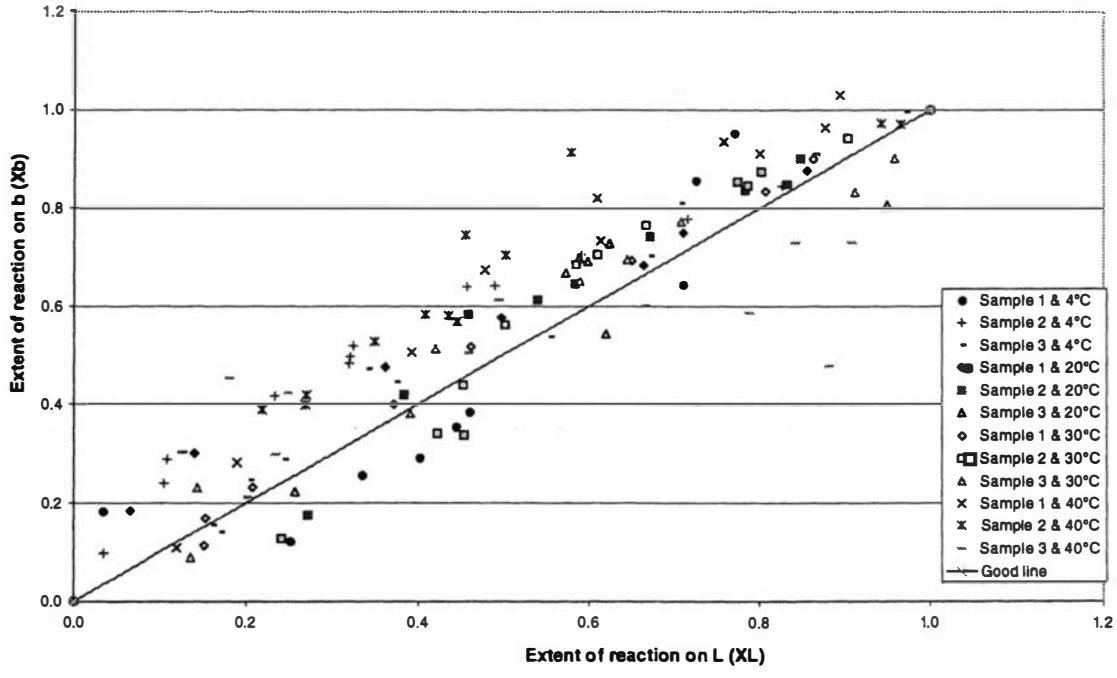

Figure 4-18 Relationship between b and L in terms of extent of reaction

The kinetic reaction parameters for the storage temperature measured in these experiments were as activation energy of 25kJmol^{-1} and an Arrhenius constant of 893min^{-1}. The activation energy found in cooked kumara was slightly lower than that found for the colour degradation in onion puree, 28kJ/mol and for non-enzymatic browning in apple juice, 83kJ mol^{-1} (Heldman and Lund, 1992; Ahmed *et al.*, 2001). However, it was higher than values reported in literature for chilli puree, 11 to 16kJmol^{-1} (Ahmed *et al.*, 2000; Ahmed *et al.*, 2001).

Often a low activation energy indicates that a reaction is diffusion limited. It follows that the observed rate constants measured in this experiment were in fact for diffusion of oxygen into the sample. The kumara samples are slightly transparent meaning the colorimeter is measuring colour from light reflected from within the sample as well as on the surface. Because of this the dynamics of colour change in oxidation step experiments could be due to oxygen diffusion alone. If this is case, the dynamics of colour change will be sample size dependent.

In order to investigate this possibility further, cooked (100°C, for 90 min) root samples cut into 5cm pieces were placed in oil (see Figure 4-19). The samples were left in this condition for three days. After that the samples were cut through the middle top to bottom, and the discoloration inside the root was inspected.

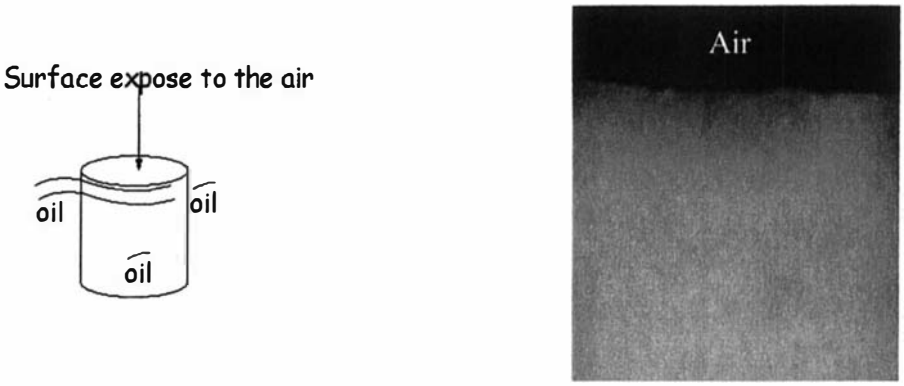

Figure 4-19 Trial outlines of kumara cylinder into oil, and one surface exposed to the air

CHAPTER 5: THE MECHANISM OFTEXTURAL CHANGE IN KUMARA

5.1. INTRODUCTION

In addition to colour changes it is important to understand and be able to control textural changes in kumara during cooking. This chapter is aimed at developing the mechanism for textural change in kumara.

Changes in the structure and properties of products occur as a results of internal (raw material composition, pH, ionic strength, etc.) and external factors (processing method, external stress, etc.) (Kunzek *et al.,* 1999). This chapter outlines work done on characterising the factors that are important to the ultimate product texture for intact cooked kumara products.

Starch is the most abundant carbohydrate present in kumara root (see Table 2-4), and therefore it follows that the reactions involving this complex polysaccharide (starch hydrolysis, starch gelatinisation and retrogradation) are likely to affect the kumara texture. These reactions depend on the temperature time history during exposure to mechanical stress and enzyme activity. Additives can also be used to influence these reactions (i.e. sugar, salts, and endogenous enzymes).

During gelatinisation the starch granule swells and changes the rheological and textural behaviour of the product. Alvarez and Canet (1998) demonstrated these changes in potato tissue. The starch granules in fresh tissue are round and oval and of crystalline structure. After cooking, they are swollen, hydrated and gelatinised and have been fused together to occupy the entire volume of the cells. This behaviour was reviewed in detail in section 2.4 of the literature review.

Starch hydrolysis can affect the texture on kumara. During hydrolysis the starch (polysaccharide) molecule is broken down into maltose and dextrin due to amylase enzyme activity. In sweet potato, starch breakdown susceptibility increases upon cooking (Woolfe, 1992). Walter Jr. and Schwartz (1993) suggested that one of the main factors in the reduction of viscosity in sweet potato puree was due to the presence of lower molecular weight polymers. In other words, the reduction in molecular weight causes a reduction in viscosity of the product due the reduction in starch content. There are no reports however on the effect of starch hydrolysis on intact potato texture. Valetudie (1999), suggested that the starch hydrolysis could possibly lead to a decrease in starch swelling and cell filling (starch gelatinisation) due to the low molecular products of hydrolysis being able to leach out of the cell.

The ability of the cell to maintain firmness is determined by the capacity of a cell wall to bind to the wall of adjacent cells. The structure or layer between two cells is called the middle lamella, which is comprised mainly of pectin. Some minerals such as calcium ions are also known to play an important role in strengthening the cell wall in some vegetables (Thakur *et al.*, 1997).

A group of enzymes generally termed pectinases promote pectin break down, especially during the ripening process. This destruction of the cell integrity in vegetable and fruit tissue can be promoted by increased cooking time and temperature (Rosenthal, 1999).

The reactions involved in this complex system can also interact. For example the combined effects of starch swelling and cell wall degradation have been shown to explain the soggy texture of cooked potato and sweet potato roots (Valetudie *et al.*, 1999; Binner *et al.*, 2000; Alvarez and Canet, 2002).

A hypothesised mechanism to explain the changes to kumara texture during cooking is presented in Figure 5-1. Both internal and external factors affect the texture with complex interactions occurring between them. The temperature plays a key role, promoting more than one reaction and affecting enzyme action (Alvarez and Canet, 2002).

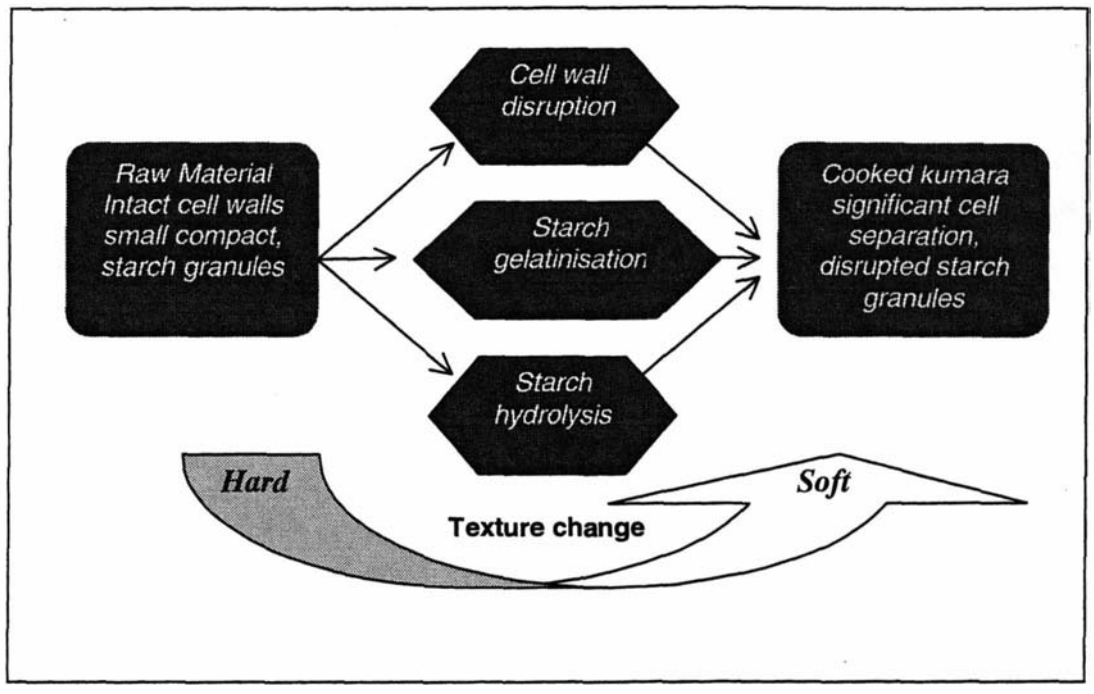

Figure 5-1 Texture change mechanism proposed for kumara

The aim of this chapter was to design and carry out experiments to characterise how the extent of each of these reactions affect cooked kumara texture, and how this varies with cooking conditions. This would then test the validity of the proposed mechanism.

5.2. EXPERIMENTAL METHODOLOGIES

Experimental methods were required in order to describe and quantify the textural changes in kumara during cooking and to relate these changes to the compositional changes identified in the proposed mechanism. Because the focus of the work was to integrate changes to the primary texture of whole or sliced kumara products, methods for quantification of mechanical strength (rather than rheological properties of a paste or puree) were required. The breakdown of the cell wall lamella is the results of pectin hydrolysis into sugars and organic acids, this reaction is likely to be evidenced by reductions in alcohol insoluble solids (AIS) and increases in total reducing sugars (TRS), and uronic acid.

Starch hydrolysis in kumara results primarily in the formation of maltose. Maltose is not

a reducing sugar, so this provides a useful method to quantify this reaction. Small levels of glucose production, as a result of starch hydrolysis may however show up in the TRS results causing some complication with data analysis.

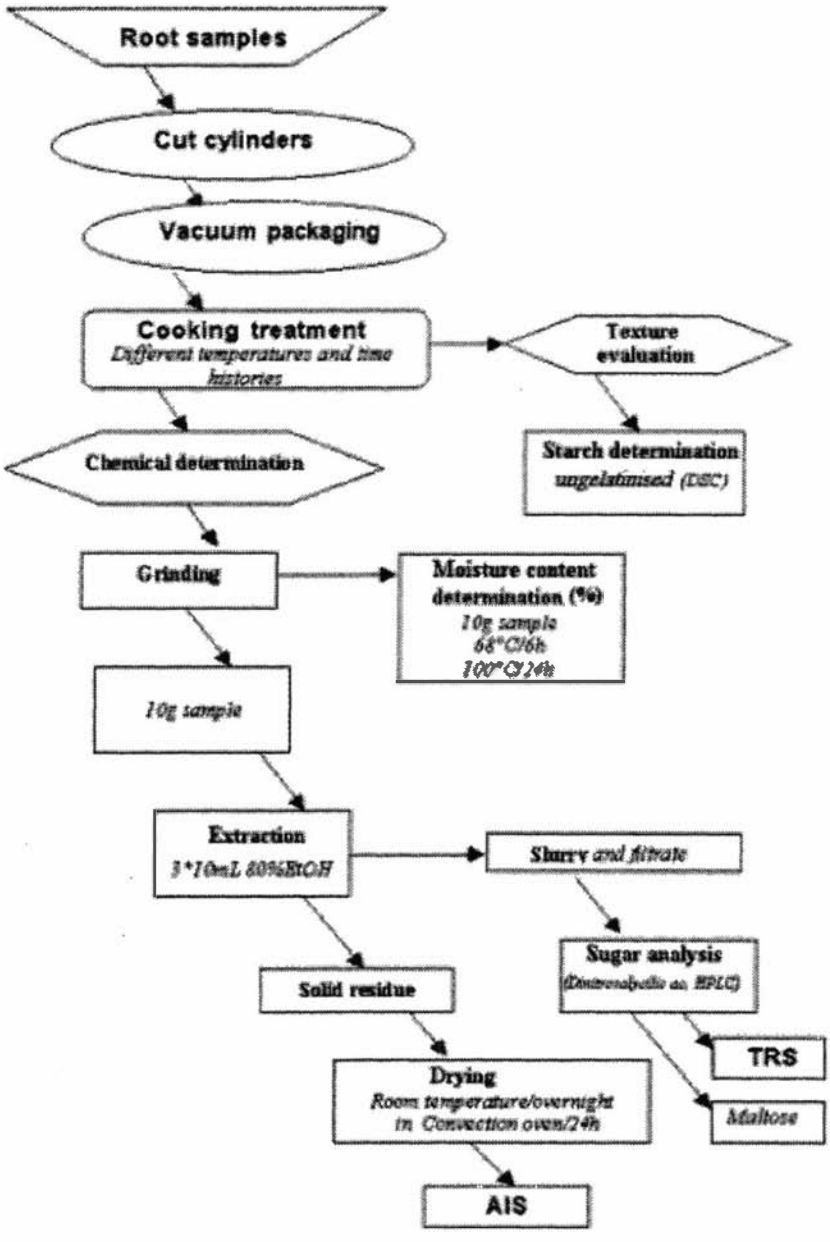

Figure 5-2 Summarises the general approach for characterisation of kumara samples

The progress of starch gelatinisation is most easily followed by changes in the levels of ungelatinised starch by differential scanning calorimetry (DSC). In addition, starch

gelatinisation and granule swelling were qualitatively assessed by scanning electron microscopy.

Figure 5-2 summarises the general approach taken for characterising kumara samples. The following sections provide details of experimental planning and analysis procedures used in the work.

5.2.1. Raw material and sample preparation

Samples from Toka Toka Gold and Owairaka Red kumara roots were used. These were supplied by Delta Produce Limited, Dargaville and from a local supermarket in Palmerston North, New Zealand. Roots from different locations, post harvest age, and storage condition were used to get a large range of expected texture change in order to link this with compositional differences in the kumara (see Table 5-1).

Table 5-1 Characteristic of kumara roots used as raw material

Samples	Varieties	Plot number	Storage state and harvested date
RA	Owairaka Red	1	2003
RB	Owairaka Red	2	Half cured 2003
RC	Owairaka Red	3	Cured, harvested 22 March 2003
RD	Owairaka Red	2	Cured and opened for cooling 2003
RE	Owairaka Red	4	Just harvested, uncured 2003
R#	Owairaka Red	5	Local market cured 2003
GA	Toka Toka Gold	1	3 days harvested 2003
GB	Toka Toka Gold	2	Just harvested, uncured 2003
GC	Toka Toka Gold	3	27 days from harvest, cured cooled 2003
GD	Toka Toka Gold	4	2002
GE	Toka Toka Gold	5	2002
GF	Toka Toka Gold	6	2002
GG	Toka Toka Gold	7	2002
GH	Toka Toka Gold	1	2002
GI	Toka Toka Gold	8	2002
G#	Toka Toka Gold	9	Local market cured 2003

The roots were selected, washed and cylinders of 1cm diameter and 1cm length were cut using a stainless steel core sampler. The cylinders were put into vacuum bags, and cooked.

5.2.2. Sample cooking

Water baths were used to cook the kumara samples at controlled temperatures specific to the experiments outlined below. Uncooked samples were used as controls. After cooking, the samples (still in bags) were cooled immediately in an ice-water slurry to arrest the rate of reactions occurring in the sample.

To be able to say that samples are cooked at particular temperatures, a step change in the temperature of the sample is required. If rapid heating to the desired cooking temperature is not achieved, then a significant amount of the cooking may occur at lower temperatures, especially at the thermal centre of the product. To assess the rate of heating in the1cm diameter cylindrical samples used in the experiments, the time taken to heat the samples was calculated.

The mass average unaccomplished temperature change (*Yav*) was determined by considering the conduction of heat in an infinite slab of thickness (*2R*) and infinite cylinder with known diameter (*2R*). The intersection of these two ideal geometries is a good approximation for the samples used in this study.

In order to know the thermal profile at different cooking times, an analytical solution for heat conduction was used for the infinite slab and infinite cylinder geometries. The infinite slab solution was determined using Equation 5-1 to Equation 5-3 below. The infinite cylinder solution was calculated using Equation 5-1, and Equation 5-4. The sample solution was obtained by interaction between both shapes and it was determined using Equation 5-5. It was assumed that the surface temperature was constant and the same as the cooking temperature (Carslaw and Jaeger, 1959). The specific heat, density, and thermal conductivity values for potatoes with similar moisture to kumara samples (71.8 ± 2.86 %w/w) (Rahman, 1995), were used due to lack of data available in the literature for kumara. The density of kumara cylinder was determined (1088 kg/m^3) by weighing fresh kumara cylinders.

$$Fo = \frac{\lambda * t}{\rho * cp * R^2}$$ *Equation 5-1*

where,

Fo is the Fourier number (dimensionless)
λ is the thermal conductivity (0.36 J s^{-1} $m^{-1}°C^{-1}$ (Rahman, 1995))
t is the time (s)
ρ is the density (1088 kg m^{-3})
cp is the specific heat capacity (3515 J kg^{-1} $°C^{-1}$ (Rahman, 1995))
Rx is the slab half of thickness (m)

$$Yav = \frac{(\theta av - \theta a)}{(\theta i - \theta a)}$$ *Equation 5-2*

where,

Yav is the mass average unaccomplished temperature change
θav is the average temperature in the solid slab (°C)
θa is the external medium temperature (°C)
θi is the slab initial temperature (°C)

$$Yav_{slab} = 8/\pi^2 * \sum_{m=0}^{\infty}\left(\frac{1}{(2m+1)^2}\exp\left[-(2m+1)^2 * \pi^2/4 * Fo\right]\right)$$ *Equation 5-3*

$$Yav_{cylinder} = \sum_{m=1}^{\infty}\left(\frac{4}{\beta m^2}\exp\left[-\beta m^2 * Fo\right]\right)$$ *Equation 5-4*

where,

βm are the roots of the Bessels function Jo(βm)=0

$$Yav = Yav_{slab} \cdot Yav_{cylinder}$$ *Equation 5-5*

It was found that the minimum required cooking time was 2min (see Figure 5-3). The samples (bags) were under thermal treatment approximately 10 times the minimum calculated, ensuring the cylinders were cooked completely.

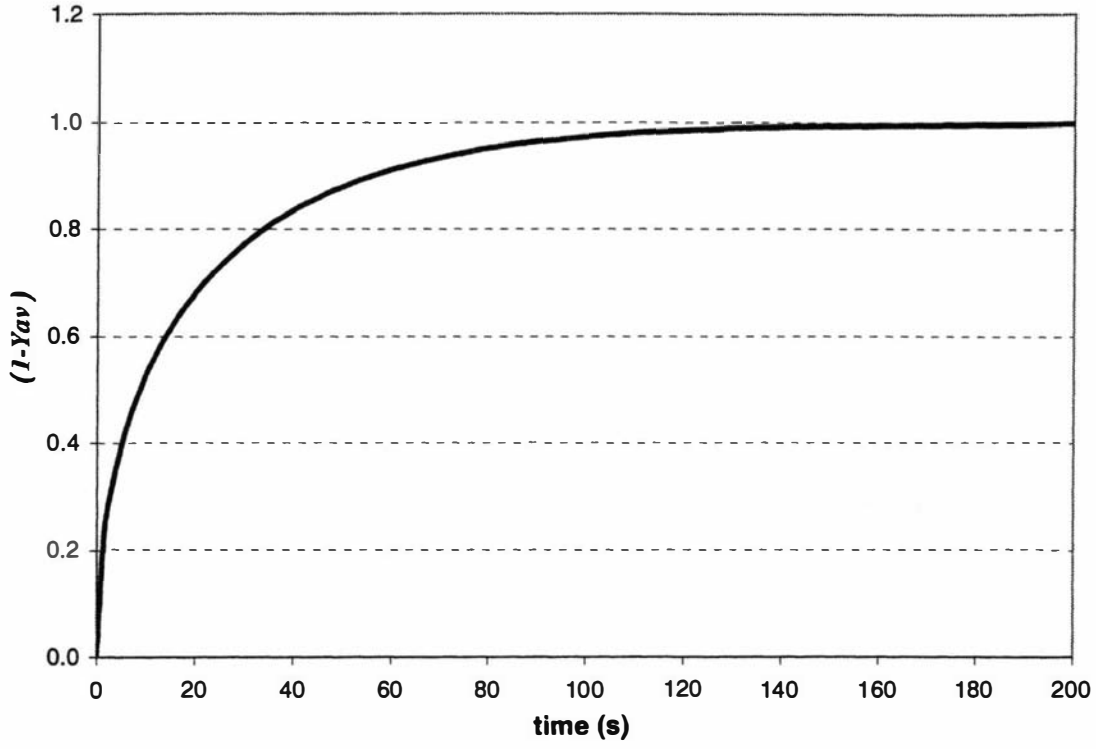

Figure 5-3 Predicted rate of heating during cooking (at any temperature) of a short cylindrical sample (diameter and length both equal to 1cm)

5.2.3. Chemical analysis

5.2.3.1. Moisture content

Kumara samples were grated using a Sunbeam food processor (Model LC-AX). Approximately 10g of grated kumara sample was weighed into pre-weighed aluminium pans and the dry matter content was determined after 68°C for 6h, followed by 18h at 100°C (Walter Jr. *et al.*, 1997). The moisture was calculated on a fresh weight basis using Equation 5-6.

$$M = 100 \cdot \frac{(fsw - dsw)}{fsw} \qquad \textit{Equation 5-6}$$

where,

M is the moisture content (%)
fsw is the fresh sample weight (g)
dsw is the dried sample weight (g)

5.2.3.2. Alcohol insoluble solids (AIS)

The AIS levels in the kumara samples were measured according to the method of Walter Jr. *et al.* (1997). The determinations were carried out by weighing 10g of grated kumara into Erlenmeyer flasks. The samples were washed three times with 30mL of boiling 80% ethanol-20% water solution. Then the solution containing the kumara sample was filtered using a sintered glass, coarse porosity filter. The solid residue was dried overnight at room temperature and then for 24h at 100°C. AIS levels were calculated according to *Equation 5-7*.

$$AIS = 100 \cdot \frac{dfw}{fsw} \qquad \textit{Equation 5-7}$$

where,

AIS is the alcohol insoluble solid (%)
fsw is the fresh sample weigh (g)
dfw is the dried weight of filtered solid (g)

5.2.3.3. Total reducing sugars (TRS)

The quantity of reducing sugars was determined using the dinitrosalicylic acid (DNS) method (Miller, 1959). This colorimetric method involves the reaction of the reducing sugar with dinitrosalicylate to give a brown-coloured complex that absorbs strongly at a wavelength of 575nm.

DNS reagent was prepared by dissolving in 600 mL distilled water, 10g sodium hydroxide, 182g potassium sodium tartrate (Rochelle Salt), 10g dinitrosalicylic acid (added slowly while stirring), 2g phenol, 0.5g sodium sulphite, and then made up to 1L with distilled water.

A standard curve was prepared by making glucose standard solutions over the range 0 to 1mg/mL in distilled water. 1mL of each standard was pipetted into separate test tubes and 1mL of distilled water was added. 2mL of distilled water was put into a test tube for the blank, and 3mL of DNS reagent was then added into each test tube and vortexed. The tubes were capped and placed in boiling water for 15min, and then cooled in cold water for at least 20min. The readings were made against the blank at 575nm using a UV spectrophotometer (Hitachi U-2000), and glucose concentrations (mg/ml) versus absorbance were plotted. A straight line was achieved between 0 and 1mg/mL.

To determine TRS in kumara samples, the filtrate samples were diluted 1/50, 1mL of this diluted solution plus 1mL of distilled water was taken in a test tube, and 3mL of DNS reagent was added. A blank was included with the samples. The tubes were placed in a boiling water bath for 15min, and then cooled for 20min. The readings were made against the blank at 575nm using the UV spectrophotometer (Hitachi U-2000). The equivalent glucose concentration was read from the standard curve and adjusted to account for the dilution factor.

5.2.3.4. Maltose

The maltose determinations were carried out by weighing 10g of grated kumara into Erlenmeyer flasks. The samples were washed three times with 30mL of boiling 80% ethanol-20% water solution. The solution containing the kumara sample was filtered using a sintered glass, coarse porosity filter. The slurries were transferred into Erlenmeyer flasks and diluted 10 times.

A Waters Associates liquid chromatograph, HPLC model 590 (Milford, MA,USA) with a refractive index detector model R401 was used to detect the maltose concentration. The Sugar-Pack column (Phenomenex model Rezex, 8μ, 8%Ca, monos, 300mm*780mm, Torrance, CA, USA) column was maintained at 90°C using the instrumental oven. The mobile phase was an EDTA solution (50mg/L) at a flow rate of 0.5 mL/min (Walter Jr., 1992).

A maltose standard (Maltose monohydrate, AR grade supplied by BDH Chemicals New Zealand) was prepared in over the concentration range between 1 to 10g/L.

5.2.3.5. Uronic acid (UA)

Determinations of uronic acid in Toka Toka Gold kumara were carried out using glucoronic and galacturonic acid as standards, following the methodology of Blumenkrantz and Asboe-Hansen (1973). Uronic acid is a good indicator of middle lamella breakdown as it is a major constituent of pectic substances which make up the sweet potato cell wall material.

Two reagents were used to determine uronic acid concentration. A 15% solution of meta-hydroxydiphenyl solution (MHS) (Aldrich Chemical Company, Inc.) was prepared in 0.5% NaOH. H_2SO_4/sodium tetraborate solution (SATS) was prepared by making a 0.0125M solution of tetraborate in concentrated sulphuric acid (98%).

Aliquots (0.2mL) of standard solution or sample containing from 0.5 to 20μg uronic acids, were put into cooled tubes that were refrigerated in crushed ice and, 1.2 mL of SATS was added and mixed. The mixture was shaken in a vortex mixer and then tubes were heated in a water bath at 100°C for 5 minutes. Tubes were then cooled in an ice-water- bath, and 20 μL the MHS reagent was added. The tubes were shaken and the absorbance at 520nm was measured in a spectrophotometer (Hitachi U-2000). Glucuronic and galacturonic acids were used as standards.

As carbohydrates produce a pinkish chromogen with sulphuric acids/tetraborate at 100°C, a blank was run without addition of the reagent, which was replaced by 20 μL of 20% NaOH.

All chemicals were sourced from The British Drugs Houses Ltd. (BDH Ltd.) and Aldrich Chemical Company, Inc.

5.2.3.6. Ungelatinised starch

A differential scanning calorimeter (DSC) (Perkin Elmer, model DSC7), with a thermal analysis controller (model TAC 7/DX) was used to determine ungelatinised starch levels. The DSC was connected to a Neslab cooler system (endocal ULT95) which recirculated ethanol coolant through the DSC at 0°C.

The onset temperature (°C), peak temperature (°C), transition energy (J/g) and total area under each peak were obtained using Pyris (version 3.81) thermal analysis system software (Perkin Elmer Instruments).

Samples from kumara were cut and weighed (approximately 10mg), placed into the aluminium pan (Perkin-Elmer Kit No. 219-0062) and sealed carefully. In order to know the sample weight, the empty aluminium pan was first weighed using a Sartorius M2P microbalance (±0.001mg), and by subtraction from the total weight (after the hermetic pan was sealed), the sample weight was determined.

The samples were heated from 30°C to 100°C, at a heating rate of 5°C/min. The equipment was calibrated (see Table 5-2) using indium and zinc as a reference following the equipment guidlines. Before each calibration a baseline was made over three different temperature ranges; 20-110°C for sample readings, 100-200°C for indium standard readings and 370-470°C for zinc standard readings.

Table 5-2 Standard elements for DSC calibration

Element	Onset (°C)	Transition energy (J)	Weight (mg)
Zinc	419.47	108.37	9.173
Indium	156.60	28.45	9.870

Thermal properties of isolated starch have been studied using DSC (Noda *et al.*, 1997, Zhang and Oates, 1999, Walter Jr. *et al.*, 2000). These results suggest there is a direct relationship between starch composition (amount of amylopectin and amylose) and the enthalpy of gelatinisation measured by DSC.

Figure 5-4 shows a typical endothermic thermogram for a kumara sample. Peak temperature, area under the curve, onset temperature and the transition energy (ΔH) of gelatinisation state were obtained. The transition energy was assumed to be proportional to the amount of ungelatinised starch present in the sample.

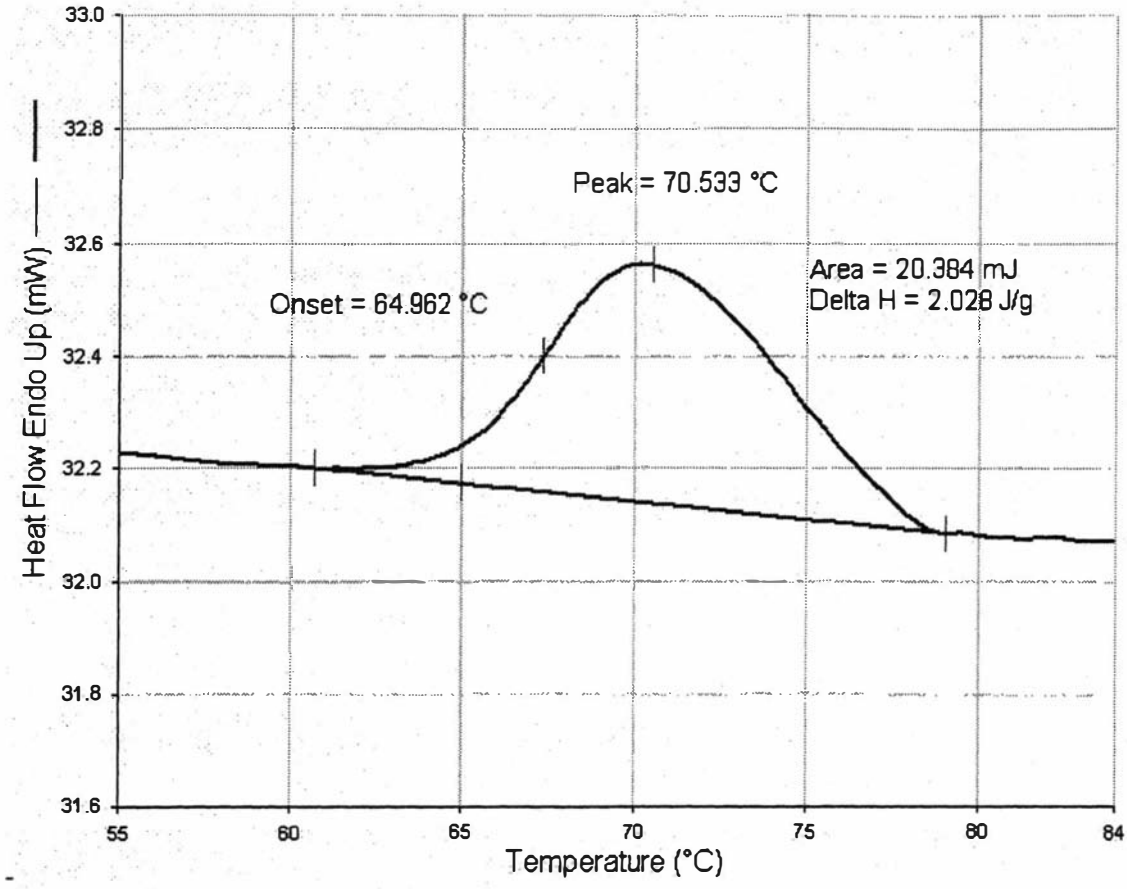

Figure 5-4 Typical endothermic thermogram (kumara) obtained from DSC

5.2.3.7. Texture

Numerous methods for quantitative evaluation of texture in vegetables have been used in the past. Watson and Jarvis (1995) measured firmness of sweet potatoes using the force required to cut tissue with a thin wire, this method was adapted from potato (Freeman *et al.*, 1992).

The fracture mechanism of uncooked potato was studied by Fahloul and Scanlon (1996). The samples were tested using a tensile test in block shape samples and the fracture toughness was quantified.

Truong *et al,*. (1997) used an Instron Universal Testing Machine to study the relationship between instrumental and sensory parameters using cylinders from cooked sweetpotato samples. They found that uniaxial compression and texture profile analysis (TPA as fracturability, hardness and gumminess) were linearly related ($R^2 \geq 0.95$), and both correlated highly with mouthfeel and mechanical-type sensory notes. Similar findings were reported by Thybo and Martens (1999) who worked with cooked potato at different storage times. They related uniaxial compression, TPA, chemical component and sensory analysis.

The uniaxial compression between two flat parallel plates is the simplest and most commonly used method for evaluation of the mechanical properties of solids, especially for determining deformation and fracture properties of food (Alvarez and Canet, 2002).

Fracture is an important property that affects the texture, and it is considered to occur when all bonds between the structural elements in a microscopic plane break, resulting in a breakdown of the structure of the material (Rosenthal, 1999).

During compression, the shape of the test piece may be affected due to friction between the test piece and the plates. Lubricant (immersion oil)was used in order to minimise this effect. Another important consideration is the length-diameter ratio of samples. If the ratio is more than 1.5 buckling may occur in this sample (Rosenthal, 1999).

Uniaxial compression tests were performed using a TA-XT2 texture analyser. An aluminium probe (35mm in diameter) was used with a calibrated 25kg load cell (25-1). The entire test was performed at room temperature (15°C) at a test speed of 1.6mm/s. The force in compression, gradient, area and distance to the fracture point data were analysed and collected using "Texture Expert" software, version 1.19 (Stable Microsystems Ltd. 1998).

5.2.3.8. Scanning electron microscopy (SEM)

In order to observe the cell wall breakdown and the fracture plane in kumara after crushing, samples were analysed using scanning electron microscopy (SEM).

Samples of gold and red kumara were prepared as above for textural analysis. Each sample was crushed in the texturometer as for a normal texture force evaluation. A thin slice of each sample was removed from the surface of the fracture plane and these were freeze dried.

Pieces of tissue taken from the region of the fracture plane, approximately 4x4mm in size, were mounted onto aluminium specimen stubs using double-sided tape and conductive silver paint, sputter coated with approximately 100nm of gold and studied using a Cambridge 250Mk 3 Scanning Electron Microscope. Photos were recorded at the chosen magnifications on Ilford FP4 black and white film.

5.3. PRELIMINARY OBSERVATIONS

A series of preliminary experiments were carried out to observe the magnitude of changes in kumara composition that occur during cooking.

5.3.1. Changes to chemical composition

Samples of gold kumara were cooked at 100°C for 30minutes and analysed as described above. The results of the preliminary experiments are shown in Table 5-3 below.

Table 5-3 Chemical composition variation in Owairaka Red and Toka Toka Gold kumara, before and after cooking at 100°C for 30min.

Samples	Condition	Moisture (% fwb)	AIS (% dw/fw)	TRS (g/100g fwb)	Maltose (% fwb)
GC	**Cooked**	74.68	16.72	4.59	7.87
GC	**Fresh**	71.73	23.87	0.01	3.37
GF	**Cooked**	72.53	19.86	3.37	7.18
GF	**Fresh**	69.70	26.38	0.00	2.87
GI	**Cooked**	71.89	19.77	5.72	7.74
GI	**Fresh**	70.49	25.10	0.00	3.30
Average	**Cooked**	73.033	18.783	4.56	7.597
Average	**Fresh**	70.64	25.117	0.003	3.18
s.e.	**Cooked**	0.8448	1.032	0.679	0.212
s.e	**Fresh**	0.591	0.725	0.003	0.156

AIS; alcohol insoluble solid: TRS; total reducing sugars

The reduction in the levels of AIS suggests that the cell integrity of the kumara decreased during cooking. This observation is supported by the marked increase in the levels of TRS in the samples as a result of cooking. These trends are consistent with the hypothesised mechanism of breakdown of the middle lamella as a result of pectin

hydrolysis.

Maltose levels increased significantly between uncooked and cooked kumara, most likely as a result of starch hydrolysis by α- and β-*amylase* activity (Striyer, 1988; Hagenimana *et al.*, 1994).

In uncooked kumara samples, an endothermic peak was evident (see **Figure 5-5**). This peak is a result of starch gelatinisation (Zhang and Oates, 1999, Walter Jr. *et al.*, 2000). The heat of reaction obtained by integrating the area under the curve divided by the scanning rate, was 1.95±0.25J/g (ΔH). The literature reported transition energy values for pure sweet potato starch of 16.5J/g (ΔH_{Lit}) (range from 13.7 to 25.63 J/g) (Rahman, 1995, Noda *et al.*, 1997, Zhang and Oates, 1999, Walter Jr. *et al.*, 2000). Using the transition energy obtained in the current experiment and the energy reported by literature from pure sweet potato starch, an estimation of starch levels in kumara samples can be calculated following *Equation 5-8*;

$$Starch = 100 \cdot \frac{\Delta H}{\Delta H_{Lit}} \qquad \textit{Equation 5-8}$$

where,

Starch is the starch content (%)
ΔH is the average of transition energy obtained in this study (J/g)
ΔH_{Lit} is the average of transition energy for pure starch from literature (J/g)

The starch content estimated was 11.8% (per 100g fresh kumara basis) which is comparable with values reported for starch levels for kumara in the literature of 5 to 29 % (see Table 2-3, in Chapter 2).

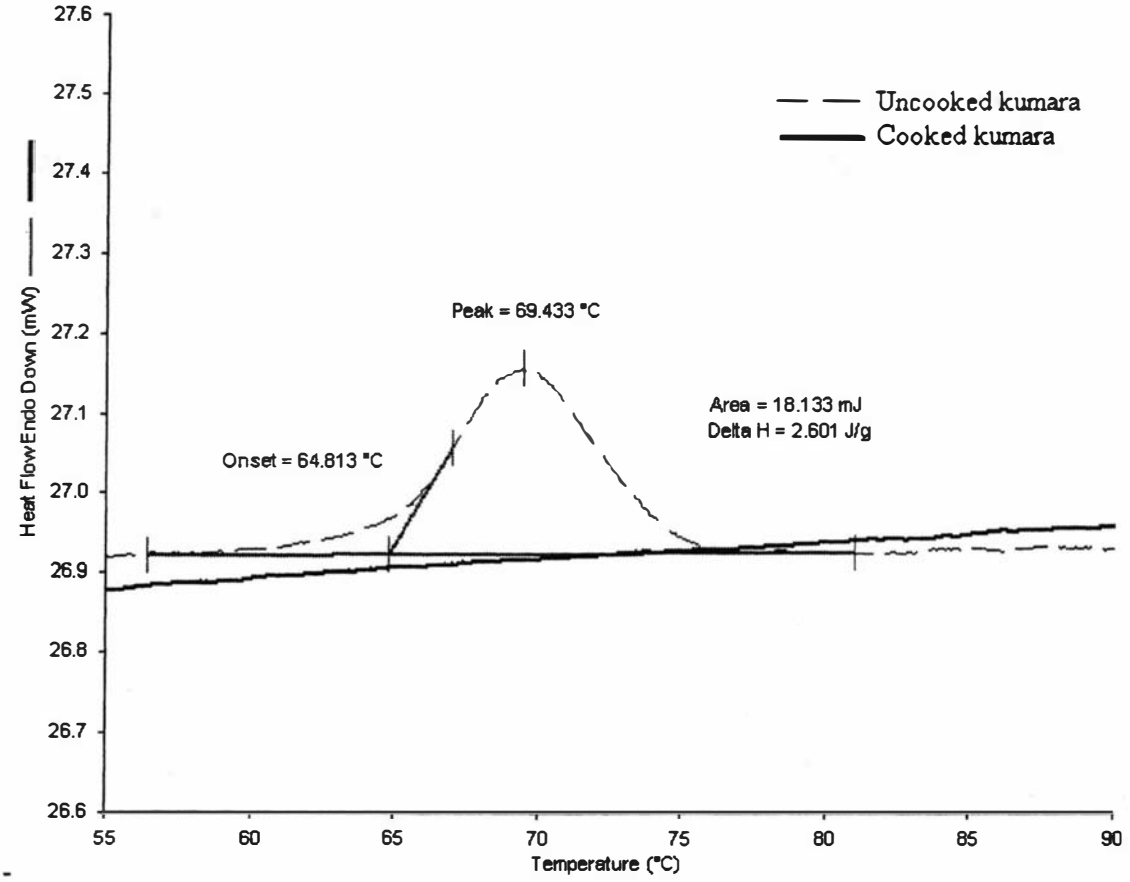

Figure 5-5 Endothermic thermogram for uncooked and fully cooked at 100°C/30min kumara samples

The DSC thermogram for the cooked kumara samples showed no evidence of starch gelatinisation (Figure 5-5) which demonstrated that all the starch had gelatinised during the sample cooking.

5.3.2. Texture

The texture was measured using a TA-XT2 texture analyser as described above in 5.2.3.6.

Figure 5-6 shows the fracture point on the gold kumara cylinder samples (1.5cm diameter and 1.5cm length) during cooking at 100°C (Note that the scale for 0 to 4 minutes samples are different to the remaining data on the graph).

This graph shows that after 4 minutes there was a dramatic drop off in peak force, strain at fracture, initial slope and area under the curve, and that this technique could demonstrate variations in texture samples during cooking.

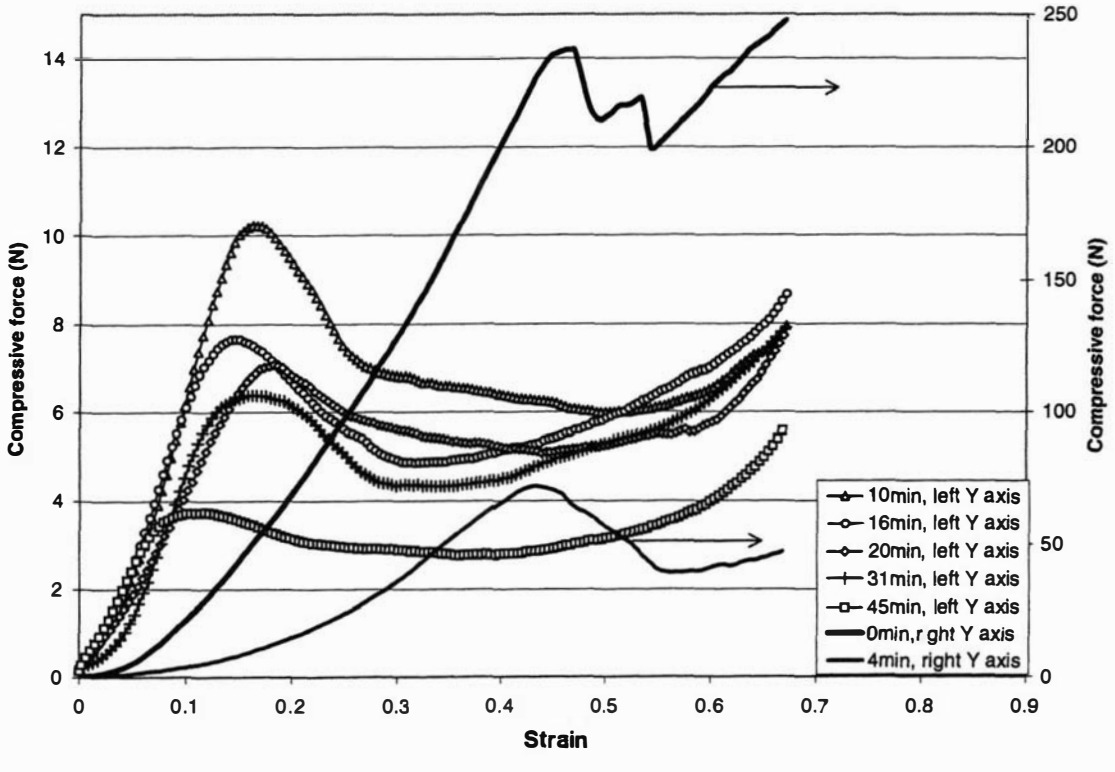

Figure 5-6 Uniaxial compressive force behaviour on kumara cylinder, cooked at different length times

Figure 5-7 is a typical force versus distance profile observed for a kumara sample. Due to the complex nature of fracture under compression, a number of possible measures of sample strength are possible. These include; force in compression (N), distance (cm) or strain to reach the fracture point (work done), the area (N*cm) under the curve until fracture point, and the initial gradient (N/cm) which is related to the Youngs Modulus of the sample (see Figure 5-7).

The strain can be calculated considering that it is the ratio of the dimensional change divided by the starting dimension of the sample (Rosenthal, 1999).

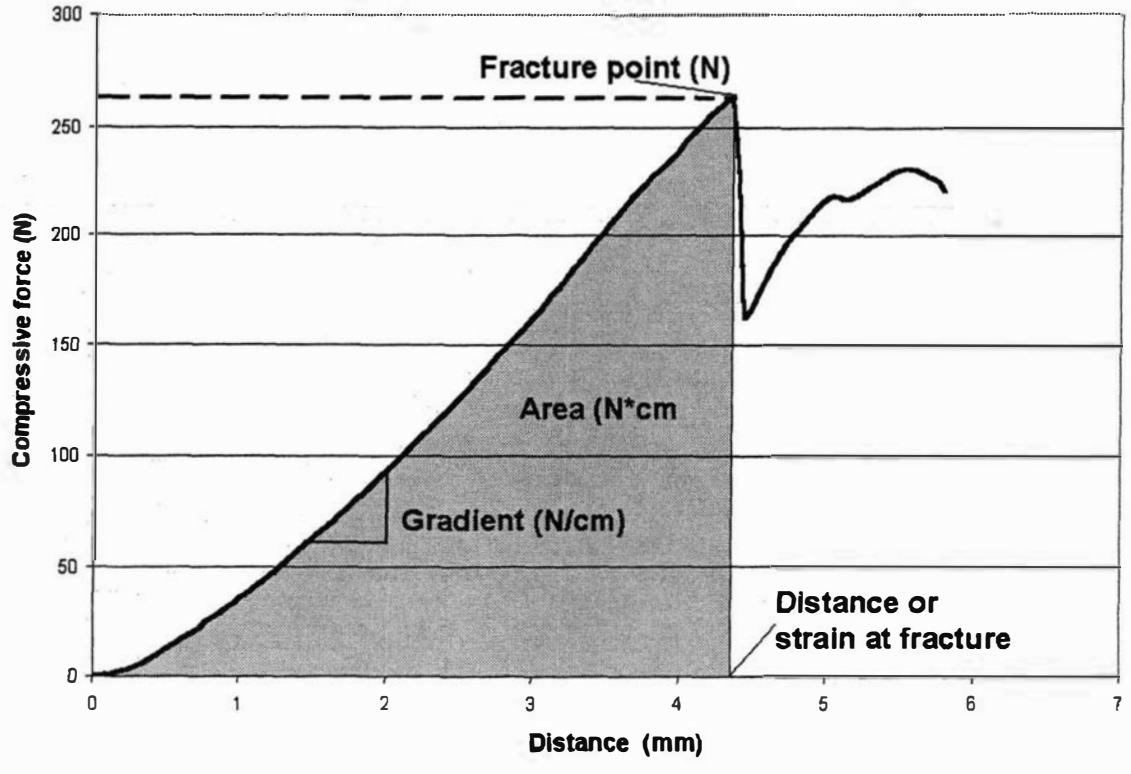

Figure 5-7 Typical chart of TA-TXS texture analyser

To test to see which of these measures is the most suitable for the evaluation of kumara, experiments were carried out in which kumara (both gold and red) were cooked as described in section above (5.2.2) at 75°C for 40 minutes. Over this time some of the cylindrical samples were removed from the water bath and rapidly cooled in an ice water slurry to halt cooking. The texture of each sample was measured, as described above, using the TX2-Texture analyser

To add clarity in analysing, data (Figure 5-8 **a** and **b**) was constructed to summarise each of these parameters as a time series for gold and red kumara respectively.

Peak texture force showed less variation between replicate samples at each cooking time than the area under the curve. The gradient decreased quickly in both types of kumara meaning this measure was not as sensitive as peak force in following changes to kumara texture. Finally, distance did not show a consistent trend during the cooking process. As a result it was decided to evaluate texture in subsequent experiments with the peak fracture force.

According to data from this preliminary experiment, AIS (%), maltose (%), TRS (gglucose/100g), ungelatinised starch (J/g), and fracture force (N) using an uniaxial compression force can be used to quantify the texture change, and the factors that are involved in the proposed mechanism (Figure 5-1).

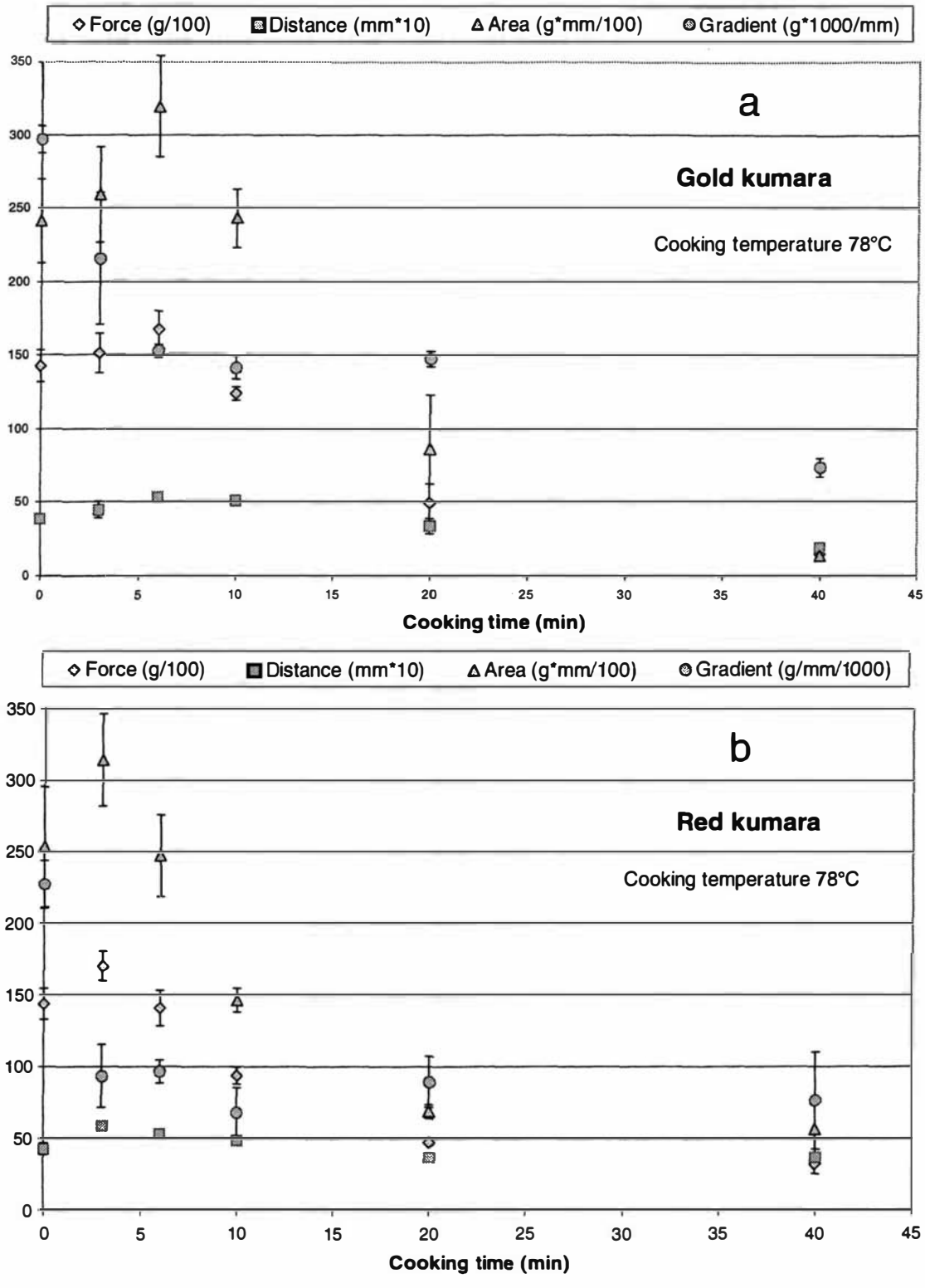

Figure 5-8 Texture parameters in Owairaka Red and Toka Toka Gold Kumara cooked at 78°C for different cooking times (see raw data Appendix A3)

5.3.3. Texture mechanism evaluation

Nine roots of Toka Toka Gold and five roots of Owairaka Red, were selected and prepared as described in section 5.2.1.

Two cooking temperatures were selected (70 and 80°C) and uncooked samples were used as controls. The experimental design was a complete randomised block design, with 9 blocks (GA, GB. GC, GD, GE, GF, GG, GH, GI, RA, RB, RC, RD, RE). Details of each kumara are summarised in Table 5-1 above.

From the fracture force analysis, four roots of gold kumara (GB, GD, GE, GH) and three from red kumara (RC, RD, RE) were selected to determinate moisture, AIS, maltose, TRS, and ungelatinised starch levels at each cooking temperature. These samples were representative of the range for observed textural changes shown in Figure 5-9.

Figure 5-9 shows the effect of temperature on the fracture force in kumara cooked at 70 and 80°C, using uncooked samples as a control. It is clear that the main effects to texture occurred after high temperature (80°C) cooking.

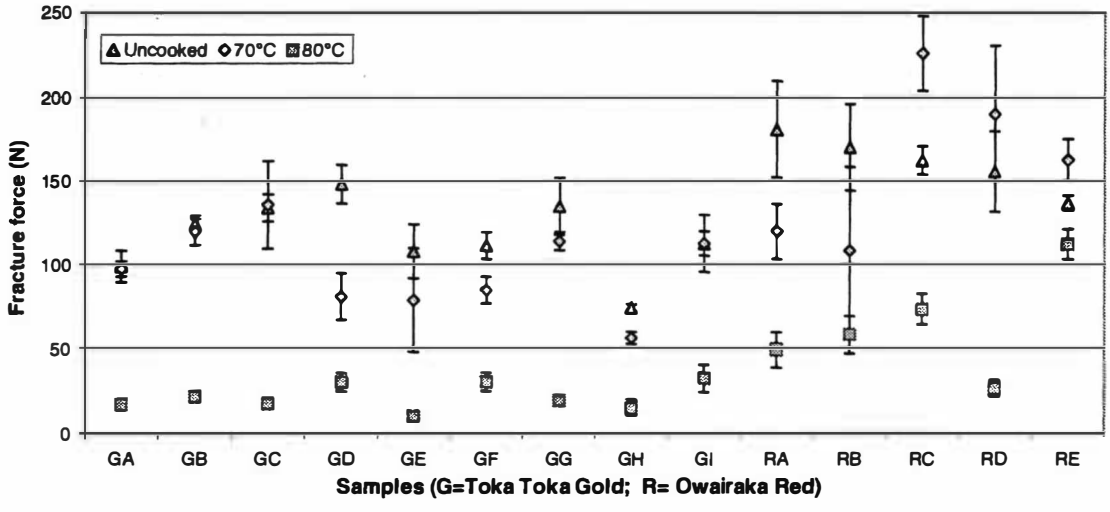

Figure 5-9 Textural behaviour in kumara cylinders cooked at different temperatures

Although the information about the samples' history during plant-growing and post harvest period is limited and was not part of the scope of this research, some observations of the raw material characteristics in the texture have been possible to obtain.

The gold kumara had an uniform behaviour in almost all the samples. Root GH had the lowest fracture force. This sample was identified as a JA cultivar harvested during the 2002 season. The long time in storage decreased the hardness' characteristics of the roots. This is evident when the GH results are compared against the GA samples, which was the same cultivar grown in the same location, but harvested one season later (2003). During storage, kumara roots have an continuous carbohydrate consumption for respiration process and other physiological activities. As a result, the carbohydrates concentrations change, specifically a decrease in starch and a increase of sucrose occurs during storage (Woolfe, 1992b). The texture decreases during storage time due to the moisture content decrease as well.

The experimental design used in this experiment allows block to block variations to be removed from the data to allow more clear observation on the effect of cooking temperature on textural and compositional changes. This was carried out using SAS software package.

Figure 5-10 shows that the texture decreased when the cooking temperature increased but note that the texture of the samples increased at 70°C in red kumara. This can be explained by the starch gelatinisation reaction.

It is also evident in Figure 5-10, that moisture levels did not change significantly.

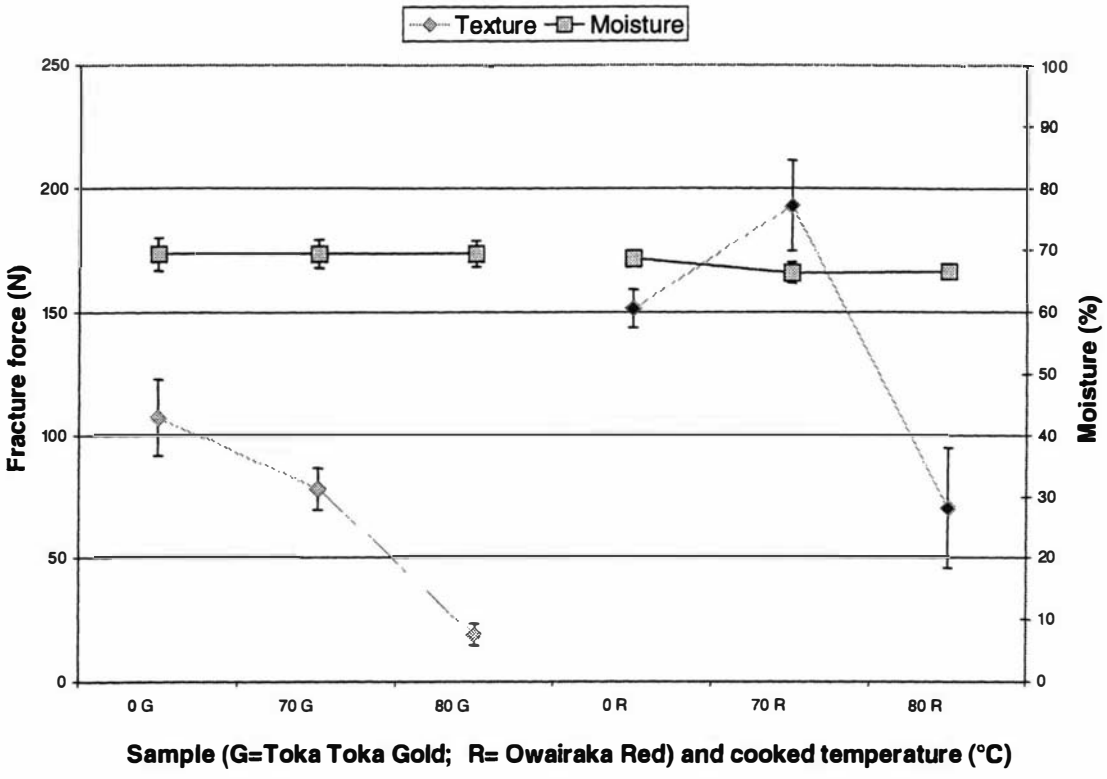

Figure 5-10 Comparison between moisture content (%) and fracture force (*N*) behaviour at different cooking temperatures in Owairaka Red and Toka Toka Gold kumara (see raw data Appendix A3)

During the cooking process at 70°C, (above the gelatinisation temperature), the starch granule located inside the cell begins to swell, and with this the pressure inside the cell is also increased (Jarvis *et al.*, 1992). This mechanical effect explains why the samples had a firmer texture at 70°C. Figure 5-11 shows the SEM images of the starch granules in uncooked sample (A) and granules present in the sample cooked at 70°C. In both cases the fracture of the kumara samples occurred across the cells suggesting that breakdown of the middle lamella has not occurred significantly at this cooking temperature and therefore the cells are still well bound to each other. Figure 5-11 clearly shows that the starch granules are a lot more swollen in samples cooked at 70°C than

those that were uncooked.

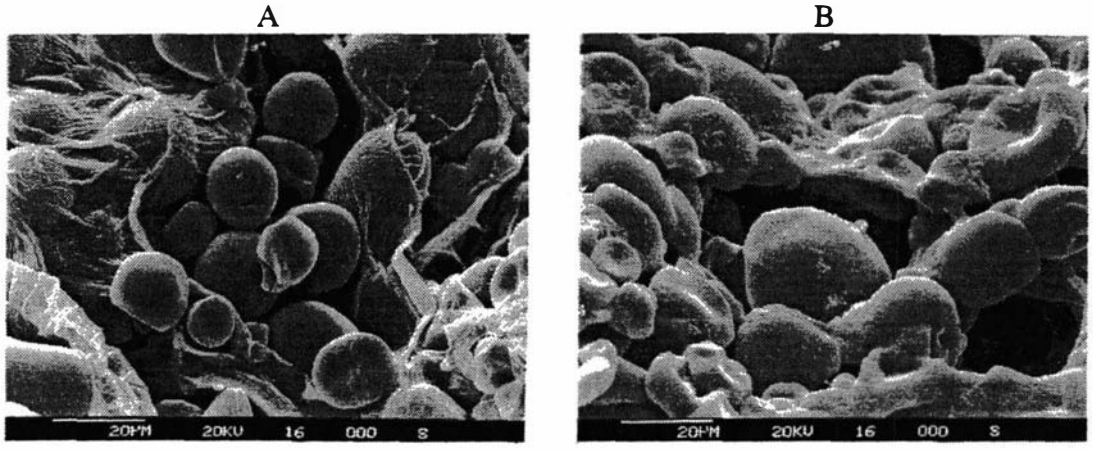

Figure 5-11 SEM photomicrograph of Owairaka Red kumara starch granules in uncooked (A), and cooked at 70°C (B) of freeze-dried samples

In other vegetables, cooking at 70°C increases the firmness of the texture by cell wall modification due to a pectin methyl esterase effect, which protects the pectin polysaccharides from thermal depolymerisation. Binner *et al.* (2000) however proved that the main effect in sweet potatoes is due to starch granule pressure.

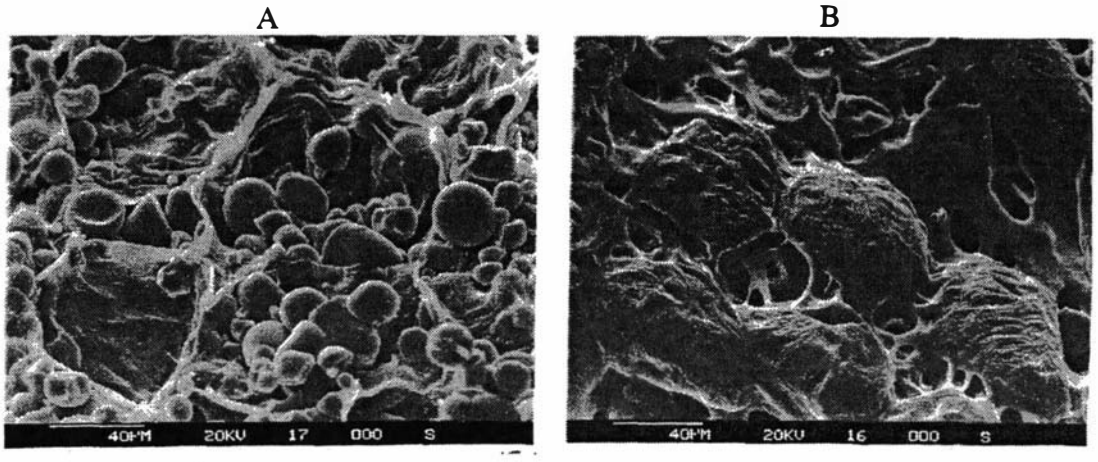

Figure 5-12 SEM photomicrograph of fracture section of uncooked of Owairaka Red kumara tissue (A) and tissue cooked at 80°C (B)

The difference of fracture force between uncooked samples and totally cooked samples (80°C) can be explained by the change in the fracture properties of the tissue. While the fracture in uncooked tissue is across cells, in cooked samples the fracture is along middle lamellae (Rosenthal, 1999). Figure 5-12 (A) shows the starch granules present in the intra-cell spaces, due to the fracture plane dividing the cell. In contrast, in **B**, the SEM photomicrograph shows intact cells. The fracture did not destroy the cell integrity, but instead fractured along the middle lamella boundary adjoining cells.

Determinations of uronic acid in Toka Toka Gold kumara were carried out using galacturonic acid as standard, and follow the methodology proposed by Blumenkrantz and Asboe-Hansen (1973). The results showed that the average of uronic acid concentration increased from 0.32±0.07 to 1.33±0.25 (Table 5-4) when the samples were cooked at 70 and 83 °C, in Toka Toka Gold. Uronic acid is a major product of pectin substance (polymers of galacturonic) in insulated sweet potato cell wall material (Binner *et al.*, 2000). Therefore these results indicate that the extent of middle lamella breakdown in samples cooked at 83°C was much greater than in those cooked at 70°C.

Table 5-4 Uronic acids (Glucoronic acid) content at different cooked time and temperature in Toka Toka Gold kumara

Cook		mg/gfb	
Temperature (°C)	*Time (min)*	*Glucoronic acid*	*Galacturonic acid*
80	0	0.36	0.31
80	40	1.12	0.98
83	0	0.36	0.31
83	40	1.65	1.44
75	0	0.33	0.29
75	40	1.14	1.00
70	0	0.21	0.18
70	40	1.39	1.21
Average	*0*	*0.315*	*0.273*
St.dev.	*0*	*0.078*	*0.068*
Average	*40*	*1.325*	*1.158*
St.dev.	*40*	*0.249*	*0.215*

Figure 5-13 confirms this finding showing that the cell wall material as measured by AIS decreased between uncooked and cooked samples. Similarly TRS levels increased significantly when cooking temperature was increased from 70 to 80°C (see Figure 5-14).

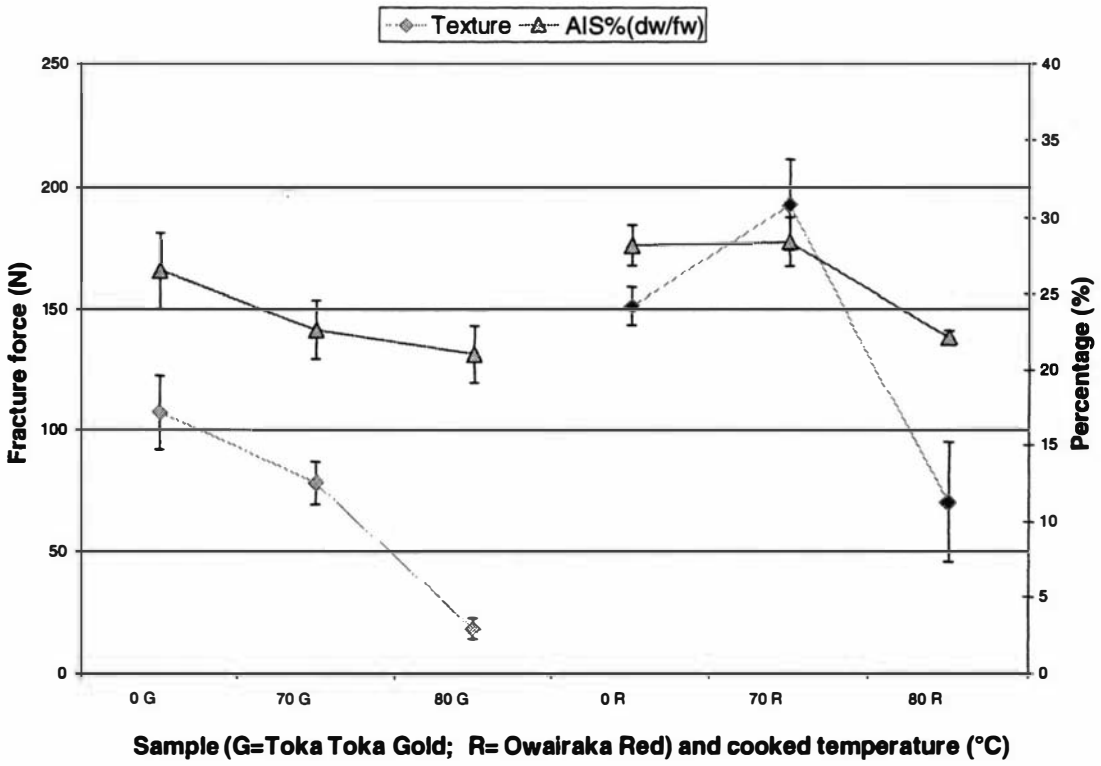

Figure 5-13 Comparison between AIS and fracture force at different cooking temperature.

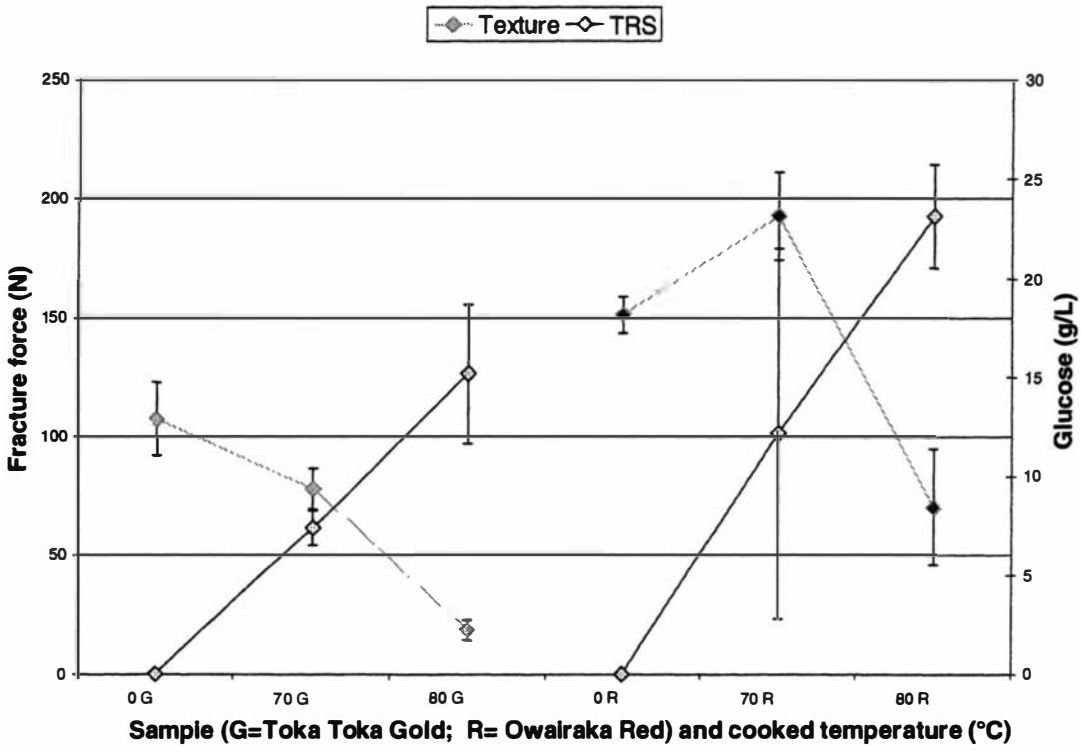

Figure 5-14 Comparisons between TRS and fracture force.

The amount of ungelatinised starch decreased during the cooking process, as shown in Figure 5-15. The transition energy (J/g) represents the amount of energy required for transformation from the granular (crystalline) to the gelatinised state (Zobel, 1984; Walter Jr. *et al.*, 2000).

On average, uncooked Red kumara had higher fracture force values than uncooked gold kumara (151.51±7.68N and 107.36±15.39N). The transition energy and peak temperatures (T_{max}) in both cases were 2.29±0.39 and 1.66±0.3 J/g respectively. This tendency supports the idea that the texture is highly influenced by the starch levels as suggested by on the texture mechanism proposed (Figure 5-1). According to Zhang and Oates (1999) low gelatinisation temperature in sweet potato starches had less amylopectin, the most complex and branched part of the starch granule. The low peak temperature in gold kumara is probably due to lower amylopectin levels in the starch constituent.

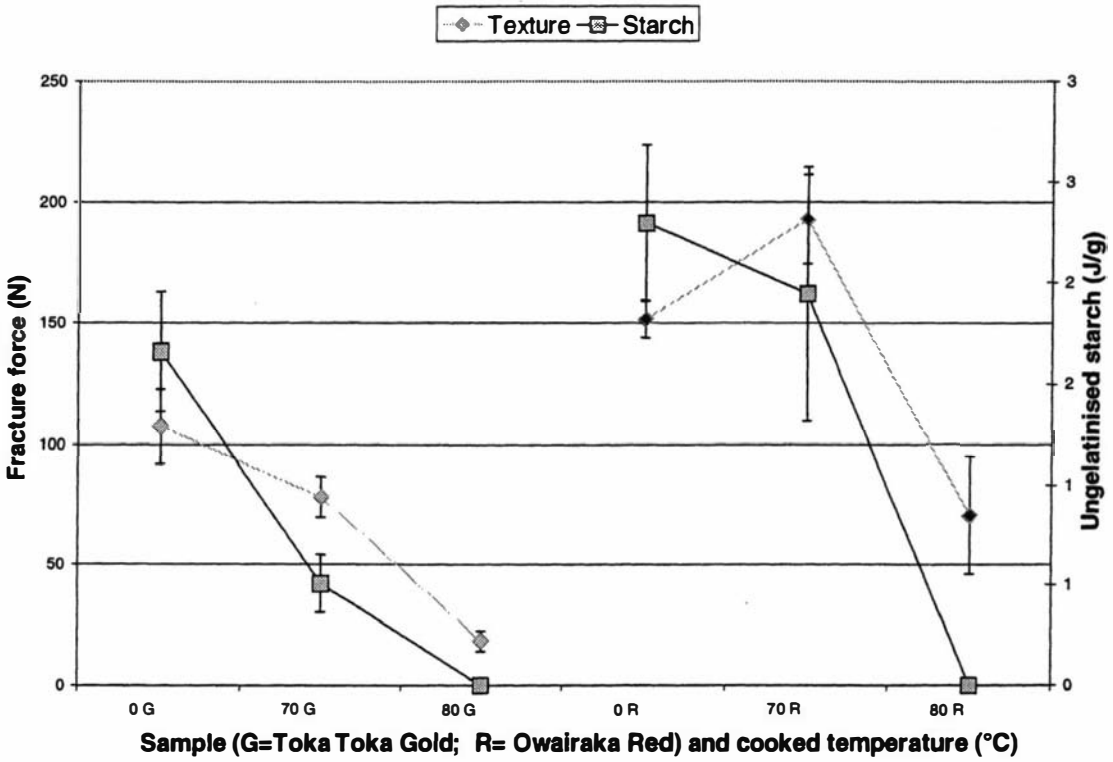

Figure 5-15 Comparison between ungelatinised starch content and fracture force

The peak and onset temperature in samples partially cooked (70°C) were higher than in uncooked samples. In Toka Toka Gold the peak temperatures were 65.25±0.52°C and 78.66±0.77°C for uncooked and kumara cooked at 70°C respectively, and in Owairaka red were 68.77±1.01°C and 77.52±0.35 for uncooked and cooked samples. The onset temperatures were 59.82±2.14°C and 75.41±1.26°C for uncooked and kumara cooked at 70°C for Toka Toka Gold, and in Owairaka red were 62.26±1.03°C and 74.73±0.93 for uncooked and cooked samples. Walter Jr. *et al.* (2000) have found onset temperature range from 55.7 to 62.1°C, and peak temperature from 62.8 to 71.9°C, although direct comparison is difficult as they worked with different cultivars of sweet potato.

The reason for the increase in peak and onset temperature observed in kumara on cooking starch is that the less ordered regions of the starch granule are hydrolysed first while the more highly structured regions remain unaltered. The more structured

portions of the granule require more energy to melt and hence increasing the peak onset temperature.

The starch hydrolysis reaction is due mainly to the group of amylase enzymes, which promote the starch conversion into less complex sugars like maltose, glucose, dextrin, etc. This results in reduction in starch content and increases in sugar levels (Figure 5-16) which could produce change in the texture and in the flavour of the product.

Hagenimana *et al.* (1994) studied the kinetics of amylases in sweet potatoes. α-amylase and β-amylase showed an optimum activity at 71.5°C and 53°C respectively. In addition α-amylases was more heat stable than β-amylases.

The results of Hagenimana *et al.* (1994) suggested that the maltose and sugar changes during the cooking process shown in Figure 5-16, were due mainly to α-amylase action.

It is interesting to note that only small changes in maltose levels were observed in kumara cooked at 70°C (particularly in Owairaka Red), even though Hagenimana *et al.*, (1994) stated that this is the optimal temperature for α-amylase activity. This suggests that starch hydrolysis is facilitated by starch gelatinisation. It is widely reported that gelatinisation greatly enhances the rate of enzymatic hydrolysis of starch (see e.g. Oates, 1997)

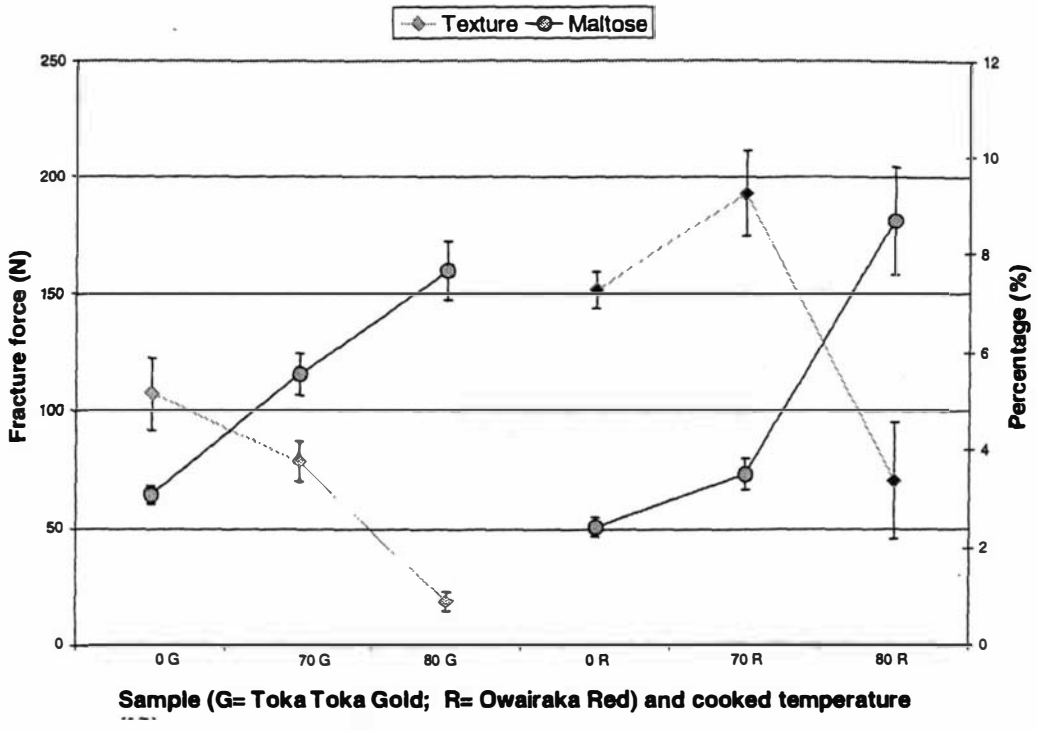

Figure 5-16 Comparison between maltose (%) and fracture force (*N*) behaviour at different cooking temperatures in Owairaka Red and Toka Toka Gold kumara

5.4. CONCLUSION

The results shown in this section support the proposed mechanism. The cooking process changed the kumara texture and consistent changes in starch gelatinisation, starch hydrolysis reaction and cell wall integrity were observed as well. These three reactions had a combined effect, and influenced the physical properties of the kumara.

The gelatinisation process produces a pressure increase inside the cell resulting in increased firmness. Starch gelatinisation also allows much more rapid amylase activity promoting hydrolysis of the starches and increases in sugar levels. Below the gelatinisation onset temperature there was no evidence of starch hydrolysis in kumara

samples.

Breakdown of the middle lamella ultimately results in softening of the texture due to a change in the fracture behaviour from across cells to along the middle lamella plane.

The cooking temperature affects all three reactions, especially when the temperature is higher than 70°C.

Understanding how the rates of each of these reactions are affected by temperature should further test the proposed mechanism and provide information to control the cooking process to optimise kumara texture. The measurement of the kinetics of these reactions and texture change is the focus of the next chapter.

CHAPTER 6: KUMARA TEXTURE KINETICS

6.1. INTRODUCTION

The kinetics of the textural changes in kumara roots is important in the processing industry as this knowledge provides the means for cooking process design and optimisation.

The thermal softening of vegetable tissue is often modelled as two first order reactions simultaneously occur (Huang and Bourne, 1983; Ramesh *et al.*, 1998). One of these reactions is believed to be the breakdown of the middle lamella layer but the second reaction is unknown. A number of researchers have been conducted with similar experiments in potato.

Alvarez and Canet (2002) found that potato texture could be modelled successfully with both first and second order kinetics. Harada *et al.*, (1985) found that potato texture changes during cooking could be modelled as a first order process.

The objective of this section was to determine the kinetics of the textural change reaction in kumara, and to compare this to the kinetics parameters of the reactions identified in chapter 5 as contributing to texture change.

6.2. EXPERIMENTAL PLAN AND METHODOLOGIES KINETICS OF TEXTURAL CHANGE

In order to describe and quantify the textural change, quantified by changes in the fracture force in uncooked and cooked kumara, samples were cooked at different temperatures. Fracture force, moisture content, alcohol insoluble solid (AIS), maltose content, total reducing sugars (TRS), and ungelatinised starch levels were determined at regular time intervals during the cooking process.

The fracture force and chemical determinations were carried out using the methodologies described in chapter 5 (section 5.2).

Temperature has a direct effect on cell wall disruption and promotes the starch hydrolysis. Maltose is a one of main products of the hydrolysed starch molecule (Woolfe, 1992b). As a result, the amount of maltose is good indicator of starch hydrolysis. Cell wall and lamella breakdown was quantified by following AIS reduction during cooking.

In order to determine the effect of the temperature and time on starch hydrolysis and cell wall disruption in kumara, slices of 1mm thickness were cut from fresh roots. The slices were packed into vacuum bags and cooked at different temperatures and times.

6.3. KINETICS OF TEXTURE CHANGES IN COOKED KUMARA

Samples from two gold roots (GA, and GB) and three red roots (RA, RC, and RD) were selected and cylinders were cut and packed into vacuum bags.

The samples were cooked at nine temperatures (60, 65, 70, 75, 78, 80, 83, 86 and 90°C) and sampled at six different cooking times (0, 3, 6, 12, 22, and 37min). The experimental design was a complete randomised block, and the samples were blocked by root.

Figure 6-1 and Figure 6-2 shows the texture variation at different cooking temperature and time in Toka Toka Gold and Owairaka Red kumara. The data are presented on separated graphs to provide clarity due to the large number of data points collected. Average results with error bars are presented as calculated using SAS.

The rate of texture change increased as a function of the cooking temperature. Samples cooked at low temperature (60 and 65°C) did not show significant reduction of texture. This was especially evident at 60°C where the texture increased during the cooking process for both cultivars. An explanation of that could be the starch granule swelling effect discussed in section 5.3.3 above.

Some trends to the texture changes are evident at 70°C and above for both gold and red kumara. At these conditions texture decreased as cooking proceeded. Between 75 and 80°C these changes were faster. From the literature information and data shown in Chapter 5, it is the range of temperature that all the reactions affecting texture have their optimum activity, especially the enzymatic reactions of pectin and starch hydrolysis.

Samples cooked at temperatures over 80°C lost firmness very quickly and reached completion of the reaction within the first five minutes.

The optimisation during thermal processing requires knowledge of kinetics of texture degradation. Kinetic parameters can provide valuable insight into understanding and predicting changes that occur from thermal processing.

Most of the literature reports for texture change or degradation in vegetables followed first order kinetics. This model is characterised by a straight line when the logarithm of the texture property is plotted against heating time (Rizvi and Tong, 1997).

The charts from 70°C to 90°C cooking temperatures were used to calculate the k value of each temperature. Figure 6-1 and 6-2 shown the texture changes at different cooking time and temperature in gold and red kumara.

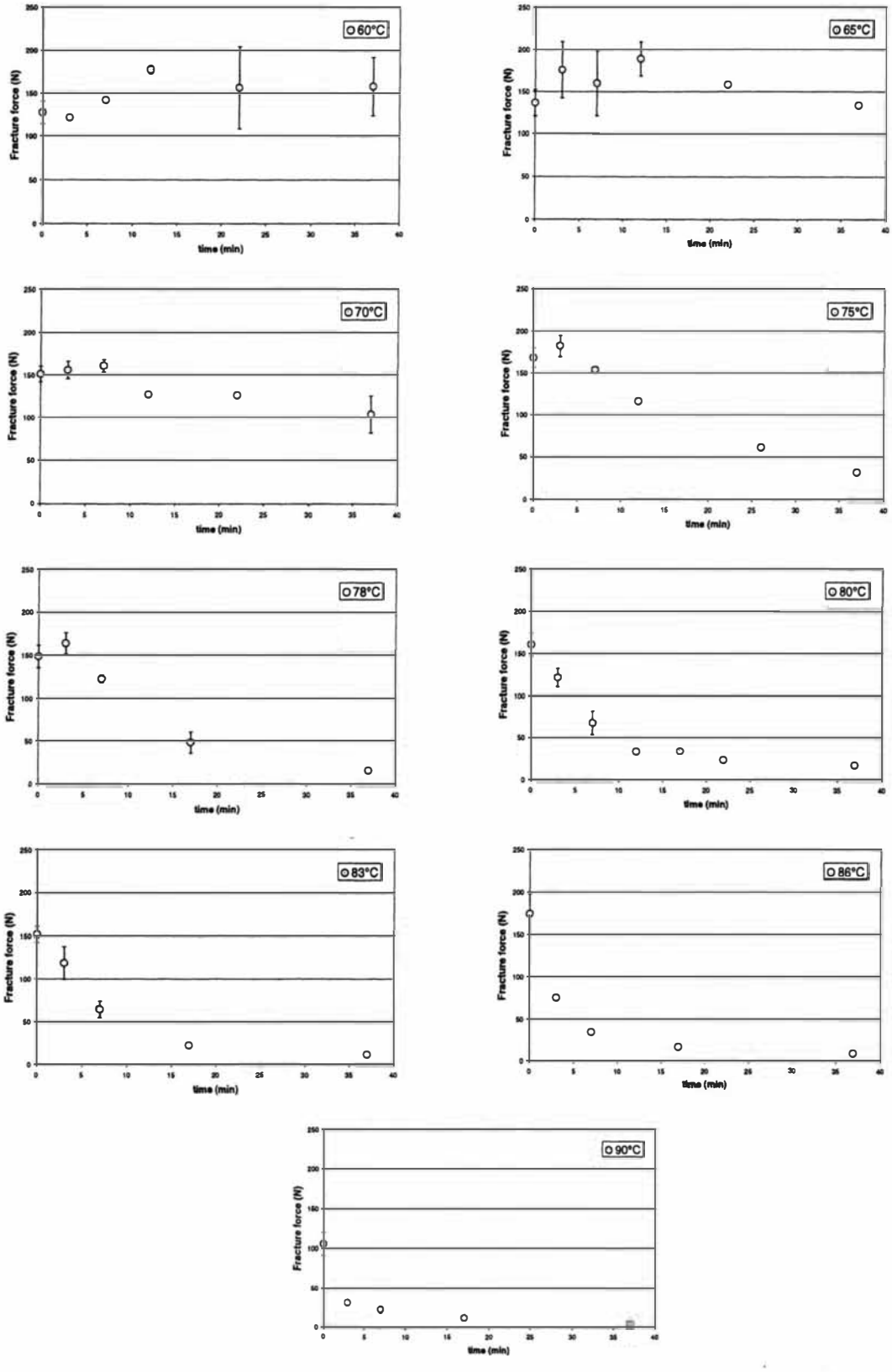

Figure 6-1 Texture (fracture force) changes in Gold kumara cooked at different temperatures (see raw data Appendix A3)

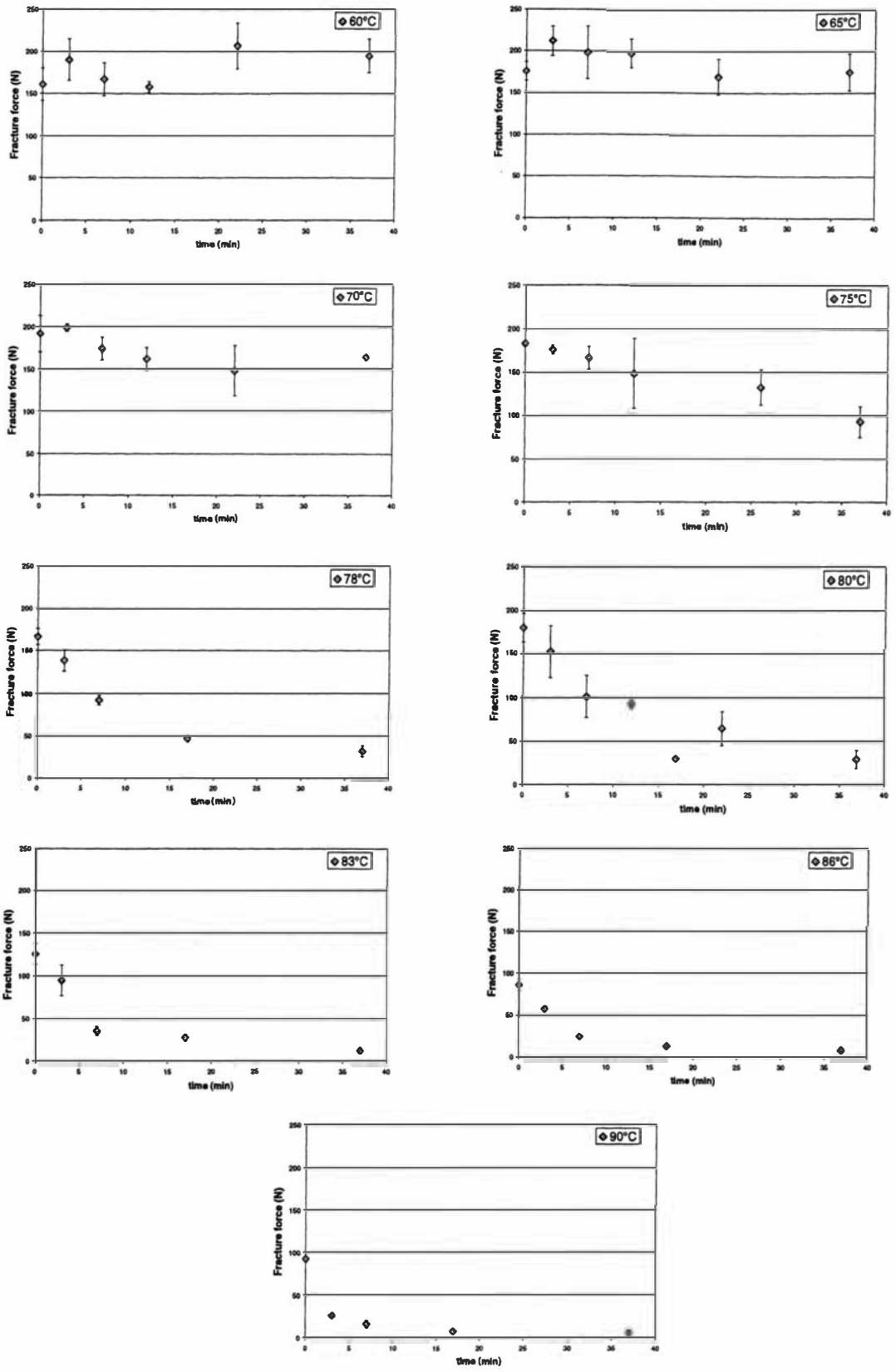

Figure 6-2 Extent of texture change in Red kumara cooked at different temperatures (see raw data Appendix A3)

From the information used in Figure 6-1 and 6-2, the extent of reactions (X) were calculated for each kind of kumara applying the follow equation,

$$X = 1 - \frac{(\Delta F_\infty - \Delta F_t)}{(\Delta F_\infty - \Delta F_i)} \qquad \textit{Equation 6-1}$$

where:

X is the extent of reaction

F_∞ is the fracture force at infinite time (N)

F_t is a the fracture force at time t (N)

F_i is the initial fracture force (t=*0min*) (N)

The rate of reaction can be obtained by plotting *ln(1-X)* versus *t (time)*, and from the Equation 6-2, it is clear that the slope is the negative of the rate constant k.

$$\ln(1 - X) = -kt \qquad \textit{Equation 6-2}$$

where:

X is extent of force change during cooking (dimensionless)

k is rate constant (min^{-1})

t is time (min)

A linear equation was fitted at each temperature and kumara cultivar, by least squares regression and the slope (-k) was obtained (see Figure 6-3 and Figure 6-4). The linearity of these plots confirm that texture degradation in kumara during the cooking process follows a first order reaction as shown by Rizvi and Tong (1997) for other vegetables.

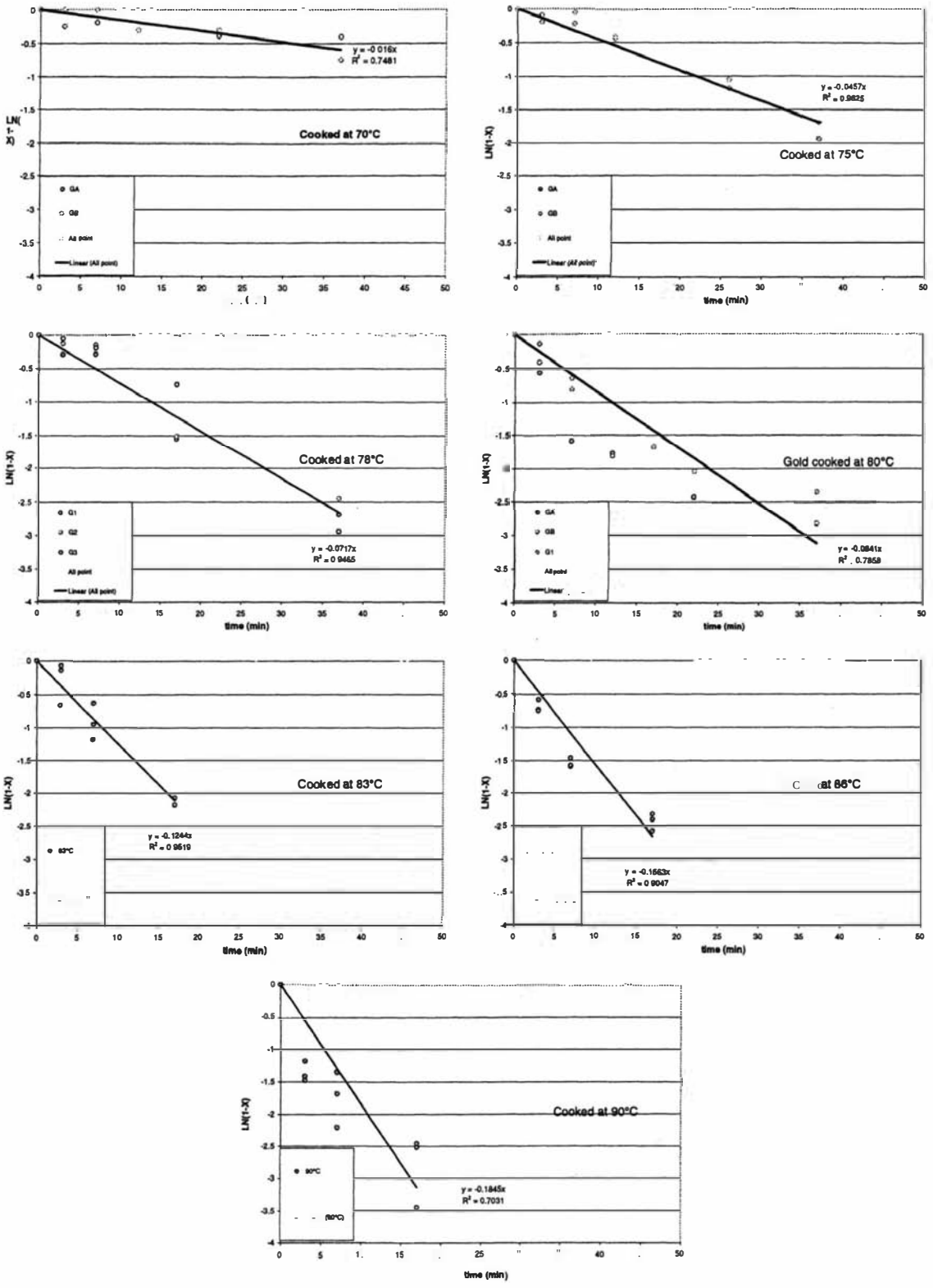

Figure 6-3 First order for Toka Toka Gold kumara cooked at different temperatures

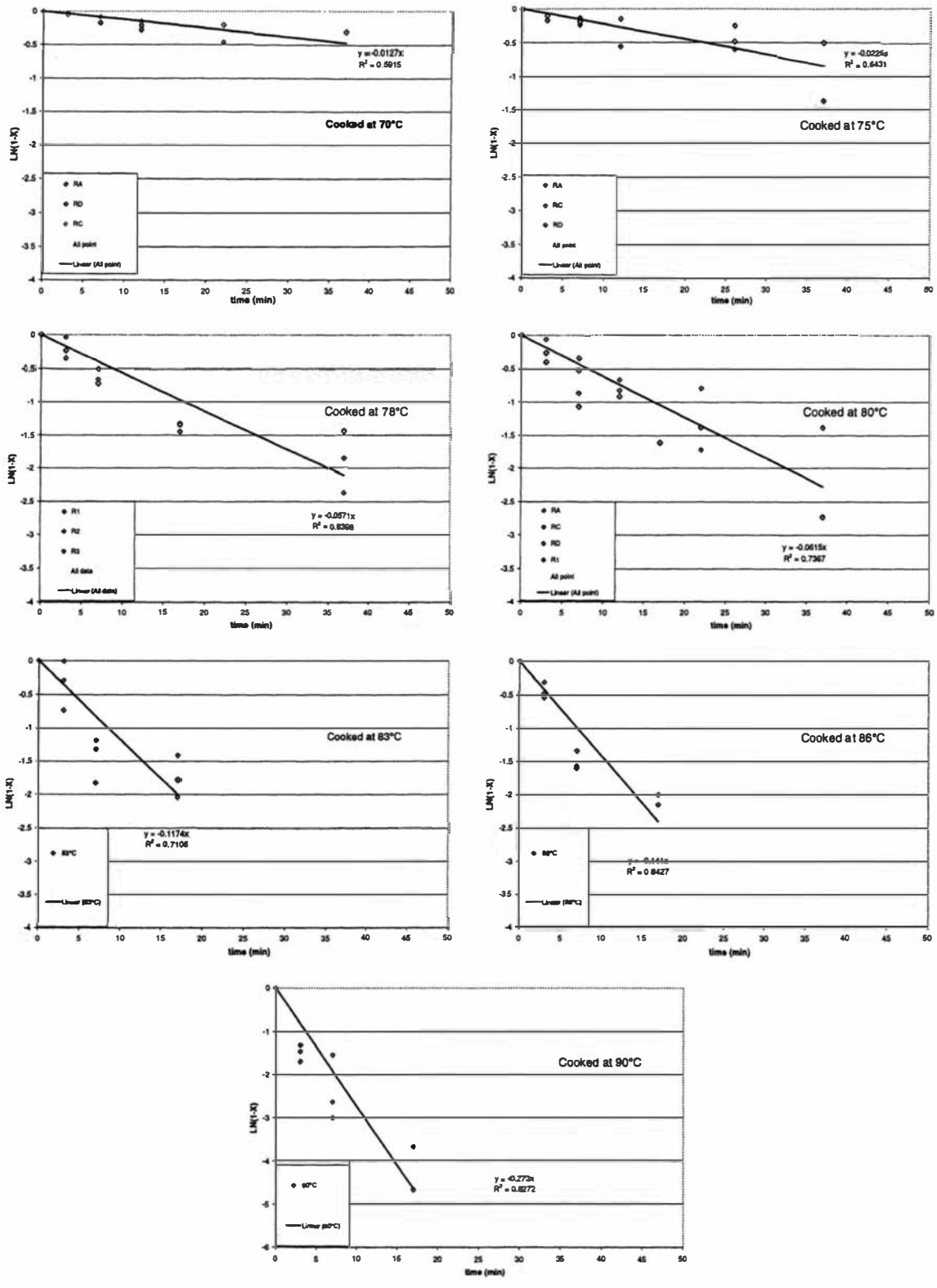

Figure 6-4 First order plots for Owairaka Red kumara cooked at different temperatures

The Arrhenius law describes the dependence of the rate constant on temperature. This relation can be described by Equation 6-3 (Levenspiel, 1999).

$$k = k_o \exp(-E_A/RT) \qquad \textit{Equation 6-3}$$

Where:

k_o is Arrhenius constant (min^{-1})

E_A is the activation energy (J)

T is absolute temperature (°K)

R is the universal gas constant (8.134 [J mol^{-1} K^{-1}]) (Cooper and Le Fevre, 1996)

The values of ln(k) for red and gold kumara were plotted against the reciprocal temperature of cooked temperature (1/T(K)) and a regression line fitted using least squares minimisation. The activation energy (E_a) of the reaction was calculated from the negative of the slope of the straight line and the Arrhenius constants (k_o) were obtained for each kumara from the intercept values (Figure 6-5).

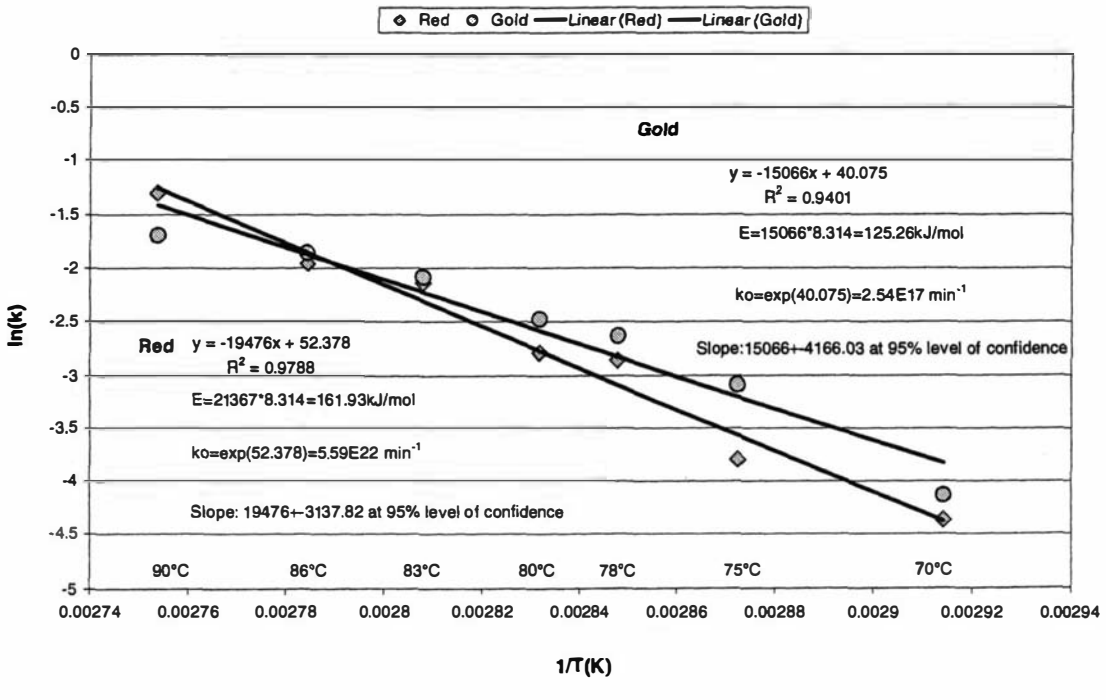

Figure 6-5 Arrhenius plot for the texture change reaction in Owairaka Red and Toka Toka Gold kumara

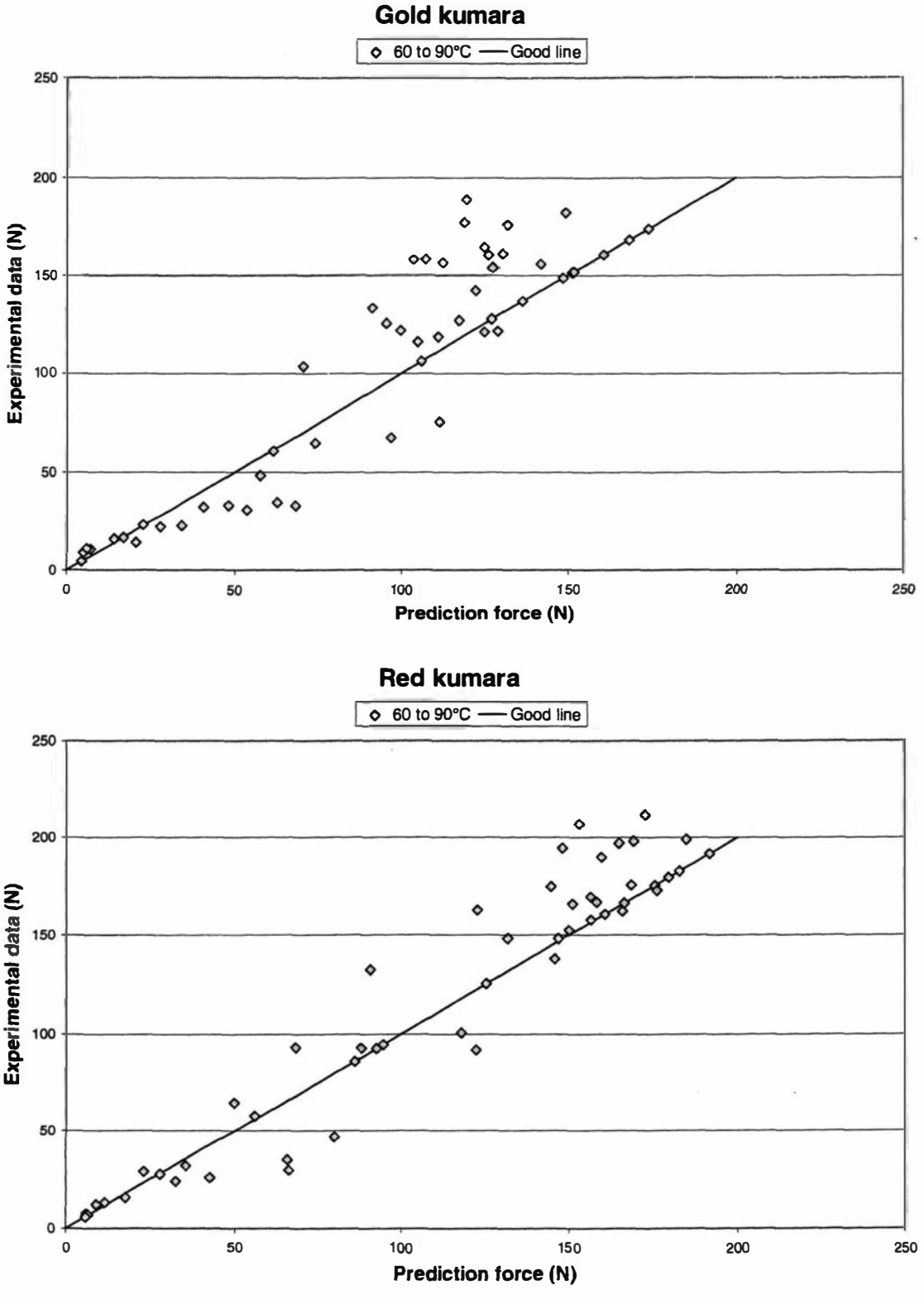

Figure 6-6 Prediction of fracture force (N) vs experimental data in kumara

The activation energies were found to be 125.26 kJ/mol and 161.93 kJ mol^{-1} for Owairaka Red and Toka Toka Gold respectively. These values are close to data obtained by Kozempel (1988) for cooked potatoes (k_o 7.8E16min^{-1}, E_a 126.95kJ mol^{-1}) for a temperature range between 74 to 110°C. Similarly, Verlinden *et al.* (1995) used values of activation energy equal to 102 kJ mol^{-1} (between 98 to 106 kJ mol^{-1}), for this simple model of texture kinetics in potatoes.

The first order model from this work was then used to predict texture for each time, and temperature data point of the experiments. This is shown in Figure 6-6 for both red and gold kumara.

This plot demonstrates that the fitted model is adequate to describe the rate of texture change in kumara during cooking.

Rearrangement of the integrated from the rate equation (Equation 6-2) and then substituting in the Arrhenius equation (Equation 6-3), the results in Equation 6-4 below.

$$t = \frac{\ln(1-X)}{\left(-k_o \exp\left(-E_a/RT\right)\right)} \qquad \textit{Equation 6-4}$$

Using this equation it is possible to calculate the time necessary to reach a specific extent of texture change (softening) as a function of cooking temperature.

Figure 6-7 shows this for X=0.1 and X=0.9 for both gold and red kumara.

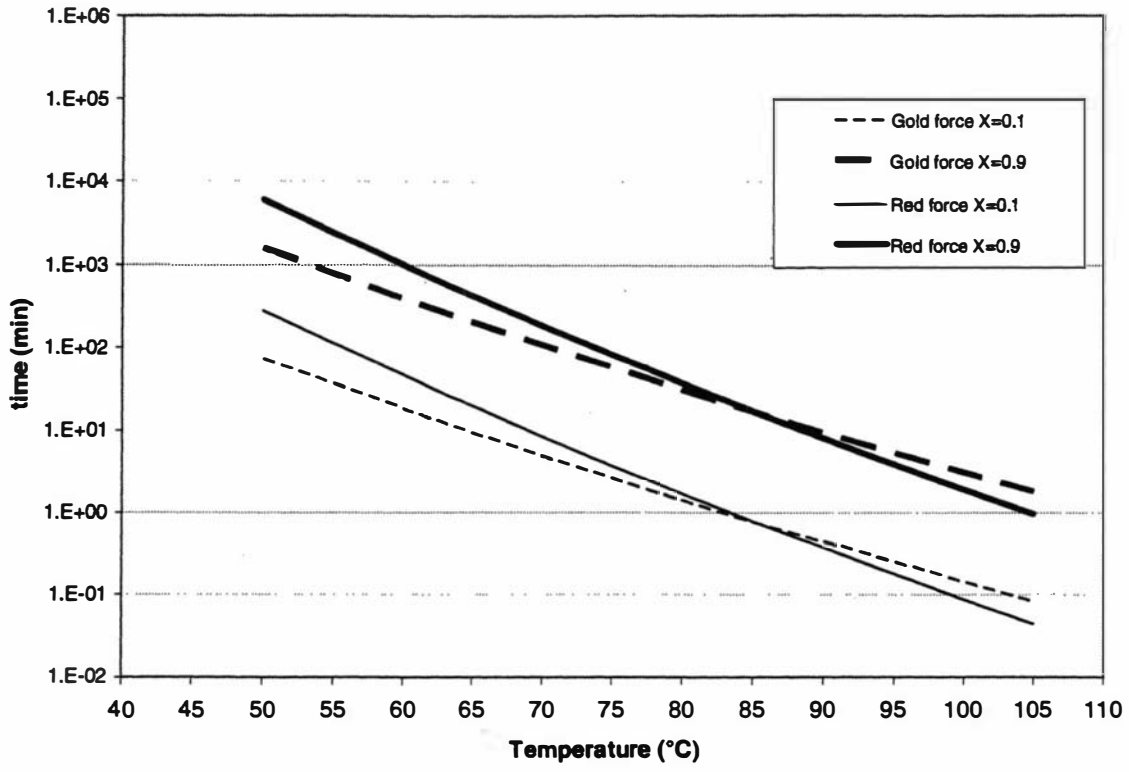

Figure 6-7 Cooking time required to achieve 10% and 90% texture change at different cooking temperatures for Toka Toka Gold and Owairaka Red kumara.

The red kumara at the lowest cooking temperature needs a longer time than the gold to reach the same completion of reaction (X=0.1 or X=0.9), however at higher temperatures (>85°C) the red kumara takes less time to reach the same extent of textural changes.

Figure 6-8 shows a comparison between kumara texture behaviour with data from literature for potatoes. The kinetics data presented by Harada *et al.*, (1985), Kozempel (1988), Rizvi and Tong (1997), and Alvarez and Canet (2002) were recalculated to provide Arrhenius constant and activation energy. In each case the kinetics data for the most closely matching method of texture measurement was used. In some case (particularly Alvarez and Canet, 2002) additional kinetics data was reported but was not included in this study. The predictions on Figure 6-8, were only made for the temperature range investigated in the original study.

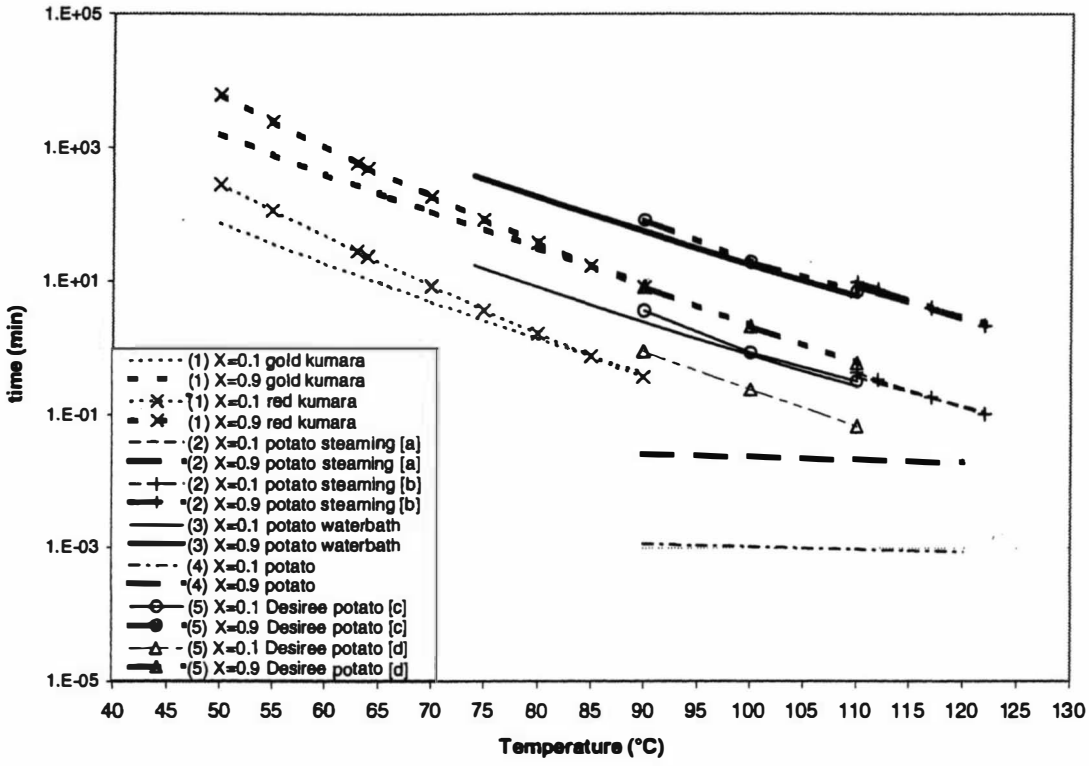

Figure 6-8 Comparison of texture change at different cooking temperatures. Note: (1) Kumara fracture force; (2) Alvarez and Canet (2002) [a: maximum compression force; b: maximum shear force]; (3) Kozempel (1988) peak force; (4) Rizvi and Tong(1997); and (5) Harada *et al.*, (1985) [c: shear force; d: sensory texture]

The results of texture kinetics obtained in the kumara are similar to those reported mentioned in the literature for cooked potato. The results from the literature used in general higher temperatures than those used in the current study. Rizvi and Tong (1997), using potato texture data from Rahardjo and Satry (1993) found much less temperature dependence on softening behaviour (number 4 in Figure 6-8) at different cooking temperatures. This result is due to the activation energy reported by Rahardjo and Satry (1993) which was very low (89.8kJ/mol). If these curves are not considered in the analysis, it is evident that a particular cooking temperature is faster than in potato, but the temperature dependence of the softening process is similar.

It is interesting to note that shear force data from Harada *et al.*, (1985) and Alvarez and Canet (2002), showed a similar slope even when the cooked temperatures range was different (see 2b, and 5c in Figure 6-8).

6.4. STARCH GELATINISATION KINETICS

In order to obtain the gelatinisation kinetics, a theoretical relationship between the heating rate and endotherm peak temperature obtained by Ozawa (Pravisani *et al.*, 1985), it was used (Equation 6-5) below.

$$\ln\left(\frac{\phi}{T_p^2}\right) = -\frac{E_a}{RT_p} + \ln\left(\frac{k_o R}{E_a}\right) \qquad \textit{Equation 6-5}$$

where:

ϕ	Heating rate (K min^{-1})
T_p	Peak temperature (K)
R	Ideal gas constant (J mol^{-1} K^{-1})
k_o	Pre exponential factor (min^{-1})
E_a	Activation energy of gelatinisation process (J)

Samples from uncooked Toka Toka Gold and Owairaka Red kumara were taken and placed into the aluminium pan and hermetically sealed. DSC equipment (more detail in section 5.2.3.5) was used and five heating rates were applied (1, 3, 5, 10, and 15 °C/min). Endothermal curves were obtained and peak temperatures were measured for each sample. The calorimeter was calibrated, as described on section 5.2.3.5 at each scanning rate prior to carry out the analyses.

From the linearity of Equation 6-5 it is evident that a plot of ($ln(\phi/Tp^2)$) versus reciprocal peak temperature ($1/Tp$) is linear with slope equal to ($-Ea/R$) and intercept ($ln(k_oR/Ea)$).

Three replicates were carried out for gold kumara and three for red at each scanning rate.

The heating rate used to obtain the DSC curve had an effect over the shape of this curve. Figure 6-9 shows that the peak temperature of the curve of the endothermic graph obtained using DSC, increases when the heating rate is increased from 1 to 15°C/min.

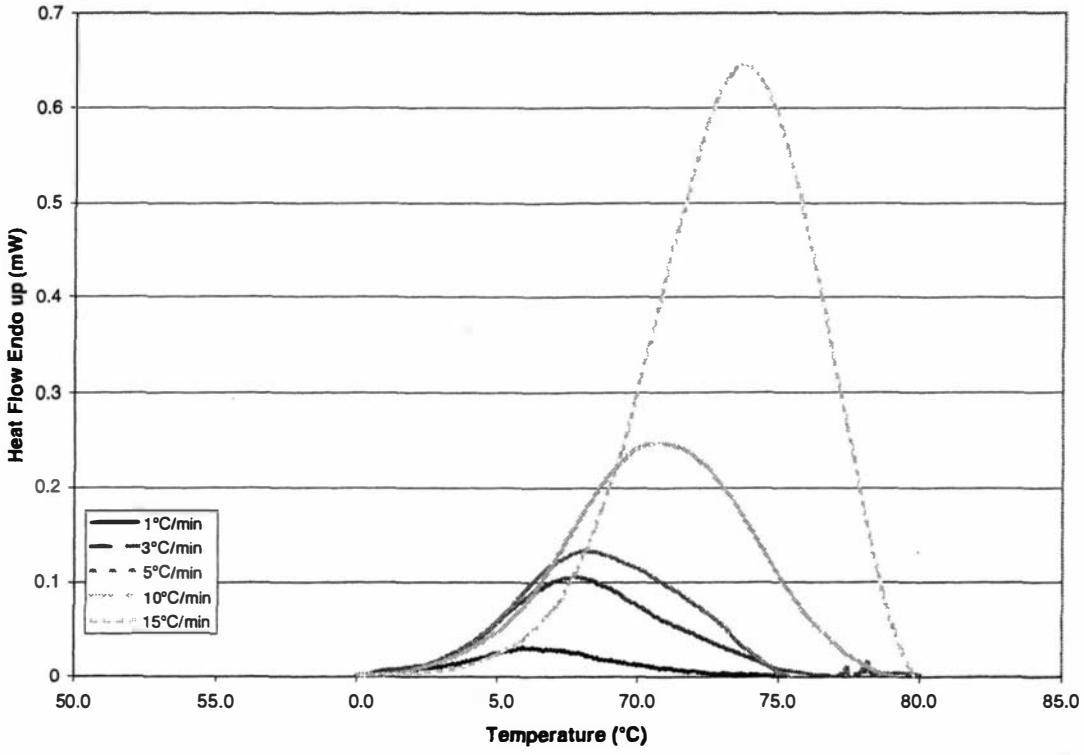

Figure 6-9 Typical endothermal graph obtained from kumara samples at different heating rates

The large increase in the area under the curve as the scanning rate increases is due to the increase in average rate of reaction at faster heating times. Because the area under the curve is proportional to $\phi \Delta h$ (where Δh *is the heat of gelatinisation*) it follows that an increase in area is expected.

The heat flow (*Y axis*) is directly proportional to the rate of reaction in the experiment. This means that the peak heat flow for each experiment corresponds to the maximum rate occurring during the DSC experiment. During a linear heating experiment there are two competing phenomena that affect the rate of reaction. This can be seen more clearly by considering the case of first order reaction, which also follows the Arrhenius with respect to temperature (see Equation 6-6).

$$\partial X/\partial t = k_o \exp\left(-E_a/RT\right)(1-X) \qquad \textit{Equation 6-6}$$

where:

X	Extent of reaction
k_o	Pre exponential factor (min^{-1})
Ea	Activation energy of gelatinisation process (J)
T	Temperature (K)
R	Ideal gas constant ($J\ mol^{-1}\ K^{-1}$)

From Equation 6-6 it is clear that $\partial X/\partial t$ increases as the temperature is increased, however as the reaction proceeds (i.e. X increases) the rate decreases. The peak heat flow (or highest reaction rate) will therefore occur at some intermediary point. For experiments at low scanning rates, more reaction is able to proceed in the lower temperature range and therefore both the peak temperature and peak heat flow are lower than for experiments conducted at high scanning rates.

The plot of Ozawa's model (Equation 6-5) for both kumara cultivars, is shown in Figure 6-10 below.

A two stage kinetic model was fitted to each data set, as can be seen in Figure 6-10. The slope and intercept of each region as well as the break point temperature were fitted by minimising of the square of the residuals using the solver tool on Microsoft Excel.

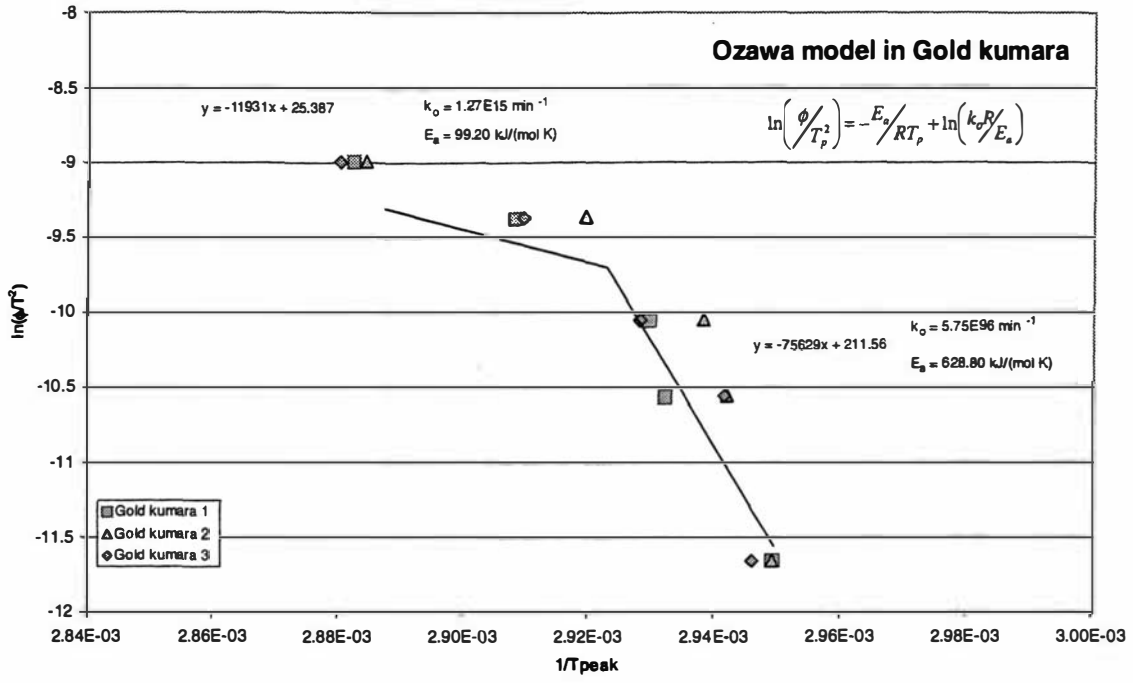

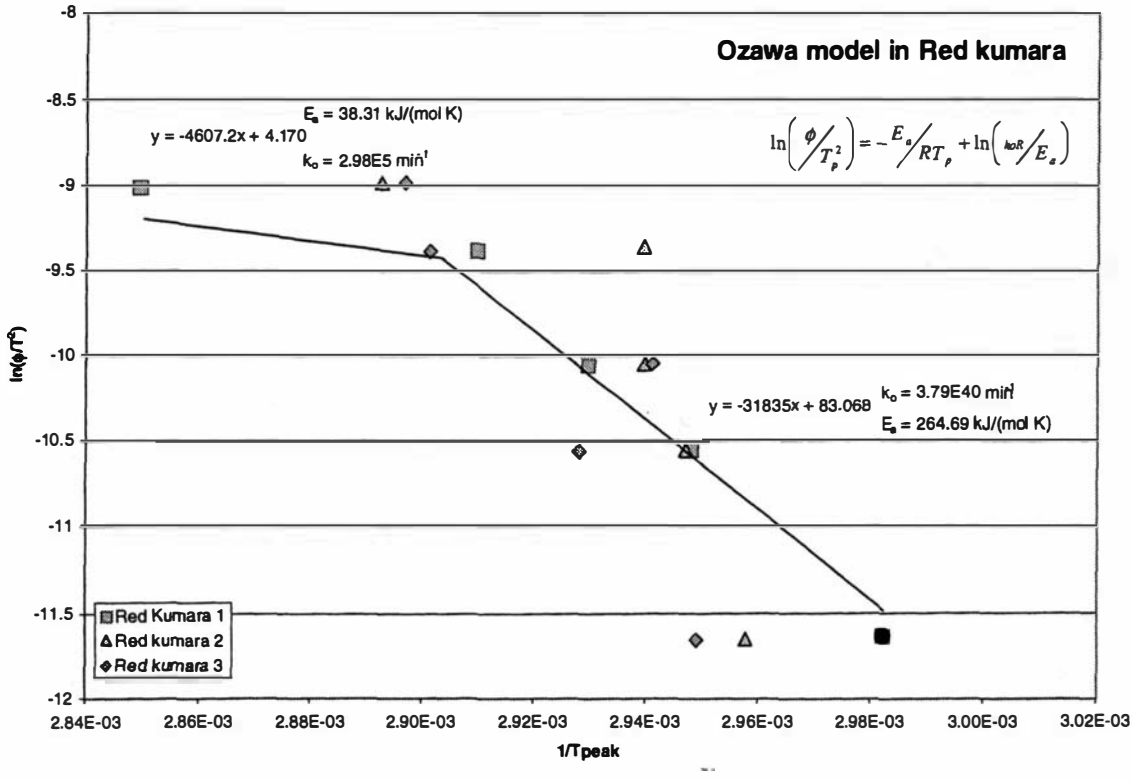

Figure 6-10 Starch gelatinisation kinetics parameters in kumara samples, according to Ozawa model

Table 6-1 summarises the kinetics constants derived for starch gelatinisation in gold and red, along with those reported by (Pravisani *et al.*, 1985) for potato.

Table 6-1 Kinetics constants for starch gelatinisation in kumara and potato

Vegetable	Temperature rage (°C)	E_a (kJ/mol)	k_o (min^{-1})
Toka Toka Gold	<65.7	629	5.75E96
Toka Toka Gold	>65.7	99	1.27E15
Owairaka Red	<63.6	265	3.79E40
Owairaka Red	>63.6	38	2.98E05
Potato (*)	<67.5	820	4.80E08
Potato (*)	>67.5	244	27.00E03

(*) Adapted from (Pravisani et al., 1985)

The activation energy (E_a) and Arrhenius constant (k_o) obtained in this study for kumara are different to the values that Pravisani *et al.* (1985) reported for potatoes. The reason for these differences is that the gelatinisation reactions depend on the kind of starch granule and amylopectin/amylose ratio or granule size.

Figure 6-10 shows that the gelatinisation in gold and red kumara had two regions, with different activation energy. Pravisani *et al.*, (1985) found the same trend for potato starch.

Pravisani *et al.*, (1985) suggest that the reason for the change in reaction mechanism observed in potato starch was that at lower temperatures the energy of the system was sufficient only to increase the disorder of amorphous regions in starch granule. At higher temperature there is enough energy present to destabilise high stability crystalline regions.

Figure 6-11 was constructed using the gelatinisation activation energy (E_a) and Arrhenius constant (k_o) obtained in this work and applying Equation 6-7 below.

$$t = \frac{\ln(1-X)}{-k_o \exp\left(-E_a/RT\right)}$$

Equation 6-7

where:

t	time (min)
k_o	Arrhenius constant (min^{-1})
Ea	Activation energy of gelatinisation process (J)
T	Temperature (K)

Differences are evident between gelatinisation in gold and red kumara. Gold kumara is shown to have more temperature dependence than red kumara.

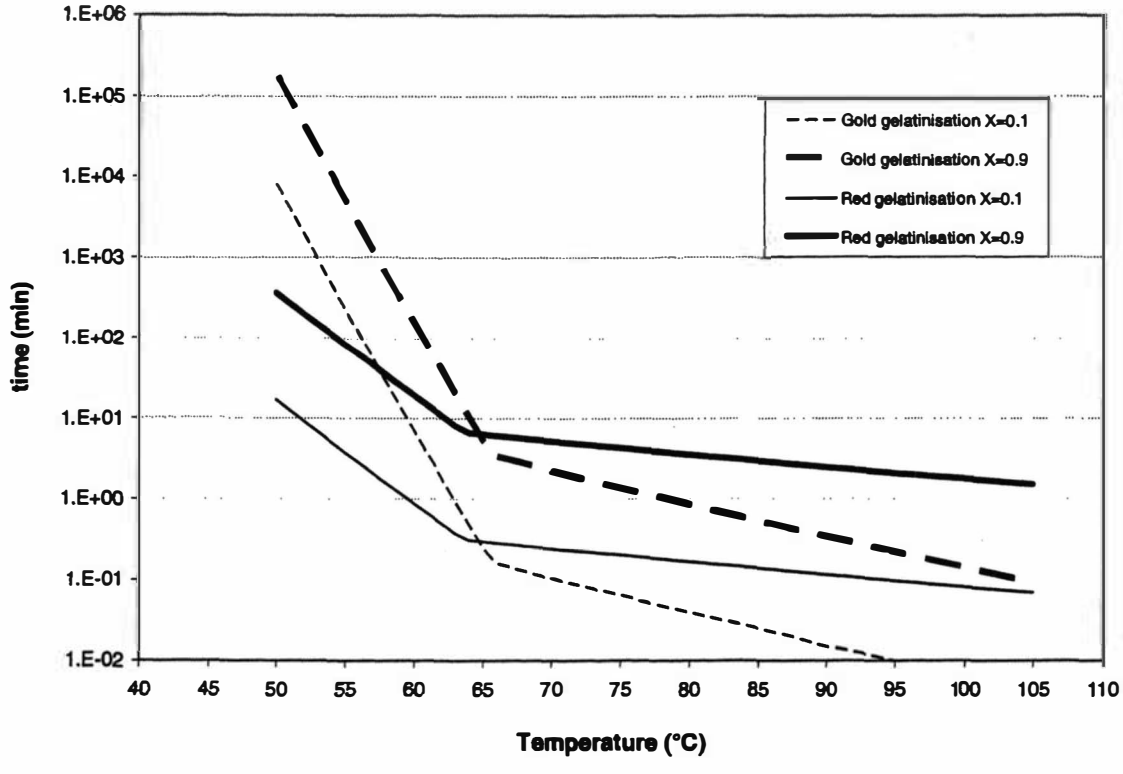

Figure 6-11 Times to reach 10 and 90%Starch gelatinisation at different cooking temperatures in gold and red kumara

There was a break in the gelatinisation reaction through the cooking process (Figure 6-10 and Figure 6-11). This break was found in both gold and red kumara at 69 and

72°C peak temperature from Figure 6-10. This corresponded to switch points between two sets of kinetics parameter of 65.6 and 63.7°C cooking temperature for gold and red kumara respectively (Figure 6-11). This break temperature was obtained by using Equation 6-8 below for temperature.

$$k_{o1} \exp\left(\frac{-E_{a1}}{RT}\right) = k_{o2} \exp\left(\frac{-E_{a2}}{RT}\right) \qquad \textit{Equation 6-8}$$

where:

$k_{o\#}$	Arrhenius constant (min^{-1})
$E_{a\#}$	Activation energy of gelatinisation process (J)
T	Temperature (K)

Figure 6-12 was constructed in the same way as Figure 6-11 using the reported kinetics parameters for starch gelatinisation described by Pravisani *et al.*, (1985).

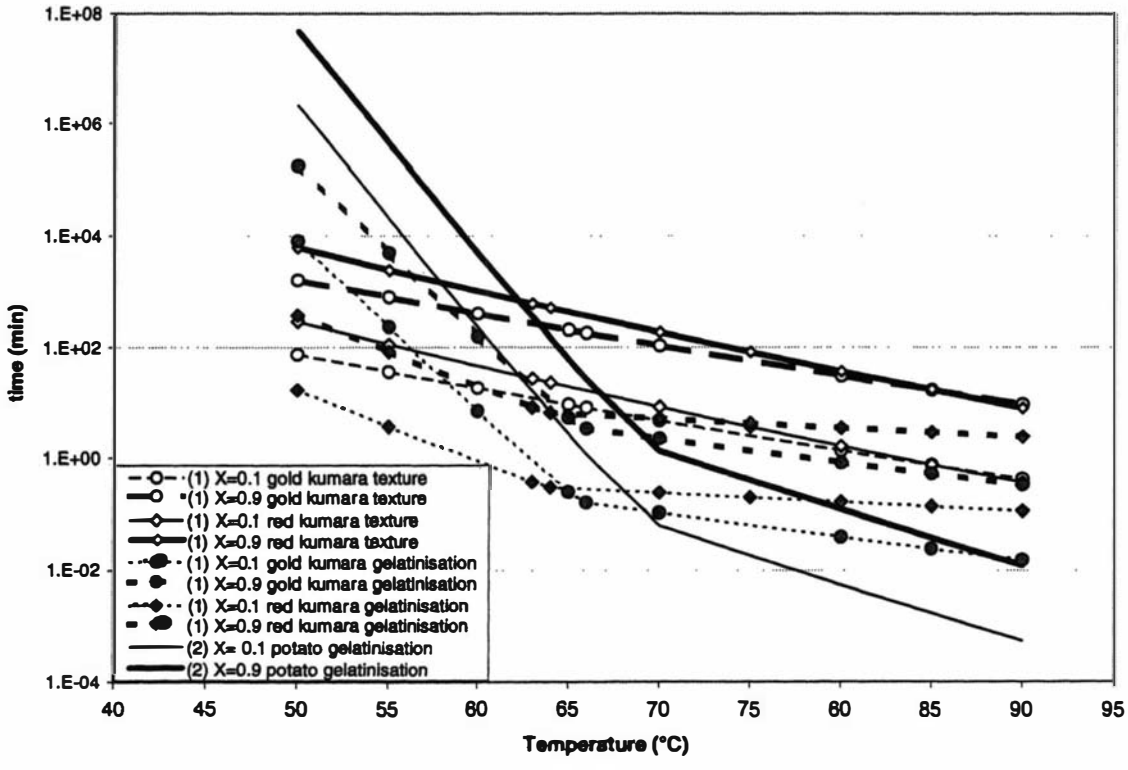

Figure 6-12 Comparison of cooking times for starch gelatinisation between kumara and potato for; (1) Toka Toka Gold and Owairaka Red Kumara data; (2) Adapted from Pravisani *et al.*, (1985)

Figure 6-12 shows the starch gelatinisation for potato was more temperature dependent than the kumara starch. In all cases it is apparent that above the transition temperature, starch gelatinisation is rapid and the starch gelatinisation reaction was complete within minutes of the cooking process. The texture change was slower. These results suggest that the gelatinisation process is important on the texture change only at the beginning of the cooking process, and another reaction such as cell separation or disruption and middle lamella is more important to the texture softening during the rest of the kumara cooking process.

Verlinden *et al.*, (1995) attempted to model texture change as a two compartment model, by assuming that the texture change occurred due to independent actions of a reduction in the level of ungelatinised starch and any other contributing reactors. They concluded that starch gelatinisation occurred faster than the observed texture change and therefore their proposed model was not better than a simple first order model. The results of the current research has shown that this approach will not explain the texture behaviour in kumara (see Figure 6-12).

To further demonstrate the much faster rate of starch gelatinisation compared to textural change in kumara, a series of ungelatinised starch measurements were made on samples that still exhibited changing texture during cooking. Figure 6-13 shows the predicted extent of the starch reaction together with fracture force measurements made during isothermal cooking experiments. It is clear from both predicted starch gelatinisation results, that this reaction has completed well before the texture had stopped changing.

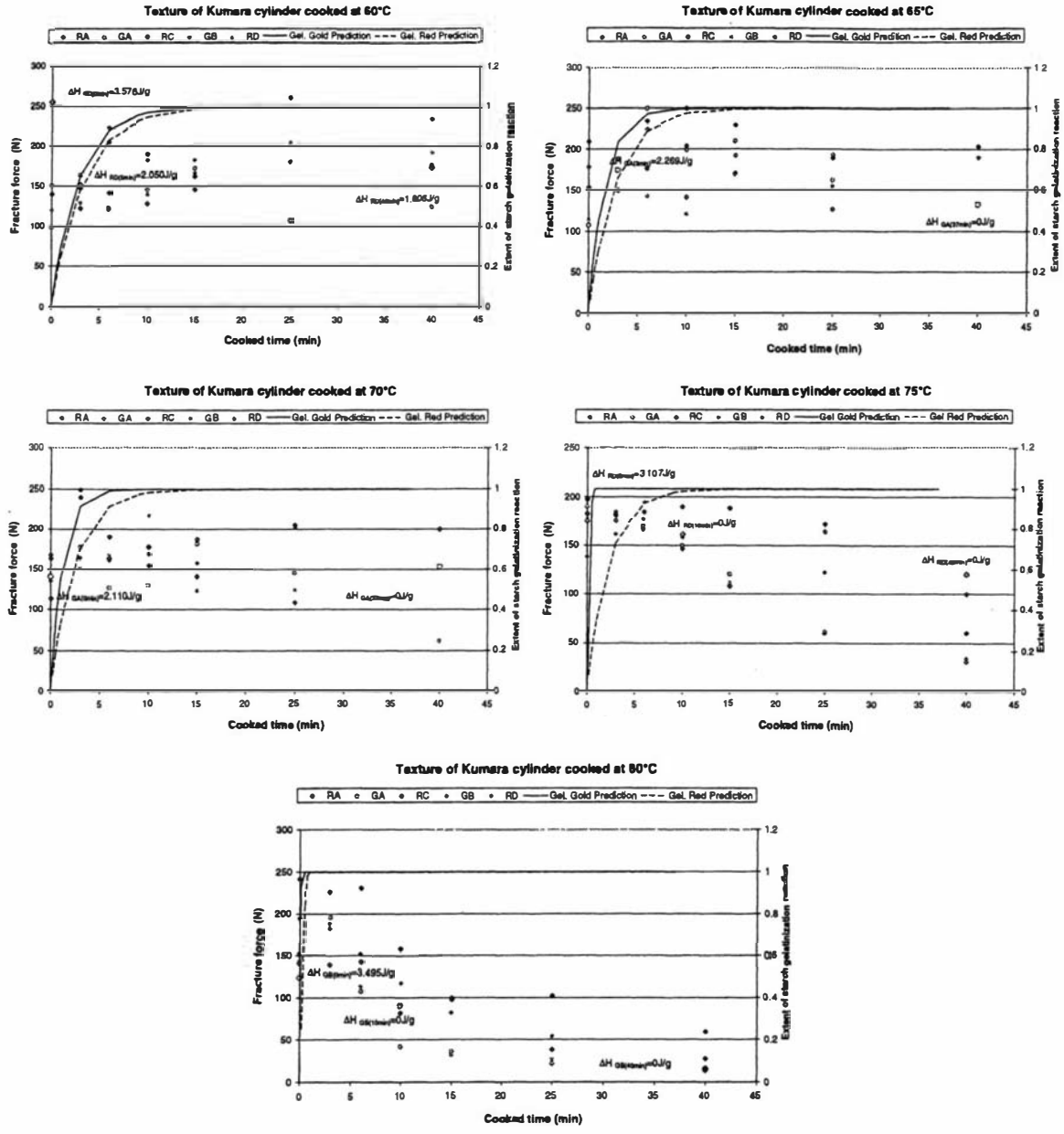

Figure 6-13 Texture comparisons of change and the starch gelatinisation reaction during cooking in Owairaka Red and Toka Toka Gold kumara

The starch granule swelling during gelatinisation, could still however explain the increase in fracture force during the initial stage of cooking as a discussed previously.

6.5. THE EXTENT OF STARCH HYDROLYSIS DURING COOKING OF KUMARA

The gelatinisation reaction changes the starch granule from a highly ordered stable structure into a more randomised amorphous mass. This reduction in the order of the starch makes it more accessible to a group of enzymes known as α- and β-amylase to promote the starch hydrolysis (Woolfe, 1992b; Hagenimana *et al.*, 1994).

According to Hagenimana *et al.*(1994) the optimum temperature for α-amylase activities is around 71.5°C and for β-amylase is at 53°C. From this it is likely that α-amylase is the primary cause of hydrolysis and the corresponding increase in maltose content observed during the cooking of kumara.

To investigate the effect of temperature on the rate and extent of starch hydrolysis, three roots of Toka Toka Gold were selected and cut into 1mm thick slices. These samples were vacuum packed into plastic bags to ensure no air gaps were present that would impede heat transfer during cooking. The samples were then cooked at 50, 70, 75, and 80°C for varying amounts of time up to 240 minutes. After cooking the samples were rapidly cooled by plunging into ice water slurry. The samples which had been cooked at the same time and temperature were then combined together by mashing. Maltose levels were evaluated according to the methodology outlined in section 5.2.3.4

Figure 6-14 shows the maltose content in gold kumara during cooking. It is clear that the cooking temperature affects the extent of the reaction. Samples cooked at 50°C did not show any increase in maltose levels. Cooking kumara at 70°C caused a rapid increase in maltose levels. A similar rate of maltose production was observed at 75 and 80°C, but the extent of the change was greater. Due to the very rapid rate of maltose production in these experiments (<5min) was not possible to determine the kinetic parameters for starch hydrolysis. To do so would require a study over much shorter time intervals which will be difficult in the whole kumara product due to the limited rate of heat transfer possible during cooking. It is clear however from the lack of maltose formation at 50°C, that gelatinisation facilitates starch hydrolysis. This phenomenon is well

reported in the literature (Oates, 1997). In terms of kumara texture, it is clear that the rate of starch hydrolysis is much faster than for texture change. This suggests that textural change is not strongly linked to starch hydrolysis and detailed kinetics for starch hydrolysis are not necessary.

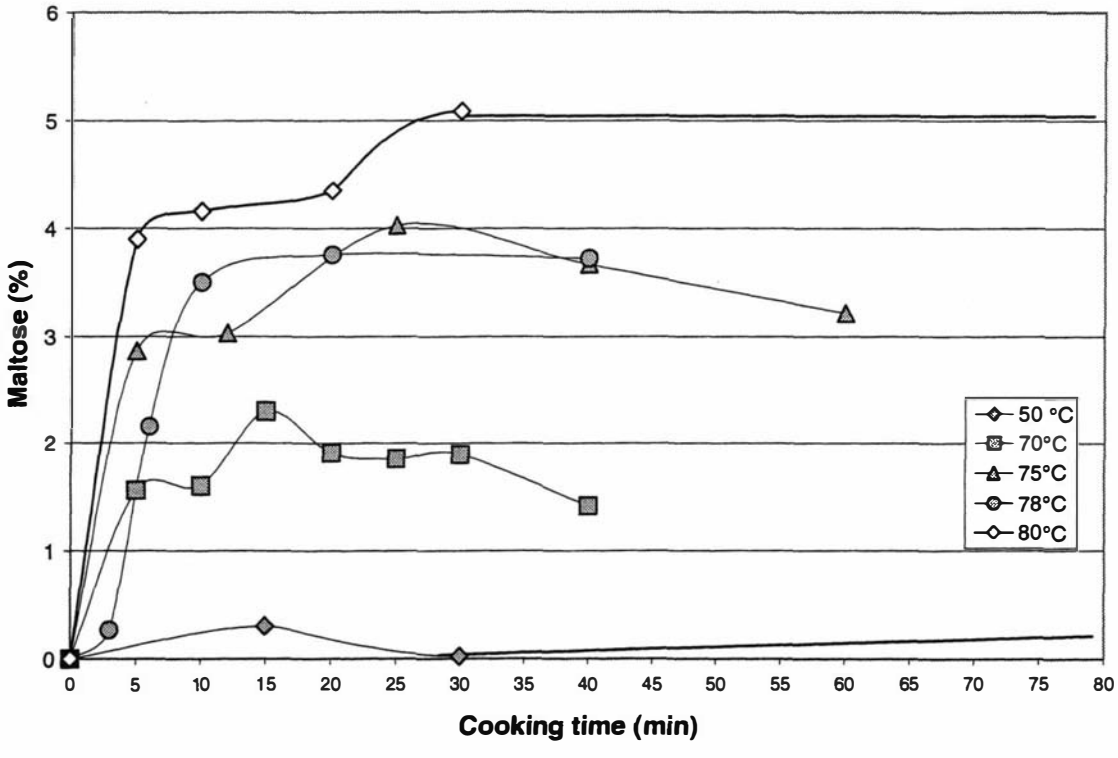

Figure 6-14 Maltose formations during cooking of Toka Toka Gold kumara

6.6. THE EXTENT AND RATE OF CELL WALL DISRUPTION DURING COOKING KUMARA

Cell separation or cell wall disruption is the other factor identified in chapter 5 as affecting the texture in kumara during cooking. Several attempts were made at trying to follow the time course of alcohol insoluble solids and total reducing sugar levels in kumara during cooking at different temperatures. These experiments were not successful and are not presented. These methodologies could demonstrate that the breakdown of

the cellular structure of the kumara occurred during cooking (see section 5.3), but the inherent variability in AIS and TRS levels in kumara meant it was not possible to evaluate kinetic trends during cooking.

The middle lamella is constituted principally of pectin. Harada *et al.*, (1985), studied the chemical component changes of three different varieties of potatoes during cooking. They reported the kinetic constants for pectin loss cooking of potato as listed in Table 6-2 below.

Table 6-2 Summary of kinetics parameters for pectin loss in potato cultivars during cooking adapted from Harada *et al.*, (1985)

Cultivar	Cooking temperature (°C)	Reaction order	Ea (kJ/mol)	ko (min^{-1})
Desiree	90	First order	5.45E+11	105868.9
Desiree	100	First order	5.79E+11	105868.9
Desiree	110	First order	5.02E+11	105868.9
Mentor	90	First order	3.19E+15	131703.5
Mentor	100	First order	4.02E+15	131703.5
Mentor	110	First order	2.81E+15	131703.5
Bintje	90	First order	1.97E+15	129418
Bintje	100	First order	2.08E+15	129418
Bintje	110	First order	1.64E+15	129418

Figure 6-15 compares the texture changes of potato and kumara with the change in pectin (data adapted from Harada *et al.*, 1985). The similar tendency between the rate of textural and pectin changes demonstrates the importance of cell wall disruption and pectin breakdown on texture. Even when the texture was evaluated by different methods (shear force, sensory texture, and fracture force), the slope of the different curves are very similar.

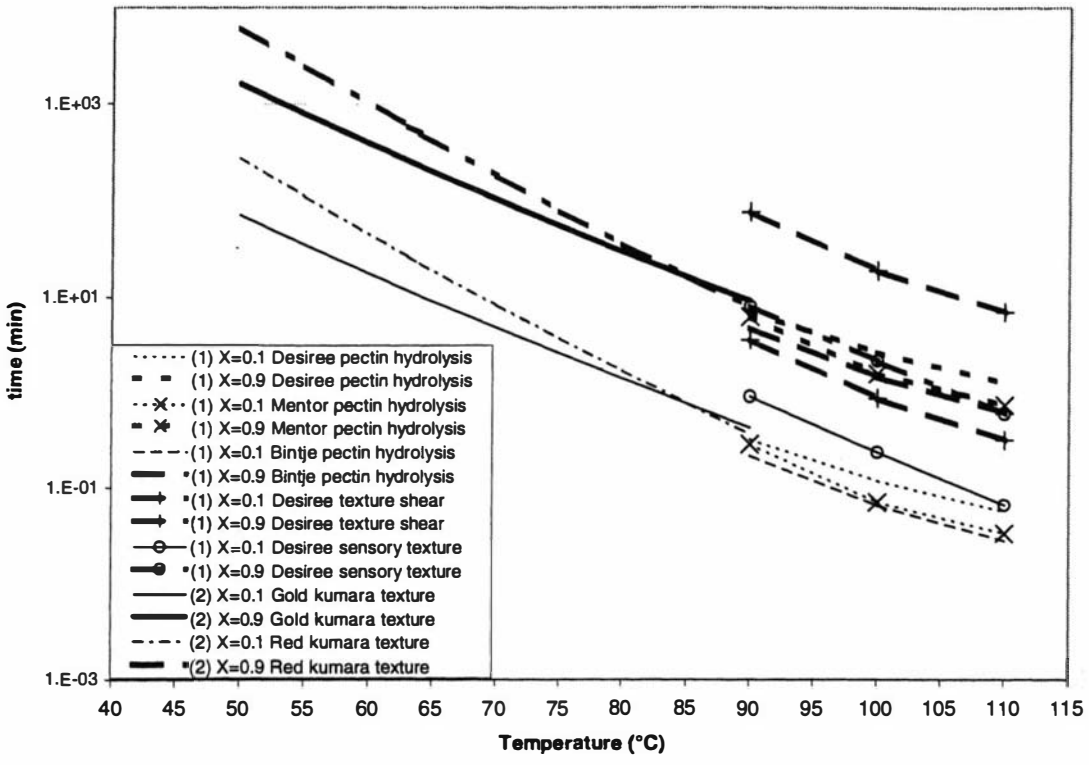

Figure 6-15 Comparison of pectin hydrolysis rate with texture changes in kumara and potato. (1) Data adapted from (Harada *et al.*, 1985); (2) Kumara texture obtained in this work.

The consistency of both the rate of reaction and the effect of temperature on reaction rate between pectin loss and textural change, clearly indicates that breakdown of the middle lamella is the primary cause of textural softening in potato and kumara.

From the kinetic results and by considering the texture mechanism analysed in chapter 5, a prediction of texture (fracture force) was carried out. The starch gelatinisation kinetics for gold and red kumara were used, along with the pectin kinetics obtained from Harada *et al.*, (1985).

The model considers uncooked kumara with fracture force (F_o). Swelling of the starch granule as a result of gelatinisation then can increase the observed fracture force by ΔF_s. It was assumed that the magnitude of this increase was independent of cooking temperature and the same for both the red and gold kumara cultivar. The breakdown of the middle lamella (as quantified by extent at pectin losses) then results in a drop in fracture force.

The overall model is summarised as in equations 6-9 to 6-11 below.

$$F = F_o + \Delta F_s X_s - (F_o + \Delta F_s - F_\infty) X_p \qquad \textit{Equation 6-9}$$

where:

F_o Uncooked fracture force (N)

ΔF_s Increase in fracture force due to starch swelling effect (N)

F_∞ Fracture force at infinite cooking time (N)

X_s Extent of starch gelatinisation reaction (dimensionless)

X_p Extent of pectin loss (dimensionless)

$$X_s = 1 - \exp(-k_s t) \qquad \textit{Equation 6-10}$$

where:

k_s Rate constant for starch gelatinisation (min^{-1})

t Time (min)

$$X_p = 1 - \exp(-k_p t) \qquad \textit{Equation 6-11}$$

where:

k_p Rate constant for pectin (min^{-1})

The rate constants for starch gelatinisation and pectin were calculated at the cooking temperature using the Arrhenius law and the constant summarised in table 6-3.

Table 6-3 Activation energy (Ea) and rate constant (k_o) values using to texture model mechanism

Component	Temperature range (°C)	E_a (kJ/mol)	k_o (min^{-1})
Starch gold kumara	<65.7	629	5.75E96
Starch gold kumara	>65.7	99	1.27E15
Starch red kumara	<63.6	265	3.79E40
Starch red kumara	>63.7	38	2.98E05
Pectin	all range	129	2.08E18

The values F_o, ΔF_s, and F_∞ were estimated from the raw texture data to be 150N, 50N, and 4N respectively.

The results of the model predictions are presented as Figure 6-16. It can be seen that the model can be used to explain the increase in fracture force observed at the onset of cooking at 65°C and 75°C, and predicts relatively well the decrease in texture at higher cooking temperatures. While this model is useful for validating the textural change mechanism, it no significant advantages over the simple first order model developed in section 6.3 for optimisation of the kumara cooking process.

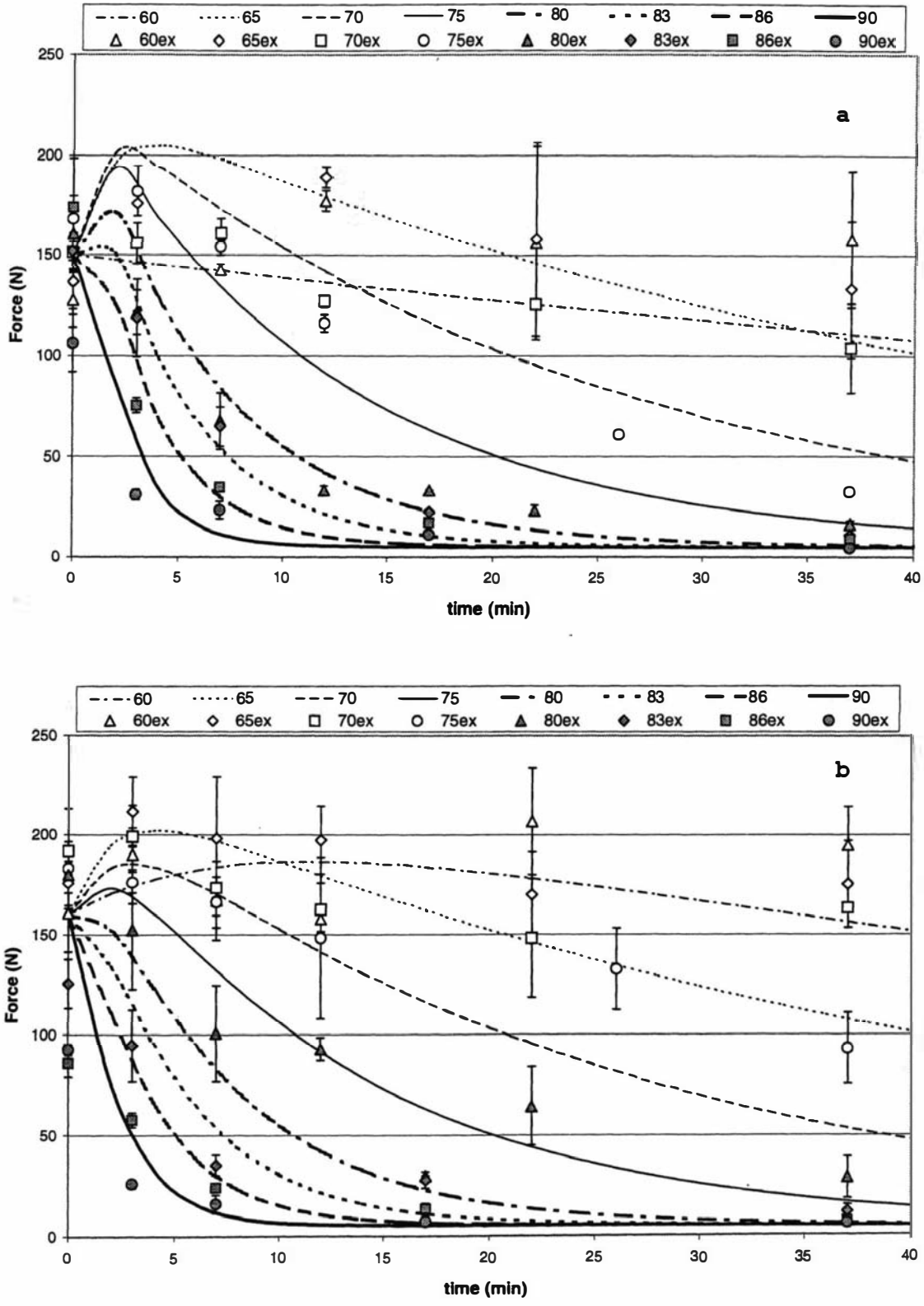

Figure 6-16 Comparison between experimental (marker) and predicted (lines) fracture force in (a) Toka Toka Gold and Owairaka Red (b) kumara

6.7. CONCLUSION

The texture kinetics in kumara were found to follow a first order equation, and the dependence of the rate on cooking temperature could be represented by the Arrhenius equation. Red and gold kumara had a slightly different behaviour and different Arrhenius parameters. The activation energy was 161.93 and 125.26kJ mol^{-1}, and the Arrhenius constants were 5.59E22 and 2.54E17min^{-1} for red and gold kumara respectively. The starch gelatinisation reaction was fast and can be used to explain the texture increase during the first period in the cooked process for product cooked at 65-75°C.

The overall rate of texture modification closely matched the changes to pectin during cooking that were reported by Harada *et al.*, (1985), identifying the breakdown of middle lamella as the primary cause of textural change.

A simple model which combined the kinetics of swelling and pectin hydrolysis was developed that could be used to successfully predict texture changes in kumara.

CHAPTER 7: PROCESS MODELLING AND OPTIMISATION

7.1. INTRODUCTION

Once the texture and colour change had been studied and the kinetics of the different reactions involved in each change had been determined, the next step was to develop a model to predict and simulate different processing scenarios.

In this competitive and changing market, to have a model is important. It can be used to show how to process kumara to achieve a desired colour and textural quality, in order to meet the customer expectation, or to predict the likely affect of changing processing parameters, like temperature or time on final product quality.

Optimisation is the act of achieving an optimal solution under a given set of circumstances (Tzia, 2003). A model that relates processing conditions to product quality is an important requirement for the optimisation process.

Figure 7-1 summarises the processing conditions typical for an industrial process. It shows the most common unit operations of the process along with the levels of key processing variables that affect product quality (temperature, oxygen, additive levels (SAPP)) and the product dimensional changes during the processing.

Raw material preparation consists of washing the roots and selection to remove those roots outside of the quality range. The peeling can be carried out using abrasive methods similar to those used in potato processing or by steaming for 3min at 121°C. After peeling, the roots can be soaked in SAPP (%) solution to prevent post cooking

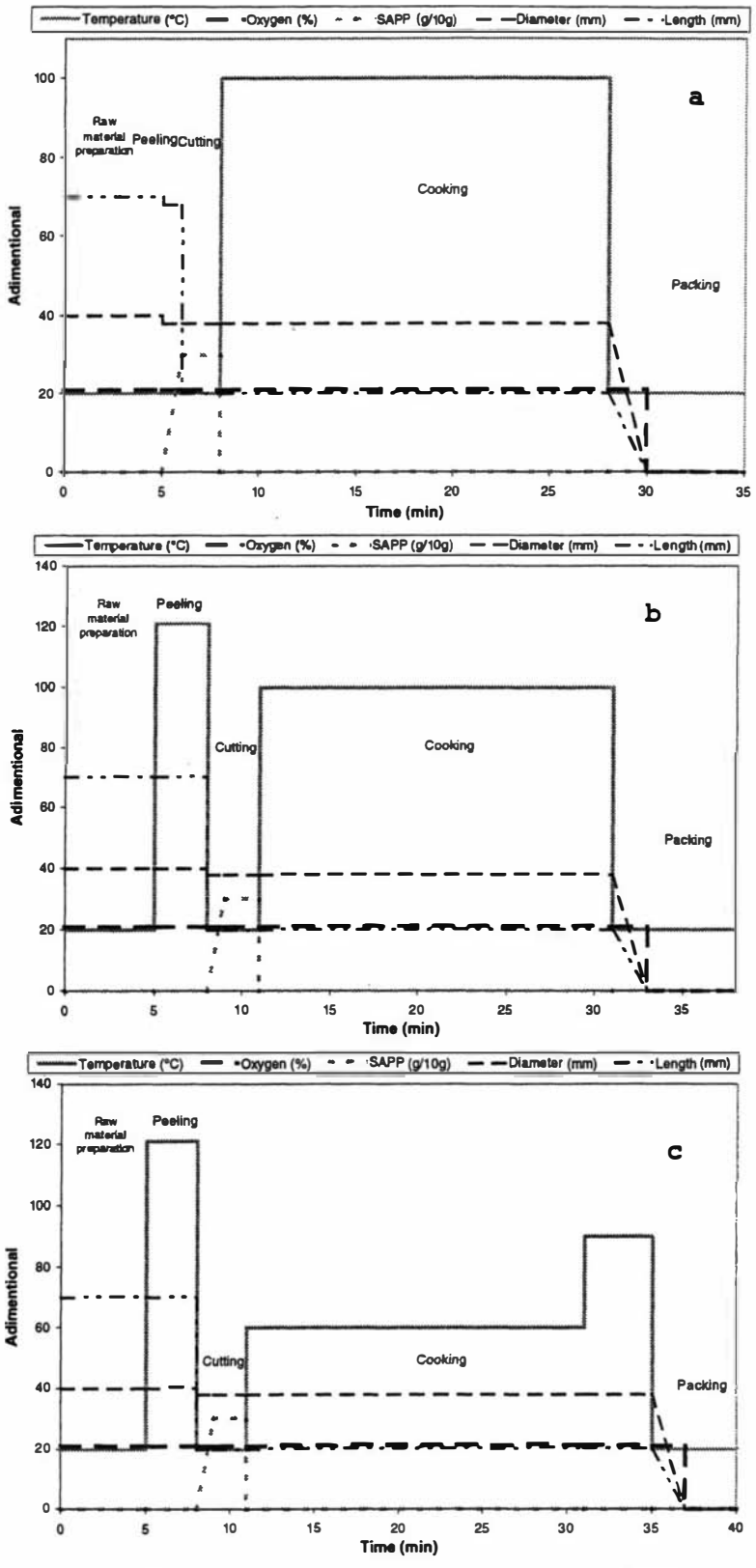

Figure 7-1 Kumara process profile (a: simple processing with abrasive peeling; b: simple processing with steam peeling; c: Steam peeling and different cooking temperatures)

darkening. Cutting is a resizing process where diced or sliced product can be made to assist the mass and heat transfer processes and achieve a uniformly cooked product.

There are a different combination of cooking time and temperature profiles that can be adopted to do the cooking. For example cooking at 100°C for 20min is the most simple approach. Cooking at 60°C for 20min is sometimes used to promote starch hydrolysis and the enzymes are inactivated by heating to 90°C for 4min. If the final product requirement is mashed, the pureeing is generally carried out at this stage. The packing can be done using a vacuum pack-machine, to reduce the oxygen levels to prevent reactions such as colour changes where the oxygen is important.

Finally in order to get a product microbiologically safe after packing, the product is most commonly retorted.

7.2. ISOTHERMAL KUMARA COOKING MODEL

Control of kumara cooking to produce product with the desired quality attributes could be achieved by selecting the optimal cooking temperature. For example, it might be possible to cook kumara under such conditions where the precursor reactions causing post cooking darkening can be avoided while starch hydrolysis and textural modification are achieved. If it is assumed that heat transfer within the product is faster than the reaction rates investigated and step change in cooking temperatures is achieved, then the kinetics model developed in chapters 4 and 6 can be applied directly.

Using Equation 7-1, the time to reach a desired extent of reaction can be calculated at any cooking temperature (see Figure 7-2).

$$t = \frac{(1 - X)}{-k_o \exp\left(-Ea/RT\right)}$$

Equation 7-1

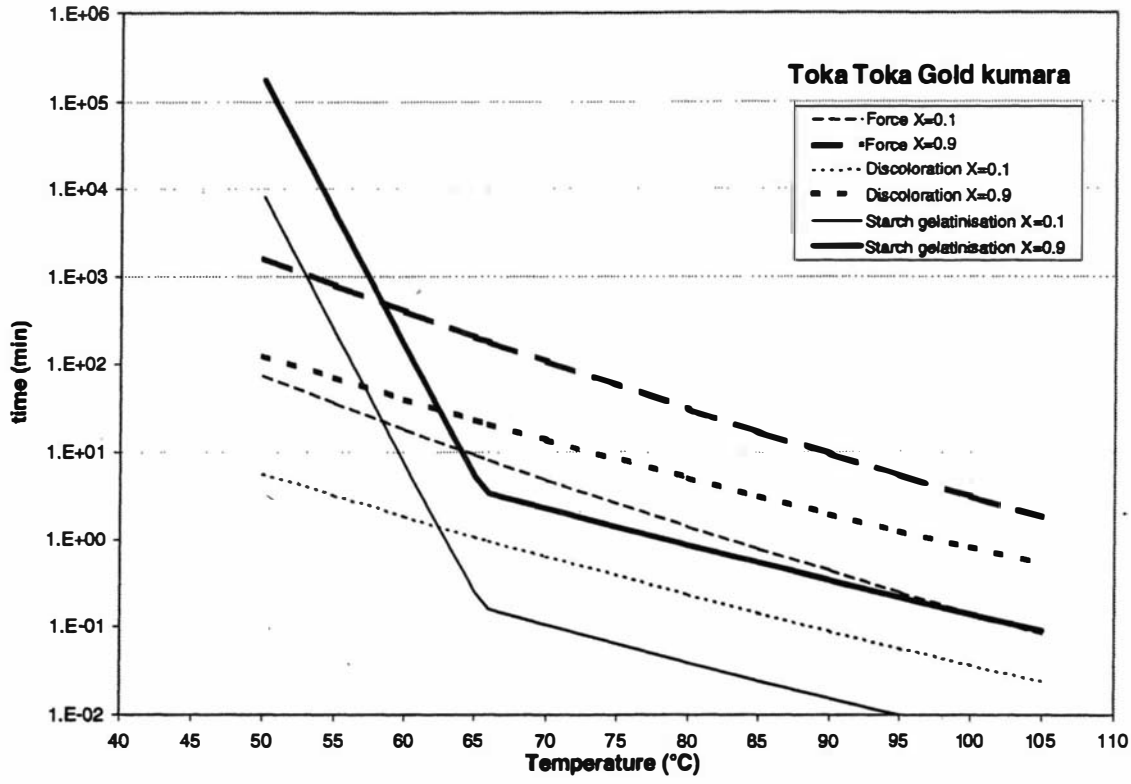

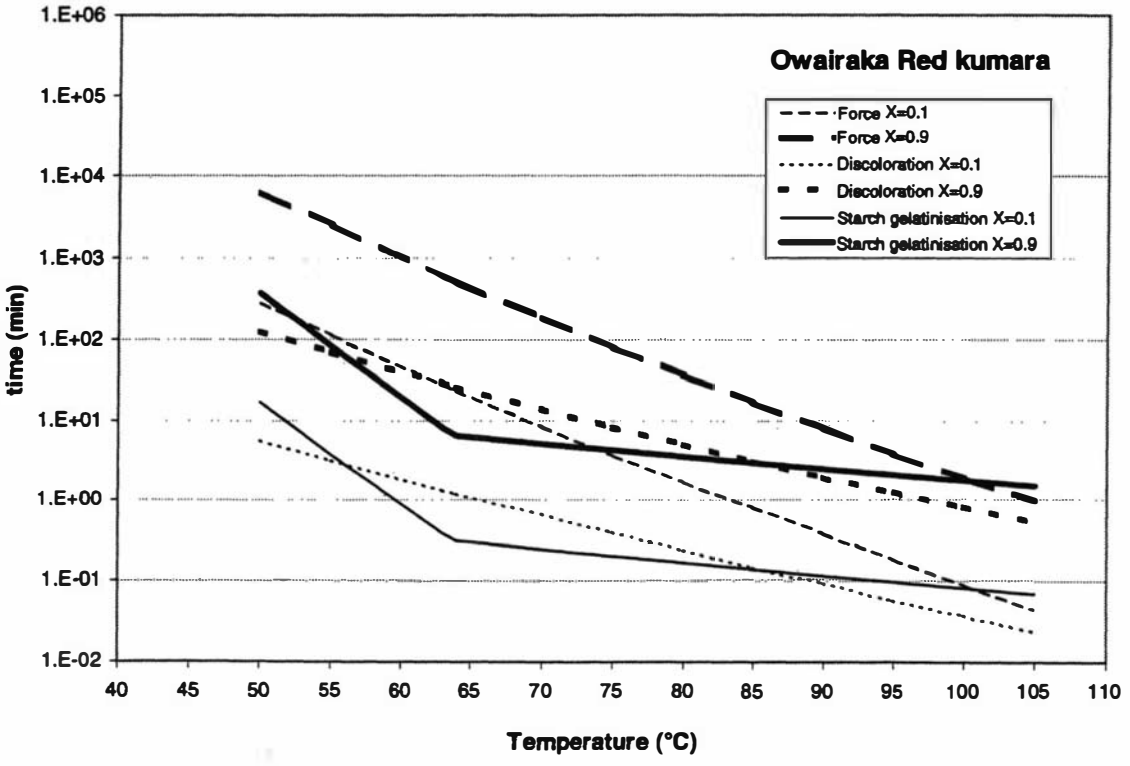

Figure 7-2 Time taken to reach 10 and 90% changes of texture, discoloration and starch gelatinisation reaction in kumara at different cooking temperatures

It is clear from Figure 7-2, that is not possible to achieve significant reduction in texture without causing release of the bound iron or phenolic acids in kumara that facilitate post cooking darkening. As a result it is necessary to chelate the iron in the sample by using an additive such as SAPP or EDTA, or to remove all oxygen from the system if colour changes are to be avoided. The rapidity of the starch gelatinisation reaction at temperatures higher than 65°C, demonstrates that cooking at high temperature for very short times should cause complete gelatinisation which could facilitate starch hydrolysis if a sweetened product is required. This could be achieved without significant colour or textural change occurring, however very rapid heat transfer would have to be achieved. In reality the productions shown in Figure 7-2, will only ever be achieved at the surface of kumara samples.

7.3. POSITION VARIABLE KUMARA COOKING MODEL

In real systems, significant temperature gradients occur within the product during cooking. The rate of heating is highly dependent on the size, shape and thermal properties of the product. In this section of the work a heat transfer model was developed for different ideal geometries. The transient temperature history can then be used to predict the extent of colour change, starch gelatinisation and textural change as a function of position.

7.3.1. Heat transfer model

Heat transfer into the fresh kumara depends on the physical characteristics of the product, like thermal conductivity, specific heat capacity, density, and shape and size.

During kumara processing the shape can be significantly changed from the raw material (see Table 1-1 in Chapter 1). The most common shapes are cylindrical, slices (slabs) or rectangular blocks (dices). So models for heat transfer for these geometrical situations were required.

7.3.1.1. Assumptions

The main assumptions for the model were;

- Constant thermal properties.
- Constant geometry (no significant swelling, or shrinkage).
- First kind boundary conditions (Bi number is large).
- Uniform initial temperature in sample.
- Instantaneous step change in cooking temperature at time zero.
- Constant external temperature over the duration of the cooking.

7.3.1.2. Model equations

The model equations for typical shapes or combinations of shapes were considered to describe the different shapes occurring during processing. An infinite slab was used to characterise the result of the slicing process. A rectangular block was used to represent diced product. A combination of infinite cylinder and slab (short cylinder) were considered for an approximations of whole kumara and very thickly sliced roots (i.e. where diameter >4 times the thickness).

7.3.1.2.1. Infinite slab

An infinite slab of thickness *2Rx* was considered as the diameter of a slice was more than four times the slice thickness. Cleland *et al.*, (1994) suggest that for such cases heat transfers in the radial direction is not significant. A first kind of boundary condition was used. It his case, the temperature at the surface of the product was equal to the cooking

temperature. For this case the model equations are given by Equation 7-2 to Equation 7-5.

$$\rho \cdot cp \frac{\partial \theta}{\partial t} = \lambda \frac{\partial^2 \theta}{\partial x^2} \qquad \text{for } t>0,\ 0<x<Rx \qquad \text{Equation 7-2}$$

$$\theta = \theta a \qquad \text{at } x=Rx,\ t>0 \qquad \text{Equation 7-3}$$

$$\partial\theta/\partial x = 0 \qquad \text{at } x=0,\ t>0 \qquad \text{Equation 7-4}$$

$$\theta = \theta i \qquad \text{at } t=0,\ 0<x<Rx \qquad \text{Equation 7-5}$$

7.3.1.2.2. Infinite cylinder

In a similar way to the infinite slab described above, the first kind of boundary condition was considered for an infinite cylinder with diameter *2Rr*. In this case, the model equations to be solved are given by Equation 7-6 to Equation 7-9.

$$\rho \cdot cp \frac{\partial \theta}{\partial t} = \lambda \frac{\partial^2 \theta}{\partial r^2} + \frac{\lambda}{r} \frac{\partial \theta}{\partial r} \qquad \text{for } t>0,\ 0<r<Rr \qquad \text{Equation 7-6}$$

$$\theta = \theta a \qquad \text{at } r=Rr \text{ for } t>0 \qquad \text{Equation 7-7}$$

$$\partial\theta/\partial r = 0 \qquad \text{at } r=0,\ t>0 \qquad \text{Equation 7-8}$$

$$\theta = \theta i \qquad \text{at } t=0 \text{ for } 0<r<Rr \qquad \text{Equation 7-9}$$

7.3.1.2.3. Short cylinder

The short cylinder was used to represent situations where the slices have diameter less than four times the thickness. In the case of a first kind of boundary condition the model equations are given by equations Equation 7-10 to Equation 7-15.

$$\rho \cdot cp \frac{\partial \theta}{\partial t} = \lambda \frac{\partial^2 \theta}{\partial x^2} + \lambda \frac{\partial^2 \theta}{\partial r^2} + \frac{\lambda}{r} \frac{\partial \theta}{\partial r} \qquad \text{for } t>0,\ 0<x<Rx,\ 0<r<Rr \qquad \text{Equation 7-10}$$

$$\partial\theta/\partial x = 0 \qquad \text{at } x=0,\ t>0,\ 0<r<Rr \qquad \text{Equation 7-11}$$

$$\theta = \theta a \qquad \text{at } x=Rx,\ 0<r<Rr,\ t>0 \qquad \text{Equation 7-12}$$

$$\partial\theta/\partial r = 0 \qquad \text{at } r=0,\ 0<x<Rx \qquad \text{Equation 7-13}$$

$$\theta = \theta a \qquad \text{at } r=Rr,\ 0<x<Rx \qquad \text{Equation 7-14}$$

$$\theta = \theta i \qquad \text{at } t=0,\ 0 \le x \le Rx \text{ and } 0 \le r \le Rr \qquad \text{Equation 7-15}$$

7.3.1.2.4. Rectangular block

Another typical shape that can be used to describe the kumara during processing is the dice, which can be represented by a rectangular block. For the situation where the first kind of boundary condition applies the model equations are Equation 7-16 to Equation 7-23.

$$\rho \cdot cp\frac{\partial\theta}{\partial t} = \lambda\frac{\partial^2\theta}{\partial x^2} + \lambda\frac{\partial^2\theta}{\partial y^2} + \lambda\frac{\partial^2\theta}{\partial z^2} \qquad \text{at } 0<x<Rx,\ 0<y<Ry,\ 0<z<Rz,\ \text{for } t>0 \qquad \text{Equation 7-16}$$

$$\partial\theta/\partial x=0 \qquad \text{at } x=0,\ 0<y<Ry,\ 0<z<Rz,\ t>0 \qquad \text{Equation 7-17}$$

$$\theta=\theta a \qquad \text{at } x=Rx,\ 0<y<Ry,\ 0<z<Rz,\ t>0 \qquad \text{Equation 7-18}$$

$$\partial\theta/\partial y=0 \qquad \text{at } 0<x<Rx,\ y=0,\ 0<z<Rz,\ t>0 \qquad \text{Equation 7-19}$$

$$\theta=\theta a \qquad \text{at } 0<x<Rx,\ y=Ry,\ 0<z<Rz,\ t>0 \qquad \text{Equation 7-20}$$

$$\partial\theta/\partial z=0 \qquad \text{at } z=0,\ 0<y<Ry,\ 0<x<Rx,\ t>0 \qquad \text{Equation 7-21}$$

$$\theta=\theta a \qquad \text{at } z=Rz,\ 0<y<Ry,\ 0<x<Rx,\ t>0 \qquad \text{Equation 7-22}$$

$$\theta=\theta i \qquad \text{for } t=0,\ 0\le x\le Rx,\ 0\le y\le Ry,\ 0\le z\le Rz \qquad \text{Equation 7-23}$$

7.3.1.3. Heat transfer model solution

In each case above with constant thermal properties dimensions, and uniform initial temperature analytical solutions exist (Carslaw and Jaeger, 1959).

7.3.1.3.1. Infinite slab

Equation 7-24 can be used to calculate the unaccomplished temperature change (Y) reached in at one specific point (x). The solution is a function of the dimensionless time (Fourier number [Fo]) that is determined from the thermal properties of the product (Equation 7-26).

$$Y_{slab} = \frac{4}{\pi}\sum_{m=0}^{\infty}\frac{-1^m}{2m+1}\cos\left[(2m+1)\frac{\pi}{2}\frac{x}{R_x}\right]\exp\left[-(2m+1)^2\frac{\pi^2}{4}Fo\right] \qquad \text{Equation 7-24}$$

$$Y = \frac{\theta - \theta_a}{\theta_i - \theta_a} \qquad \textit{Equation 7-25}$$

$$Fo = \frac{\lambda t}{\rho c p R_x^2} \qquad \textit{Equation 7-26}$$

7.3.1.3.2. Infinite cylinder

The analytical solution for Equation 7-6 to Equation 7-9 is given by Equation 7-27. Where βm, (m is equal 1, 2, 3, etc.), are the roots of $Jo(\beta)=0$. Jo is a first order Bessel's function.

$$Y_{cylinder} = \sum_{m=1}^{\infty} \frac{2J_o\left(\beta_m \frac{r}{Rr}\right)}{\beta_m J_1(\beta_m)} \exp\left[-\beta^2 Fo\right] \qquad \textit{Equation 7-27}$$

7.3.1.3.3. Short cylinder

3D model solutions for the short cylinder are achieved by intersection between the infinite slab and infinite cylinder solutions as shown by Equation 7-28.

$$Y_{(x,r)} = Y_{slab(x)} \cdot Y_{cylinder(r)} \qquad \textit{for any particular point} \qquad \textit{Equation 7-28}$$

7.3.1.3.4. Rectangular block

The rectangular block solution was achieved by intersecting the solutions of three slabs as given by Equation 7-29.

$$Y_{(x,y,z)} = Y_{slab(x)} \cdot Y_{slab(y)} \cdot Y_{slab(z)} \qquad \textit{for any particular point} \qquad \textit{Equation 7-29}$$

In each case the analytical solutions were calculated using Matlab 6.5. The Matlab code for these calculations can be found in Appendix A2. At least 13 terms in the series solutions were used to ensure no numerical errors arose in the calculation.

7.3.2. Kinetic models

The kinetics for texture, discoloration, and starch gelatinisation were determined from isothermal cooking experiments. Because the temperature changes as a function of time at each position in the kumara during cooking, it is necessary to solve the differential equations for rate of reactions extent to predict the progress of these reactions as a function of time.

7.3.2.1. Texture fracture force

The ordinary differential equation (ode) for textural changes in kumara, at each position in the slab is given by Equation 7-30.

$$\frac{\partial X_{F(x,y,z)}}{\partial t} = k_F\left(1 - X_{F(x,y,z)}\right) \qquad \textit{Equation 7-30}$$

Where the rate is constant dependent on the temperature (θ) predicted from the heat transfer model using the Arrhenius law (Equation 7-31).

$$k_F = k_o \exp\left(-E_{aF} \Big/ \left(R\left(\theta_{(x,y,z)} + 273.15\right)\right)\right) \qquad X_F=0 \text{ at } t=0, \text{ for all } x, y, z \qquad \textit{Equation 7-31}$$

7.3.2.2. Discoloration (ΔE) reaction

Similarly the ode for discoloration is given by Equation 7-32 and Equation 7-33 below.

$$\frac{\partial X_{D(x,y,z)}}{\partial t} = k_D\left(1 - X_{D(x,y,z)}\right) \qquad \textit{Equation 7-32}$$

$$k_D = k_{oD} \exp\left(-E_{aD} \Big/ \left(R\left(\theta_{(x,y,z)} + 273.15\right)\right)\right) \qquad X_D=0 \text{ at } t=0, \text{ for all } x, y, z \qquad \textit{Equation 7-33}$$

7.3.2.3. *Starch gelatinisation*

The extent of starch gelatinisation can be predicted by solving Equation 7-34 and Equation 7-35 below, remembering that the value of the kinetic constants E_{aSt} and k_{oSt} change at specific break temperature as discussed in section 6.4.

$$\frac{\partial X_{St(x,y,z)}}{\partial t} = k_{St}\left(1 - X_{St(x,y,z)}\right) \qquad \textit{Equation 7-34}$$

$$k_{St} = k_{oSt}\exp\left(-E_{aSt}\Big/\left(R\left(\theta_{(x,y,z)} + 273.15\right)\right)\right) \quad X_{St}=0 \text{ at } t=0, \text{ for all } x, y, z \qquad \textit{Equation 7-35}$$

7.3.2.4. *Kinetics model solution*

To provide a temperature history at each position in the kumara, the kumara was divided into 20 equally sized regions in each dimension. At the centre of each region (21 nodes) the heat transfer model was applied for the duration of the simulated cooking period. These temperature profiles were then used as inputs into the kinetic model equations.

The odes for quality change in kumara (Equation 7-30 to Equation 7-35) were solved numerically using the ode 45, Runge Kutta solver in Matlab 6.5, for each position in the kumara product. At each time step, the current temperature at each position was looked up and used to calculate the rate constant. The function solution files are included in Appendix A2.

7.4. INPUT DATA

In order to solve the model, thermophysical and kinetic properties for kumara were required.

7.4.1. Physical and thermal properties

There have been no reported data for thermal properties of kumara in literature and this was not a major focus of this project, so literature values for product of similar consistency to kumara were used.

Thermal conductivity (λ) for potato with similar water content (72.3%) and density to the kumara or sweet potato studied in this work was selected. This data is summarised in Table 7-1 below.

Table 7-1 Thermal properties of kumara used for model predictions

Property	Value	Unit	Product	Reference
Cp	*3640*	*$J\,kg^{-1}.°C^{-1}$*	*Sweet potato*	*(Wadsworth and Spadaro, 1970)*
λ	*0.36*	*$W\,m^{-1}\,°C^{-1}$*	*Potato*	*(Rahman, 1995)*
ρ	*1088*	*m^3kg^{-1}*	*Kumara*	*Calculated in this research*

7.4.2. Kinetics properties

In previous chapters the Arrhenius parameter were calculated for the different reactions occurring during cooking process. For convenience they are summarised in Table 7-2.

Table 7-2 Kinetics parameters for the kumara cooking process

Reaction	*Samples*	$k_o (min^{-1})$	$E_a (kJ\ mol^{-1})$	*Conditions*
Discoloration	Gold kumara	4.56E14	101.40	
Texture change	Gold kumara	2.54E17	125.26	
	Red kumara	5.59E22	161.93	
Starch gelatinisation	Gold kumara	5.75E96	628.80	<65.63°C
		1.27E15	99.20	>65.63°C
	Red kumara	3.79E40	264.69	<63.71°C
		2.98E05	38.31	>63.71°C

7.5. PREDICTION FOR TYPICAL COOKING OPERATIONS

7.5.1. Definition of cooking operation

In order to show some results from the model in the cooking process, using the data from Table 7-1 and Table 7-2, the cooking operation was formally defined. Typically for the cooking process, in potatoes or other tubers, the raw material is cut into two regular shapes before cooking. These are the slab and the rectangular block. These two shapes were used to carry out example simulations the results of which are shown in Figure 7-3 and Figure 7-4. A third shape the short or finite cylinder was considered because it could represent the raw materials if thickly sliced. The simulated cooking process for this case is seen as (Figure 7-5).

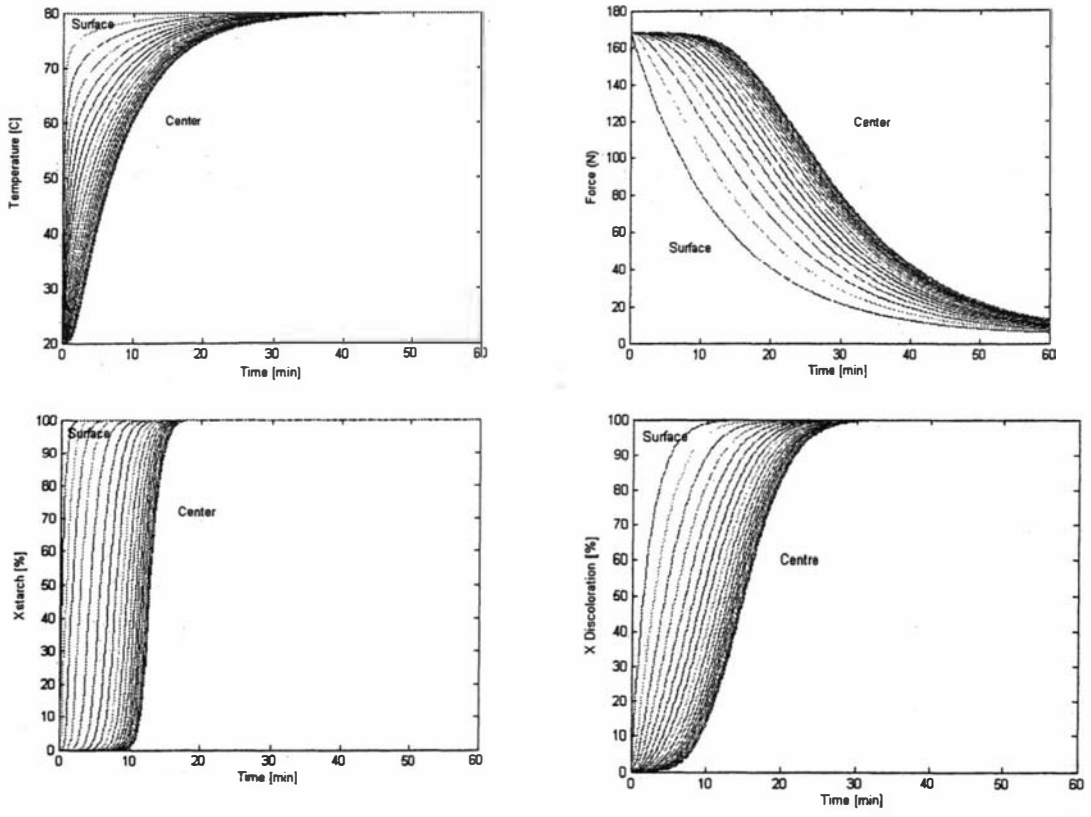

Figure 7-3 Simulation of the cooking process (80°C) in gold kumara slices (slab 2cm thickness)

The cooking temperature in each of these simulations was 80°C, with 20°C as the initial temperature of the product. The dimensions of the slab were 0.02m thickness and infinite length. The rectangular block was 0.01m thick (x), 0.01m in length (y), and 0.01m deep (z). The short cylinder simulated in Figure 7-5 was 0.02m thick, and 0.02m in diameter.

From the simulation results, it easy to see that the shapes of the product to be processed and their size have a large effect on the texture (fracture force), gelatinisation and discoloration reaction behaviour.

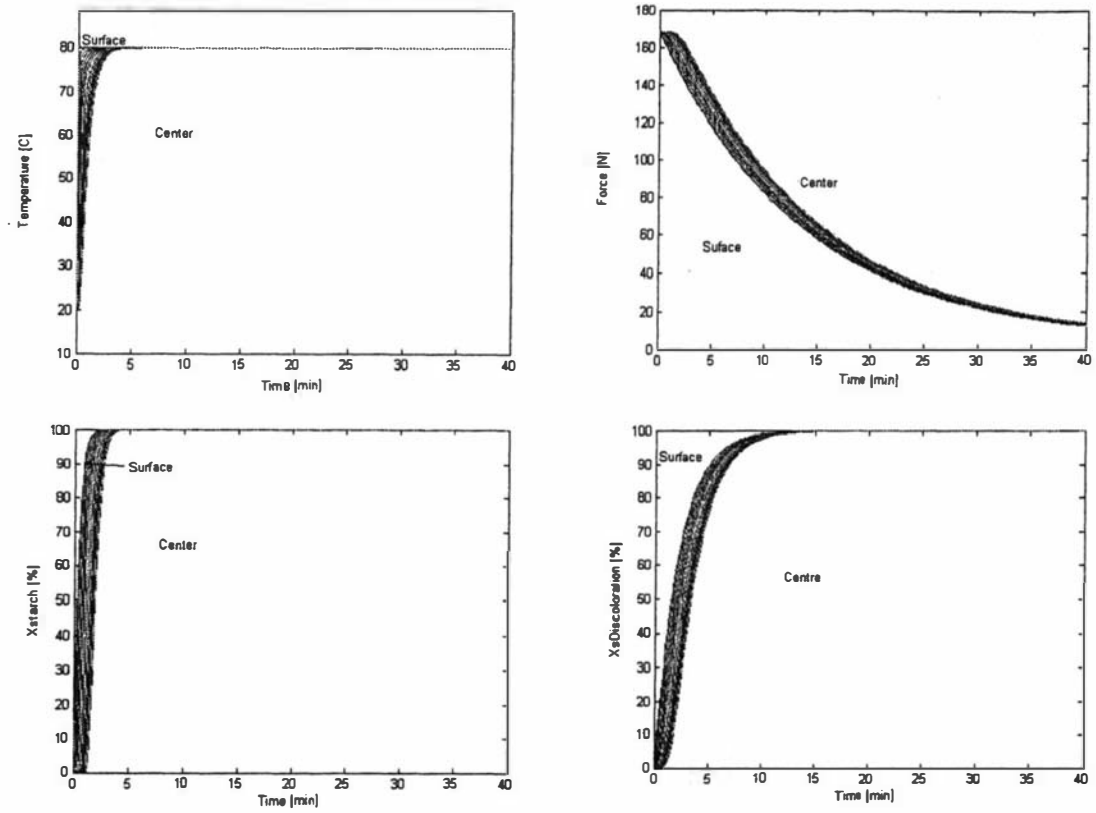

Figure 7-4 Simulation of the cooking process (80°C) in Gold kumara in a rectangular block arrangement (0.01m thick, 0.01m long, and 0.01m deep)

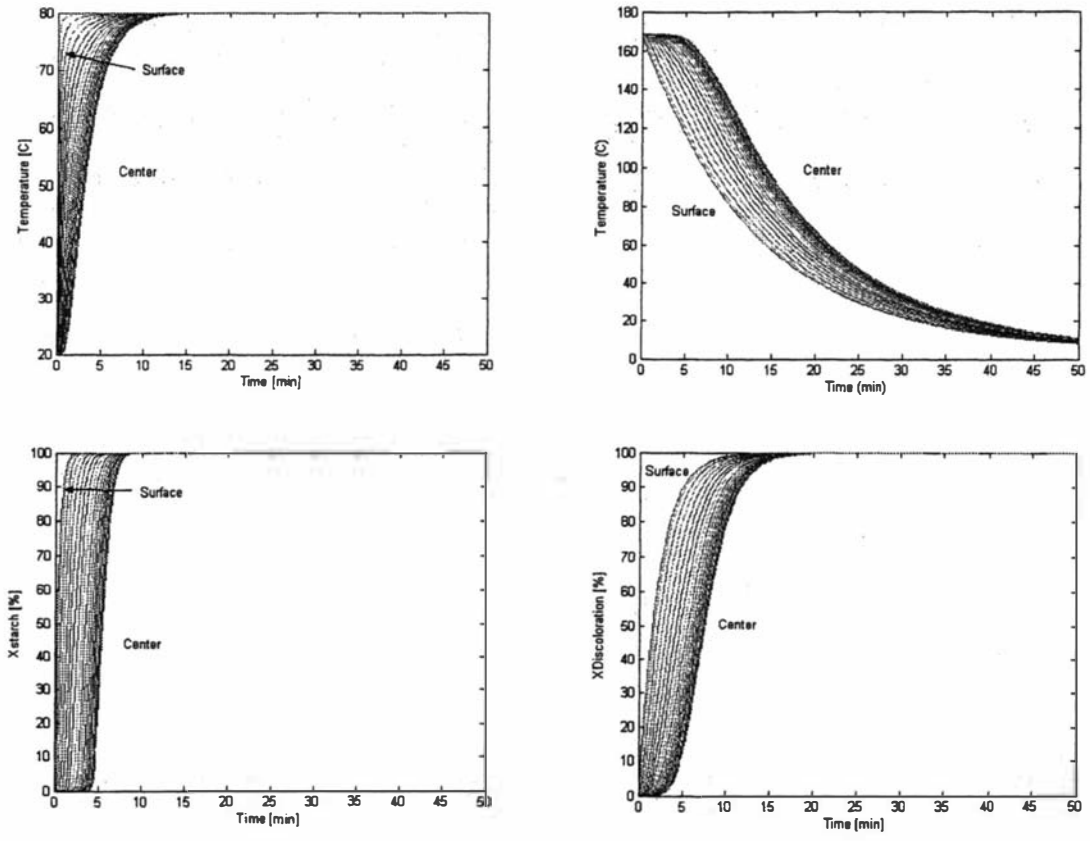

Figure 7-5 Simulation of the cooking process in gold kumara short cylinder arrangement (0.02m thickness, and radius 0.01m). Note the predictions are aligned in the x direction for radial centre

7.5.2. Rationalisation

From the simulation curves it is easy to see that the texture change is slower than the discoloration reaction in gold kumara, as previously discussed in section 7.2. In addition, at this cooking temperature the starch gelatinisation was very fast, being the first reaction to reach the completion.

The temperature profiles in all the cases have a similar shape but the time to reach the cooking temperature in each case is totally different. If the rectangular and short

cylinder predictions are compared, the time necessary to get all the product to the cooking temperature and to reach final texture levels is more than three times less for the rectangular block arrangement.

In addition there is much less variation in the extent of reaction in relation to position for the diced kumara predictions. Both of these factors (cooking time and variation in quality at a particular time) are key considerations to commercial processing operations.

7.6. MODEL VALIDATION

7.6.1. General considerations

To demonstrate the model predictions for texture and colour at different positions in kumara during the thermal treatment (cooking or cooling) were accurate, the model was validated against experimental data.

7.6.2. Experimental design

7.6.2.1. Roots preparation

Large roots of gold kumara were cleaned and cut into rectangular blocks. The dimensions were 3cm (x axis), 6cm (y axis), and more than 9cm in the z direction. The z dimension was made more than 3 times the others dimensions to avoid edge effects, and in this way ensuring 2 dimensional cooking. Cleland *et al.* (1994), found that if the a dimension is more than 3 times that of the other dimension, edge effects are minimal. These dimensions were the largest that could be cut from a single kumara root in order to facilitate a crude estimation of colour and texture profile through the sample after cooking.

7.6.2.2. *Samples locations and methodologies*

The rectangular blocks were vacuum packed into plastic bags.

After cooking, samples were taken from the centre of the block (z axis) by cutting three 1cm slices. From each slice samples were taken to determine texture and colour (see Figure 7-6). Texture was determined by uniaxial compression and the samples were cylindrical, 10mm in length, and 5mm radius. The methodology was described in Chapter 5 (5.2.2.6). For colour changes (discoloration), the equipment and methodology was described in Chapter 3 (3.3.5). Due to the large diameter of the test samples necessary for fracture force measurement and the large area (approx. $1cm^2$) that is used by the Minolta colorimeter to evaluate ΔE, it was possible to determine only a very coarse texture and colour profile.

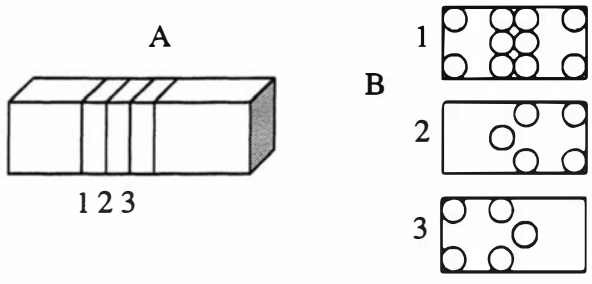

Figure 7-6 Layout of the trial experiment A) Slices location, B) Point samples from each slice

Data were analysed statistically using SAS, as a block design.

7.6.2.3. *Cooking temperature*

Simulations were run to select the temperature and time combinations to cook the samples prior to texture and colour determination (Figure 7-7, and Figure 7-8). The criteria to select the temperature was to be able to see the variation in each parameter.

For the texture validation 70°C was selected (Figure 7-7), and 50 and 60°C were used for discoloration validation. The analytical solution for heat transfer in a 2D slab was used to predict both the heating and cooking regions of the cooking process. For the cooking predictions it was assumed that the whole kumara slice had reached relatively uniform temperature in order to apply the solutions.

After cooking, the samples were placed into the cooling water (water and ice) at 5°C for 50min.

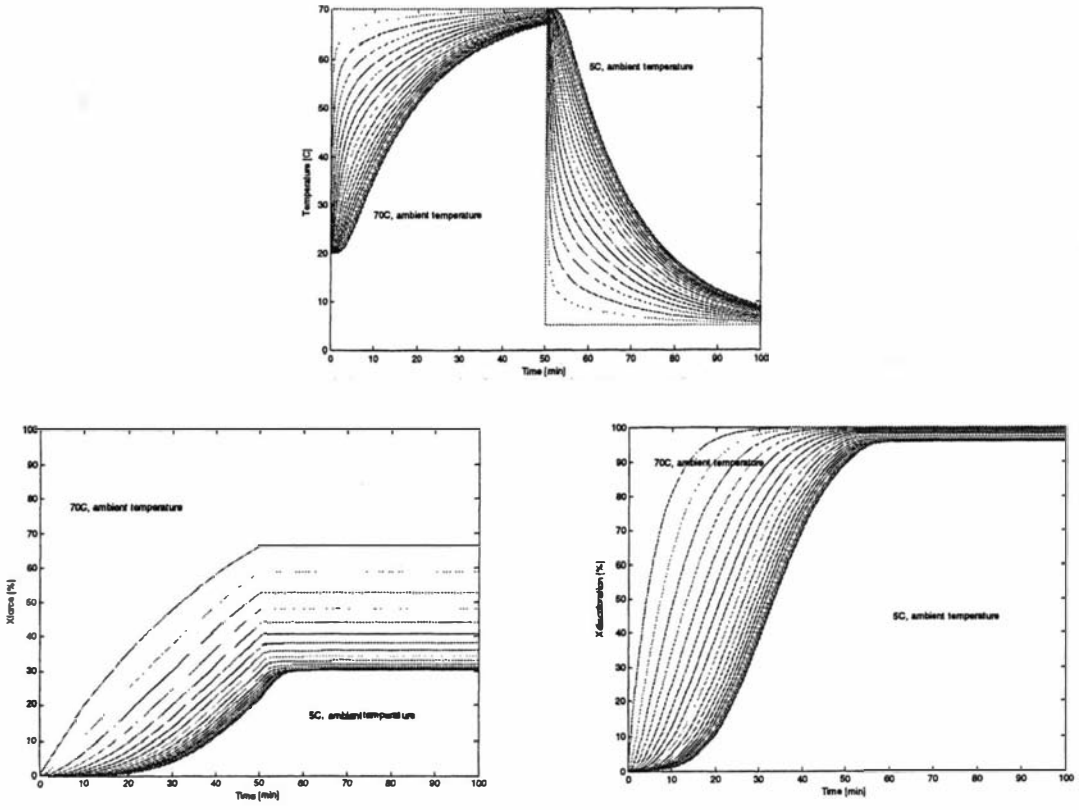

Figure 7-7 30mm slab cooked at 70°C for 50min and cooled with water at 5°C for 50min

The simulations show the impossibility of using one cooking temperature to validate both parameters. Cooking at 70°C, all the colour reaction change is completed before significant texture change occurred. At 50 or 60°C good validation in the colour was predicted but the change in fracture force was very small.

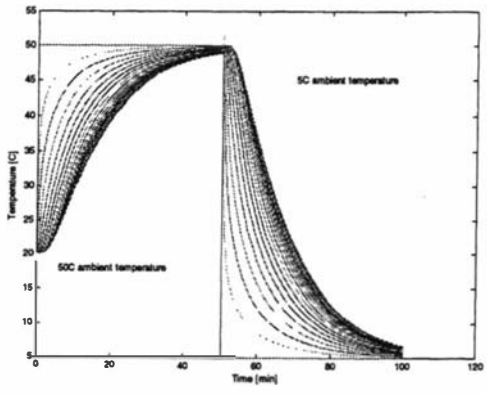

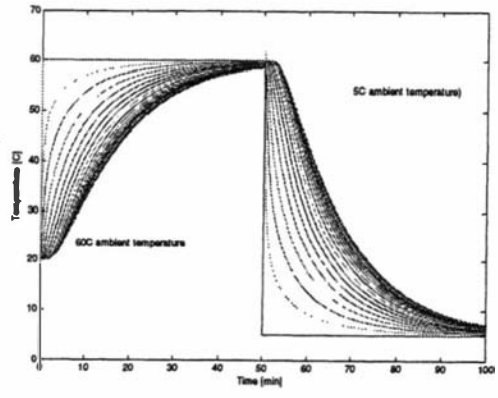

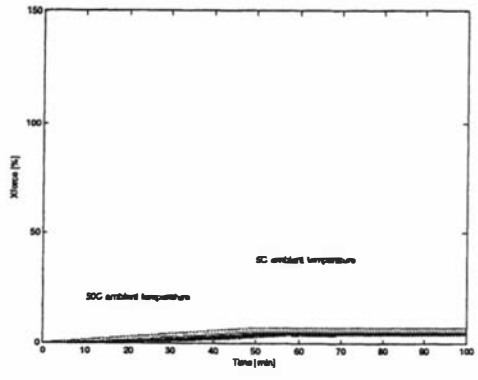

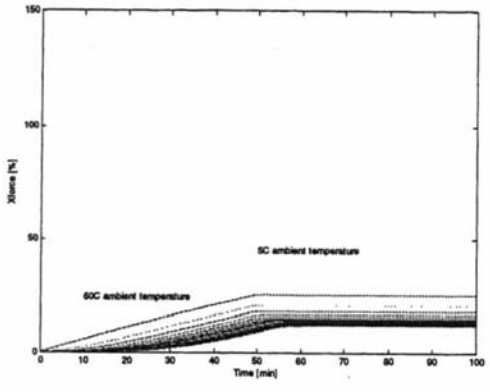

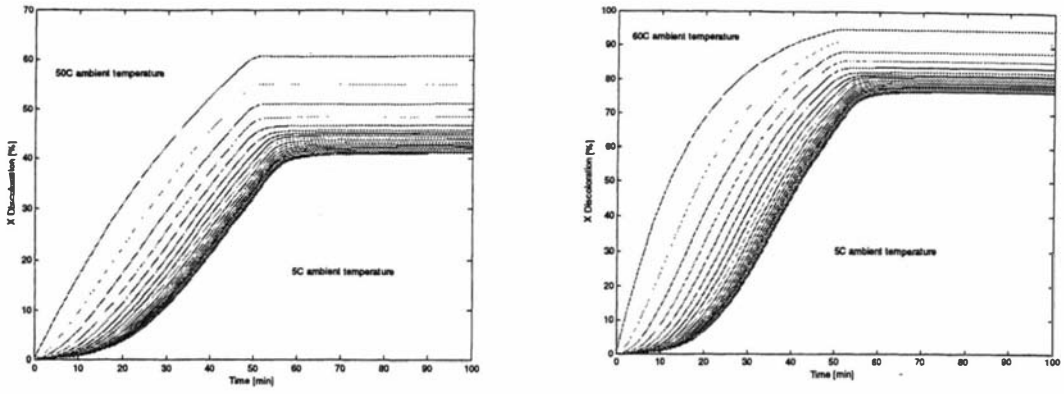

Figure 7-8 30mm slab cooked at 50 and 60°C for 50min and then cooled with water at 5°C for 50min

7.6.3. Model predictions and trial results

Texture and discoloration were simulated and are shown in Figure 7-7, and Figure 7-8 respectively.

Figure 7-9, and Figure 7-10 show the predicted texture profile through the sample, after the cooking was completed along with measured values of fracture force. The large sample sizes needed for the texture determination meant that the measurements are really an average of quite a large area of the sample. This is indicated on the plots within the error bars. Better validation of the model was not possible using the methods selected in this work.

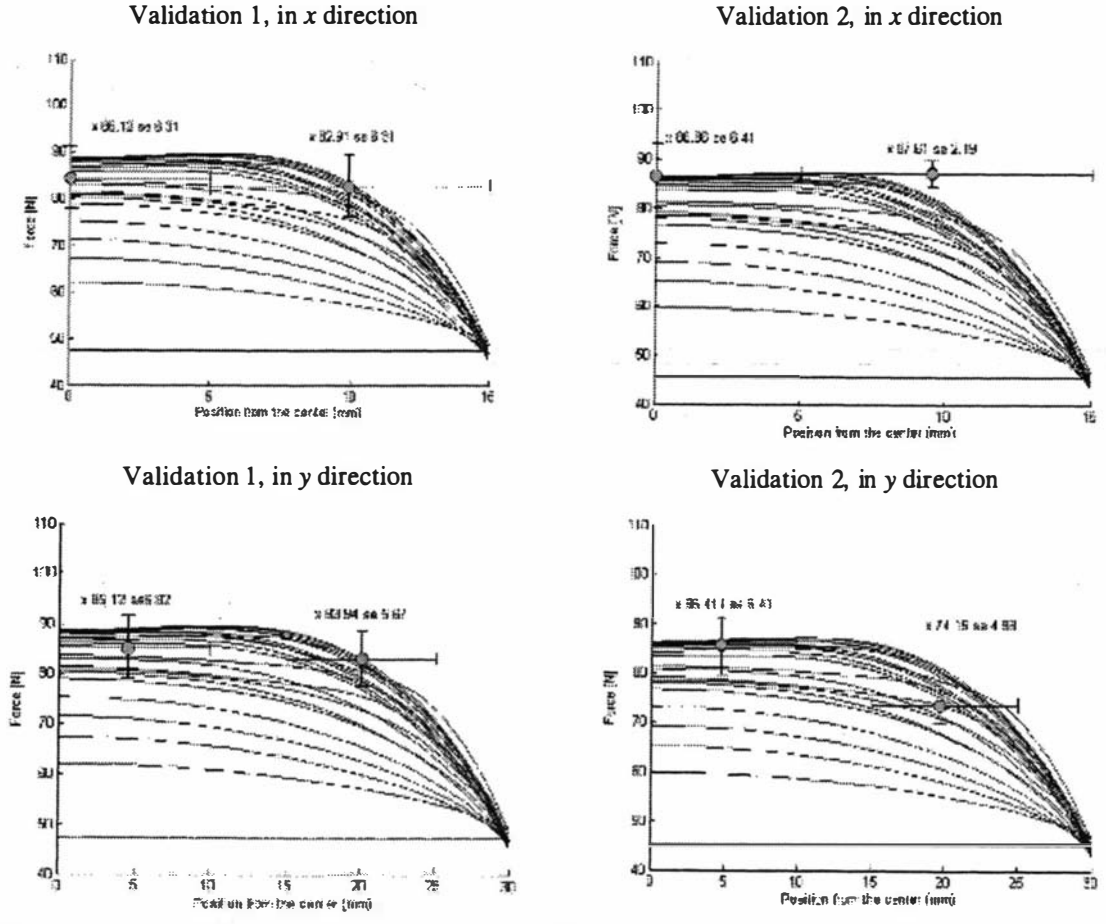

Figure 7-9 Fracture force prediction for 2D 60mm by 30mm slabs cooked at 70°C for 50min and cooled with water at 5°C for 50min

Unfortunately time constraints prohibited development of methods that would allow a more refined texture profile across the kumara.

The colour evaluation measurements also lacked resolution which meant it was difficult to accurately measure the colour profile across the slab. Image analysis techniques may offer an alternative approach to allow better model validation but time constraints prohibited this being carried out in this study.

The different values of discoloration obtained are very close to the model data.

Validation 1, in *x* direction 60°C

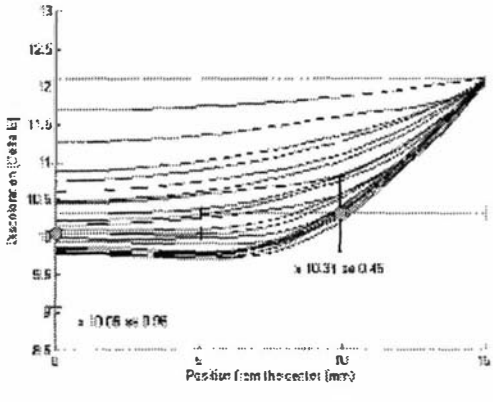

Validation 2, in *x* direction 50°C

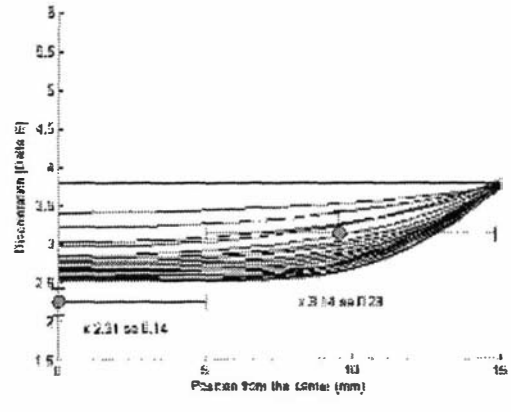

Validation 1, in *y* direction 60°C

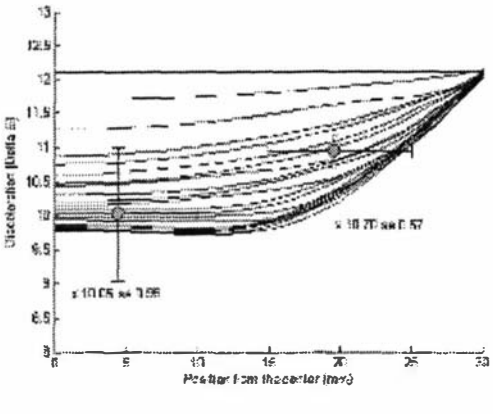

Validation 2, in *y* direction50°C

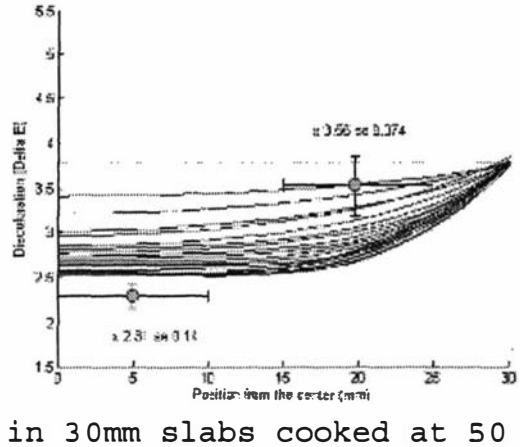

Figure 7-10 Discoloration (ΔE) in 30mm slabs cooked at 50 and 60°C for 50min and cooled with water at 5°C for 50min

Despite the problems with the measurement methods, the data from the experimental trials was close to the model results for both parameters studied. While not a comprehensive model validation, these experiments do offer some confidence that the models developed in this study are correct.

7.7. SENSITIVITY ANALYSIS

7.7.1. Temperature and size changes

In order to identify the effect of the processing parameters, such as cooking time and temperature and product sizes, on the temperature profile, texture (fracture force), starch gelatinisation and discoloration (ΔE) reactions in the product, a sensitivity analysis was carried out. This is as shown Figure 7-11 to Figure 7-14.

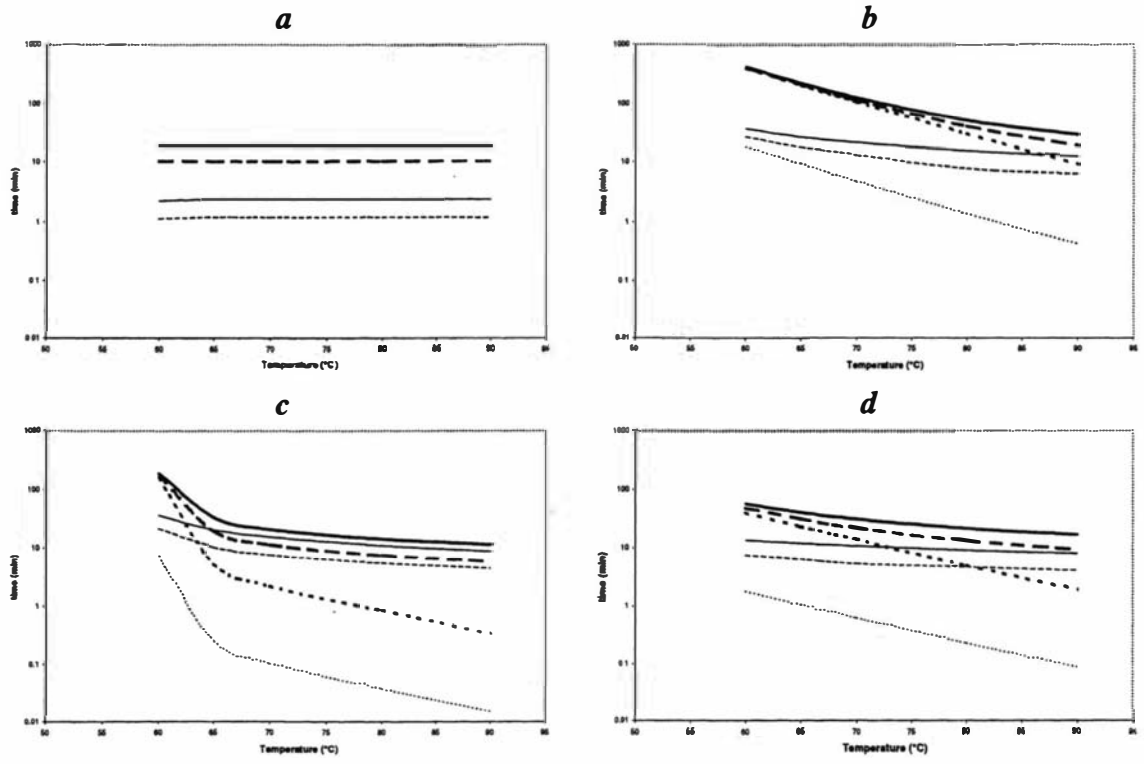

Figure 7-11 Time treatment required to achieve X=0.1(-) and X=0.9(-) for centre (–), average (- -) and surface (···) of a 2cm slab at different cooking temperature for *a*) Temperature, *b*) Fracture force, *c*) Gelatinisation, and *d*) Discoloration (ΔE) reaction

The time to reach 10% or 90% (*1-Y*) of the cooking temperature change in the samples is independent of the cooking temperature. This because the temperature profile inside the sample is dependent on the products thermal characteristics and not on the external temperature (see ***a*** in Figure 7-11 and Figure 7-12).

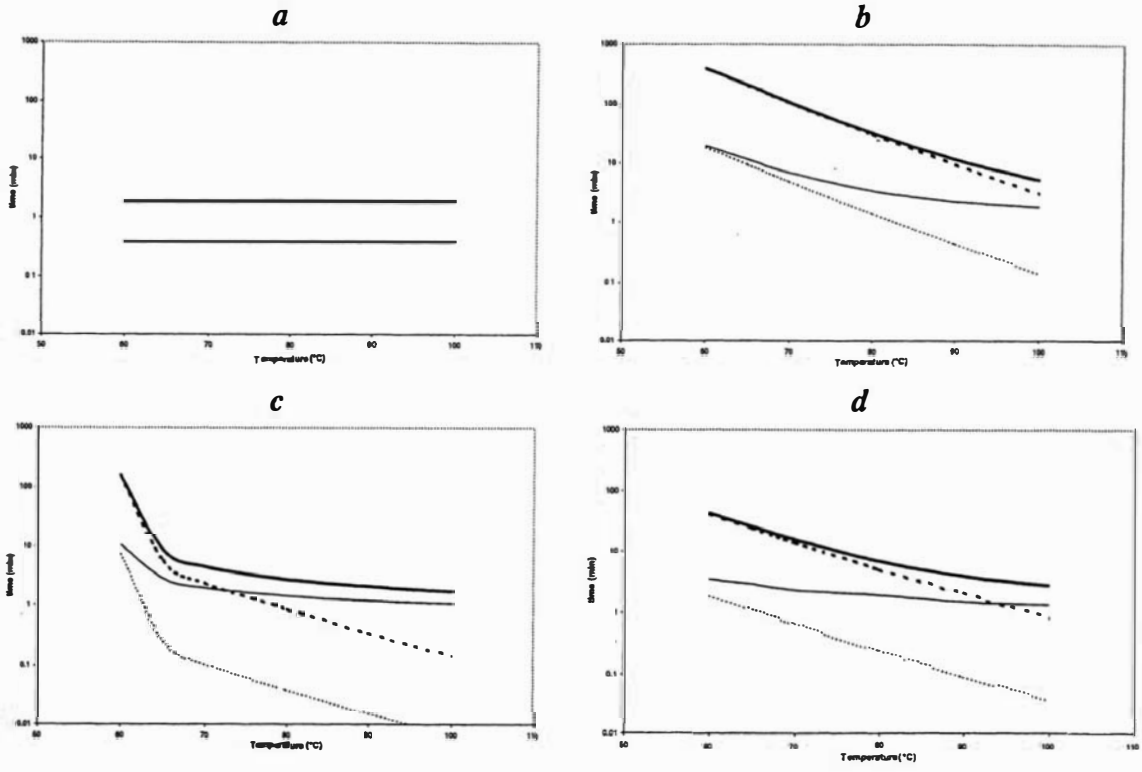

Figure 7-12 Time treatment required to achieve X=0.1(-) and X=0.9 (-) for centre (–) and surface (···) of rectangular block (1cm*1cm*1cm) at different cooking temperature for *a*) Temperature, *b*) Fracture force, *c*) Gelatinisation, and *d*) Discoloration (ΔE) reaction

At the lowest cooking temperature (60°C) the force, gelatinisation and discoloration (ΔE) reactions are approximately the same for the infinite slab and rectangular blocks. Under this condition, the rates of reactions are much slower than the heating rate and therefore the reaction are much more uniform with respect to position. The counter to this however, is that the cooking time is very long.

At high cooking temperatures more variation of the product with position is evident in all three reactions during the cooking process. It easy to see in Figure 7-11 and Figure 7-12 that the distance between the X=0.1 and X=0.9 curves increase as cooking temperature increases.

The discoloration reaction is more sensitive to temperature change than texture, for both shapes. The time range for discoloration reaction reduced to a greater extent than the texture changes (fracture force changes) by changing the geometry from a slice to a diced shape, as shown Figure 7-11 and Figure 7-12.

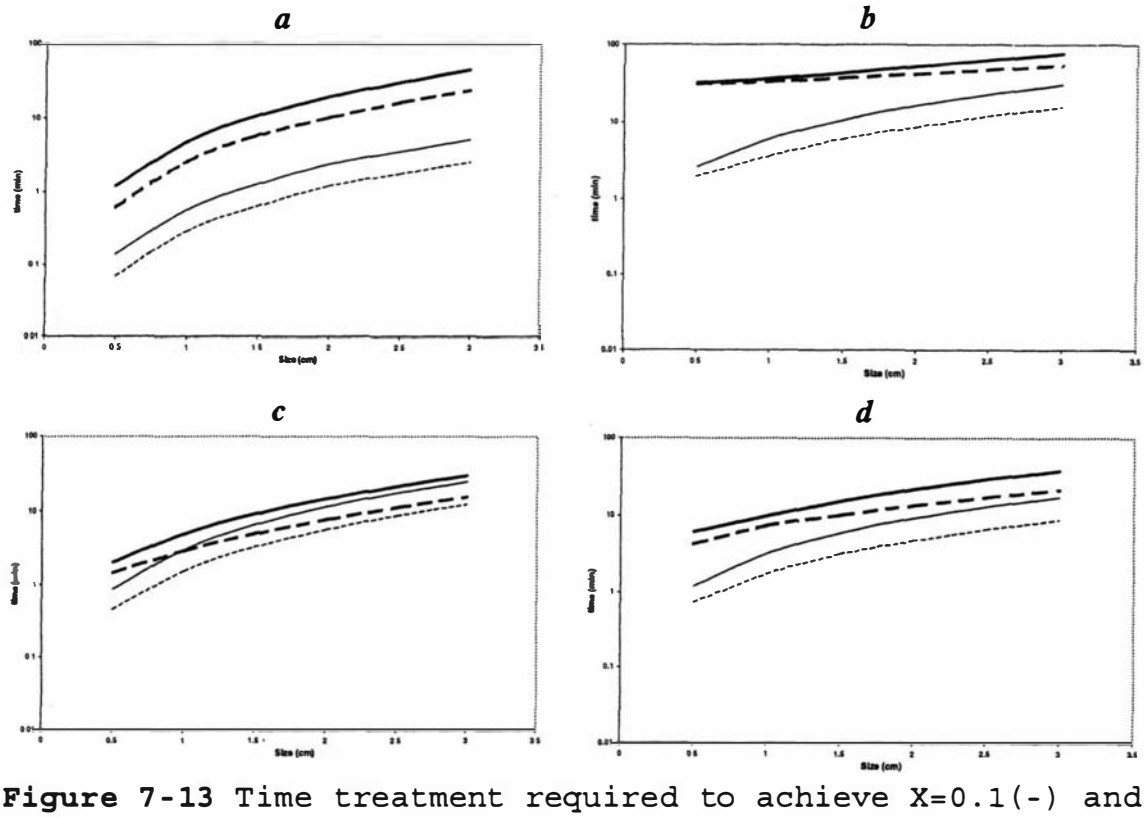

Figure 7-13 Time treatment required to achieve X=0.1(-) and X=0.9 (-) for centre (–), and surface (- -) at different slab sample sizes, cooked at 80°C, for *a*) Temperature, *b*) Fracture force, *c*) Gelatinisation, and *d*) Discoloration (ΔE) reaction

The size is another parameter that can be used to optimise the process to get well controlled and uniform product quality.

Figure 7-13 and Figure 7-14 show the times required to reach 10% or 90% of reaction completion, for different sized slices and dices cooked at 80°C respectively.

These figures show that the time required to achieve a desired degree of cooking increases significantly as the dimensions of the product increase. This trend translates through to dramatic increases in the time required for textural, colour and gelatinisation reactions to occur throughout the product.

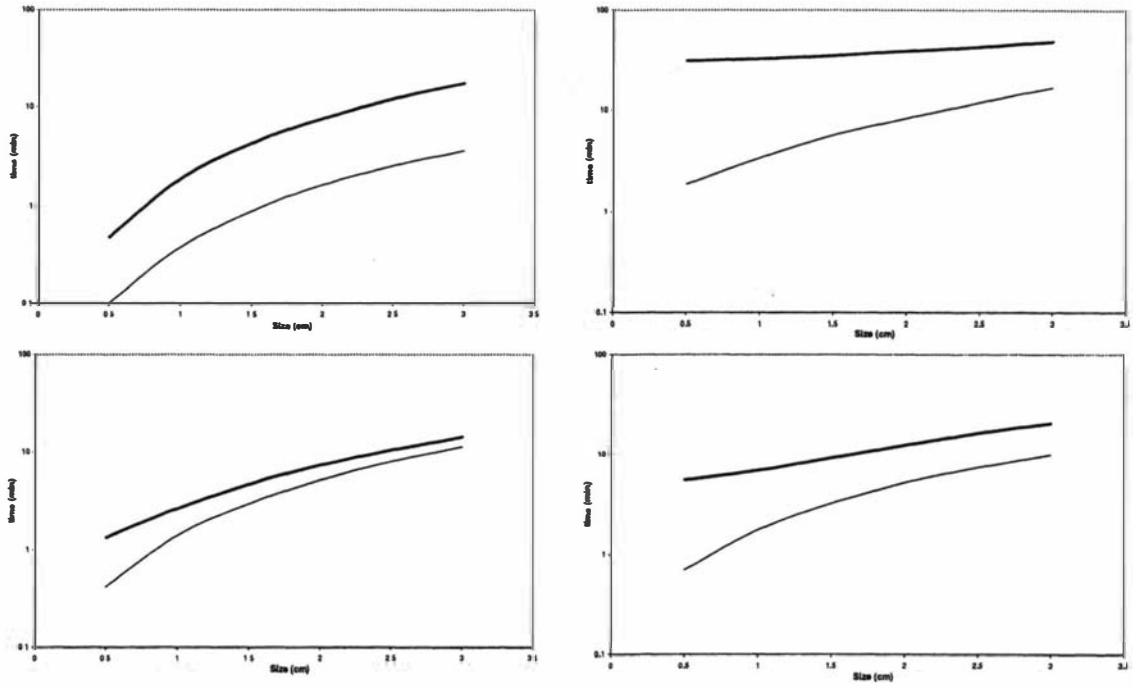

Figure 7-14 Time treatment required to achieve X=0.1(-) and X=0.9 (-) for centre at different rectangular block sizes at 80°C cooking temperature for *a*) Temperature, *b*) Fracture force, *c*) Gelatinisation, and *d*) Discoloration (ΔE) reaction

7.7.2. Variation inside the product (uniformity) at different samples sizes

The uniformity in the final product is an important quality characteristic.

The uniformity in force and discoloration in the product during the cooking process, was defined as the fraction of the kumara volume that was less than a critical percentage of the extent of kinetic change at the surface of kumara. This critical value can be interpreted as the level of variation that is tolerated in the product. The uniformity is then the fraction of the kumara that meets this requirement.

In order to analyse the affect of cooking conditions on the uniformity in force and discoloration of slices and dices of kumara, different simulations were carried out using the model and the uniformity was then calculated. These results are shown in Figure 7-15 to Figure 7-22.

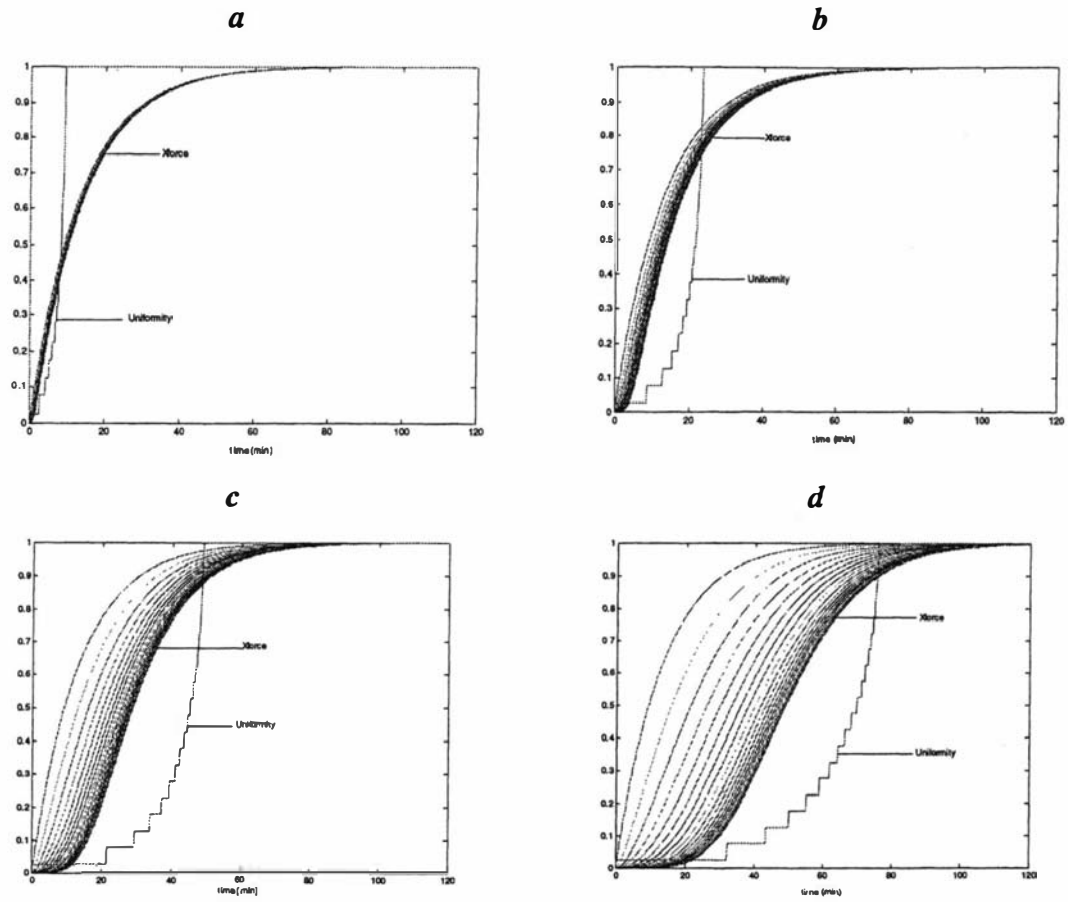

Figure 7-15 Texture (fracture force) profile and uniformity in samples cooked at 80°C for 120min in: a) 5mm slab, b) 10mm slab, c) 20mm slab, and c) 30mm slab in thickness using 10% as the critical value

It can be seen in Figure 7-15 that the time taken until all the kumara volume meets the uniformity criteria increases as the slice thickness increases. This can be seen more clearly on Figure 7-16. While this result is not surprising, this approach to quantifying the uniformity of texture in kumara is useful in terms of optimising an industrial operation. A key trend which is made clear from this analysis is that the range of possible textures that a product can have and yet still meet the uniformity criteria, is much greater for the thinner samples (e.g. X_f >0.4 for a 5mm slice but only X_f >0.9 for a 20mm thick slice). As the slice thickness increases or the uniformity criteria becomes more strict, the possible range of texture in the cooked product decreases to approach that of completely cooked product.

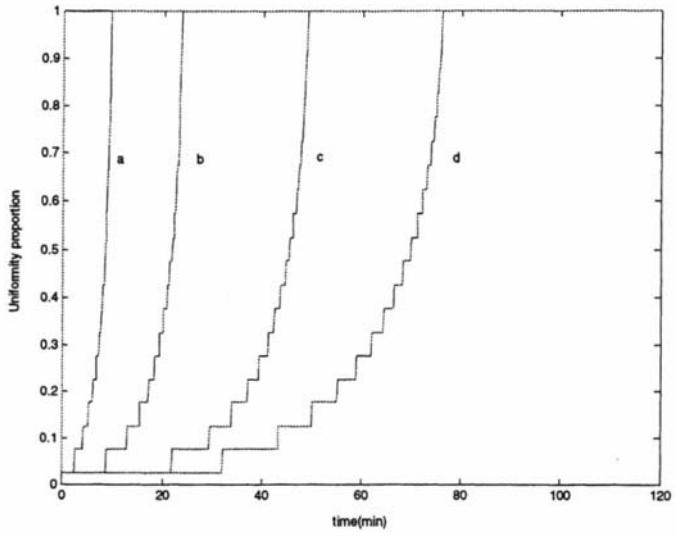

Figure 7-16 Comparison of (fracture force) uniformity in samples cooked at 80°C for 120min in: a) 5mm slab, b) 10mm slab, c) 20mm slab, and c) 30mm slab in thickness, using 10% as critical value

Figure 7-17 and Figure 7-18 presents a similar analysis for the uniformity in discoloration reaction.

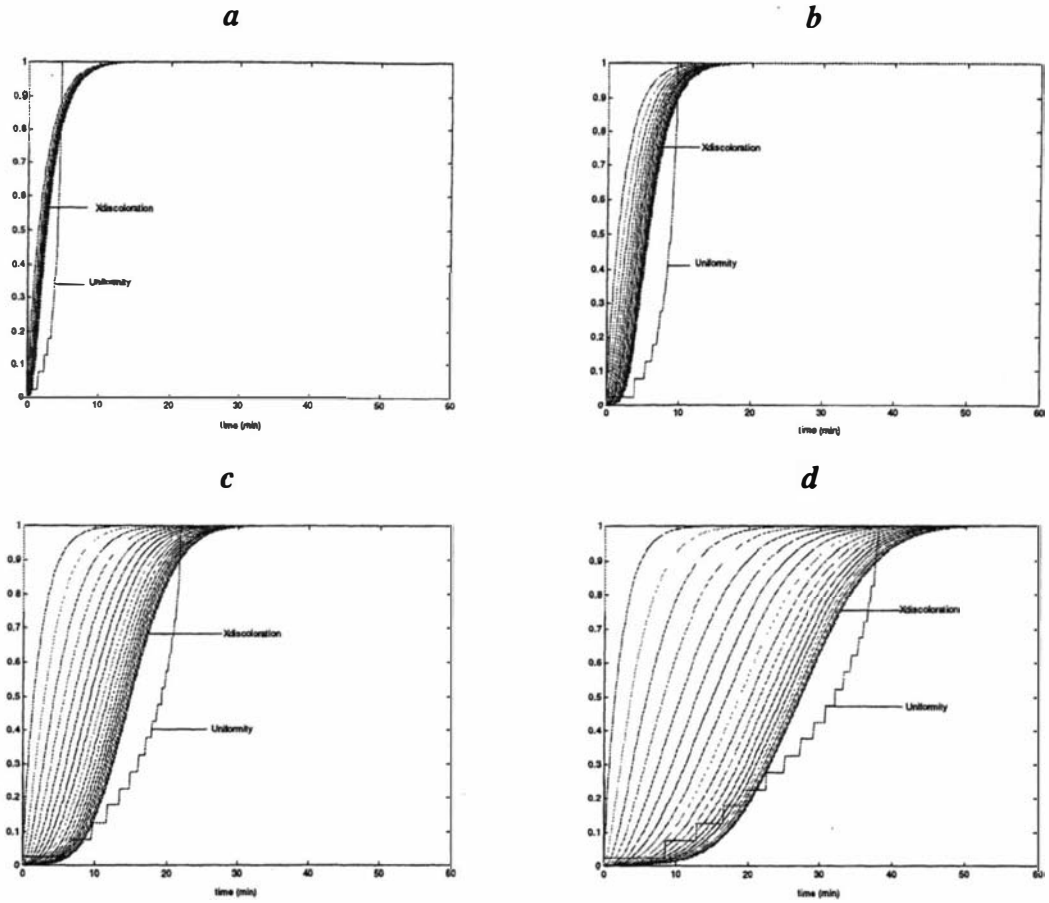

Figure 7-17 Discoloration (ΔE) profile and uniformity in samples cooked at 80°C in a) 5mm slab, b) 10mm slab, c) 20mm slab, and d) 30mm slab in thickness, using 10% as critical value

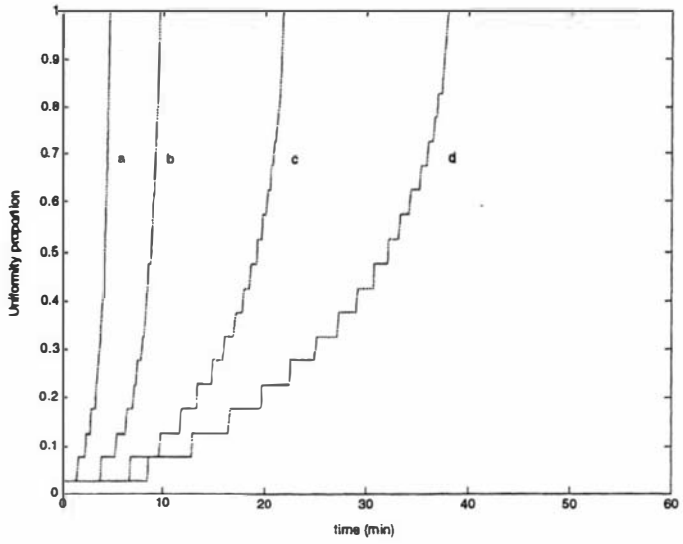

Figure 7-18 Discoloration (ΔE) uniformity in samples cooked at 80°C in: a) 5mm slab, b) 10mm slab, c) 20mm slab, and c) 30mm slab in thickness, using 10% as critical value

Similar observations are evident from these plots. It is clear that at a 80°C cooking temperature there is a little scope for avoiding significant colour change if the 10% uniformity criteria is to be met. Figure 7-19 and Figure 7-20 summarises this analysis for the texture changes reaction in dice. Again, there is a trend that as the sample size increases so do the gradients of reaction progress in the sample. As a result the stability criteria can only be met in thick samples of the reaction approaches completion. By moving to a diced product, heating is more even due to now having three dimensional heat transfers. As a result there is greater scope to achieve a specific textural requirement without compromising uniformity of product.

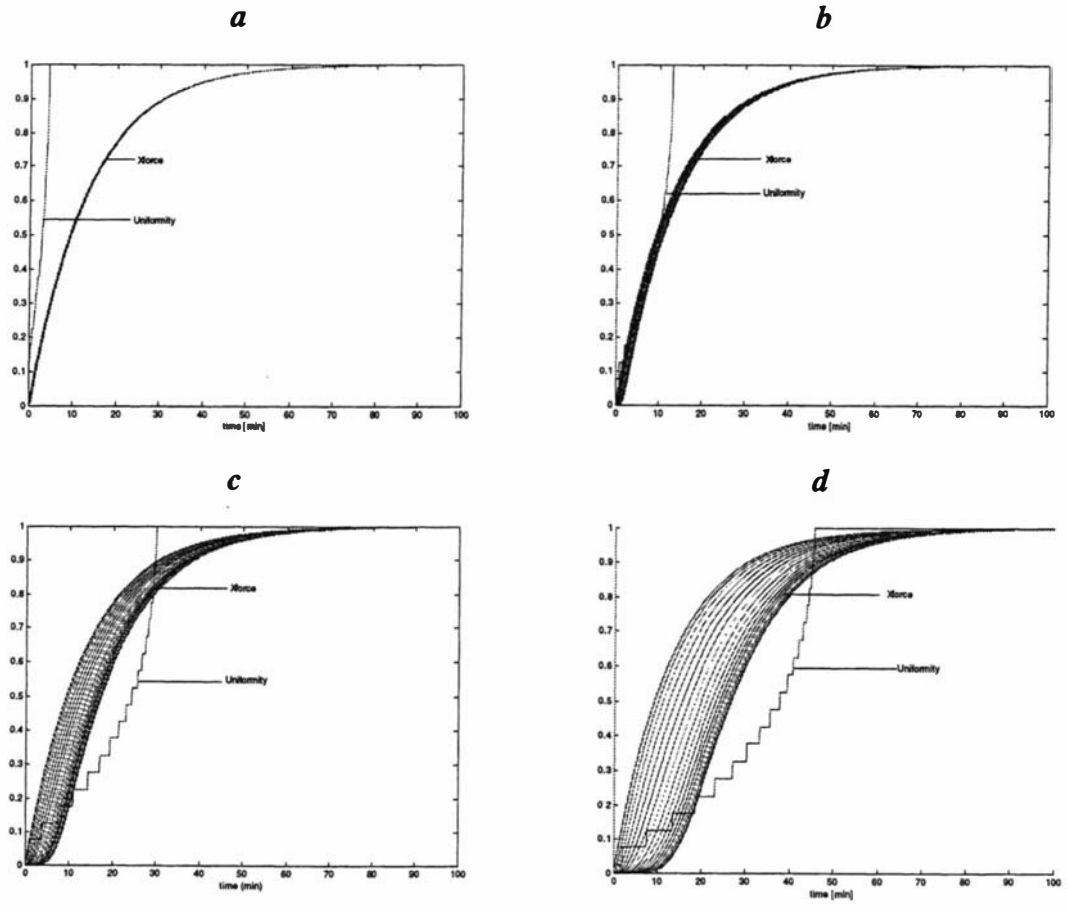

Figure 7-19 Texture (fracture force) profile and uniformity in samples cooked at 80°C in a) 5*5*5 [mm^3] dice, b) 10*10*10 [mm^3] dice, c) 20*20*20 [mm^3] dice, and c) 30*30*30 [mm^3] dice using 10% as critical value

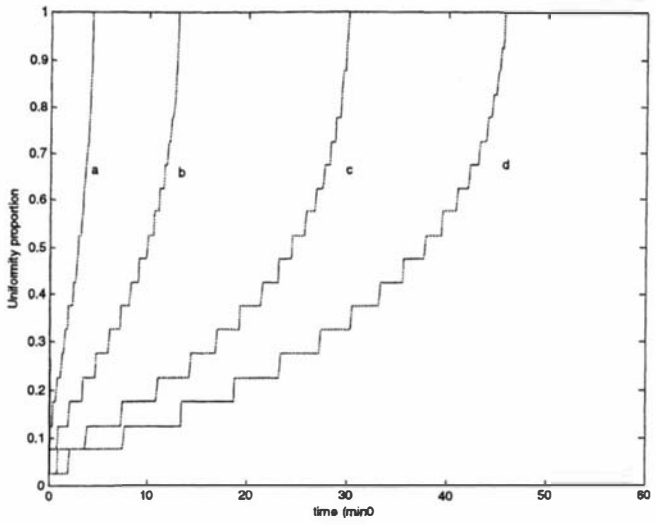

Figure 7-20 Texture (fracture force) uniformity in samples cooked at 80°C for 100min in a) 5*5*5 [mm^3] dice, b) 10*10*10 [mm^3] dice, c) 20*20*20 [mm^3] dice, and d) 30*30*30 [mm^3] dice, using 10% as critical value

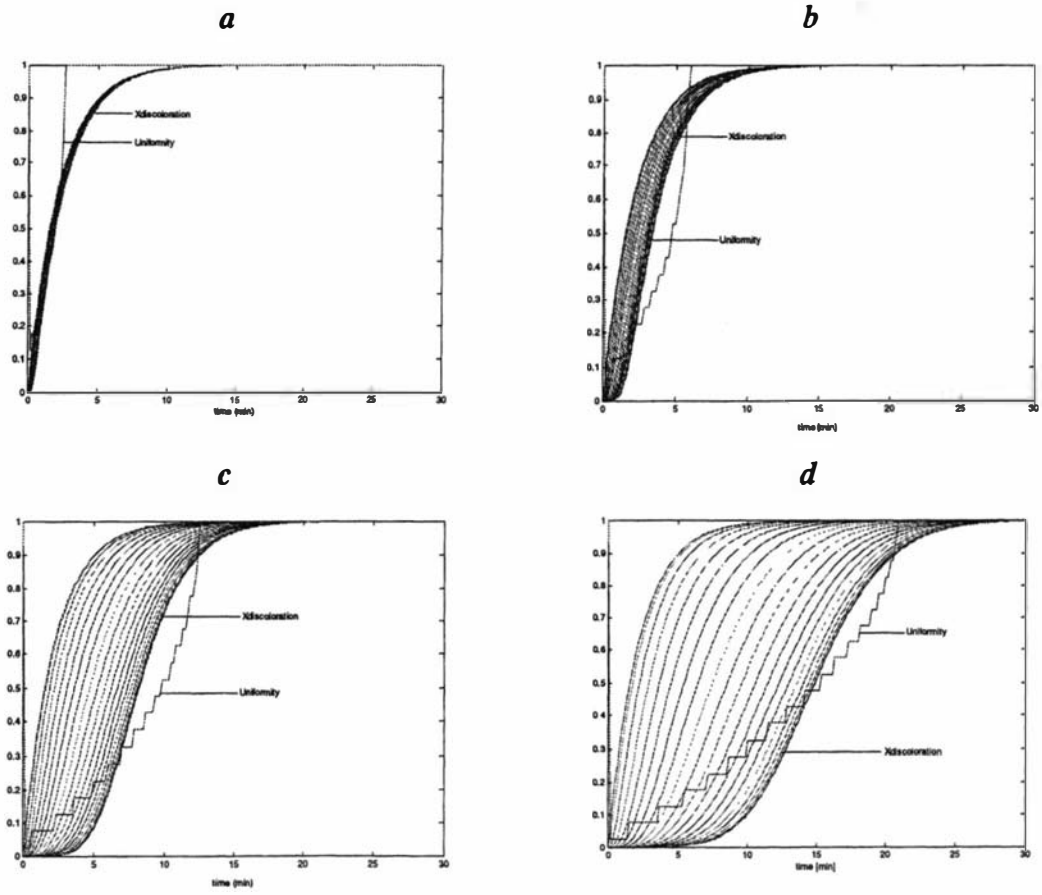

Figure 7-21 Discoloration (ΔE) profile and uniformity in samples cooked at 80°C in a) 5*5*5 [mm^3] dice, b) 10*10*10 [mm^3] dice, c) 20*20*20 [mm^3] dice, and c) 30*30*30 [mm^3] dice, using 10% as critical value

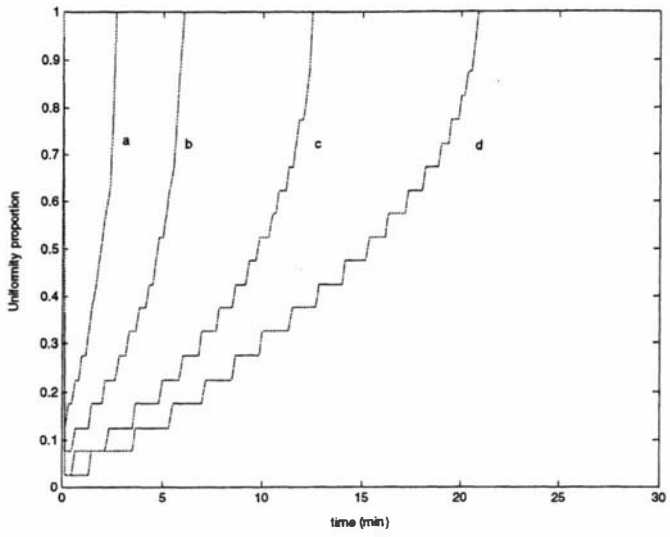

Figure 7-22 Discoloration (ΔE) uniformity in samples cooked at 80°C in a) Dice 5*5*5 [mm^3] dice, b) 10*10*10 [mm^3] dice, c) 20*20*20 [mm^3] dice, and c) 30*30*30 [mm^3] dice, using 10% as critical value

Similar conclusions can be drawn with respect to the discoloration reaction uniformity in diced kumara product (see Figure 7-21 and Figure 7-22)

The information (cooking time, cooking temperature, shape and size effect over the kumara processing, etc) that the model provides, constitutes a helpful tool for in problem solving processing, in the design of the process line or for identifying how the product quality required for a customers can be achieved using the current equipment in the plant.

7.8. MODEL APPLICATION

In order to demonstrate the potential application of the model for industrial problem solving, two case studies were carried out for different hypothetical scenarios with typical questions that the process manager might have to answer.

Traditionally such questions would be resolved either by trial and error or by application of years of industrial experience, if indeed it is available in the company.

These case studies are intended to demonstrate how the understanding of the changes to kumara, once integrated with the heat transfer model, can provide a value tool to industry.

7.8.1. Case 1

The first case is aimed at being able to produce a product that is specified by an overseas client. The customer is a food processing manufacturer, and they want to have a cooked kumara to make a new desert formulation for 2 to 4 years old children. The product has contain a cooked kumara, have a colour with no evidence of darkening, and the final product must preserve at least 50% of the initial colour. In addition, it has to be moderately soft, in other words it has to have lost at least 40% of the initial texture because it will be mixed with other ingredients without additional cooking. Finally, the product cannot contain any additives to improve the colour or texture. Under the scenario described many questions about the process must be answered.

What is the cooking temperature and time during the process in order to reach the quality of texture and colour required?

Is it possible to manufacture the product required with out additives, such as SAPP to prevent discoloration, just by managing the cooking temperature and size and shape of the product during processing?

To clarify if the product required by the client is possible to make, a traditional process was considered including the peeling, cutting (dice and slab) and cooking operations. To solve the problem, the extent of discoloration and texture (force) behaviour must be predicted for the cooking operation. Consequently, simulations were carried out using the traditional shapes after cutting, of rectangular block or dice and infinite slab geometries. A short cylinder was considered as well to simulate the extreme shape of the roots.

Figure 7-23 to Figure 7-25 shown the extent of force and discoloration reaction during cooking at 80°C. In all the predictions, the discoloration reaction was faster than the force change. The client requires that the product preserve at least 50% of the initial colour, which means that the extent of the discoloration reaction has to be less than 50%.

In a slab (10mm in thickness) the cooking time has to be less than 14.25min to preserve the colour, but at this time the product has lost only around 5% of the initial texture. The colour meets the required specifications but the product is too hard for the client.

In the same manner other arrangements of size analysis can be made. It is clear however from the results that the conclusion is the same, "it is impossible to meet the customers objectives unless an additive is used to control the texture, or the product is handled by in the complete absence of oxygen." This result is clearly shown in Figure 7-2 of this chapter for the extreme case where no heat transfer limitations exist in the product.

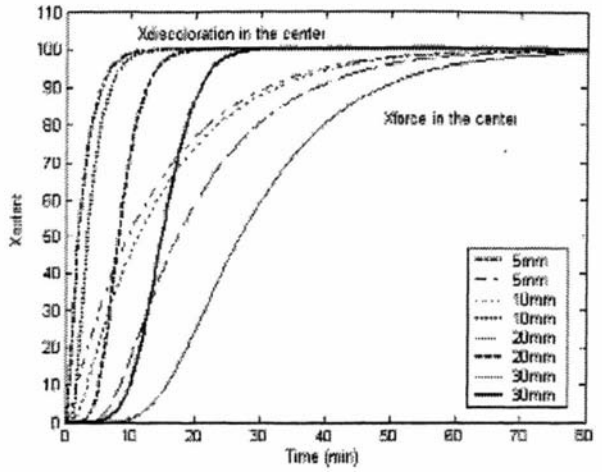

Figure 7-23 Simulation of force and discoloration changes in cooking operation at 80°C in kumara with different dice's size configurations

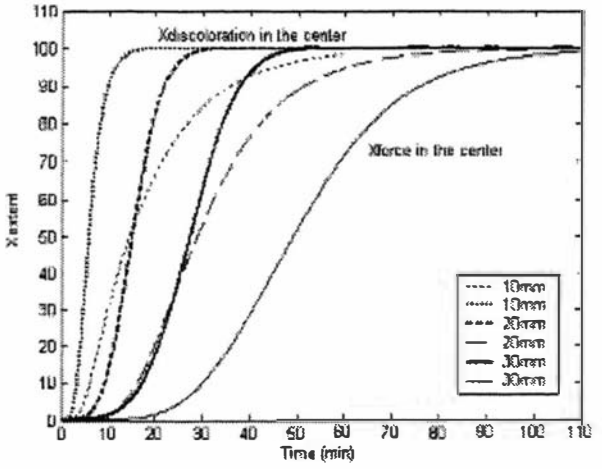

Figure 7-24 Simulation of force and discoloration changes in cooking operation at 80°C in kumara with different slab thickness

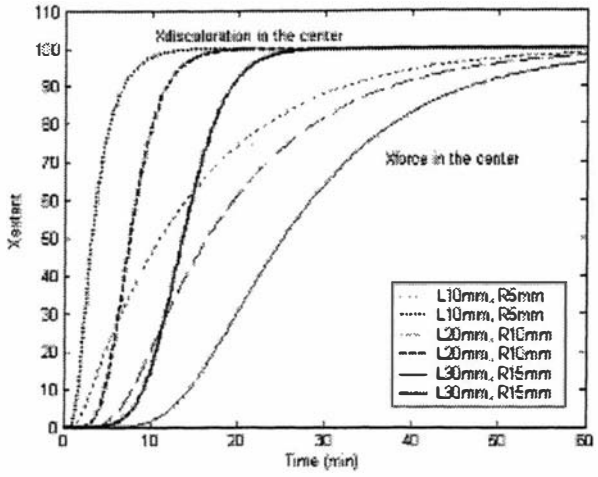

Figure 7-25 Simulation of force and discoloration changes in cooking operation at 80°C in kumara with different short cylinder length and ratio configurations

7.8.2. Case 2

The uniformity of products is always an important factor in product quality which must be controlled. In most cases the client specifies what levels of variation in product functionality is allowable.

To define what range of uniformity of values that is acceptable, it is necessary to consider that it has a process cost implication, and different scenarios can be used to reach the same values of variation or quality uniformity.

The simulation of different process configurations, is a good way to quantify the impact of changing specifications on processing and product characteristics. As an example a case study was carried out to quantify the importance of a change between 5 to 10% of tolerance in the uniformity criteria for the final product in texture (measured as a fracture force) and colour change in a kumara cooking process.

In this case one shape was considered, the slab or slice. Simulations were carried out to identify; the relationship between uniformity, slab dimensions, and cooking time, and

the relationship between the extent of reaction (force and discoloration) and uniformity at different slab sizes.

Different levels of the critical values of variation were considered, 5 10, 20 and 30%. The 5% level represents the highest specification of those studied. The results of the simulations are summarised in Figure 7-26, to Figure 7-28.

From the Figure 7-26 the effect of tighter control on permitted variability in the product is clearly demonstrated. Certainly the cooking operation is an expensive and important unit operation.

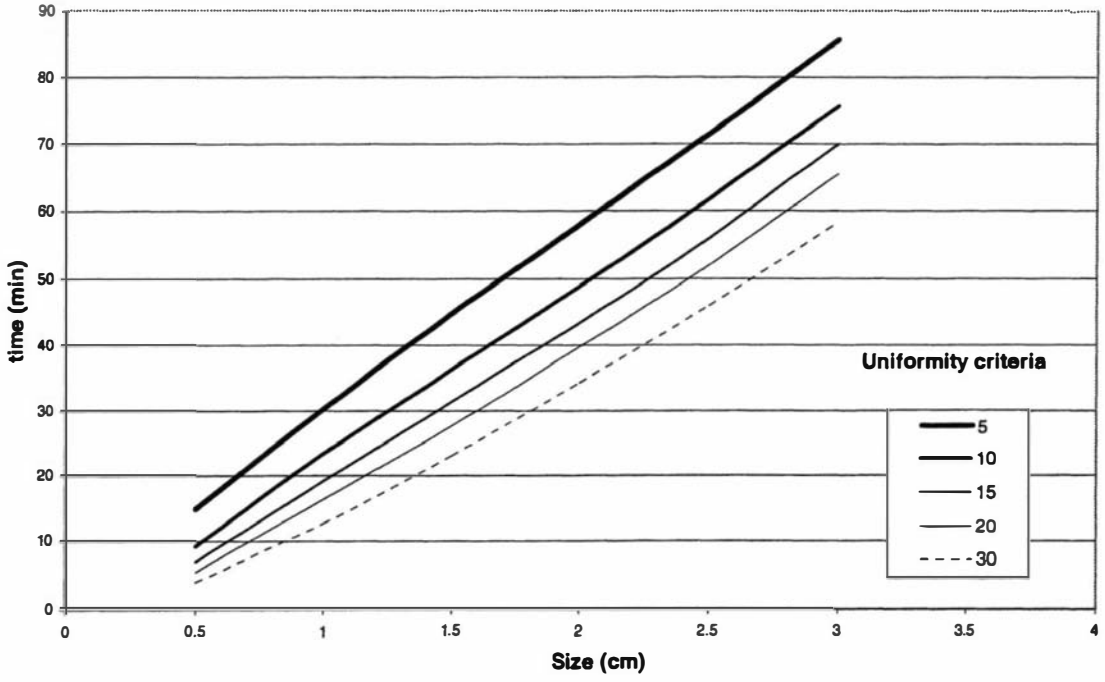

Figure 7-26 Cooking time to reach different uniformity in kumara slabs at different thicknesses cooked at 80°C

Considering a slab of 2cm thickness, an increase in the uniformity of 5% (i.e. a variation decrease from 10 to 5%) means an increase in the cooking time of around 9min (from 50 to 58min).

From the Figure 7-27, and Figure 7-28, it is possible to see that there is a cost for this reduction in variability due to heat transfer through the product. The cost is that the range of possible texture and colour is significantly reduced. In order to have only 5% of variation in the product, 93% of texture reaction must be reached (very soft). If the variation criteria related to is 10% the product texture change can be stopped at 87%. In the same way for the discoloration, in order to have 5% of variation in the same slice dimension, 95% of the reaction has completed, while at 10% this value reduces to 90%. In small samples this effect has an even greater impact on cooking time and possible product functionality.

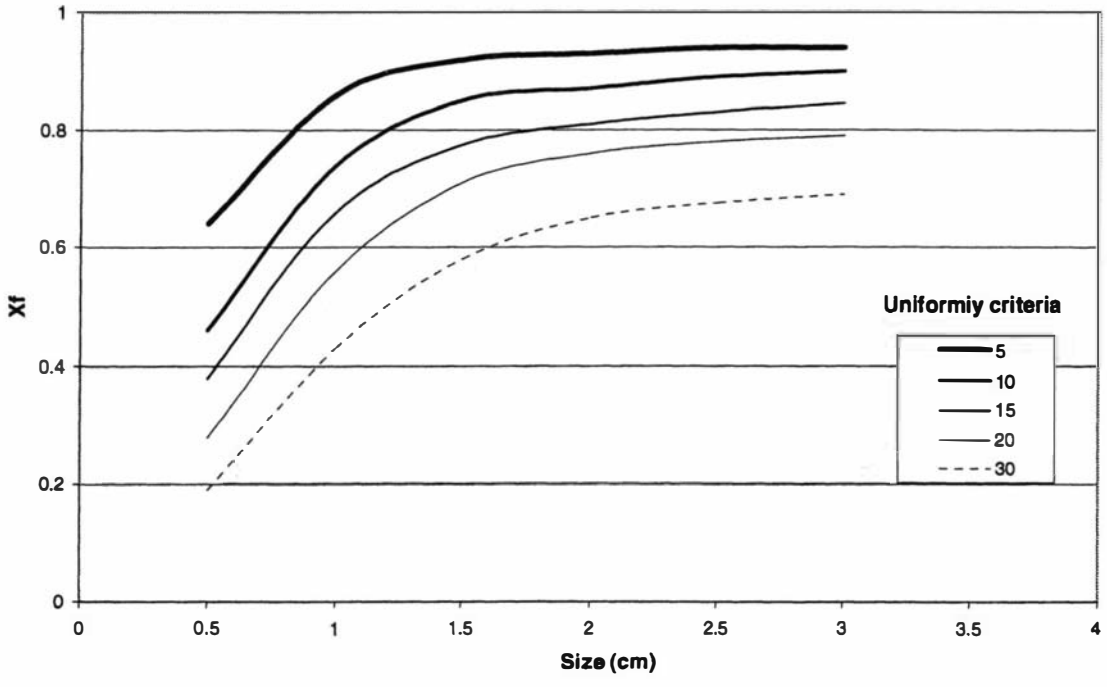

Figure 7-27 Extent of force (X_f) to reach different uniformity in kumara slabs at different thicknesses cooked at 80°C

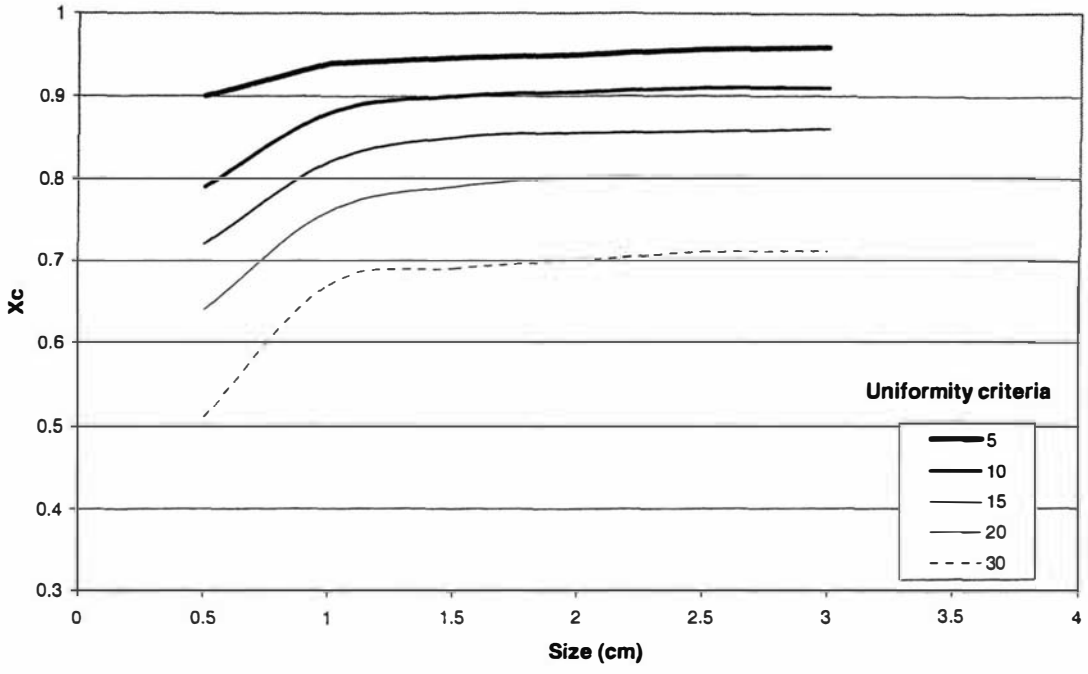

Figure 7-28 Extent of discoloration reaction (X_c) to reach different uniformity criteria in kumara slabs of different thickness cooked at 80°C

7.9. CONCLUSION

The model developed from the kinetics data during previous chapter, can be used to predict texture and colour in kumara using different time and temperature histories, or to simulate the final kumara quality processed under different condition.

A limited validation process was carried out which provided some confidence that the model predicted reality correctly. Force and colour determination methods with greater resolution (i.e. smaller area for sample measurement) are required to more fully validate the model.

The model can be used as a tools for the process design and optimisation. Two case studies were carried out to demonstrate how the model could be applied to industrial situations.

CHAPTER 8: CONCLUSIONS AND RECOMMENDATIONS

8.1. CONCLUSIONS

Colour and texture quality characteristics were studied in Owairaka Red and Toka Toka Gold kumara (*Ipomoea batatas* L).

A post cooking darkening mechanism was proposed and demonstrated experimentally. This mechanism was comprised of three steps; cell modification causing release of iron and phenolic, iron-phenolic complex formation and oxidation of Fe^{2+} to Fe^{3+} from this complex. The kinetics for the cellular modifications causing release of free iron and phenolic were measured for a range of cooking temperatures. It was shown that this reaction occurs more quickly than textural modification demonstrating that its prevention by manipulating cooking conditions is not possible.

The control of post cooking discoloration, using SAPP as a metal chelating agent, showed that free iron levels could be made the limiting element for the discoloration reaction in kumara. This offers a good method for prevention of after cooking darkening.

After cooking, the rate of the kinetic of darkening in kumara was found to be limited by the rate of diffusion of oxygen into the sample, rather than by the rate of the chemical oxidation reaction of Fe^{2+} to Fe^{3+} phenolic complex. Colour formation can be avoided by vacuum packing into foil bags, but colour development will occur within an hour after exposure to oxygen by opening the bags. As a result it is suggested that for products in which colour is an important factor, chelation of iron is the best approach to achieve good quality product.

Starch gelatinisation, and loss of cell wall integrity had a combined effect to influence the textural properties of the kumara.

The gelatinisation process causes starch granule swelling that produces a pressure increase inside the cell. This results in an increased firmness. Starch gelatinisation also significantly increases the rate of starch hydrolysis and a corresponding increase in sugar levels results. This allows a sweeter product to be produced.

Breakdown of the cell wall, in particular the middle lamella, ultimately results in the softening of the texture due to a change in the fracture behaviour from across cells to along the middle lamella plane.

The cooking temperature affects both the gelatinisation and cell wall degredation reactions, especially when the temperature is higher than 70°C.

The texture kinetics in gold and red kumara were found to follow a first order equation, and the dependence of the rate on cooking temperature could be represented by the Arrhenius equation. Red and gold kumara had a slightly different behaviour during cooking and different Arrhenius parameters.

The starch gelatinisation reaction was fast and can be used to explain the texture increase during the first period in the cooked process for product cooked at 65-75°C.

A simple model which combined the kinetics of swelling and pectin hydrolysis was developed that could be used to successfully predict texture changes in kumara.

A model was developed from the kinetics data measured in this work that could be used to predict texture and colour in kumara as a function of time and position in the kumara processed under different conditions. A limited validation process was carried out which provided some confidence that the model predicted relatively correctly. The

model can be used as a tool for process design and optimisation. Two case studies were carried out to demonstrate how the model could be applied to industrial situations.

8.2. RECOMMENDATIONS

The colour of kumara flesh presented high variation within each slice but colour development could be followed using the Minolta chromameter if it were placed consistantly. In order to more completely evaluate the colour, another technique such as image analysis could be useful. This technique may allow greater insight into how position within the kumara affects colour changes. It would also provide more complete data for positional variation during cooking which, in turn, would allow more comprehensive validation of the models developed in chapter 7 of this work.

The pectin kinetics in kumara can be studied further. Kinetics for pectin loss were not determined in this study due to time constraints but would be useful to further prove the texture mechanisms developed in this study.

In order to have a full validation of the model, force and colour determination methods with greater resolution (i.e. smaller area for sample measurement) are required, to study the change between positions in the samples. It is recommended that evaluation of penetrometry and image analysis for measurement of texture and colour profiles in kumara be carried out for these purposes.

REFERENCES

Ahmed, J., Shivhare, U. S. and Raghavan, G. S. V. (2000). "Rheological Characteristics and Kinetics of Colour Degradation of Green Chilli Puree." Journal of Food Engineering 44: 239-244.

Ahmed, J., Shivhare, U. S. and Raghavan, G. S. V. (2001). "Color Degradation Kinetics and Rheological Characteristics of Onion Puree." Transactions of the ASAE 44(1): 95-98.

Alvarez, M. D. and Canet, W. (1998). "Rheological Characterization of Fresh and Cooked Potato Tissues (cv. Monalisa)." *Zeitschrift fur Lebensmittel-Untersuchung und –Forschung.* 207: 55-65.

Alvarez, M. D. and Canet, W. (2002). " A Comparison of Various Rheological Properties for Modelling the Kinetics of Thermal Softening of Potato Tissue (c.v. Monalisa) by Water Cooking and Pressure Steaming." *International Journal of Food Science and Technology.* 37: 41-55.

Anonymous (2002). Sodium Acid Pyrophosphate. Asteris. http://www.astaris.com/products.asp?ProducID=118&Grade=Food.

Balasingham, A. N. (1984). "Kumara: An Export Crop Suitable for Rangitaiki Plains." *NZ Society for Horticultural Science.* 18(2): 46-48.

BeMiller, J. N. and Whistler, R. L. (1996). "Carbohydrates". In *Food Chemistry.* Fennema, O. Marcek Dekker, Inc. 157-224. New York.

Binner, S., Jardine, W. G., Renard, C. M. C. G. and Javis, M. C. (2000). "Cell Wall Modifications During Cooking of Potatoes and Sweet Potatoes." *Jounal of the Science of Food and Agriculture.* 80: 216-218.

Blumenkrantz, N. and Asboe-Hansen, G. (1973). "New Method for Quantitative Determination of Uronic Acids." *Analytical Biochemistry.* 54: 484-489.

Bradbury, J. H. and Holloway, W. D., Eds. (1988). Chemistry of Tropical Root Crops: significance for nutrition and agriculture in the Pacific. Australian Centre for International Agricultural Research (ACIAR). Melbourne

Carslaw, H. S. and Jaeger, J. C. (1959). Conduction of Heat in Solids. Clarendon Press. Oxford.

Clark, C. A. and Moyer, J. M. (1988). *Compendium of Sweet Potato Diseases*. The American Phytopathological Society (APS) Press. Minnesota.

Cleland, D.J, Cleland, A.C. and Jones, R.S. (1994). "Collection of Accurate Experimental Data for Testing the Performance of Simple Methods for Food Freezing Time Prediction. " Journal of Food Processing Engineering. 17,93-117.

Collado, L. S. and Corke, H. (1996). "Use of Wheat-Sweet Potato Composite Flours in Yellow-Alkaline and White-Salted Noodles." *Cereals Chemistry*. 73(4): 439-444.

Cooper, J. and Le Fevre, E. (1996). Thermophysical Properties of Water Substance. Arnold (Hodder Headline Group). London.

Cunniff, P., Ed. (1996). Official Methods of Analysis of AOAC International. AOAC International. Gaithersburg, Maryland

Damodaran, S. (1996). Amino Acids, Peptides, and Proteins. In Food Chemistry. Fennema, O. Marcel Dekker, Inc.: 412-413. New York.

Decoteau, D. R. (2000). Vegetables Crops. New Jersey.

Enachescu, D. M. (1995). Fruit and Vegetable Processing. FAO Agricultural Service. Rome.

Fahloul, D. and Scanlon, M. G. (1996). "A Fracture Mechanics Analysis of the Texture of Potatoes." *Journal of Texture Studies*. 27: 545-557.

FAO (1990). Roots Tubers Plantains and Bananas in a Human Nutrition. Food and Agriculture Organisation of the United Nations. Rome.

Fennema, O., Ed. (1996). Food Chemistry. Marcel Dekker, Inc. New York

Freeman, M., Jarvis, M. C. and Duncan, H. J. (1992). "The Textural Analysis of Cooked Potato. 3. Simple Methods for Determining Texture." *Potato Research* 35: 103-109.

Griffiths, D. W., Brain, H. and Dale, M. F. B. (1992). "Development of a Rapid Colorimetric Method for the Determination of Chlorogenic Acid in Freeze-Dried Potato Tubers." *Journal of the Science of Food and Agriculture.* 58: 41-48.

Haard, N. F. and Chism, G. W. (1996). Characteristics of Edible Plant Tissues. In *Food Chemistry*. Fennema, O. Marcek Dekker, Inc. 993. New York.

Hagenimana, V., Vézina, L. P. and Simard, R. E. (1994). "Sweetpotato α- and ß-Amylases: Characterization and kinetic studies with endogenous inhibitors." *Journal of Food Science.* 59(2): 373-377.

Harada, T., Tirtohusodo, H. and Paulus, K. (1985). "Influence of Temperature and Time on Cooking Kinetics of Potatoes." *Journal of Food Science* 50: 459-462, 472.

Harrington, W. O. and Shaw, R. (1967). Peeling Potatoes for Processing. In book Potato Processing. Talburt, W. and Smith, O. The AVI Publishing Company, Inc. Chapter 9: 242-261. Connecticut.

Harwood, J. J., Temkar, P., M., ASCE., M. and Schltze, R. J. (1995). "Determination of Sequestration Capacities of Iron Control Chemicals." *Journal of Environmental Engineering* 121(1): 108-112.

Heldman, D. R. and Lund, D. B., Eds. (1992). Handbook of Food Engineering. Marcel Dekker, Inc. New York

Hoover, R. (1995). "Starch Retrogradation." *Food Review International.* 11(2): 331-335.

Huaman, Z. (1991). Descriptor for Sweet Potato. International Board for Plant Genetic Resources (International Potato Centre [CIP]; Asian Vegetable Research and Development Centre [AVRDC] and [IBPGR]. Rome.

Huang, Y. T. and Bourne, M. C. (1983). "Kinetics of Thermal Softening of Vegetables." *Journal of Texture Studies* 14(1): 1-9.

Hughes J.C. (1958). "Chlorogenic Acid in the Potato." *Chemistry and Industry*, 214.

Hughes J.C. and Swain T. (1962). "After-cooking Blackening in Potatoes II. Core experiments." *Journal of the Science of Food and Agriculture.* 13: 229-236.

Irani, R. R. and Morgenthaler, W. W. (1963). "Iron Sequestration by Polyphosphates." *The Journal of the American Oil Chemists' Society* 40: 283-285.

Kays, S. J. (1992). The Chemical Composition of the Sweet Potato. In book Sweetpotato for the 21st Century. Technology. Hill, W., Bonsi, C. and Loretan, P.: 201-262. Alabama.

Keetels, C. J. A. M., Van Vliet, T. and Walstra, P. (1996). "Gelation and Retrogradation of Concentrated Starch System: 1. Gelation." *Food Hydrocolloids.* 10(3): 343-353.

Koch, K. and Jane, J. L. (2000). "Morphological Charges of Granules of Different Starches by Surface Gelatinization with Calcium Chloride." *Cereal Chemistry.* 77(2): 115 - 120.

Kozempel, M. F. (1988). "Modeling the Kinetics of Cooking and Precooking Potatoes." *Journal of Food Science.* 53(3): 753-755.

Kunzek, H., Kabbert, R. and Gloyna, D. (1999). "Aspects of Material Science in Food Processing: Changes in plants cell walls of fruits and vegetables." *Zeitschrift fur lebensmittel-untersuchung und-forschung a-food research and technology.* 208: 233-250.

Lamikanra, O., Ed. (2002). Fresh-cut Fruits and Vegetables. Science, Technology, and Market. CRC Press. Boca de Raton, Florida

Lattanzio, V., Cardinali, A., Di Venere, D., Linsalata, V. and Palmieri, S. (1994). "Browning Phenomena in Stored Artichoke (Cynara scolymus L.) Heads: enzymatic or chemical reactions?" *Food Chemistry.* 50: 1-7.

Levenspiel, O. (1999). Chemical Reaction Engineering. John Wiley & Sons. New York.

Lima, I. and Singh, P. (1993). "Objective Measurement of Retrogradation in Cooked Rice During Storage." *Journal of Food Quality.* 16: 321-337.

Liu, H. X., Wang, Y. R. and Guo, J. Y. (1989). "Mechanism of Low Temperature Effect on Injury of Cell Membrane System in Plants." *Acta Botanica Austro Sinica.* 5: 31-38.

Lugasi, A., Almeida, D. P. F. and Dworschak, E. (1999). "Chlorogenic acid content and antioxidant properties of potato tubers as related to nitrogen fertilisation." *Acta Alimentaria.* 28(2): 183-195.

Ma, S., Silva, J. L., Hearnsberger, J. O. and Garner, J. O. J. (1992). "Prevention of Enzymatic Darkening in Frozen Sweet Potatoes [Ipomoea batatas (L.) Lam.] by Water Blanching: Relationship among Darkening, Phenols, and Polyphenol Oxidase Activity." *Journal of Agricultural and Food Chemistry.* 40: 864-867.

Mann, J. D. and De Lambert, C. (1989). "A Fast Test for Darkening in Potatoes." *New Zealand Journal of Crop and Horticultural Science.* 17: 207-209.

Mayhew, S. and Penny, A. (1988). Tropical and Sub-tropical Foods. Published by Macmillan Publishers Ltd. Hong Kong.

McArdle, R.N. and Bouwkamp, J.C. (1986). "Use of Heat Treatments for Saccharification of Sweet Potato Mashes." *Journal of Food Science.* 51(2):364-366.

Miller, G. L. (1959). "Use of Dinitrosalicylic Acid Reagent for Determination of Reducing Sugar." *Analytical Chemistry.* 31: 426 - 428.

Morris, V. J. (1990). "Starch Gelation and Retrogradation." *Trends in Food Science & Technology.* 1(1): 2-6.

Muneta P. (1959). Studies of after-cooking darkening in potatoes. PhD thesis, Cornell University, Ithaca, New York. (Cited from Smith 1977).

Muneta, P. and Kaisaki, F. (1985) Ascorbic acid-ferrous iron (Fe++) complexes and after cooking darkening of potatoes. " *American Potato Journal*", 62, (10):531-536,.

Navas, P. B., Carrasquero, A. and Mantilla, J. (1999). "Advances in the Kumara (Ipomoea batatas) Flour Chemical Characterisation var. Carolina." *Rev. Fac. Agron. (LUZ).* 16: 11-18.

Noda, T., Takada, Y., Sato, T., Ikoma, H. and Mochida, H. (1997). "Combined Effects of Planting and Harvesting Dates on Starch Properties of Sweet Potato Roots" *Carbohydrate Polymers.* 33: 169-176.

Noda, T., Kobayashi, T. and Suda, I. (2001). "Effect of Soil Temperature on Starch Properties of Sweet Potatoes." *Carbohydrate Polymers.* 44: 239-246.

Oates, C. G. (1997). "Towards an Understanding of Starch Granule Structure and Hydrolysis." *Trends in Food Science and Technology* 8: 375-382.

Oduro, I., Ellis, W. O., Aryeetery, S. K., Ahenkora, K. and Otoo, J. A. (2000). "Pasting Characteristics of Starch from new Varieties of Sweet Potato." *Tropical Science.* 40(1): 25-28.

Olaofe, O. and Sanni, C. (1988). "Mineral Content of Agricultural Products." *Food Chemistry.* 30: 73-77.

Onwueme, I. C. and Charles, W. B. (1994). Sweet Potato. In book Tropical Root and Tuber Crops. Production, Perspectives and Future Prospects. . FAO. FAO plant production and Protection Paper. 126: 115-135. Rome.

Orford, P. D., Ring, S. G., Carrol, V., Miles, M. J. and Morris, V. J. (1987). "The Effect of Concentration and Botanical Source on the Gelation and Retrogradation of the Starch." *J. Sci. Food Agric.* 39: 169-177.

Pilnik and Voragen (1989). Enzyme Treatment and Quality. In book Quality Factor of *Fruits and Vegetables. Chemistry and Technology.* Ed. Jen, J. J. American Chemical Society. 263-266. Washington, DC.

Pravisani, C. I., Califano, A. N. and Calvelo, A. (1985). "Kinetics of Starch Gelatinization in Potato." *Journal of Food Science.* 50(3): 657 - 660.

Purcell, A. E. and Sistrunk, W. A. (1982). Sweet Potatoes: Effects of cultivar and curing on sensory quality. In book Evaluation of Quality of Fruits and Vegetables. Patte, H. A. AVI Publishing Company, Inc.: 257-276. Westport. Connecticut.

Rahardjo, B. and Sastry, S. K. (1993). "Kinetics of Softening of Potato Tissue During Thermal Treatment." *Trans. I. ChemE.* 71: 235.

Rahman, S., Ed. (1995). Food Properties Handbook. CRC Press. New York

Ramesh, M. N., Sathyanarayana, K. and Girish, A. B. (1998). "Biphasic Model for Kinetics of Vegetable Cooking at 100°C." *Journal of Food Engineering* 35: 127-133.

Rao, V. N. M., Hamann, D. D. and Humphries, E. G. (1975). "Flow Behaviour of Sweet Potato Puree and Its Relation to Mouthfeel Quality." *Journal of Texture Studies.* 6: 197-209.

Rao, V. N. M. and Graham, L. R. (1982). "Rheological, Chemical and Textural Characteristics of Sweet Potato Flakes." *Transactions of ASAE.* 25(6): 1792-1798.

Rizvi, A. F. and Tong, C. H. (1997). "Factorial Conversion for Determining Texture Degradation Kinetics of Vegetables." *Journal of Food Science.* 62(1): 1-7.

Rogers, L. B. and Reynolds, C. A. (1949). "Interation of Pyrophosphate Ion with Certain Multivalent Cations in Aqueous Solution." *Journal of American Chemical Society* 71(6): 2081-2085.

Rosenthal, A. J. (1999). Food Texture: Measurement and Perception. Aspen Publisher, Inc. Maryland.

Saravacos, G. and Maroulis, Z. (2001). Transport Properties of Foods. Marcel Deckker, Inc. New York.

Savage, G. P. and Bolitho, K. M. (1993). "Kumara -a Traditional Food for Maori." Proceedings of the Nutrition Society of New Zealand. 18: 19-30.

Sears, F. W., Zemansky, M. W. and Young, H. D. (1987). *University Physics.* Addison-Wesley Publishing Company. Massachusetts.

Sloss, T. (1994). Develop of the Vegetable Flour Using Kumara. Food Technology. Palmerston North, Massey University.

Smith O. (1977). Potatoes: Production, Storing, Processing. 2nd Ed. AVI Publishing, Westport.

Stryer, L. (1988). Biochemistry. W.H.Freeman and Company. New York.

Szyperski, R. J., Hamann, D. D. and Walter Jr., W. M. (1986). "Controlled Alpha Amylase Process for Improved Sweet Potato Puree." *Journal of Food Science.* 51(2): 360-363.

Thakur, B. R., Singh, R. K. and Handa, A. K. (1997). "Chemistry and Uses of Pectin- A Review." *Critical Review in Food Science and Nutrition.* 37(1): 47-73.

Thybo, A. K. and Martens, M. (1999). "Instrumental and Sensory Characterization of Cooked Potato Texture." *Journal of Texture Studies.* 30(3): 259-278.

Tian, S. J., Rickard, J. E. and Blanshard, J. M. V. (1991). "Physicochemical Properties of Sweet Potato Starch." *Journal of the Science of Food and Agriculture.* 57: 459-491.

Tzia, C. and Liadakis, G. (2003). Extraction Optimization in Food Engineering. Ed. Marcel Dekker, Inc. New York

Truong, V. D., Walter JR, W. M. and Hamann, D. D. (1997). "Relationship Between Instrumental and Sensory Parameters of Cooked Sweetpotato Texture." *Journal of Texture Studies.* 28: 163-185.

Valetudie, J.-C., Gallant, D. J., Bouchet, B., Colonna, P. and Champ, M. (1999). "Influece of Cooking Procedures on Structure and Biochemical Changes in Sweet Potato." *Starch.* 51(11-12): 389-397.

van Den, T. (1992). Transfer of Sweetpotato Processing Technologies: Some experiences and key factors. In book Product Development for Root and Tuber Crops. International Workshop. Scott, G., Wiersema, S. and Ferguson, P. I. Visayas State College of Agriculture (VISCA). I Asia. Baybay, Leyte.

van Hal, M. (2000). "Quality of Sweetpotato flour during Processing and Storage." *Food Reviews International.* 16(1): 1-37.

Vegfed (2001). 'New Zealand Vegetable & Potato Growers' Federation (Inc). Download on August 2001 from http:// www.vegetables.co.nz.

Verlinden, B. E., Nicolai, B. and de Baerdenemaeker, J. (1995). "The Starch Gelanization in Potato During Cooking in Relation to the Modelling of Texture Kinetics." *Journal of Food Engineering.* 24(2): 165-179.

Visser, F. R., Hannah, D. J. and Bailey, R. W. (1990). Composition of New Zealand Foods. 2. Export fruits and vegetables. Published as DSIR. Tauranga.

Wadsworth, J. I. and Spadaro, J. J. (1970). "Transient Temperature Distribution in Whole Sweetpotato Roots During Immersion Heating: 2. Computer Simulation." *Food Technology.* 24: 77-84.

Walter Jr., W. M., Purcell, A. E. and McCollum, G. K. (1979). "Use of high-pressure liquid chromatography for analysis of sweet potato phenolics." *Journal of Agricultural and Food Chemistry.* 27(5): 938-941.

Walter Jr., W. M. and Purcell, A. E. (1980). "Effect of Substrate Levels and Polyphenol Oxidase Activity on Darkening in Sweet Potato Cultivars." *Journal of Agricultural and Food Chemistry.* 28: 941-944.

Walter Jr., W. M. and Schadel, W. E. (1982). "Effect of Lye Peeling Conditions on Sweet Potato Tissue." *Journal of Food Science.* 47: 813-817.

Walter Jr., W. N. (1992). "Use of Refractive Index to Monitor Changes in Sugar Content of Stored Sweet Potatoes." *HortScience* 27(4): 333-335.

Walter Jr., W. M. and Schwartz, S. J. (1993). "Controlled Heat Processing of Jewel Sweet Potatoes for Puree Production." *Journal of Food Quality.* 16: 71-80.

Walter Jr., W. M., Collins, W. W., Truong, V.-D. and Fine, T. I. (1997). "Pysical, Compositional, and Sensorial Properties of French Fry-Type Products from Five Sweetpotato Selections." *Journal of Agricultural and Food Chemistry.* 45(2): 383-388.

Walter Jr., W. M., Truong, V. D., Wiesenborn, D. P. and Carvajal, P. (2000). "Rheological and Physicochemical Properties of Starches from Moist- and Dry-Type Sweetpotatoes." *Journal of the Science of Food and Chemistry.* 48: 2937-2942.

Walter Jr., W. M., Truong, V. D., Simunovic, N. and McFeeters, R. F. (2003). "Low-temperature Blanching of Sweetpotatoes to Improve Firmness Retention: Effect on compositional and Textural Properties." *Journal of Food Science.* 68(4): 1244-1247.

Watson, S. and Jarvis, M. C. (1995). "The Origin and Measurement of Texture in Sweet Potatoes." *Tropical Science.* 35(3): 229-235.

Whitaker, J. R. (1996). Enzymes. In book Food Chemistry. Fennema, O. Marcek Dekker, Inc.: 492-494. New York.

Woolfe, J. A. (1992a). The Contribution of Sweetpotato and its Products to Human Diets. Technology. In book In book Sweetpotato for the 21st Century. Hill, W., Bonsi, C. and Loretan, P.: 367-380. Alabama.

Woolfe, J. A. (1992b). Sweet Potato. An untapped food resource. Published by Press Syndicate of the Cambridge University. Cambridge.

Wurster R.T. and Smith O. (1965). "Potato Quality XX. After-cooking Darkening in Potatoes as Related to the Distribution of Radioiron." *American Potato Journal.* 42: 37-44.

Yen, D. E. (1974). The Sweet Potato and Oceania. Bernice Pauahi Bishop Museum. Honolulu. Hawaii.

Zhang, T., and Oates, C.G. 1999. "Relationship Between α-Amylase Degradation and Physico-chemical Properties of Sweet Potato Starches. " *Food Chemistry.* 65: 157-163

Zobel, H. (1984). Gelatinization of Starch and Mechanical Properties of Starch Pastes. In book *Starch.* Whistler, R. L., BeMiller, J. N. And Paschall, E. Academic Press, Inc. Chapter IX: 285-310.

APPENDIX A1

1.1. NOMENCLATURE

a	Colour value to measure the red-blue range	-
b	Colour value to measure the yellow-green range	-
c_p	Specific heat capacity	$J\,kg^{-1}.°C^{-1}$
D_m	Mass diffusivity	m^2/s
dsw	Dried sample weight	g
E_A	Activation energy	$J\,mol^{-1}$
Fo	Fourier number	-
fsw	Fresh sample weight	g
k	Rate constant	min^{-1}
k_o	Arrhenius equation constant	min^{-1}
L	Colour parameter to measure white-black range	-
M	Moisture content	%
r	Any radial position between centre and Rr	m
R	Universal gas constant (8.134)	$J\,mol^{-1}.K^{-1}$
Rr	Radius of cylinder	m
Rx	Distance in X axis (half thickness)	m
Ry	Distance in Y axis (half thickness)	m
Rz	Distance in Z axis (half thickness)	m
sd	Standard deviation	-
se	Standard error	-
T	Absolute temperature	K
t	Time	min or s
Tp	Peak temperature	K
x	Any position between centre and Rx over X axis	m
X	Extent of reaction	-
y	Any position between centre and Ry in Y axis	m
Yav	The extent of thermal profile(average)	-
z	Any postion between centre and surface in Z axis	m
ΔE	Colur difference	-
ΔE_∞	Colour difference at infinite time	-
ΔEa	Colour difference at anytime	-
ΔEi	Initial colour difference (t=0min)	-
ΔF_∞	Fracture force at infinite time	N
ΔFa	Fracture force at anytime	N
ΔFi	Initial fracture force (t=0min)	N

1.2. NOMENCLATURE GREEK LETTERS

ρ	Density	$kg\ m^{-3}$
ϕ	Heating rate	$K\ min^{-1}$
θ	Temperature	$°C$
θa	external medium temperature	$°C$
θav	average temperature	$°C$
θi	Initial temperature	$°C$
β	Roots of Bessels function	-
λ	Thermal conductivity	$W m^{-1}\ °C^{-1}$

APPENDIX A2

2.1. PROGRAM SOURCE CODE

```
clear all
tic
%-------------------------------------------------------------
% Main program. Get general data
%-------------------------------------------------------------
filename=input('What is the file name?','s');
tc=0.36;            %thermal conductivity [W/mC]
cp=3643;            %specific heat capacity [J/kgC]
rho=1088;           %density [kg/m3]
tstep=input('How often do you want temperatures predicted
      (each 2s) ');
tstop1=input('What is the cooking time (min [60]) ');
tstop=tstop1*60;
t=[0:tstep:tstop+10];   %time [s]
J=input ('How many space steps do you want ([20]) ');

Ta=input ('What is the cooking temperature? ([80] C) ');
Ti=input ('What is the initial product temperature? ([20]C)
');
Fi=input('The initial fracture force is [av 168N]) ');
Finf=input('The infinite force is [av 4.5N]) ');

%-------------------------------------------------------------
% Decide geometries
%-------------------------------------------------------------
Simtype=input ('Press 1 for infinite 1Dslab, 2 for infinite
       1D  cylinder,  3  for  short  cylinder,  4  for
       Rectangular block   ');
if Simtype==1
   slabcook;
end;
if Simtype==2
    cylcook;
end;
if Simtype==3
    shcylcook;
end;
```

```
if Simtype==4
    rectangular;
end;

%save(['C:\Documents and Settings\jacanumi\Simulation1\',
filename]);

%saveas(GraphExtent,          ['C:\Documents          and
Settings\jacanumi\Simulation1\', filename 'ext'], 'fig');
    %saveas(GraphTemperature,      ['C:\Documents      and
Settings\jacanumi\Simulation1\', filename 'temp'], 'fig');
        %saveas(GraphForce,        ['C:\Documents       and
Settings\jacanumi\Simulation1\' filename 'force'], 'fig');
            %saveas(GraphStarch,     ['C:\Documents     and
Settings\jacanumi\Simulation1\' filename 'starch'], 'fig');
                %saveas(GraphColour,   ['C:\Documents   and
Settings\jacanumi\Simulation1\' filename 'colour'], 'fig');

toc

%-------------------------------------------------------
% ODE Discoloration kinetics
%-------------------------------------------------------

function dXc=odeColour(time,Xc)

global t T J;

%-------------------------------------------------------
% Get kinetic parameters
%-------------------------------------------------------
Ea=101397.54;     % J/mol
ko=4.56e14/60;  % 1/s
R= 8.314;       % J/mol/K

%-------------------------------------------------------
% Lookup correct temperatures in T array
%-------------------------------------------------------

dt=t(2);
i=floor(time/dt)+1;
Temp=T(:,i)+(T(:,i+1)-T(:,i))*(time-t(i))/(t(i+1)-t(i));

k=ko*exp(-Ea/R./(Temp+273.15));

dXc=zeros(J+1,1);
dXc=k.*(1-Xc);
```

```
%-------------------------------------------------------
% ODE Force kinetics
%-------------------------------------------------------
function dXf=odeForce(time,Xf)
global t T J;

%-------------------------------------------------------
% Get kinetic parameters
%-------------------------------------------------------
Ea=125260;      % J/mol
ko=2.54e17/60;  % 1/s
R= 8.314;       % J/mol/K

%-------------------------------------------------------
% Lookup correct temperatures in T array
%-------------------------------------------------------
dt=t(2);
i=floor(time/dt)+1;
Temp=T(:,i)+(T(:,i+1)-T(:,i))*(time-t(i))/(t(i+1)-t(i));
k=ko*exp(-Ea/R./(Temp+273.15));
dXf=zeros(J+1,1);
dXf=k.*(1-Xf);

%-------------------------------------------------------
% ODE starch gelatinisation kinetics
%-------------------------------------------------------
function dXs=odeStarch(time,Xs)
global t T J;
%-------------------------------------------------------
% Get kinetic parameters
%-------------------------------------------------------
R= 8.314;       % J/mol/K
%-------------------------------------------------------
% Lookup correct temperatures in T array
%-------------------------------------------------------
dt=t(2);
i=floor(time/dt)+1;
Temp=T(:,i)+(T(:,i+1)-T(:,i))*(time-t(i))/(t(i+1)-t(i));
for j=1:J+1
    if Temp(j)<68.99 %Gold break for Red 71.96
        Ea=628804.5;      % J/mol Gold
        %Ea=264689.04;      % J/mol Red
        ko=5.75e96/60;  % 1/s Gold
        %ko=3.79e40/60;  % 1/s Red
    else
        Ea=99201.47;
        %Ea=38305.23;
        ko=1.27e15;
        %ko=2.98E19;
```

```
    end
k(j)=ko*exp(-Ea/R./(Temp(j)+273.15));
end;
dXs=zeros(J+1,1);
dXs=k'.*(1-Xs);



%-------------------------------------------------------------
% Analytical solution for cylinder profile
%-------------------------------------------------------------

function y=y1dcylinder(J,Fo)

NumberOfTimes=size(Fo);
beta=[2.40482556046450, 5.52007708970830, 8.65372796706966,
11.79153445795890,   14.93091771689720,   18.07106398088790,
21.21163687527850,   24.35246762705590,   27.49348191011570,
30.63460380630730,   33.77582697461230,   36.91710172451060,
40.05842572797020];
y=zeros(J+1,NumberOfTimes(2));
for n=1:J+1
    for m=1:13
        y(n,:)=y(n,:)+2*besselj(0,beta(m)*(n-
1)/J)/beta(m)/besselj(1,beta(m))*exp(-beta(m)^2*Fo);
    end;
end;
y(:,1)=1;

%-------------------------------------------------------------
% Analytical solution for slab profile
%-------------------------------------------------------------
function y=y1dslab(J,Fo)

NumberOfTimes=size(Fo);

y=zeros(J+1,NumberOfTimes(2));
for n=1:J+1
    for m=0:20
        y(n,:)=y(n,:)+(-1)^m/(2*m+1)*cos((2*m+1)*pi/2*(n-
1)/J)*exp(-(2*m+1)^2*pi^2/4*Fo);
    end;
end;
y=y*4/pi;
y(:,1)=1;
```

```
%-------------------------------------------------------
% Cook slab. Get the general data
%-------------------------------------------------------
global t T J

Rx1=input ('What is the slab thickness (mm[10]) ');
Rx=Rx1/2/1000;
%drx=Rx/J;              %distance between positions [m]

%-------------------------------------------------------
% Solve heat transfer equations
%-------------------------------------------------------
Fox=tc*t/rho/cp/Rx^2;
yx=y1dslab(J,Fox);

GraphExtent=figure;
plot(t/60,yx);
axis ([0 10 0 1]);
xlabel('Time [min]');
ylabel('Incompletion reaction');
title([num2str(Rx*100*2) 'mm thickness.  One D Slab extent
temperature profile at 80C']);

%-------------------------------------------------------
% Convert to temperatures
%-------------------------------------------------------
T=yx*(Ti-Ta)+Ta;
%GraphTemperature=figure;

%plot(t/60,T);
%axis ([0 15 20 Ta]);
%xlabel('Time [min]');
%ylabel('Temperature [C]');
%title([num2str(Ta)  'C  cooked  temperature.   One  D  Slab
temperature predictions']);

%-------------------------------------------------------
% Set up force kinetics model
%-------------------------------------------------------

Xfi=zeros(1,J+1);
tinterval=10;
options=[];
[time,Xf]=ode45('odeForce',[0:tinterval:tstop],Xfi,options)
;
F=Finf-(1-Xf)*(Finf-Fi);

GraphForce=figure;
axis ([0 tstop1 0 1]);
```

```
plot(time/60,Xf*100);
xlabel('Time [min]');
ylabel('Force [%]');
title([num2str(Rx*100*2) 'mm thickness.  One D Slab force
prediction at 80C']);

%-----------------------------------------------------------
% Set up starch gelatinisation kinetics model
%-----------------------------------------------------------
Xsi=zeros(1,J+1);
[time,Xs]=ode45('odeStarch',[0:tinterval:tstop],Xsi,options
);
GraphStarch=figure;
plot(time/60,Xs*100);
axis ([0 3 0 100]);
xlabel('Time [min]');
ylabel('Xstarch [%]');
title([num2str(Rx*100*2) 'mm thickness.  One D Slab starch
gelatinisation prediction at 80C']);

%-----------------------------------------------------------
% Set up Colour stage  kinetics model
%-----------------------------------------------------------
Xci=zeros(1,J+1);
[time,Xc]=ode45('odeColour',[0:tinterval:tstop],Xci,options
);
GraphColour=figure;
plot(time/60,Xc*100);
axis ([0 20 0 100]);
xlabel('Time [min]');
ylabel('X Discoloration [%]');
title([num2str(Rx*100*2)  'mm  thickness.    One  D  Slab
Discoloration prediction at 80C']);


%-----------------------------------------------------------
% Cook infinite cylinder general data
%-----------------------------------------------------------
global  t T J

Rc=input ('What is the cylinder ratio (m[0.005]) ');
%drc=Rc/J;              %distance between positions [m]

%-----------------------------------------------------------
% Solve heat transfer equations
%-----------------------------------------------------------
Fo=tc*t/rho/cp/Rc^2;
yc=y1dcylinder(J,Fo);
```

```
%-------------------------------------------------------
% Convert to temperatures
%-------------------------------------------------------
T=yc*(Ti-Ta)+Ta;
GraphTemperature=figure;
plot(t/60,T);
xlabel('Time [min]');
ylabel('Temperature [C]');
title('Infinite cylinder temperature predictions');

%-------------------------------------------------------
% Set up force kinetics model
%-------------------------------------------------------
tinterval=10;

Xfi=zeros(1,J+1);
options=[];
[time,Xf]=ode45('odeForce',[0:tinterval:tstop],Xfi,options)
;
F=Finf-(1-Xf)*(Finf-Fi);
GraphForce=figure;
plot(time/60,F);
xlabel('Time [min]');
ylabel('Force [N]');
title('Infinite cylinder force predictions');

%-------------------------------------------------------
% Set up starch gelatinisation kinetics model
%-------------------------------------------------------
Xsi=zeros(1,J+1);
[time,Xs]=ode45('odeStarch',[0:tinterval:tstop],Xsi,options
);
GraphStarch=figure;
plot(time/60,Xs*100);
xlabel('Time [min]');
ylabel('X starch [%]');
title('Infinite     cylinder     starch     gelatinisation
predictions');

%-------------------------------------------------------
% Set up Colour stage 1 kinetics model
%-------------------------------------------------------
Xci=zeros(1,J+1);
[time,Xc]=ode45('odeColour',[0:tinterval:tstop],Xci,options
);
GraphColour=figure;
plot(time/60,Xc*100);
xlabel('Time [min]');
ylabel('X Discoloration [%]');
```

```
title('Infinite cylinder discoloration predictions');


%-----------------------------------------------------------
% Cook finite cylinder general data
%-----------------------------------------------------------

Rx=input ('What is the slab thinckness (m[0.005]) ');
Rc=input ('What is the cylinder ratio (m[0.005]) ');
t=[0:2:62*60];       %time [s]
J=20;                %number of positions -1
%drx=Rx/J;             %distance between positions [m]

%-----------------------------------------------------------
% Solve heat transfer equations
%-----------------------------------------------------------
Fox=tc*t/rho/cp/Rx^2;
yx=y1dslab(J,Fox);

Focs=tc*t/rho/cp/Rc^2;
ycs=y1dcylinder(J,Focs);
n=size(t);
y=zeros(J+1,J+1,n(2));
for j=1:J+1
    for jj=1:J+1
       y(j,jj,:)=yx(j,:).*ycs(jj,:);
    end
end
figure;
hold on;

yc=zeros(J+1,n(2));

for p=1:J+1
    yc(p,:)=squeeze(y(p,p,:))';
end
    plot(t/60,yc); %plot from centre to corner
    xlabel('Time [min]');
    ylabel('Completion (y)');
    title('Predictions of reaction completion [centre to
corner] in short cylinder ');

    %figure;
    %plot(t,squeeze(y(:,1,:)),'r'); %plot from centre to
the tope (in x direction)
    %hold on
    %plot(t,squeeze(y(1,:,:)),'b'); %plot from centre to
centre of top face in (r direction)
```

```
%-------------------------------------------------------------
% Convert to temperatures
%-------------------------------------------------------------
Ta=80;
Ti=20;
T=yc*(Ti-Ta)+Ta;
GraphTemperature=figure;
plot(t/60,T);
xlabel('Time [min]');
ylabel('Temperature [C]');
title('Short cylinder temperature predictions');

%-------------------------------------------------------------
--------------
% Set up force kinetics model
%-------------------------------------------------------------
global t T J

Xfi=zeros(1,J+1);
tinterval=10;
tstop=60*60;
options=[];
[time,Xf]=ode45('odeForce',[0:tinterval:tstop],Xfi,options)
;
Finf=4.5;
Fi=168;
F=Finf-(1-Xf)*(Finf-Fi);
GraphForce=figure;
plot(time/60,F);
xlabel('Time [min]');
ylabel('Force [N]');
title('Short cylinder Force predictions');

%-------------------------------------------------------------
% Set up starch gelatinisation kinetics model
%-------------------------------------------------------------
Xsi=zeros(1,J+1);
[time,Xs]=ode45('odeStarch',[0:tinterval:tstop],Xsi,options
);
GraphStarch=figure;
plot(time/60,Xs*100);
xlabel('Time [min]');
ylabel('Xstarch [%]');
title('Short cylinder starch gelatinisation predictions');

%-------------------------------------------------------------
% Set up Colour stage 1 kinetics model
%-------------------------------------------------------------
Xci=zeros(1,J+1);
```

```
[time,Xc]=ode45('odeColour',[0:tinterval:tstop],Xci,options
);
GraphColour=figure;
plot(time/60,Xc*100);
xlabel('Time [min]');
ylabel('X Discoloration [%]');
title('Short cylinder discoloration predictions');

%-------------------------------------------------------------
% Cook rectangular block general dimensions
%-------------------------------------------------------------
global t T J

Rx1=input('What is the thinckness (x axe [mm]) ');
Rx=Rx1/2/1000;

Ry1=input('What is the lengthness (y axe [mm]) ');
Ry=Ry1/2/1000;

Rz1=input('What is the deepness (z axe [mm]) ');
Rz=Rz1/2/1000;

%-------------------------------------------------------------
% Solve heat transfer equations
%-------------------------------------------------------------
Fox=tc*t/rho/cp/Rx^2;
yx=y1dslab(J,Fox);

Foy=tc*t/rho/cp/Ry^2;
yy=y1dslab(J,Foy);

Foz=tc*t/rho/cp/Rz^2;
yz=y1dslab(J,Foz);

n=size(t);
y=zeros(J+1,J+1,J+1,n(2));

for j=1:J+1
    for jj=1:J+1
        for jjj=1:J+1
            y(j,jj,jjj,:)=yx(j,:).*yy(jj,:).*yz(jjj,:);
        end
    end
end
GraphExtent=figure;
hold on;
xyz=zeros(J+1,n(2));
for p=1:J+1
    xyz(p,:)=squeeze(y(p,p,p,:))';
```

```
end


    plot(t/60,xyz); %plot from centre to corner
     axis ([0 30 0 1]);
    xlabel('Time [min]');
    ylabel('Completion (y)');
    title([num2str(Ta) 'Prediction of reaction completion
[centre to corner] in rectangular block ']);
    %title([num2str(Rx1) 'cm dice. Temperature profile
[centre to corner] in rectangular block at 80C']);
    %figure;
    %plot(t,squeeze(y(:,1,1,:)),'r'); %plot from centre to
centre of right face (in x direction)
    %hold on
    %plot(t,squeeze(y(1,:,1,:)),'b'); %plot from centre to
centre of top face in (y direction)
    %plot(t,squeeze(y(1,1,:,:)),'k'); %plot from centre to
centre of back face in (z direction)

%-------------------------------------------------------------
% Convert to temperatures
%-------------------------------------------------------------
%GraphTemperature=figure;
%hold on;
T=xyz*(Ti-Ta)+Ta;
%plot(t/60,T);
%xlabel('Time [min]');
%ylabel('Temperature [C] ');
%title('Temperature predictions from centre to corner in
rectangular block ');

%-------------------------------------------------------------
% Set up force kinetics model
%-------------------------------------------------------------
Xfi=zeros(1,J+1);
tinterval=10;
options=[]; %?
[time,Xf]=ode45('odeForce',[0:tinterval:tstop],Xfi,options)
;
F=Finf-(1-Xf)*(Finf-Fi);
GraphForce=figure;
axis ([0 tstop1 0 100]);
plot(time/60,Xf*100);
xlabel('Time [min]');
ylabel('Force [%]');
title([num2str(Ta) 'C cooked temperature. Rectangular block
force prediction']);
```

```
%title([num2str(Rx1) 'cm dice.  Rectangular block force
prediction at 80C']);
%-------------------------------------------------------
% Set up starch gelatinisation kinetics model
%-------------------------------------------------------
Xsi=zeros(1,J+1);
[time,Xs]=ode45('odeStarch',[0:tinterval:tstop],Xsi,options
);
GraphStarch=figure;
axis ([0 tstop1 0 100]);
plot(time/60,Xs*100);
xlabel('Time [min]');
ylabel('Xstarch [%]');
title([num2str(Ta) 'C cooked temperature. Rectangular block
starch gelatinisation prediction']);
%title([num2str(Rx1) 'cm dice.  Rectangular block starch
gelatinisation prediction at 80C']);

%-------------------------------------------------------
% Set up Colour stage 1 kinetics model
%-------------------------------------------------------
Xsi=zeros(1,J+1);
[time,Xs]=ode45('odeColour',[0:tinterval:tstop],Xsi,options
);
GraphColour=figure;
axis ([0 tstop1 0 100]);
plot(time/60,Xs*100);
xlabel('Time [min]');
ylabel('XsDiscoloration [%]');
title([num2str(Ta) 'C cooked temperature. Rectangular block
discoloration prediction']);
%title([num2str(Rx1) 'cm dice.  Rectangular block force
discoloration at 80C']);
```

APPENDIX A3

Raw data Figure 3-2: Hunter values

Sample	Loc	a	b	L	Blk	Col	Loc	DE
SAPP I	1	-3.22	37.26	64.03	1	Good	1	12.0
	2	-1.99	42.32	68.71	1	Good	2	5.3
	3	-3.16	36.75	59.04	1	Good	3	16.5
	4	-2.48	39.49	63.5	1	Good	4	11.2
	5	-3.1	37.63	67	1	Good	5	9.5
SAPP II	1	-4.27	38.06	66.6	2	Good	1	9.7
	2	-3.01	41.02	69.81	2	Good	2	5.2
	3	-3.93	41.07	66.01	2	Good	3	8.4
	4	-4.67	38.16	68.81	2	Good	4	8.2
	5	-4.75	40.56	70.71	2	Good	5	5.4
SAPP III	1	-4.19	36.44	66.06	3	Good	1	11.2
	2	-3.59	41.09	70.4	3	Good	2	4.8
	3	-2.56	44.6	73.5	3	Good	3	0.0
	4	-4.77	39.27	68.48	3	Good	4	7.6
	5	-4	39.5	66.85	3	Good	5	8.5
Water I	1	0.56	40.18	59.23	1	Inter	1	15.3
	2	-0.48	37.64	58.35	1	Inter	2	16.8
	3	-1.59	39.05	60.78	1	Inter	3	13.9
	4	-1.69	40.04	60.45	1	Inter	4	13.9
	5	-1.22	34.68	54.79	1	Inter	5	21.2
Water II	1	-0.05	39.67	59.77	2	Inter	1	14.8
	2	-0.74	38.53	61.41	2	Inter	2	13.7
	3	-1.99	37.69	58.96	2	Inter	3	16.1
	4	-1.22	34.96	55.19	2	Inter	4	20.7
	5	-1.93	39.88	61.67	2	Inter	5	12.8
Water III	1	-0.23	40.54	61.27	3	Inter	1	13.1
	2	-0.98	35.77	56.79	3	Inter	2	19.0
	3	-1.67	40.16	61.4	3	Inter	3	12.9
	4	-1.39	38.43	60.8	3	Inter	4	14.2
	5	-1.14	42	63.56	3	Inter	5	10.4
Water I	1	-2.96	35.32	52.32	1	Bad	1	23.1
	2	-2.61	38.59	58.89	1	Bad	2	15.8
	3	-1.87	38.45	57.3	1	Bad	3	17.3
	4	-1.39	39.33	58.7	1	Bad	4	15.8
	5	-1.81	38.42	58.04	1	Bad	5	16.7
Water II	1	-2.94	36.17	58.46	2	Bad	1	17.2
	2	-1.48	40.37	59.47	2	Bad	2	14.7
	3	-1.26	37.81	55.59	2	Bad	3	19.2
	4	-2.03	39.08	58.6	2	Bad	4	15.9
	5	-0.58	36.57	55	2	Bad	5	20.3
Water III	1	-3.01	31.16	55.59	3	Bad	1	22.4
	2	-1.78	33.04	55.52	3	Bad	2	21.4
	3	-2.44	38.75	59.15	3	Bad	3	15.5
	4	-1.44	33.24	54.69	3	Bad	4	22.0
	5	-3.29	37.33	60.19	3	Bad	5	15.2

Raw data Figure 3-3: Hunter values

Gold				Red				
Bk	a	b	L	Bk	a	b	L	
G1		-0.72	37.52	64.98 R1		-0.02	16.98	47.64
G2		0.04	35.6	60.19 R2		-2.45	16.15	48.75
G3		-1.56	29.29	55.59 R1		-1.14	18.66	48.75
G1		-1.09	34.9	57.16 R2		-1.76	15.55	48.26
G2		-0.78	30.69	54.89 R1		-0.78	20.21	49.21
G3		-1.21	28.52	52.18 R2		-2.24	21.08	50.08
G1		3.13	46.45	65.83 R1		-1.23	23.52	52.26
G2		-0.3	39.62	64.83 R2		-2.46	23.88	54.62
G3		-0.49	34.1	56.16 R1		-0.93	19.78	49.07
G1		2.29	48.15	70.43 R2		-1.36	19.62	45.11
G2		-0.72	44.02	64.13 R1		-0.52	21.83	48.79
G3		-1.29	38.58	61.58 R2		-2.48	16.32	48.31
G1		1.71	44.55	68.29 R1		-1.97	23.26	53.3
G2		1.55	40.44	68.1 R2		-2.7	20.25	51.83
G3		-1.5	33.32	59.87 R1		-1.89	24.07	54.08
G1		0.97	40.98	65.92 R2		0.79	22.49	52.36
G2		-0.06	37.94	63.68 R3		-1.96	17.72	46.79
G3		-1.65	30.66	54.13 R4		-1.21	20.62	51.29
G1		3.3	47.27	67.37 R3		-2.66	16	48.38
G2		-0.31	40.08	63.52 R4		-2.36	21.25	55.11
G3		-1.19	35.28	58.28 R3		-1.37	22.07	49.91
G1		-1.43	42.18	64.7 R4		-1.13	25.76	55.98
G2		-1.58	41.63	66.1 R3		-3.36	24.88	53.59
G3		-1.63	37.63	62.57 R4		-2.23	23.87	58.87
G4		1.44	35.1	53.54 R3		-1.91	22.05	52.3
G5		-1.14	34.3	55.17 R4		-2.32	21.1	54.87
G6		-2.08	34.09	55.47 R3		-2.97	23.17	54.49
G4		-1.23	36.64	60.77 R4		-2.47	22.87	59.5
G5		-2.7	32.61	57.72 R3		-1.85	24.43	56.47
G6		-1.01	35.97	61.54 R4		-3.17	20.36	53.65
G4		1.15	42.71	63.22 R3		-2.38	28.35	61.61
G5		-1.7	42.95	68.61 R4		-3.46	23.11	58.15
G6		-0.64	40.91	66.14 R5		-1.67	21	48.19
G4		-2.01	41.82	69.96 R6		-0.29	18.08	48.42
G5		-1.99	45.67	69.35 R5		-2.51	19.63	51.07
G6		-3.75	39.74	67.74 R6		-1.98	17.69	49.19
G4		-0.62	35.95	60.06 R5		-1.61	22.18	50.09
G5		-2.5	32.34	64.76 R6		0.08	21.67	50.7
G6		-1.03	36.22	63.38 R5		-1.87	26.93	53.86
G4		0.26	42.23	63.1 R6		-2.05	23.59	55.75
G5		-2.8	37.75	62.45 R5		-2.3	22.3	51.17
G6		-1.95	36.07	63.07 R6		-0.89	21.49	54.51
G4		-1.73	42.54	69.23 R5		-3.05	19.08	52.28
G5		-1.7	38.67	64.36 R6		-1.62	21.93	55.01

G6	-1.83	39.3	67.3 R5	-1.67	21.14	50.12
G4	-3.43	41.16	69.67R6	-1.71	19.32	51.76
G5	-3.53	39.86	68.83 R5	-1.53	25.27	55.98
G6	-0.89	43.22	67.74 R6	-0.81	24.38	57.41
G7	-1.7	35.02	60.27 R7	-1.75	17.8	48.19
G8	-1.54	33.65	56.49 R8	-1.61	18.47	51.79
G9	1.37	36.17	55.76 R7	-1.76	19.19	50.82
G7	-1.35	37.28	59.26 R8	-2.32	17.5	50.8
G8	-0.46	31.52	54.53 R7	-3.86	21.27	54.64
G9	-2.43	33.28	58.65 R8	-3.43	20.81	53.61
G7	1.21	40.53	67.53 R7	-2.31	25.17	55.64
G8	-0.46	35.37	60.99 R8	-2.1	26.75	59.46
G9	-1.33	36.09	63.15 R7	-2.75	20.88	50.04
G7	-0.95	43.7	69.22 R8	-3.1	23.64	55.14
G8	2.34	46.93	67.77 R7	-3.13	23.04	55.87
G9	2.02	41.16	68.23 R8	-2.76	20.2	54.28
G7	-1.72	31.16	55.54 R7	-3.46	24.44	56.05
G8	-0.98	31.77	58.76 R8	-3.08	22.7	52.12
G9	-2.74	32.36	56.55 R7	-3.03	24.18	57.32
G7	-1.21	36.6	60 R8	-1.79	24.39	54.49
G8	-2.16	32.45	59.26			
G9	-2.29	35.28	61.6			
G7	1.9	43.49	66.49			
G8	3.04	40.33	61.62			
G9	-0.29	40.33	64.46			
G7	-1.05	45.41	71.2			
G8	3.22	46.91	66.91			
G9	-0.8	42.4	68.97			
G10	-2.46	33.8	58.51			
G11	-2.75	24.07	51.74			
G12	-2.01	30.09	54.62			
G10	-2.38	30.86	53.05			
G11	-3.58	24.12	52.05			
G12	-3.94	29.26	58.24			
G10	-0.46	36.98	61.64			
G11	-1.07	37.23	59.83			
G12	-1.31	34.35	57.53			
G10	-1.32	40.7	64.94			
G11	-1.82	39.73	61.11			
G12	-1.89	33.1	59.85			
G10	-0.4	36.12	62.56			
G11	-0.85	34.46	58.58			
G12	-2.76	29.62	57.11			
G10	-2.12	36.92	64.36			
G11	-2.48	32.36	57.11			
G12	-3.2	31.6	60.4			
G10	-0.86	40.19	64.7			
G11	0.26	38.78	59.87			
G12	-2.45	33.21	60.81			

G10	-1.38	40.14	65.7
G11	-1.94	40.05	61.76
G12	-1.08	37.79	59.89

Raw data Figure 3-4: L values and resistance (ohms)

	Block											
Temp	A	B	C	D	E	F	G	H	I	J	K	L
	L value											
15	79	82.66	80.15	84.02	82.9	82.43	85.66	82.24	83.45	83.2	80.1	80.57
35	78	82.89	81.78	81.01	80.1	82.89	83.6	79.98	84.03	83.88	82.4	80.62
53	78	82.07	81.35	78.77	77.1	79.74	81.16	77.95	81.89	80.33	80.9	77.43
58	71	75.48	74.17							76.97	73.2	72.22
63				66.37	59.2	70.11	75	65.7	74.14			
68							72.93	61.76	73.48			61.62
73	49	49.16	55.33	49.29	47.8	54.2	63.02	50.2	61.11	55.65	55.9	51.09
80	53	56.25	56.25	51.23	52.5	52.11						
	Resistance (ohms)											
15	24	45	32	29	20	35	43	23.5	35	29	39	29
35	23	33	26	35	17	32	42	18	25	33	33	38
53	14	27	30	20	13.5	15	28	16.5	24	19	19	35
58	12	16	22							15	12	12
63				15	18	19	20	18	16			
68							16	13	19			15
73	13	13	18	14	18	19	19	11	18.5	15.5	17	19
80	19	14	14	17	15	17						

Raw data Figure 4-3: Hunter values

		1ST Read			2ND Read			
Temp	Bk	a	b	L	a	b	L	DE
50	A1	4.362	28.962	85.4	5.24	25.31	82.9025	4.51
50	B1	6.528	27.756	83.484	7.246	25.188	81.42	3.37
50	C1	5.166	28.328	85.438	4.84	25.542	84.216	3.06
50	A2	4.38	30.274	84.232	4.62	25.28	82.14	5.44
50	B2	9.186	32.14	81.706	8.268	25.68	81.184	6.55
50	C2	5.674	26.816	85.364	5.106667	24.16667	83.50333	3.29
50	A3	3.838	30.198	84.162	4.84	24.586	82.026	6.09
50	B3	9.35	31.608	81.708	7.448	26.024	81.724	5.90
50	C3	6.798	26.886	84.074	6.28	24.322	81.6	3.60
50	A4	3.506	30.494	84.472	4.224	24.302	82.258	6.61
50	B4	7.978	33.248	81.91	7.348	26.25	81.122	7.07
50	C4	2.086	28.54	86.556	2.83	24.902	84.45	4.27
50	A5	4.942	28.936	84.888	5.17	24.53	82.528	5.00
50	B5	5.906	30.346	83.334	6.958	24.922	80.238	6.33
50	C5	3.97	27.784	85.874	3.982	23.894	83.846	4.39
55	A1	5.36	25.6	84.788	5.606	21.706	81.95	4.82
55	B1	4.032	26.318	80.544	4.472	23.316	78.968	3.42
55	C1	7.31	31.216	81.304	7.256	26.532	78.588	5.41
55	A2	4.97	32.106	82.262	5.548	25.494	78.544	7.61

55	B2	4.164	29.586	79.232	4.342	23.228	77.898	6.50
55	C2	5.924	32.588	83.906	5.784	25.274	82.736	7.41
55	A3	5.086	35.186	81.414	4.898	27.03	77.226	9.17
55	B3	3.664	31.806	75.094	4.346	23.476	73.33	8.54
55	C3	6.874	36.272	82.386	7.466	30.282	79.454	6.70
55	A4	5.272	38.246	80.96	5.296	30.094	73.77	10.87
55	B4	4.96	37.592	76.068	6.502	31.42	69.138	9.41
55	C4	6.312	41.458	82.234	6.624	36.226	77.912	6.79
55	A5	4.894	43.03	80.524	4.838	31.896	70.328	15.10
55	B5	5.07	40.984	80.66	6.208	31.396	68.38	15.62
55	C5	9.742	42.666	78.196	9.306	35.55	68.93	11.69
60	A1	2.422	35.872	84.826	4.032	27.382	82.05	9.08
60	B1	1.89	31.238	85.278	3.056	25.658	83.138	6.09
60	C1	6.862	39.6	81.462	6.952	34.604	77.936	6.12
60	A2	3.376	39.438	83.056	4.57	34.382	75.774	8.95
60	B2	4.65	42.17	82.804	5.436	36.186	75.766	9.27
60	C2	7.406	42.434	80.956	7.598	38.844	74.976	6.98
60	A3	3.332	40.734	83.416	4.462	31.996	72.222	14.25
60	B3	3.952	42.582	82.636	3.4	34.428	74.55	11.50
60	C3	8.406	45.916	81.226	6.684	35.812	69.028	15.93
60	A4	5.18	40.964	81.558	4.86	30.368	69.36	16.16
60	B4	4.562	43.182	82.598	5.158	33.098	71.05	15.34
60	C4	7.236	44.016	78.286	5.966	33.072	68.216	14.93
60	A5	2.848	42.602	83.156	3.802	29.942	65.866	21.45
60	B5	3.9575	43.865	83.23	4.244	31.762	70.882	17.29
60	C5	5.354	45.926	81.42	5.914	32.302	66.202	20.43
65	A1	0.404	30.446	87.198	1.324	25.73	84.728	5.40
65	B1	5.288	39.616	80.976	6.064	33.834	77.274	6.91
65	C1	9.15	37.076	81.048	7.96	33.278	76.302	6.19
65	A2	0.212	41.95	84.874	1.036	35.56	73.156	13.37
65	B2	6.216	44.026	77.9	5.646	30.346	66.992	17.51
65	C2	6.9	42.902	81.646	5.9875	32.4775	68.335	16.93
65	A3	0.098	45.614	83.92	1.586	30.878	65.43	23.69
65	B3	5.294	44.718	80.406	5.228	30.636	66.442	19.83
65	C3	9.02	43.862	78.244	8.1025	30.1325	61.7975	21.44
65	A4	-0.688	46.092	83.48	2.014	31.532	65.578	23.23
65	B4	7.756	45.24	79.676	5.398	30.442	63.376	22.14
65	C4	5.368	46.312	78.3	6.898	29.396	61.062	24.20
65	A5	-1.688	45.492	84.572	-0.106	34.116	72.816	16.44
65	B5	2.748	47.634	80.306	6.584	30.13	61.84	25.73
65	C5	3.592	47.438	80.688	6.122	31.072	63.788	23.66
70	A1	4.292	44.262	82.924	4.18	34.366	70.7	15.73
70	B1	9.68	42.104	78.65	7.956	31.052	67.468	15.82
70	C1	3.836	47.28	81.464	4.384	32.394	65.946	21.51
70	A2	3.54	46.958	81.784	3.118	32.234	67.242	20.70
70	B2	8.1	39.628	73.334	7.27	28.342	61.394	16.45
70	C2	6.19	43.522	76.994	6.35	27.56	59.632	23.58
70	A3	2.416	45.872	79.324	3.394	30.538	62.652	22.67
70	B3	6.166	38.264	73.99	5.782	27.77	60.192	17.34

70	C3	4.64	44.354	77.448	6.038	29.242	59.25	23.70
70	A4	2.24	47.432	78.77	3.916	30.314	62.634	23.58
70	B4	5.04	42.564	76.456	4.902	30.59	63.8	17.42
70	C4	1.62	45.734	76.532	6.14	31.264	57.054	24.68
70	A5	0.832	44.38	75.57	3.082	29.516	59.35	22.12
70	B5	3.232	40.44	72.09	3.624	33.14	57.308	16.49
70	C5	2.628	44.558	77.174	5.804	30.078	58.848	23.57
80	A1	7.034	42.516	81.178	6.27	35.75	76.57	8.23
80	B1	7.128	43.07	77.91	7.06	31.33	66.29	16.51
80	C1	0.372	44.098	83.136	2.96	30.68	67.62	20.68
80	A2	4.984	46.056	74.5	4.27	34.11	62.20	17.16
80	B2	5.49	40.11	71.168	5.93	26.03	55.33	21.20
80	C2	-1.492	46.978	79.908	2.53	28.09	59.69	27.96
80	A3	-2.166	37.618	61.112	1.16	25.92	50.25	16.31
80	B3	5.05	35	56.52	5.89	25.63	45.66	14.37
80	C3	-1.896	44.634	68.99	3.51	28.89	52.75	23.25
80	A4	-0.15	34.034	52.354	3.26	22.14	43.92	14.98
80	B4	1.754	33.372	55.536	0.48	27.05	46.04	11.48
80	C4	-3.644	38.334	63.04	2.67	24.39	46.27	22.70
80	A5	3.752	37.578	61.112	2.73	27.36	45.64	18.57
80	B5	1.672	34.97	57.766	1.94	25.78	47.36	13.88
80	C5	-4.118	31.664	54.864	1.33	21.59	41.76	17.41

Raw data Figure 4-5: Hunter values

			1s Read																											
	time	Temp	Rep	a	b	L	Temp	Rep	a	b	L	Temp	Rep	a	b	L	Temp	Rep	a	b	L	Temp	Rep	a	b	L	Temp	Rep	a	b	L
Sample1 t1		50	1	4.2	27	86	55	1	5	25	85	60	1	2.5	33	84	65	1	0.9	31	87	70	1	4.7	44	83	80	1	7.4	43	81
Sample1 t1		50	2	3.3	31	85	55	2	4.7	26	83	60	2	1.5	40	85	65	2	-0	31	87	70	2	3.1	43	84	80	2	6.8	42	82
Sample1 t1		50	3	5.5	29	85	55	3	5.6	27	85	60	3	3.1	38	85	65	3	1.7	32	87	70	3	3.9	44	84	80	3	6.8	44	81
Sample1 t1		50	4	5.3	28	85	55	4	6.2	24	85	60	4	2.2	34	86	65	4	0.4	30	87	70	4	2.8	46	83	80	4	9	43	79
Sample1 t1		50	5	3.5	30	86	55	5	5.2	26	85	60	5	2.9	35	85	65	5	-1	28	88	70	5	7	44	81	80	5	5.2	42	82
Sample1 t1		50		4.4	29	85	55		5.4	26	85	60		2.4	36	85	65		0.4	30	87	70		4.3	44	83	80		7	43	81
Sample2 t1		50	1	6	25	83	55	1	5.7	28	81	60	1	0.8	31	87	65	1	5.8	38	82	70	1	8.9	41	77	80	1	8.1	43	76
Sample2 t1		50	2	4.7	30	84	55	2	2.6	27	82	60	2	1.2	31	85	65	2	3	40	81	70	2	8.8	41	81	80	2	5.2	44	82
Sample2 t1		50	3	6	28	83	55	3	5.7	25	74	60	3	3.7	31	85	65	3	5.8	40	80	70	3	10	44	79	80	3	8.3	42	78
Sample2 t1		50	4	6.1	27	85	55	4	2.1	25	84	60	4	2.4	32	84	65	4	3.7	41	82	70	4	11	42	77	80	4	6.9	42	75
Sample2 t1		50	5	9.9	29	82	55	5	4.2	27	81	60	5	1.4	32	86	65	5	8.2	39	79	70	5	9.7	42	79	80	5	7.1	44	79
Sample2 t1		50		6.5	28	83	55		4	26	81	60		1.9	31	85	65		5.3	40	81	70		9.7	42	79	80		7.1	43	78
Sample3 t1		50	1	6.6	28	85	55	1	6.1	29	84	60	1	5.6	38	84	65	1	11	36	81	70	1	4.4	49	82	80	1	-2	45	82
Sample3 t1		50	2	2.8	28	87	55	2	9.6	34	78	60	2	7.4	39	81	65	2	9.4	39	80	70	2	2.8	50	83	80	2	0.7	46	82
Sample3 t1		50	3	5.4	27	85	55	3	6.9	30	83	60	3	9.2	43	79	65	3	8.6	42	81	70	3	3.4	45	82	80	3	0.9	42	83
Sample3 t1		50	4	6.6	30	84	55	4	6.8	33	79	60	4	6.8	39	82	65	4	8.4	39	81	70	4	4.8	46	80	80	4	0.2	44	83
Sample3 t1		50	5	4.4	29	86	55	5	7.1	30	83	60	5	5.3	39	81	65	5	8.7	29	82	70	5	3.9	47	81	80	5	1.7	43	84
Sample3 t1		50		5.2	28	85	55		7.3	31	81	60		6.9	40	81	65		9.2	37	81	70		3.8	47	81	80		0.4	44	83
Sample1 t2		50	1	4.1	31	84	55	1	4.6	34	83	60	1	4.4	35	82	65	1	0	41	86	70	1	3.2	47	82	80	1	6.2	46	75
Sample1 t2		50	2	3.2	32	83	55	2	5.2	31	83	60	2	2.8	41	84	65	2	-2	40	86	70	2	3.8	46	83	80	2	4.5	48	78
Sample1 t2		50	3	6.4	30	85	55	3	3.5	33	83	60	3	4.4	40	84	65	3	1.6	44	85	70	3	5.2	47	81	80	3	4.3	45	74
Sample1 t2		50	4	3.2	29	85	55	4	6	30	82	60	4	2.3	41	83	65	4	0.4	45	83	70	4	2.2	49	82	80	4	6.1	46	72
Sample1 t2		50	5	5	30	84	55	5	5.6	32	80	60	5	3	40	83	65	5	0.6	40	85	70	5	3.3	47	80	80	5	3.8	46	74
Sample1 t2		50		4.4	30	84	55		5	32	82	60		3.4	39	83	65		0.2	42	85	70		3.5	47	82	80		5	46	75
Sample2 t2		50	1	9.4	32	82	55	1	4.1	29	81	60	1	6	42	82	65	1	6.4	44	80	70	1	7.5	38	74	80	1	5.8	41	72
Sample2 t2		50	2	6.3	33	82	55	2	3.5	28	79	60	2	4	43	82	65	2	4.6	45	80	70	2	7	41	73	80	2	4.8	40	75
Sample2 t2		50	3	7.6	32	83	55	3	5	31	80	60	3	2.8	42	84	65	3	8.2	43	69	70	3	8.9	40	73	80	3	3.9	40	69
Sample2 t2		50	4	9.5	33	82	55	4	4.5	32	76	60	4	4.5	41	84	65	4	6.7	45	80	70	4	6.6	39	75	80	4	4.7	40	70
Sample2 t2		50	5	13	31	80	55	5	3.8	28	80	60	5	5.9	43	82	65	5	5.2	44	81	70	5	11	39	72	80	5	8.2	40	70
Sample2 t2		50		9.2	32	82	55		4.2	30	79	60		4.7	42	83	65		6.2	44	78	70		8.1	40	73	80		5.5	40	71

Sample3t2	50	1	5.1	26	86	55	1	5.7	34	85	60	1	6	42	82	65	1	7.6	41	83	70	1	6.5	42	76	80	1	-2	47	81
Sample3t2	50	2	2.2	27	87	55	2	4.7	33	83	60	2	7.3	44	81	65	2	5.4	44	82	70	2	2.7	44	80	80	2	0.1	48	81
Sample3t2	50	3	7.5	29	84	55	3	6.2	31	84	60	3	8.9	43	80	65	3	7.3	44	81	70	3	2.7	45	78	80	3	-2	45	80
Sample3t2	50	4	5	26	86	55	4	6.7	36	84	60	4	8.1	40	80	65	4	8.6	44	80	70	4	9.4	42	76	80	4	-2	48	75
Sample3t2	50	5	8.6	27	84	55	5	6.3	29	84	60	5	6.8	43	81	65	5	5.6	42	82	70	5	9.7	44	75	80	5	-2	47	83
Sample3t2	50		5.7	27	85	55		5.9	33	84	60		7.4	42	81	65		6.9	43	82	70		6.2	44	77	80		-1	47	80
Sample1 t3	50	1	4.9	29	84	55	1	4	32	85	60	1	3.6	41	84	65	1	1.7	46	83	70	1	2.7	47	82	80	1	-2	32	55
Sample1 t3	50	2	2.8	31	83	55	2	4.7	34	80	60	2	1.7	41	85	65	2	-2	44	85	70	2	2.3	47	81	80	2	-2	44	66
Sample1 t3	50	3	4.2	31	84	55	3	6.6	37	80	60	3	5.6	42	82	65	3	1.3	46	84	70	3	1.8	45	77	80	3	-2	42	65
Sample1 t3	50	4	2.3	30	85	55	4	5	36	83	60	4	3.8	40	83	65	4	0.3	47	84	70	4	3.4	44	78	80	4	-2	34	61
Sample1 t3	50	5	5.1	29	85	55	5	5.2	37	80	60	5	2	40	83	65	5	-1	45	84	70	5	2	46	80	80	5	-4	37	59
Sample1 t3	50		3.8	30	84	55		5.1	35	81	60		3.3	41	83	65		0.1	46	84	70		2.4	46	79	80		-2	38	61
Sample2 t3	50	1	11	31	81	55	1	5.4	33	77	60	1	2.3	44	84	65	1	5	47	81	70	1	4.9	30	76	80	1	5	30	52
Sample2 t3	50	2	5.5	33	83	55	2	2.2	29	73	60	2	2	43	83	65	2	1.8	46	83	70	2	5.7	41	75	80	2	2.8	37	60
Sample2t3	50	3	9.6	32	83	55	3	4.2	33	73	60	3	5.7	41	80	65	3	7.8	42	79	70	3	8.6	41	70	80	3	6.7	38	59
Sample2 t3	50	4	9.5	32	82	55	4	3.5	31	75	60	4	5.6	43	82	65	4	6.5	44	80	70	4	4.6	40	74	80	4	4.3	33	52
Sample2t3	50	5	11	30	80	55	5	3.2	34	78	60	5	4.2	42	83	65	5	5.4	45	79	70	5	7	40	74	80	5	6.3	38	61
Sample2 t3	50		9.4	32	82	55		3.7	32	75	60		4	43	83	65		5.3	45	80	70		6.2	38	74	80		5.1	35	57
Sample3 t3	50	1	9.3	26	82	55	1	7.7	36	83	60	1	7.3	44	82	65	1	7.3	44	80	70	1	10	41	76	80	1	-3	40	71
Sample3t3	50	2	2.1	27	86	55	2	5.7	39	81	60	2	10	47	80	65	2	9.9	44	77	70	2	2.5	46	79	80	2	-2	48	56
Sample3t3	50	3	6.3	27	85	55	3	6.5	36	84	60	3	10	47	80	65	3	8.9	45	79	70	3	2.8	46	78	80	3	-2	45	72
Sample3t3	50	4	7.8	28	84	55	4	6.9	36	82	60	4	7.6	46	81	65	4	11	41	78	70	4	3.1	43	76	80	4	-2	47	75
Sample3 t3	50	5	8.5	27	84	55	5	7.5	36	82	60	5	6.7	46	84	65	5	7.8	45	78	70	5	4.6	46	78	80	5	-1	43	71
Sample3t3	50		6.8	27	84	55		6.9	36	82	60		8.4	46	81	65		9	44	78	70		4.6	44	77	80		-2	45	69
Sample1 t4	50	1	5.2	30	85	55	1	4	38	84	60	1	5.7	41	82	65	1	0.7	46	84	70	1	1	45	77	80	1	-1	31	50
Sample1 t4	50	2	2	34	84	55	2	5.1	38	79	60	2	3.9	42	81	65	2	-2	45	83	70	2	0.8	47	81	80	2	0.3	40	56
Sample1 t4	50	3	3.6	29	85	55	3	5.7	38	82	60	3	3.1	44	83	65	3	0	48	83	70	3	4.2	50	79	80	3	-2	34	52
Sample1 t4	50	4	3.8	29	85	55	4	6.4	38	80	60	4	9.5	41	79	65	4	-1	46	84	70	4	0.4	47	78	80	4	0.7	33	51
Sample1 t4	50	5	3	32	84	55	5	5.2	39	79	60	5	3.7	38	82	65	5	-1	46	83	70	5	4.8	48	79	80	5	1	33	53
Sample1 t4	50		3.5	30	84	55		5.3	38	81	60		5.2	41	82	65		-1	46	83	70		2.2	47	79	80		-0	34	52
Sample2 t4	50	1	4.8	34	84	55	1	6.9	38	74	60	1	4.3	42	84	65	1	7.7	47	79	70	1	5.7	43	76	80	1	2.3	32	54
Sample2 t4	50	2	5.3	34	83	55	2	2.6	36	75	60	2	4.2	43	83	65	2	8.8	45	77	70	2	5	44	77	80	2	-0	36	60
Sample2 t4	50	3	9.7	34	80	55	3	4.7	38	78	60	3	6.1	43	82	65	3	9.7	42	84	70	3	5	42	76	80	3	2.6	30	59
Sample2 t4	50	4	10	36	80	55	4	4.7	40	77	60	4	3.8	44	81	65	4	7	46	80	70	4	3.5	43	77	80	4	1.8	37	54

Sample2 t4	50	5	9.8	29	82	55	5	6	36	76	60	5	4.4	44	83	65	5	5.6	47	79	70	5	6.1	41	77	80	5	2.4	32	51
Sample2 t4	50		8	33	82	55		5	38	76	60		4.6	43	83	65		7.8	45	80	70		5	43	76	80		1.8	33	56
Sample3t4	50	1	2	29	87	55	1	7.5	41	83	60	1	7.3	45	80	65	1	6.7	45	78	70	1	3.1	46	75	80	1	-5	39	64
Sample3 t4	50	2	2.3	30	86	55	2	5.5	42	82	60	2	7.2	45	81	65	2	4.5	47	80	70	2	-1	48	80	80	2	-4	42	68
Sample3 t4	50	3	2.6	28	87	55	3	6.6	42	82	60	3	7.3	43	80	65	3	6.3	47	78	70	3	2	45	77	80	3	-4	35	60
Sample3 t4	50	4	2.3	28	87	55	4	4.6	41	83	60	4	8.4	44	79	65	4	4.1	46	78	70	4	-1	44	75	80	4	-1	39	62
Sample3 t4	50	5	1.4	28	86	55	5	7.4	42	82	60	5	6.1	42	72	65	5	5.2	47	78	70	5	4.5	46	75	80	5	-4	36	61
Sample3 t4	50		2.1	29	87	55		6.3	41	82	60		7.2	44	78	65		5.4	46	78	70		1.6	46	77	80		-4	38	63
Sample1 t5	50	1	6.7	31	84	55	1	4.3	45	83	60	1	3.2	40	84	65	1	0.5	48	84	70	1	-1	44	75	80	1	5.4	32	55
Sample1 t5	50	2	2.3	30	84	55	2	6.4	43	79	60	2	2	42	83	65	2	-2	44	84	70	2	1.6	46	78	80	2	4.1	43	66
Sample1 t5	50	3	6.8	27	86	55	3	4.3	42	81	60	3	2.1	45	84	65	3	-2	45	84	70	3	1.3	43	76	80	3	2.8	42	65
Sample1 t5	50	4	3.1	29	86	55	4	3.5	40	80	60	4	3.8	42	82	65	4	-2	46	84	70	4	-1	41	73	80	4	3.2	34	61
Sample1 t5	50	5	5.9	28	85	55	5	5.9	45	81	60	5	3.1	43	82	65	5	-3	44	86	70	5	2.7	47	76	80	5	3.2	37	59
Sample1 t5	50		4.9	29	85	55		4.9	43	81	60		2.8	43	83	65		-2	45	85	70		0.8	44	76	80		3.8	38	61
Sample2 t5	50	1	4.6	32	85	55	1	5.3	41	81	60	1	5.5	43	84	65	1	2.2	48	81	70	1	3.9	41	71	80	1	2.8	32	52
Sample2 t5	50	2	4.5	30	85	55	2	2.1	41	82	60	2	1.4	43	84	65	2	1.2	48	81	70	2	2.7	42	74	80	2	-0	38	61
Sample2 t5	50	3	8.7	32	80	55	3	5.9	42	81	60	3	3.8	46	82	65	3	2.4	49	81	70	3	4.1	39	71	80	3	1.7	36	57
Sample2 t5	50	4	5.3	29	85	55	4	7.1	42	79	60	4	5.2	44	83	65	4	5.9	46	78	70	4	1.8	40	73	80	4	2	29	59
Sample2 t5	50	5	6.5	29	82	55	5	5	40	81	60	5				65	5	2.1	47	81	70	5	3.7	40	72	80	5	2.1	40	60
Sample2 t5	50		5.9	30	83	55		5.1	41	81	60		4	44	83	65		2.7	48	80	70		3.2	40	72	80		1.7	35	58
Sample3 t5	50	1	4.6	28	87	55	1	8.8	43	80	60	1	3.5	46	81	65	1	4.7	47	81	70	1	1.6	45	76	80	1	-5	30	56
Sample3 t5	50	2	1.5	27	86	55	2	12	46	76	60	2	6.2	46	81	65	2	3.1	48	81	70	2	1.4	45	78	80	2	-5	31	56
Sample3 t5	50	3	5.4	26	86	55	3	11	41	77	60	3	5.7	45	82	65	3	3.7	47	81	70	3	3.8	43	82	80	3	-3	33	55
Sample3 t5	50	4	4.1	28	85	55	4	9.3	43	77	60	4	6	46	82	65	4	1.2	48	82	70	4	2.6	43	74	80	4	-4	32	55
Sample3t5	50	5	4.4	29	85	55	5	7.4	41	81	60	5	5.3	47	81	65	5	5.3	47	79	70	5	3.8	47	76	80	5	-3	33	52
Sample3t5	50		4	28	86	55		9.7	43	78	60		5.4	46	81	65		3.6	47	81	70		2.6	45	77	80		-4	32	55

2d Read

time	Temp	Rep	a	b	L	Temp	Rep	a	b	L	Temp	Rep	a	b	L	Temp	Rep	a	b	L	Temp	Rep	a	b	L	Temp	Rep	a	b	L
Sample1 t1	50	1	5.0	21.8	83.2	55	1	5.0	21.8	83.2	60	1	5.3	25.2	81.6	65	1	0.9	24.0	86.7	70	1	4.7	35.9	72.6	80	1	6.8	36.1	75.9
Sample1 t1	50	2	5.2	21.4	77.4	55	2	5.2	21.4	77.4	60	2	3.0	29.5	82.0	65	2	0.4	25.7	84.8	70	2	3.3	31.6	70.0	80	2	6.3	36.2	78.2
Sample1 t1	50	3	6.4	23.5	83.0	55	3	6.4	23.5	83.0	60	3	2.8	29.2	82.3	65	3	2.3	28.5	82.3	70	3	4.2	35.5	72.6	80	3	6.9	36.7	75.0
Sample1 t1	50	4	5.2	19.9	83.1	55	4	5.2	19.9	83.1	60	4	6.0	25.5	82.6	65	4	1.6	26.1	84.4	70	4	4.4	32.5	66.2	80	4	6.7	33.7	75.1
Sample1 t1	50	5	6.3	22.0	83.1	55	5	6.3	22.0	83.1	60	5	3.1	27.5	81.8	65	5	1.4	24.4	85.5	70	5	4.4	36.3	72.2	80	5	4.8	36.1	78.7
Sample1 t1	50		5.6	21.7	82.0	55	3	5.6	21.7	82.0	60	3	4.0	27.4	82.1	65	3	1.3	25.7	84.7	70	3	4.2	34.4	70.7	80	3	6.3	35.7	76.6
Sample2 t1	50	1	5.0	24.2	82.8	55	1	5.0	24.2	82.8	60	1	3.0	26.6	83.2	65	1	5.1	31.0	80.1	70	1	8.0	32.8	69.5	80	1	6.9	29.5	61.6
Sample2 t1	50	2	3.4	22.4	78.7	55	2	3.4	22.4	78.7	60	2	2.6	25.0	82.4	65	2	4.0	33.5	75.2	70	2	7.8	29.7	68.6	80	2	5.8	32.6	67.1
Sample2 t1	50	3	6.2	23.1	71.1	55	3	6.2	23.1	71.1	60	3	3.5	25.1	83.2	65	3	7.4	35.8	77.3	70	3	7.7	29.9	65.0	80	3	8.0	32.5	68.5
Sample2 t1	50	4	2.8	22.8	83.5	55	4	2.8	22.8	83.5	60	4	3.6	26.3	82.4	65	4	5.3	34.6	79.5	70	4	8.4	30.3	65.4	80	4	7.4	27.8	67.8
Sample2 t1	50	5	5.0	24.2	78.7	55	5	5.0	24.2	78.7	60	5	2.5	25.4	84.5	65	5	8.7	34.3	74.3	70	5	7.9	32.7	68.8	80	5	7.3	34.3	66.5
Sample2 t1	50		4.5	23.3	79.0	55	3	4.5	23.3	79.0	60	3	3.1	25.7	83.1	65	3	6.1	33.8	77.3	70	3	8.0	31.1	67.5	80	3	7.1	31.3	66.3
Sample3 t1	50	1	6.8	24.5	81.5	55	1	6.8	24.5	81.5	60	1	5.9	33.8	81.3	65	1	9.6	31.4	76.3	70	1	4.6	32.4	67.3	80	1	2.7	28.4	64.6
Sample3 t1	50	2	7.8	29.2	73.9	55	2	7.8	29.2	73.9	60	2	6.9	32.1	77.4	65	2	8.2	31.0	72.7	70	2	5.0	33.4	69.1	80	2	3.7	29.0	62.7
Sample3 t1	50	3	7.5	26.8	80.0	55	3	7.5	26.8	80.0	60	3	8.4	35.3	76.2	65	3	7.7	34.8	77.2	70	3	3.6	33.1	66.8	80	3	3.0	33.3	72.9
Sample3 t1	50	4	7.1	26.9	76.4	55	4	7.1	26.9	76.4	60	4	5.5	35.2	79.4	65	4	8.3	36.3	78.9	70	4	4.2	32.4	64.7	80	4	2.3	28.8	66.0
Sample3 t1	50	5	7.2	25.3	81.3	55	5	7.2	25.3	81.3	60	5	8.1	36.7	75.5	65	5	6.0	32.8	76.4	70	5	4.5	30.7	61.8	80	5	3.1	34.0	72.0
Sample3 t1	50		7.3	26.5	78.6	55	3	7.3	26.5	78.6	60	3	7.0	34.6	77.9	65	3	8.0	33.3	76.3	70	3	4.4	32.4	65.9	80	3	3.0	30.7	67.6
Sample1 t2	50	1	6.1	27.4	77.1	55	1	6.1	27.4	77.1	60	1	3.9	33.7	77.7	65	1	0.8	34.1	73.7	70	1	2.7	32.5	69.0	80	1	5.0	36.4	64.3
Sample1 t2	50	2	5.2	23.5	78.2	55	2	5.2	23.5	78.2	60	2	5.2	35.5	75.1	65	2	0.6	35.7	75.1	70	2	3.8	29.9	64.7	80	2	3.9	31.3	62.2
Sample1 t2	50	3	5.3	27.0	80.6	55	3	5.3	27.0	80.6	60	3	3.9	35.8	77.0	65	3	2.0	35.6	69.1	70	3	3.3	32.6	66.8	80	3	3.4	33.9	62.2
Sample1 t2	50	4	5.8	25.0	79.8	55	4	5.8	25.0	79.8	60	4	3.2	36.7	78.3	65	4	1.5	35.7	74.0	70	4	2.2	33.9	69.1	80	4	3.9	38.1	63.9
Sample1 t2	50	5	5.5	24.6	77.1	55	5	5.5	24.6	77.1	60	5	6.7	30.3	70.8	65	5	0.3	36.8	73.9	70	5	3.6	32.3	66.6	80	5	5.2	30.8	58.6
Sample1 t2	50		5.5	25.5	78.5	55	3	5.5	25.5	78.5	60	3	4.6	34.4	75.8	65	3	1.0	35.6	73.2	70	3	3.1	32.2	67.2	80	3	4.3	34.1	62.2
Sample2 t2	50	1	3.5	22.7	79.0	55	1	3.5	22.7	79.0	60	1	6.2	36.9	76.4	65	1	5.9	30.7	67.5	70	1	7.8	30.5	62.0	80	1	6.8	25.4	51.9
Sample2 t2	50	2	3.9	23.1	76.1	55	2	3.9	23.1	76.1	60	2	4.5	34.5	74.2	65	2	4.8	29.6	66.1	70	2	5.8	26.6	60.5	80	2	5.2	25.3	57.5
Sample2 t2	50	3	5.0	23.6	78.3	55	3	5.0	23.6	78.3	60	3	6.5	35.3	75.1	65	3	5.6	30.7	68.4	70	3	7.1	27.0	60.9	80	3	6.8	27.2	54.3
Sample2 t2	50	4	4.8	23.7	78.2	55	4	4.8	23.7	78.2	60	4	3.5	37.8	78.3	65	4	6.0	30.9	66.1	70	4	7.0	28.9	62.6	80	4	5.7	26.4	54.4

Sample2 t2	50	5	4.5	23.0	77.9	55	5	4.5	23.0	77.9	60	5	6.5	36.5	74.8	65	5	5.9	29.9	66.8	70	5	8.6	28.6	60.9	80	5	5.2	25.9	58.6
Sample2t2	50		4.3	23.2	77.9	55	3	4.3	23.2	77.9	60	3	5.4	36.2	75.8	65	3	5.6	30.3	67.0	70	3	7.3	28.3	61.4	80	3	5.9	26.0	55.3
Sample3 t2	50	1	6.1	25.0	83.2	55	1	6.1	25.0	83.2	60	1	6.9	39.8	76.7	65	1	7.3	35.1	72.8	70	1	7.7	29.8	61.3	80	1	2.6	28.3	62.3
Sample3t2	50	2	4.8	24.8	82.2	55	2	4.8	24.8	82.2	60	2	6.9	38.3	73.7	65	2	5.2	29.5	63.2	70	2	3.8	24.8	58.1	80	2	3.1	26.9	57.7
Sample3 t2	50	3	5.8	24.3	83.2	55	3	5.8	24.3	83.2	60	3	8.7	40.5	74.1	65	3	6.6	31.6	65.4	70	3	6.1	25.8	56.8	80	3	1.6	26.8	59.9
Sample3 t2	50	4	5.8	27.3	82.9	55	4	5.8	27.3	82.9	60	4	8.7	37.6	75.6	65	4				70	4	6.5	27.4	61.0	80	4	2.6	30.2	57.0
Sample3t2	50	5	6.5	25.1	82.1	55	5	6.5	25.1	82.1	60	5	6.8	38.0	74.8	65	5	4.9	33.7	71.8	70	5	7.7	30.0	60.9	80	5	2.8	28.4	61.6
Sample3 t2	50		5.8	25.3	82.7	55	3	5.8	25.3	82.7	60	3	7.6	38.8	75.0	65	3	6.0	32.5	68.3	70	3	6.4	27.6	59.6	80	3	2.5	28.1	59.7
Sample1 t3	50	1	3.8	25.9	80.8	55	1	3.8	25.9	80.8	60	1	6.7	30.6	67.7	65	1	3.3	31.6	64.1	70	1	4.2	31.3	63.0	80	1	-0.3	23.9	46.5
Sample1 t3	50	2	5.3	22.8	73.4	55	2	5.3	22.8	73.4	60	2	3.4	33.7	74.1	65	2	1.0	27.7	63.2	70	2	3.7	27.5	59.4	80	2	2.3	27.3	53.3
Sample1 t3	50	3	5.6	30.2	77.8	55	3	5.6	30.2	77.8	60	3	4.6	32.8	71.6	65	3	1.2	32.4	66.1	70	3	2.8	32.8	63.5	80	3	2.4	28.1	51.0
Sample1 t3	50	4	4.7	27.8	80.1	55	4	4.7	27.8	80.1	60	4	4.6	28.9	71.9	65	4	1.4	31.3	64.9	70	4	3.2	30.3	63.9	80	4	1.1	24.0	50.0
Sample1 t3	50	5	5.1	28.5	74.1	55	5	5.1	28.5	74.1	60	5	3.0	33.9	75.9	65	5	1.0	31.5	68.9	70	5	3.2	30.8	63.5	80	5	0.4	26.3	50.5
Sample1 t3	50		4.9	27.0	77.2	55	3	4.9	27.0	77.2	60	3	4.5	32.0	72.2	65	3	1.6	30.9	65.4	70	3	3.4	30.5	62.7	80	3	1.2	25.9	50.3
Sample2 t3	50	1	5.8	25.0	75.6	55	1	5.8	25.0	75.6	60	1	3.8	35.6	76.0	65	1	5.3	31.7	67.3	70	1	5.7	25.6	58.3	80	1	4.3	23.6	44.4
Sample2 t3	50	2	3.5	20.6	71.5	55	2	3.5	20.6	71.5	60	2	3.0	32.8	73.1	65	2	4.0	29.5	66.0	70	2	5.6	26.3	59.6	80	2	5.6	23.0	43.5
Sample2 t3	50	3	4.2	23.2	71.4	55	3	4.2	23.2	71.4	60	3	3.6	33.0	73.5	65	3	4.8	29.6	67.1	70	3	6.4	27.1	59.4	80	3	6.5	30.9	50.3
Sample2t3	50	4	4.2	24.0	72.8	55	4	4.2	24.0	72.8	60	4	3.1	34.6	75.3	65	4	4.9	31.7	67.7	70	4	5.3	30.3	60.7	80	4	7.1	23.7	43.1
Sample2 t3	50	5	4.0	24.5	75.3	55	5	4.0	24.5	75.3	60	5	3.6	36.2	74.9	65	5	7.2	30.6	64.1	70	5	5.9	29.6	63.0	80	5	6.0	27.0	47.0
Sample2 t3	50		4.3	23.5	73.3	55	3	4.3	23.5	73.3	60	3	3.4	34.4	74.6	65	3	5.2	30.6	66.4	70	3	5.8	27.8	60.2	80	3	5.9	25.6	45.7
Sample3 t3	50	1	8.0	31.7	80.6	55	1	8.0	31.7	80.6	60	1	4.9	36.7	72.3	65	1	8.6	26.1	54.6	70	1	9.8	30.9	58.8	80	1	2.1	28.3	56.8
Sample3 t3	50	2	5.9	29.6	77.0	55	2	5.9	29.6	77.0	60	2	7.5	34.1	63.3	65	2	7.8	31.6	63.4	70	2	5.0	26.7	57.3	80	2	4.9	34.0	49.6
Sample3t3	50	3	7.7	29.2	81.6	55	3	7.7	29.2	81.6	60	3	8.8	36.2	68.2	65	3	7.6	30.0	63.6	70	3	5.4	28.2	58.7	80	3	4.1	28.8	52.7
Sample3t3	50	4	7.8	30.7	79.2	55	4	7.8	30.7	79.2	60	4	5.6	37.5	73.0	65	4	8.5	32.8	65.6	70	4	4.0	32.6	64.2	80	4	2.8	26.5	51.6
Sample3t3	50	5	7.9	30.3	78.9	55	5	7.9	30.3	78.9	60	5	6.6	34.5	68.4	65	5				70	5	6.0	27.8	57.2	80	5	3.8	26.9	53.1
Sample3t3	50		7.5	30.3	79.5	55	3	7.5	30.3	79.5	60	3	6.7	35.8	69.0	65	3	8.1	30.1	61.8	70	3	6.0	29.2	59.3	80	3	3.5	28.9	52.8
Sample1 t4	50	1	4.9	32.9	76.2	55	1	4.9	32.9	76.2	60	1	4.0	31.2	72.8	65	1	2.2	34.2	69.1	70	1	3.7	33.1	63.8	80	1	3.5	23.5	48.0
Sample1 t4	50	2	5.8	27.9	68.3	55	2	5.8	27.9	68.3	60	2	4.3	28.6	73.4	65	2	2.2	28.0	61.0	70	2	3.1	27.8	60.5	80	2	3.6	24.2	47.3
Sample1 t4	50	3	6.0	30.5	75.2	55	3	6.0	30.5	75.2	60	3	4.6	33.4	68.9	65	3	2.3	33.7	66.6	70	3	5.4	28.1	66.0	80	3	2.7	21.0	40.9
Sample1 t4	50	4	4.2	29.7	78.6	55	4	4.2	29.7	78.6	60	4	6.8	30.1	65.7	65	4	1.0	32.4	68.1	70	4	2.8	33.2	62.2	80	4	3.5	19.9	40.9

Sample1 t4	50	5	5.5	29.6	70.5	55	5	5.5	29.6	70.5	60	5	4.6	28.6	66.0	65	5	2.4	29.3	63.1	70	5	4.6	29.4	60.8	80	5	3.0	22.2	42.5
Sample1 t4	50		5.3	30.1	73.8	55	3	5.3	30.1	73.8	60	3	4.9	30.4	69.4	65	3	2.0	31.5	65.6	70	3	3.9	30.3	62.6	80	3	3.3	22.1	43.9
Sample2 t4	50	1	7.7	31.2	68.4	55	1	7.7	31.2	68.4	60	1	3.8	35.5	74.3	65	1	6.2	31.2	63.6	70	1	5.0	29.8	63.5	80	1	-0.8	25.8	47.0
Sample2 t4	50	2	5.3	30.4	67.3	55	2	5.3	30.4	67.3	60	2	5.3	32.1	69.1	65	2	5.0	29.9	62.6	70	2	4.9	31.1	63.3	80	2	2.7	28.9	47.2
Sample2 t4	50	3	6.3	32.0	72.4	55	3	6.3	32.0	72.4	60	3	5.6	32.3	69.8	65	3	4.5	32.2	66.5	70	3	4.6	31.2	64.5	80	3	0.1	25.8	44.8
Sample2 t4	50	4	6.1	32.4	69.6	55	4	6.1	32.4	69.6	60	4	6.0	34.4	72.1	65	4	4.3	30.5	64.8	70	4	4.4	30.7	63.8	80	4	0.1	27.7	45.7
Sample2 t4	50	5	7.1	31.1	68.0	55	5	7.1	31.1	68.0	60	5	5.2	31.3	70.0	65	5	6.9	28.4	59.4	70	5	5.7	30.2	63.9	80	5	0.4	27.1	45.5
Sample2 t4	50		6.5	31.4	69.1	55	3	6.5	31.4	69.1	60	3	5.2	33.1	71.1	65	3	5.4	30.4	63.4	70	3	4.9	30.6	63.8	80	3	0.5	27.1	46.0
Sample3 t4	50	1	6.8	33.8	80.4	55	1	6.8	33.8	80.4	60	1	7.2	33.1	66.1	65	1	6.9	29.9	61.6	70	1	7.3	35.0	54.0	80	1	3.3	25.1	48.0
Sample3 t4	50	2	6.0	36.6	75.0	55	2	6.0	36.6	75.0	60	2	5.9	31.2	65.7	65	2	7.0	26.9	56.7	70	2	6.4	27.5	55.2	80	2	4.7	19.2	43.2
Sample3 t4	50	3	7.0	38.2	78.8	55	3	7.0	38.2	78.8	60	3	5.8	33.7	71.1	65	3	8.5	29.2	59.6	70	3	4.8	30.3	58.9	80	3	0.4	25.7	46.6
Sample3 t4	50	4	6.6	35.7	78.4	55	4	6.6	35.7	78.4	60	4	5.6	34.7	68.0	65	4	5.7	31.2	65.2	70	4	4.7	33.7	61.3	80	4	2.6	26.7	46.2
Sample3t4	50	5	6.7	36.9	77.0	55	5	6.7	36.9	77.0	60	5	5.4	32.7	70.1	65	5	6.4	29.7	62.2	70	5	7.5	29.8	55.8	80	5	2.4	25.3	47.3
Sample3t4	50		6.6	36.2	77.9	55	3	6.6	36.2	77.9	60	3	6.0	33.1	68.2	65	3	6.9	29.4	61.1	70	3	6.1	31.3	57.1	80	3	2.7	24.4	46.3
Sample1 t5	50	1	3.1	36.1	78.0	55	1	3.1	36.1	78.0	60	1	4.3	29.2	69.6	65	1	0.4	37.0	72.3	70	1	2.8	31.6	60.9	80	1	1.9	25.9	43.3
Sample1 t5	50	2	6.5	27.6	62.3	55	2	6.5	27.6	62.3	60	2	3.7	27.6	64.6	65	2	-0.1	33.3	72.4	70	2	3.2	27.8	59.0	80	2	4.4	30.1	47.5
Sample1 t5	50	3	4.1	27.2	71.2	55	3	4.1	27.2	71.2	60	3	3.3	31.3	69.0	65	3	-0.1	33.5	72.4	70	3	2.9	29.7	61.2	80	3	1.9	27.9	46.6
Sample1 t5	50	4	4.4	32.9	70.2	55	4	4.4	32.9	70.2	60	4	4.6	29.2	55.5	65	4	-0.5	33.4	73.5	70	4	1.7	31.4	61.5	80	4	0.2	26.1	46.2
Sample1 t5	50	5	6.2	35.7	70.1	55	5	6.2	35.7	70.1	60	5	3.2	32.5	70.7	65	5	-0.3	33.3	73.6	70	5	4.9	27.1	54.3	80	5	5.3	26.9	44.6
Sample1 t5	50		4.8	31.9	70.3	55	3	4.8	31.9	70.3	60	3	3.8	29.9	65.9	65	3	-0.1	34.1	72.8	70	3	3.1	29.5	59.4	80	3	2.7	27.4	45.6
Sample2t5	50	1	7.8	31.9	69.3	55	1	7.8	31.9	69.3	60	1	4.7	33.7	72.5	65	1	6.0	32.9	65.5	70	1	3.2	31.7	57.6	80	1	1.4	23.7	45.7
Sample2 t5	50	2	4.8	29.0	67.6	55	2	4.8	29.0	67.6	60	2	4.2	29.9	67.9	65	2	6.4	27.0	58.3	70	2	5.5	31.1	60.4	80	2	1.8	26.4	48.8
Sample2t5	50	3	5.6	33.9	71.8	55	3	5.6	33.9	71.8	60	3	4.6	31.4	69.1	65	3	6.0	29.7	61.2	70	3	4.1	33.5	54.4	80	3	2.0	26.0	47.0
Sample2t5	50	4	4.7	32.5	71.2	55	4	4.7	32.5	71.2	60	4	2.9	32.1	74.6	65	4	7.0	33.0	64.6	70	4	2.1	33.8	56.4	80	4	2.0	23.6	44.1
Sample2 t5	50	5	8.1	29.6	62.0	55	5	8.1	29.6	62.0	60	5	4.9	31.7	70.4	65	5	7.5	28.1	59.5	70	5	3.2	35.6	57.8	80	5	2.5	29.2	51.3
Sample2 t5	50		6.2	31.4	68.4	55	3	6.2	31.4	68.4	60	3	4.2	31.8	70.9	65	3	6.6	30.1	61.8	70	3	3.6	33.1	57.3	80	3	1.9	25.8	47.4
Sample3 t5	50	1	7.2	38.2	66.0	55	1	7.2	38.2	66.0	60	1	7.8	33.4	66.0	65	1	7.3	30.8	60.8	70	1	6.5	29.8	60.4	80	1	-0.5	23.6	43.8
Sample3t5	50	2	11.3	34.4	67.2	55	2	11.3	34.4	67.2	60	2	6.4	30.1	63.1	65	2	6.9	27.7	67.1	70	2	6.3	28.5	56.0	80	2	2.6	17.1	37.8
Sample3 t5	50	3	9.4	34.4	65.7	55	3	9.4	34.4	65.7	60	3	5.0	32.5	67.7	65	3	5.2	35.0	67.4	70	3	6.3	29.3	57.1	80	3	0.7	24.4	44.4
Sample3t5	50	4	9.7	35.5	69.7	55	4	9.7	35.5	69.7	60	4	5.1	34.7	70.1	65	4	5.1	33.6	65.4	70	4	4.6	32.2	61.1	80	4	2.2	20.3	40.1

Sample3t5	50	5	8.9	35.3	76.1	55	5	8.9	35.3	76.1	60	5	5.4	30.9	64.1	65	5	6.1	28.3	58.3	70	5	5.3	30.6	59.6	80	5	1.7	22.5	42.8
Sample3 t5	50		9.3	35.6	68.9	55	3	9.3	35.6	68.9	60	3	5.9	32.3	66.2	65	3	6.1	31.1	63.8	70	3	5.8	30.1	58.8	80	3	1.3	21.6	41.8

Raw data Figure 4-10 12: Color diference at diferent oxygen concentration

	Sample 1				Sample 2				Sample 3				Sample 4			
	t	a	b	L	t	a	b	L	t	a	b	L	t	a	b	L
6.1%	0	-0.06	37.4	53	0	1.45	44.8	59.1	0	-5.05	32.1	50.4	0	-4.87	28	49.4
	5	0.26	36.8	52.5	5	1.14	44.2	58.5	5	-4.95	31	49.8	5	-4.79	27.3	48.6
	10	-0.63	34.4	52.9	10	0.73	42	57.6	10	-4.05	30.5	48.6	10	-4.67	26.5	47.7
	20	0.32	33.3	51.8	20	0.82	40.5	56.6	20	-3.82	29.2	47.8	20	-4.43	25.9	47.1
	30	0.2	32.9	50.5	30	0.43	40	56.5	30	-4.34	28.6	47.4	30	-4.47	25.2	46
	45	-0.05	32	50.6	45	0.55	39.1	55.7	45	-4.5	28.3	47.6	45	-3.65	24.2	45.5
	60	-0.24	31.7	50.5	60	0.58	37.9	54.9	60	-4.55	27	46.2	60	-4.21	23.4	44.6
	90	-0.54	29.1	49.3	90	-0.63	37.7	54	90	-4.65	26.4	46	90	-3.35	22.1	43.5
	120	-1.69	28.5	49.4	120	-1.9	36	54.4	120	-4	24.5	44.6	120	-3.51	21.6	42.8
	180	-0.39	27.5	47.8	180	-1.41	34.8	51.1	180	-3.76	24.5	44.5	180	-2.79	20.9	42.1
	240	-1.95	27.4	47.9	240	-1.56	34.6	51.1	240	-3.8	24.3	44.2	240	-2.7	20.9	41.3
9.9%	0	0.14	39.5	56.7	0	-1.25	37.1	55.3	0	-3.73	33.9	52.5	0	-3.7	28.1	48.8
	3	0.01	37.5	55.6	3	-1.36	35.9	54	3	-3.93	33.5	52.2	3	-3.37	27.2	47.4
	5	-0.02	37.1	55.5	5	-1.15	35.2	54	5	-3.97	33.4	52.2	5	-3.51	26.8	47.1
	10	-0.39	36.7	55	10	-1.66	35.9	53.8	10	-4.03	33.1	52.1	10	-3.93	26.3	47.1
	15	-0.5	36	54.6	15	-1.23	34.2	52.5	15	-4.12	32.7	51.8	15	-4.03	25.4	46.6
	20	-0.32	34.1	53.1	20	-1.49	33.5	52.5	20	-4.15	32.3	51.4	20	-3.74	25.1	46
	30	0.02	33.7	52.8	30	-2.07	32.9	52.2	30	-4.3	31.9	51.2	30	-4.14	23.5	45.2
	45	-0.52	32.5	51.4	45	-1.71	31.9	51	45	-4.48	31.5	51.1	45	-3.84	23	44.4
	60	-0.14	32.2	51.2	60	-0.67	31.5	50.6	60	-4.28	30.5	49.8	60	-3.95	22.5	44.2
	90	-0.78	31.9	51.5	90	-1.91	30.9	50.3	90	-4.42	29.6	49.6	90	-3.87	21	42.5
	120	-0.57	31.7	50.6	120	-1.79	30.8	50.2	120	-4.27	29.1	48.8	120	-2.73	20.4	41.9
	180	0.16	31.4	50.2	180	-1.71	30.5	49.7	180	-4.24	29.1	48.6	180	-2.17	20.4	41.9
	240	0.87	30.7	50.1	240	-1.75	30.3	49.3	240	-4.22	28.9	48	240	-2.13	20.3	41.8
13.8%	0	-1.14	36.8	56.6	0	1.69	44.8	59.6	0	-3.91	29.1	48.6	0	-4.18	26.9	47.6
	2	-0.93	36	56.1	2	1.47	44	58.9	2	-3.82	27.4	46.6	2	-4.15	26.7	47.2
	5	-0.44	36.7	55.7	5	1.74	42.4	57.9	5	-3.97	27.5	47.6	5	-4.3	26.2	47.3
	7	-0.49	36.7	55.7	7	1.7	42.3	57.6	7	-3.86	27	46.5	7	-4.27	25.2	46.6
	10	-0.56	36	55.3	10	1.37	41.4	57.4	10	-4.31	26.8	46.8	10	-4.26	24.8	46.3
	15	-0.82	34.9	54.6	15	1.08	41.1	57.2	15	-4.35	26.8	46.9	15	-4.26	24.6	46.2
	20	-0.79	33.9	53.6	20	1	40.9	56.1	20	-4.48	26.6	47	20	-4.12	23.7	45.7
	30	-0.93	33.2	53.3	30	0.54	39.5	56	30	-4.33	25.4	45.8	30	-4.22	23.2	45
	40	-1.09	31.9	52.2	40	0.39	39.5	56	40	-4.48	24.8	45.3	40	-4.29	22.3	43.6
	50	-1.24	31.8	52	50	0.08	39	55.4	50	-4.48	24.3	44.8	50	-4.2	21.9	43.3
	60	-1.2	31.8	51.9	60	0.72	38.3	54.4	60	-4.34	23.8	44.3	60	-4.08	21.3	42.7
	90	-1.33	31.4	51.7	90	0.1	37.9	53.9	90	-4.49	23.4	44.2	90	-3.76	20.2	42.5
	120	-1.53	31.3	51.3	120	0.99	37.8	53.6	120	-4.03	22.7	43.3	120	-3.19	20.1	42.5
	180	-1.52	31.1	51.3	180	-0.6	37.6	53.6	180	-4.1	21.8	42.4	180	-3.47	19.6	42.2
20.0%	0	0.95	38.7	54	0	2.95	46.6	56.6	0	-3.07	47.9	65.3	0	-2.4	35.5	55.6
	1	0.83	36.3	53.7	1	3.04	43.2	55.5	1	-3.37	46.7	64.6	1	-2.32	34.9	55.1
	3	0.84	34.7	52.2	3	2.77	41	54.7	3	-3.35	44.8	63.1	3	-2.22	34.1	54.2
	5	-0.13	33.5	52.5	5	2.69	39.2	53.2	5	-3.13	44.6	62.3	5	-2.28	34.5	54.8
	7	-0.2	31.6	51.1	7	1.13	40.6	56.1	7	-3.31	43.7	61.7	7	-2.03	32.4	52.5
	10	-0.14	31.2	50.6	10	2.07	39.7	54.9	10	-3.09	42	59.8	10	-1.68	32.5	52.7
	15	-0.48	29.2	49.9	15	-1.54	39.4	55.2	15	-3.45	40.7	59.9	15	-1.28	31.7	51.7
	25	-0.81	28.6	48.7	20	1.99	38.9	54.4	20	-3.53	40.7	59.9	20	-1.41	31.4	51.4
	30	-0.19	29.2	48.6	25	-1.85	39.1	54.1	25	-3.53	39.3	57.8	25	-0.95	29.6	49.3
	40	-2.11	28.4	48.9	30	0.16	37.8	55	30	-3.58	39.5	59	30	-0.84	29.7	49
	50	-1.81	28.8	49	40	-1.59	37.3	54.1	40	-3.64	38.8	57.7	40	-1.64	28.8	47.9
	60	-2.33	28.6	47.9	50	-0.56	37.9	54.3	50	-3.85	37	56.9	50	-0.76	27.6	47.4

90	-1.15	26.7	46.7	60	-2.31	36.5	54	60	-4.66	36.3	57.5	60	-1.23	26.7	46.7
120	-2.76	26	47.3	90	-2.2	36.1	52.6	90	-3.77	38.1	56.9	90	-2.99	25.2	47.7
20	-0.3	27.9	47.3	120	-1.1	35.6	51.3	120	-4.79	36.1	56.9	120	-3.37	24.8	47.6

Raw data Figure 4-14: Color diference at diferent storage temperature

Sample1

4°C

t	a	b	L
0	-3	28	48
5	-3	26	47
10	-3	27	45
15	-3	25	46
20	-3	25	46
25	-3	24	46
30	-3	24	46
40	-3	24	45
50	-3	24	46
60	-3	23	45
85	-3	22	46
100	-3	23	45
120	-4	23	46
180	-3	22	45

20°C

t	a	b	L
0	-4	28	47
3	-3	27	47
5	-4	27	46
10	-3	27	45
15	-3	26	45
20	-2	26	46
30	-2	25	46
45	-3	24	45
60	-3	23	45
120	-3	23	44
300	-3	24	45

30°C

t	a	b	L
0	-2	29	48
3	-3	27	47
5	-2	27	46
8	-3	26	47
10	-1	27	46
15	-1	26	46
20	-2	27	47
25	-1	25	45
30	-1	25	45
40	-1	25	43
50	-1	25	43
60	-1	25	43
90	-1	24	44
120	-1	24	44

40°C

t	a	b	L
0	-3	28	44
2	-3	25	46
3	-3	25	45
5	-3	26	45

Sample2

4°C

t	a	b	L
0	-0	32	51
5	-0	31	51
10	-0	31	50
15	-0	30	49
20	-0	30	49
25	-0	30	48
30	-0	30	48
40	-1	28	47
50	-1	26	47
60	-1	26	46
85	-1	26	45
100	-1	24	44
120	-1	24	45
180	-1	25	45

20°C

t	a	b	L
0	-3	32	50
3	-3	30	49
5	-3	30	49
10	-2	28	48
15	-2	28	47
20	-2	27	46
30	-2	27	46
45	-2	26	45
60	-1	25	44
120	-1	25	44
300	-1	25	44

30°C

t	a	b	L
0	-1	37	54
3	-0	38	55
5	-0	36	53
8	-0	35	53
10	-0	34	52
15	-0	33	51
20	-1	32	50
25	-1	30	48
30	-1	30	48
40	-1	28	47
50	-1	28	48
60	-1	27	46
90	-1	27	45
120	-1	29	47

40°C

t	a	b	L
0	-3	32	47
2	-2	31	46
3	-2	30	46
5	-2	28	45

Sample3

4°C

t	a	b	L
0	-4	41	57
5	-4	40	56
10	-3	38	56
15	-4	37	56
20	-4	35	55
25	-4	34	54
30	-3	34	54
40	-3	34	54
50	-3	32	53
60	-3	32	53
80	-4	32	52
100	-4	31	51
120	-4	30	50
180	-4	28	49

20°C

t	a	b	L
0	-4	39	56
3	-4	37	54
5	-4	35	53
10	-4	33	53
15	-4	32	52
20	-4	32	52
30	-3	31	51
45	-4	30	50
60	-3	30	50
120	-4	29	50
260	-3	28	49

30°C

t	a	b	L
0	-3	33	51
3	-3	32	49
5	-3	29	48
8	-3	29	48
10	-3	28	48
15	-3	27	47
20	-2	26	47
25	-3	25	46
30	-2	25	46
40	-2	24	45
50	-2	24	45
60	-3	23	45
90	-3	23	44
120	-2	22	43

40°C

t	a	b	L
0	-4	36	52
2	-4	31	50
3	-4	32	51
5	-4	31	50

Sample4

4°C

t	a	b	L
0	-5	30	51
5	-5	29	50
10	-5	29	50
15	-5	29	50
20	-5	28	50
25	-5	27	49
30	-5	27	49
40	-5	27	47
50	-4	25	46
60	-4	25	46
80	-4	24	45
100	-5	24	46
120	-3	23	44
180	-5	23	44

20°C

t	a	b	L
0	-5	30	51
3	-5	29	50
5	-5	27	49
10	-4	28	49
15	-5	27	49
20	-5	27	49
30	-5	27	49
45	-4	27	47
60	-4	26	46
120	-4	25	46
260	-3	26	47

30°C

t	a	b	L
0	-2	32	51
3	-2	31	50
5	-2	30	50
8	-2	29	49
10	-2	28	48
15	-2	27	47
20	-2	26	47
25	-2	26	46
30	-3	25	45
40	-3	25	45
50	-3	25	44
60	-3	24	43
90	-3	24	43
120	-3	24	45

40°C

t	a	b	L
0	-5	32	51
2	-5	30	50
3	-3	29	49
5	-3	29	50

8	-3	24	44	8	-2	26	44	8	-4	30	50	8	-4	28	49
10	-3	24	45	10	-2	26	45	10	-4	29	49	10	-4	28	50
13	-2	24	44	13	-1	24	43	13	-3	30	49	13	-4	27	48
15	-3	23	44	15	-2	25	44	15	-3	29	50	15	-4	26	48
20	-3	24	44	20	-2	25	43	20	-3	28	49	20	-4	26	46
25	-3	23	44	25	-1	24	43	25	-3	28	49	25	-1	27	45
30	-2	22	43	30	-1	24	43	30	-3	26	48	30	-3	25	45
40	-2	22	43	40	-1	23	42	40	-3	25	46	40	-4	25	45
45	-3	23	44	45	-1	24	43	45	-3	25	46	45	-3	26	45
60	-3	23	43	60	-1	23	42	60	-3	24	45	60	-3	23	45
90	-2	22	43	90	-1	24	42	90	-3	25	46	90	-4	22	44

Raw data Figure 5-8: Texture data

Red

		Force 1	Distance 1	Area-FD 1:2	Grad.-FD 1:2
	time	g	mm	g mm	g/mm
R1000	0	12378.4	3.52	17469.53	259654
R1003	3	16158.2	5.40	31299.94	132540
R1006	6	16452.2	5.76	29935.83	91983
R1010	10	9028.5	4.48	14448.61	101858
R1020	20	4967.9	3.17	6135.61	119737
R1040	40	2136.4	3.38	2623.71	39069
R2000	0	16075.4	4.83	31849.41	218472
R2003	3	18940.4	6.24	37112.61	91290
R2006	6	12203.1	4.86	20047.56	112063
R2010	10	10533.8	5.14	16155.24	57720
R2020	20	4452.8	4.32	7719.09	58371
R2040	40	3179.0	4.01	4990.16	47209
R3000	0	14681.7	4.62	26725.07	203991
R3003	3	15827.7	5.88	25962.58	56441
R3006	6	13580.2	5.44	24201.87	86011
R3010	10	8570.6	5.07	13278.39	43605
R3020	20	4897.0	3.62	6812.24	90760
R3040	40	4452.4	3.78	9311.85	143269

Gold

		Force 1	Distance 1	Area-FD 1:2	Grad.-FD 1:2
	time	g	mm	g mm	g/mm
G1000	0	14629.7	3.78	23732.6	309060
G1003	3	16263.4	4.13	25948.7	263509
G1006	6	18838.8	5.70	37984.9	161807
G1010	10	11540.3	4.82	21702.9	146041
G1020	20	3584.8	3.05	5580.9	142158
G1040	40	1460.1	2.00	1354.9	71984
G2000	0	15951.6	4.37	29234.6	278345
G2003	3	12501.7	3.79	20294.0	258030
G2006	6	16901.3	5.32	31915.9	148272
G2010	10	13114.2	5.61	28179.9	126553
G2020	20	3709.7	2.69	4413.6	142351
G2040	40	1723.1	1.98	1652.7	85755
G3000	0	12259.7	3.52	19429.9	303630
G3003	3	16692.1	5.58	31559.2	125573
G3006	6	14419.7	5.00	25964.9	149030
G3010	10	12584.6	4.84	23063.6	152545
G3020	20	7515.6	4.44	15970.4	158228
G3040	40	1229.3	1.90	1090.3	63468

Raw data Figure 5-10 15: Chemical analysis

									TRS		DSC			
Var	Rep	Bk	Cooktemp	%Moiture	AIS%(dw/fw)	%(dw/dw)	Maltose(%fwb)	%(dw/dw)	Glucose (g/100gfwb)	%(dw/dw)	Peak (J/g)	Peak	onset	Texture Force (N)
G	R1	GB	0	75.50	20.90	85.34	2.60	10.61	0.01	0.05	1.91	65.02	61.07	99.20
G	R1	GB	70	75.01	18.19	72.77	4.51	18.04	2.45	9.82	0.74	76.60	73.80	97.62
G	R1	GB	80	73.90	16.15	61.88	7.53	28.85	6.42	24.58	0.00	.	.	17.43
G	R2	GD	0	64.92	30.91	88.13	3.41	9.73	0.01	0.02	1.20	63.93	56.85	148.30
G	R2	GD	70	64.88	26.85	76.44	5.92	16.86	2.49	7.10	0.76	79.85	76.88	80.84
G	R2	GD	80	63.98	24.99	69.37	8.78	24.38	6.20	17.22	0.00	.	.	30.46
G	R3	GE	0	72.12	23.79	85.34	3.29	11.80	0.01	0.05	2.17	65.68	59.68	107.76
G	R3	GE	70	71.07	20.92	72.31	6.55	22.66	2.90	10.03	0.34	79.85	75.44	78.70
G	R3	GE	80	70.94	20.54	70.69	6.06	20.86	2.35	8.10	0.00	.	.	10.51
G	R4	GH	0	64.92	30.50	86.95	3.09	8.79	0.01	0.03	2.17	66.35	61.66	74.19
G	R4	GH	70	66.64	24.72	74.10	5.27	15.80	1.60	4.79	0.19	78.35	75.52	55.85
G	R4	GH	80	68.56	22.67	33.07	8.30	26.40	4.05	12.88	0.00	.	.	15.07
R	R1	RC	0	67.49	29.90	44.30	2.49	7.67	0.01	0.04	3.02	68.35	62.46	162.30
R	R1	RC	70	64.25	29.14	45.35	4.13	11.54	1.71	4.77	1.69	77.68	74.43	225.90
R	R1	RC	80	66.50	21.57	32.44	9.26	27.63	7.74	23.11	0.00	.	.	73.02
R	R2	RD	0	67.35	29.19	43.34	2.77	8.49	0.00	0.00	2.16	70.68	63.17	155.60
R	R2	RD	70	65.20	30.79	47.23	3.05	8.76	0.06	0.18	3.14	78.02	75.77	190.02
R	R2	RD	80	65.36	21.90	33.51	6.54	18.88	5.35	15.43	0.00	.	.	26.70
R	R3	RE	0	71.03	25.56	35.98	2.09	7.22	0.01	0.03	1.70	67.27	61.14	136.64
R	R3	RE	70	69.61	25.36	36.44	3.38	11.11	1.69	5.56	1.00	76.85	73.98	162.51
R	R3	RE	80	67.86	23.06	33.98	10.26	31.93	7.62	23.72	0.00	.	.	111.61

Raw data Figure 6-1 and 6-2: Texture (fracture force)

	Red				Gold		
	Temp (°C)	time	Fracture point (N)		Temp (°C)	time	Fracture point (N)
RA	60	0	150.7	GA	60	0	98.6
RA	60	0	121.8	GA	60	0	163.4
RA	60	3	223.1	GA	60	3	121.8
RA	60	7	127.8	GA	60	7	144.8
RA	60	12	145.3	GA	60	12	172.3
RA	60	22	180.2	GA	60	22	107.9
RA	60	37	176.6	GA	60	37	123.6
RA	65	0	153.2	GA	65	0	107.3
RA	65	0	149.0	GA	65	0	174.1
RA	65	3	176.5	GA	65	3	209.6
RA	65	7	140.9	GA	65	7	198.9
RA	65	12	170.2	GA	65	12	209.4
RA	65	22	126.8	GA	65	22	161.6
RA	65	37	132.0	GA	65	37	132.9
RA	70	0	163.7	GA	70	0	140.8
RA	70	0	239.3	GA	70	0	177.5
RA	70	3	190.4	GA	70	3	145.6
RA	70	7	155.4	GA	70	7	153.5
RA	70	12	141.3	GA	70	12	129.7
RA	70	22	118.5	GA	70	22	126.3
				GA	70	37	125.5
RA	75	0	182.9	GA	75	0	190.2
RA	75	0	175.7	GA	75	0	182.8
RA	75	3	166.3	GA	75	3	169.6
RA	75	7	146.8	GA	75	7	149.9
RA	75	12	108.0	GA	75	12	120.2
RA	75	26	103.9	GA	75	26	60.0
RA	75	37	99.5	GA	75	37	30.5
RA	80	0	194.8	GA	80	0	142.0
RA	80	0	138.6	GA	80	0	195.8
RA	80	3	142.1	GA	80	3	107.5
RA	80	7	81.2	GA	80	7	41.5
RA	80	12	97.8	GA	80	12	35.3
RA	80	22	37.9	GA	80	22	20.3
RA	80	37	26.5	GA	80	37	15.2
RC	60	0	139.3	GB	60	0	119.6
RC	60	0	147.1	GB	60	0	127.8
RC	60	3	205.4	GB	60	3	119.9
RC	60	7	190.2	GB	60	7	139.3
RC	60	12	161.8	GB	60	12	182.5
RC	60	22	261.0	GB	60	22	204.4
RC	60	37	234.2	GB	60	37	192.0
RC	65	0	209.0	GB	65	0	114.1
				GB	65	0	150.3
RC	65	3	234.2	GB	65	3	142.2
RC	65	7	203.6	GB	65	7	121.0
RC	65	12	229.1	GB	65	12	168.4

RC	65	22	189.3	GB	65	22	154.3
RC	65	37	203.2				
RC	70	0	113.7	GB	70	0	135.2
RC	70	0	248.9	GB	70	0	151.7
RC	70	3	205.1	GB	70	3	166.0
RC	70	7	199.9	GB	70	7	168.3
RC	70	12	187.3	GB	70	12	123.7
RC	70	22	177.8	GB	70	22	124.0
RC	70	37	163.0	GB	70	37	81.8
RC	75	0	197.9	GB	75	0	138.6
RC	75	0	180.9	GB	75	0	161.3
RC	75	3	184.6	GB	75	3	194.7
RC	75	7	189.9	GB	75	7	158.0
RC	75	12	188.6	GB	75	12	111.5
RC	75	26	172.0	GB	75	26	61.4
RC	75	37	59.8	GB	75	37	34.3
RC	80	0	241.3	GB	80	0	124.1
RC	80	0	224.9	GB	80	0	187.1
RC	80	3	230.4	GB	80	3	113.0
RC	80	7	157.4	GB	80	7	89.8
RC	80	12	99.2	GB	80	12	31.0
RC	80	22	102.2	GB	80	22	25.6
RC	80	37	59.2	GB	80	37	14.2
RD	60	0	254.8	G1	80	0	154.5
RD	60	0	150.8	G1	80	3	142.9
RD	60	3	141.6	G1	80	7	71.6
RD	60	7	182.7	G1	80	17	33.2
RD	60	12	166.2	G1	80	37	19.2
RD	60	22	179.1				
RD	60	37	173.0				
RD	65	0	178.7				
RD	65	0	188.0				
RD	65	3	224.2				
RD	65	7	249.5				
RD	65	12	192.2				
RD	65	22	193.0				
RD	65	37	190.0				
RD	70	0	168.2				
RD	70	0	217.2				
RD	70	3	201.2				
RD	70	7	163.7				
RD	70	12	158.0				
RD	75	0	175.5				
RD	75	0	184.9				
RD	75	3	176.5				
RD	75	7	161.3				
RD	75	26	122.2				
RD	75	37	120.3				
RD	80	0	152.4				
RD	80	0	182.1				
RD	80	3	151.8				
RD	80	7	117.6				

RD	80	12	81.7	
RD	80	22	53.4	
RD	80	37	15.3	
R1	80	0	123.9	19.47
R1	80	3	85.2	3.687
R1	80	7	46.8	3.458
R1	80	17	29.7	1.916
R1	80	37	14.7	3.061